

# Toward synthesis of novel thermoelectric organic semiconductors



John William Ritchie, MSc

Thesis submitted to the University of Nottingham  
for the degree of Doctor of Philosophy

## Contents

Acknowledgements.....	3
Abbreviations.....	5
Abstract.....	8
Introduction to Tetracenes: Application to Thermoelectric Materials and Syntheses	10
1.1. Semiconductors .....	11
1.2 Thermoelectric Materials.....	13
1.3. Organic Semiconductors .....	15
1.4. Synthesis of Tetracenes .....	19
1.4.1. Friedel-Crafts approaches.....	19
1.4.2 Diels-Alder Approaches to Tetracenes .....	26
1.4.3 Aldol Approaches to Tetracenes.....	31
1.4.4 Bergman Approach to Tetracenes .....	33
1.4.5. Organometallic and Transition Metal-catalysed Approaches to Tetracenes .....	33
1.4.6. Late-stage Modification of Tetracene .....	37
1.5 Aims.....	44
2.1. Results and discussion .....	46
2.1.1. Optimisation and Scope of the Sigmatropic Rearrangement Cascade.....	46
2.1.2. Mechanistic Investigation of the rearrangement cascade .....	52
2.1.3. Density Functional Theory Calculations and Electrooptic properties .....	60
2.1.4. Crystal Structures of Dithiocarbamate Tetracenes.....	63
2.2. Conclusions and Future Work.....	65
Synthesis of 8-membered rings via a [1,5]-hydride rearrangement-propargyl Michael addition cascade .....	67
3.1. Introduction .....	68
3.1.1. Ring Closing Metathesis (RCM) Approaches to 8-Membered Rings .....	70
3.1.2. Aldol Approaches to 8-Membered Rings.....	73
3.1.3. Radical Approaches to 8-Membered rings .....	74
3.1.4. Transition Metal-catalysed Approaches to 8-Membered Rings.....	76
3.1.5. Gold Catalysed Approaches to 8-Membered Rings.....	80
3.1.6. Synthesis of 8-Membered Rings via Ring expansions, Fragmentations and Rearrangements.....	82

3.2. Results and Discussion .....	85
3.2.1. Optimisation and Mechanistic Investigation .....	85
3.2.2. Diversification of the 8-Ring Structure .....	89
Knoevanagel Cyclisation Approach to Tetracenes.....	91
4.1. Introduction .....	92
4.2 Results and discussion .....	92
4.3 Future Work.....	96
Carbometallation Approach to Tetracenes .....	98
5.1. Introduction .....	99
5.2. Results and Discussion .....	100
5.2.1. Carbometalation and Negishi Cross-Coupling of Vinyl Iodides .....	100
5.2.2. Oxidation of the Diols .....	108
5.2.3. Cyclisation of the Dialdehydes.....	110
5.2.4. Calculated and Electrooptic properties .....	116
5.3. Conclusions and Future Work.....	117
Appendices.....	118
Appendix 1 – Experimental Data for Chapter 2.....	118
General information .....	118
Appendix 2 – Experimental Data for Chapter 3.....	143
Appendix 3 – Experimental Data for Chapter 4.....	146
Appendix 4 – Experimental Data for Chapter 5.....	149

# Acknowledgements

I thank Professor Simon Woodward for provision of the project and valuable input, and at times his patience and understanding in the campaign toward the project's completion. I am furthermore indebted to Kevin Simpson and European Thermodynamics Ltd for funding my research in conjunction with the EPSRC.

I am immensely grateful to the Woodward and Ball research groups for interesting and stimulating discussions, convivial atmosphere and continuing friendship throughout my time within the group. My sincere thanks to Dr Laurence Burroughs, Dr Benoit Wahl, Dr Darren Lee, Dr Mary-Robert Garrett, Dr Liam Ball, Dr Maria Durán-Peña, Dr Melchior Cini, Dr Lee Eccleshare, Alex Kingsbury, Ryan Nouch, Mustafa Al-Jumaili, Mohammed Abid, Mark Jurrat, Lorenzo Maggi, Tom Barber, Jonathan Shine, Miriam Ackermann, Antonio Pedrina-McCarthy, Byörk Tyril, Evie Newby, Ellen Nichols, Doriana Dobрева, Sean Selzer, Saurabh Ariwhar and Omkar Kulkarni. It has been a pleasure to support and to be supported by them in our successes and frustrations throughout our time working together.

I am particularly grateful toward Dr Laurence Burroughs, whose insight and assistance through my research have been instrumental to its success: without his guidance early within the project, I have no doubt this volume would be a shadow of what you will read hence. Furthermore, I am immensely grateful to Dr. Lee Eccleshare for graciously allowing me to assist in his doctoral project discussed within Chapter 3 of this thesis. Furthermore, I must give special thanks to Professor Simon Woodward and Dr Mary-Robert Garrett for assistance in synthesising many of the derivatives discussed in Chapter 5, and to Drs Garrett and Burroughs for proofreading and helpful suggestions.

Within the body of this thesis, some results were generated by other members of the Woodward group. The individual responsible and their work is highlighted at the start of each chapter. I do however, wish to thank them here for their contribution to the body of this thesis.

I must finally give thanks to my partner Emma Ishmael and my family, for inestimable patience in the preparation of this manuscript, and at times, tirelessly working to synthesise some sanity for me through my PhD: they are the makers of this thesis.

## *Abbreviations*

Ac – Acetyl

Acac – Acetylacetonate

9-BBN – 9-Borabicyclo[3.3.1]nonane

Bn – Benzyl

Bz – Benzoyl

1,4-CHD – 1,4-Cyclohexadiene

cod – Cyclooctadiene

CuBr.DMS – Copper bromide dimethylsulfide complex

CuTc – Cuprous thiophene-2-carboxylate

DBU – 1,8-Diazabicyclo[5.4.0]undec-7-ene

DCE – 1,2-Dichloroethane

DDQ – 2,3-Dichloro-5,6-dicyano-*p*-benzoquinone

DEAD – Diethyl azodicarboxylate

DFT – Density functional theory

DIBAL-H – Diisobutyl aluminium hydride

DMAD – Dimethyl acetylenedicarboxylate

DME – 1,2-Dimethoxyethane

DMF – Dimethylformamide

DMP – Dess-Martin periodinane

Dtbpy – Di-*tert*-butyl-2,2'-bipyridine

Et – Ethyl

facam – 3-(Trifluoromethylhydroxymethylene)-(+)-camphorate

HFIP – Hexafluoroisopropanol

HMDS – Hexamethyldisilazane

HMPA – Hexamethylphosphoramide

HOMO – Highest occupied molecular orbital

<sup>i</sup>Pr – *iso*-Propyl

LUMO – Lowest occupied molecular orbital

Me – Methyl

MeCN – Acetonitrile

Mes – Mesityl

MOM – Methoxymethyl

Ms – Mesyl

<sup>n</sup>BuLi – *n*-Butyl lithium

<sup>n</sup>BuOH – *n*-Butyl alcohol

NBS – *N*-Bromosuccinamide

NMP – *N*-Methyl-2-pyrrolidone

*o*-DCB – *Ortho*-dichlorobenzene

PCC – Pyridinium chlorochromate

PEDOT – Poly(3,4-ethylenedioxythiophene)

PhH – Benzene

PhLi – Phenyllithium

PhMe – Toluene

PPA – Polyphosphoric acid

SET – Single electron transfer

SPhos – 2-Dicyclohexylphosphino-2',6'-dimethoxybiphenyl

TBAF – Tetrabutylammonium fluoride

TBDPS – *tert*-Butyl diphenylsilyl

<sup>t</sup>Bu – *tert*-Butyl

TCE – Trichloroethylene

TE - Thermoelectric

Tf – Triflyl

TIPS – Triisobutyl silyl

THF – Tetrahydrofuran

TMEDA – Tetramethylethylenediamine

TMS – Trimethylsilyl

Ts – Tosyl

TTT – Tetrathiotetracene

TW – Terrawatt

## Abstract

Thermoelectric devices provide an excellent method for the generation of electrical power from low grade waste heat from energy production, but the current best inorganic materials used for such devices are expensive and require dwindling resources. Organic semiconductors derived from tetracenes may therefore provide an excellent alternative. However existing synthetic methods are step and atom inefficient and as such would provide poor yield and cost efficiency in mass production, and there is a paucity of n-type organic materials compared to p-type, which limits device design.

This report details attempts to develop rapid, general and scalable syntheses of tetracenes. A two-step process for the synthesis of substituted tetracenes *via* [3,3]-sigmatropic rearrangement cascade reaction from a series of *bis*-propargyl diols is disclosed. This method furnished a variety of tetracenes in up to quantitative yield from commercially available materials. Mechanistic insights into the novel anionic Chugaev cascade derived from DFT calculations are disclosed along with computed and experimentally derived HOMO-LUMO gaps. A brief analysis of the predicted electronic properties of some of the materials synthesised is then presented.

In investigating *bis*-allenic cascades, an 8-membered ring was isolated in low yield. Mechanism of formation and the scope of the cascade which formed the carbocycle are briefly discussed.

A second method toward the synthesis of tetracenes *via* an attempted nitrile cyclisation reaction is disclosed. The method suffered from the rapid oxidation of the derived *peri*-diaminotetracene, and attempts to temper the reactivity of the resultant tetracene were stymied by a difficulty in forcing a second ring closure, which proved resistant to further attempts to force cyclisation.

A final method derived from an (*E*)-selective carbomagnesiation of 2-butyne-1,4-diol with various benzylmagnesium chlorides and trapping with iodine is disclosed. This allowed for a facile and high yielding Negishi-cross coupling with various benzylzinc halides to allow for various substitution patterns on the outermost aryl rings. A high yielding Stahl oxidation gave access to various dialdehydes in excellent to

quantitative yields, allowing for a Lewis acid-mediated double closure with  $\text{TiCl}_4$ . This step proved to be limited by the necessity of electron-donating groups to facilitate the double Bradsher closure, but allowed access to multiple substituted tetracenes.

# ***Chapter One***

## ***Introduction to Tetracenes: Application to Thermoelectric Materials and Syntheses***

## 1.1. Semiconductors

Semiconductors are materials which display the properties of a resistor, but at elevated temperatures begin to display electrical conductivity.<sup>1</sup> This behaviour is caused by the thermal excitation of electrons from the valence band into the conductance band populating an energetically higher band with electrons and generating a hole in the energetically lower valence band (Figure 1.1). This creation of charge carriers can therefore be used to generate a current at elevated temperatures.

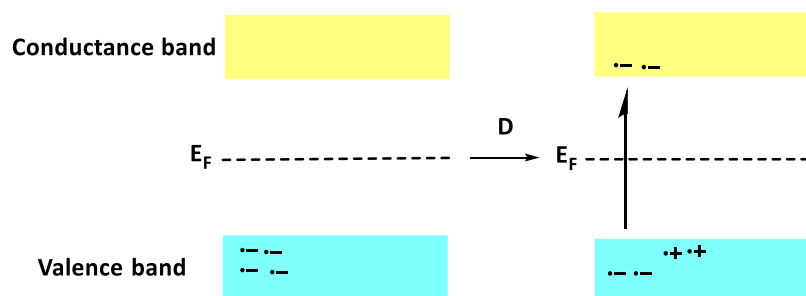


**Figure 1.1** - Thermal excitation of electrons from the valence band to the conductance band in an intrinsic semiconductor, with  $\cdot$  denoting electrons and  $\cdot^+$  denoting holes.  $E_F$  denotes the Fermi level

The above described behaviour is for an intrinsic semiconductor, that is a pure elemental material for which the number of conductance band electrons is equal to the number of valence band holes. In this treatment, the size of the gap gives an insight into how conducting the material will be at a temperature. In elemental Si the band gap is 1.1 eV making it a poor semiconductor. However, elemental Ge has a band gap of 0.66 eV, making it a better semiconductor displaying greater conductivity.

Upon addition of dopant atoms to a pure intrinsic semiconductor such as Si, the material becomes an extrinsic semiconductor. By introducing atoms of phosphorus, which has 5 valence electrons compared with silicon which has 4 valence electrons, a greater number of electrons are present in the substance which can occupy empty orbitals within the conductance band. This creates a new narrow donor band at higher energy, reducing the band gap and reducing the amount of thermal energy necessary to excite electrons to the conductance band.

This is termed n-doping, where the n signifies the negative charge of the electrons which act as the major charge carrier in the substance. If a dopant with fewer valence electrons, such as boron, is introduced to silicon, positive holes are introduced to the silicon. This withdraws valence electrons and creates a new narrow acceptor band, similarly reducing the band gap. This is termed as p-doping, from the positive charge of the holes (Figure 1.2).

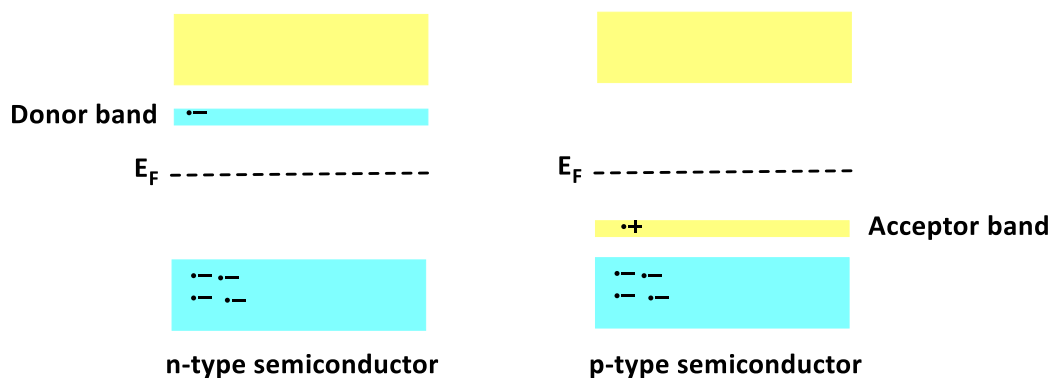


Figure 1.2 - Effect of introducing dopants to electronic band structure in extrinsic semiconductors

In the case of organic semiconductors, built out of discrete separate molecules, the molecular HOMO and LUMO energy levels can be treated as indicative of the valence band and conduction band respectively and the gap to be the lowest energy difference to excitation. This can be seen in the orbital diagrams for hexatriene (Figure 1.3).

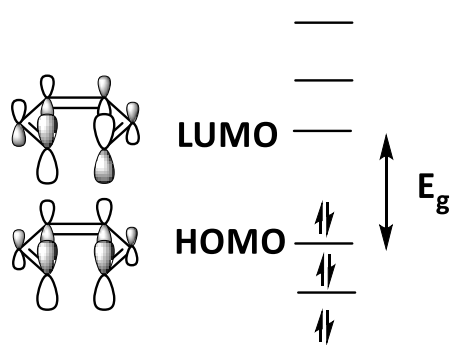


Figure 1.3 - The HOMO-LUMO gap of hexatriene as an example of an organic bandgap.  $E_g$  denoted the HOMO-LUMO energy gap.

## 1.2 Thermoelectric Materials

Thermoelectric modules are devices which utilise semiconducting materials in the generation of an electrical current from a source of heat (Figure 1.4).<sup>2</sup>

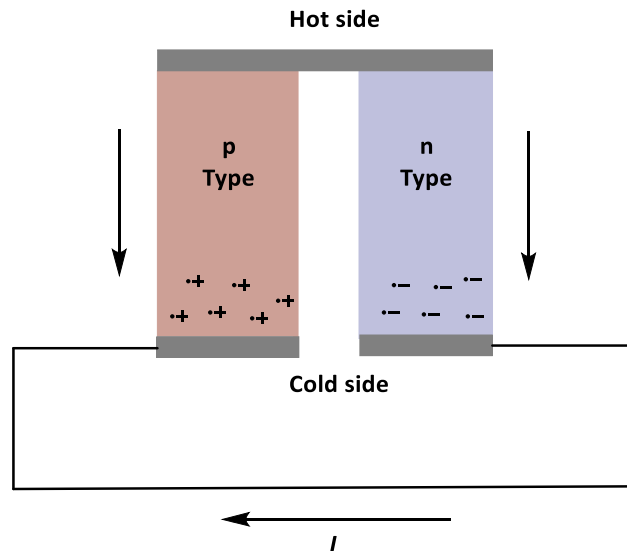


Figure 1.4 - A Simplified Thermoelectric module,  $I$  denotes induced current.

The generation of a current from a temperature difference is described by the Seebeck effect. Simple theoretical treatments describe how charge carriers in semiconductors act as molecules in an ideal gas. Upon the application of a heat difference upon a simple thermocouple (shown above), the charge carriers diffuse from the hot end to the cold end creating a potential difference. Ideal thermoelectric materials should transport energy only by electrical conduction (*via* charge carrier mobility) and not thermally (*via* lattice vibrations). In practice, it is challenging to achieve this but if efficient thermoelectric materials can be developed huge opportunities exist for meaningful energy recovery. It was estimated in 2008 that the efficiency of fossil fuel burning around the world is currently 30-40% with an approximate loss of 15 TW energy as low grade heat (heat up to 200°C).<sup>3</sup>

The design and optimisation of thermoelectric modules therefore presents a means to generate electrical energy for the waste heat and improve the sustainability of energy generation. Thermoelectric devices are judged by the dimensionless figure of merit or  $ZT$  (Equation 1.1), where  $\sigma$  is the electrical conductivity,  $S$  the Seebeck

coefficient (Equation 1.2),  $T$  is temperature and  $\kappa$  is the thermal conductivity, and by power factor, or PF (Equation 1.3).<sup>2</sup>

$$ZT = \sigma S^2 T / \kappa \quad (1.1)$$

$$S = \frac{\Delta V}{\Delta T} \quad (1.2)$$

$$PF = \sigma S^2 \quad (1.3)$$

Issues arise on increasing temperature, both  $\sigma$  and  $\kappa$  increase and  $S$  decreases, lowering the  $ZT$  of the material. Furthermore, as a heat engine, a thermoelectric module is limited by Carnot efficiency. The overall device efficiency is therefore a product of the Carnot efficiency and the  $ZT$  for any thermoelectric module (a  $ZT$  of 1 correlates to a device efficiency of 5% with a temperature difference of 100 K, without taking into effect the Carnot efficiency). This means that  $ZT$  is dependent on both temperature and the tuning of several material properties to give high device efficiency.<sup>4,5</sup> Therefore, significant research effort has gone into optimising  $ZT$  through modifying materials to lower  $\kappa$  by introducing heavy elements into TE materials to scatter phonons (quantum mechanical descriptions of lattice vibrations contributing to heat transport in solids) and increase  $ZT$ . Superlative  $ZT$  values ( $2.6 \pm 0.3$  at 928 K) have been observed in SnSe due to low  $\kappa$  along the  $b$  axis of the unit cell.<sup>6</sup> Currently, the most commonly used and highest performing thermoelectric devices are based around bulk and thin film  $\text{Bi}_2\text{Te}_3$  superlattices. High  $ZT$  values in superlattices have been attained through doping with some devices attaining  $>2=ZT$  values at room temperature upon doping with heavy element tellurides such as  $\text{Sb}_2\text{Te}_3$ .<sup>7, 8</sup> However, the development of these devices is marred by their cumbersome and costly production, and by the scarcity of tellurium, reducing the sustainability of the technology.<sup>9</sup>

### 1.3. Organic Semiconductors

One potential method of obviating the cost issues of thermoelectric devices based upon  $\text{Bi}_2\text{Te}_3$  is the usage of semiconducting materials of greater abundance, lower cost and greater ease of production. Although the electrical conductivity of organic materials is orders of magnitude lower than that of metallic alternatives, the low thermal conductivity of organic alternatives can be exploited to maximise the thermodynamic figure of merit of organic semiconductors and potentially make them comparable. Furthermore, modification of the substitution patterns of organic molecules has been shown to introduce perturbations in the HOMO-LUMO gaps of organic molecules allowing for the relatively facile tuning of their electronic properties for increased p or n-type properties and stability to oxidation.<sup>10</sup> For example, addition of electron-withdrawing and donating groups has been shown to lower the LUMO of oligoacenes.<sup>11, 12</sup> As such, the ability to tune organic semiconductor properties facilely through substitution presents a simple means to optimise the various factors thermoelectric device efficiency depends upon.

The reasons stated above have made the research of organic thermoelectric semiconductors a fertile and rapidly developing field, with many organic systems fast approaching similar ZT values to  $\text{Bi}_2\text{Te}_3$  at r.t.<sup>13</sup> The greatest advances have been made in the development of conductive polymers,<sup>14</sup> with air stable oxidised PEDOT-Tos polymers **1** (Figure 1.5) with simple synthetic operations capable of optimising  $\kappa$ ,  $\sigma$ , and  $S$ , engendering an optimised  $\text{ZT} = 0.42$  and power factors  $\text{PF} = 469 \mu\text{W m}^{-1} \text{K}^{-2}$ .<sup>15</sup>

16

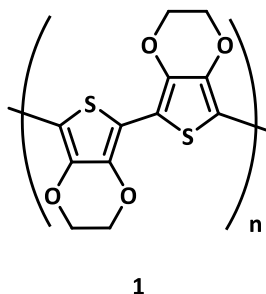


**Figure 1.5** – A generalised PEDOT polymer

Furthermore, theoretical studies of similar PEDOT nanowires are calculated to possess an upper limit to ZT of 15.2, indicating significant room for improvement of these parameters.<sup>17</sup> Furthermore, progress has been made in the development of n-type polymers, achieving good power factors and conductivities allowing for the potential design of high performance organic thermocouples.<sup>18</sup>

Other materials which show favourable semiconducting properties include linear oligoacenes such as tetracene **1** and pentacene **2** (Figure 1.6).<sup>19, 20</sup>

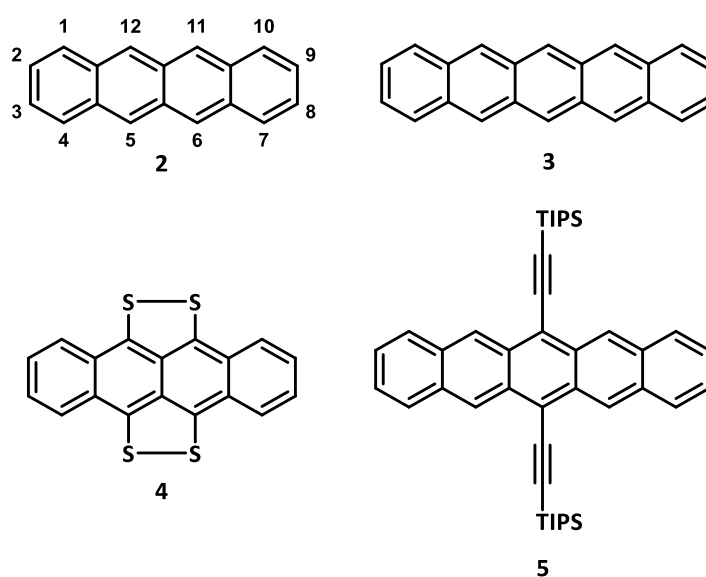


**Figure 1.6** - Examples of oligoacene molecules, **1**- tetracene and numbering convention, **2**- pentacene, **3**- (tetrathio)tetracene (TTT), **4**- 6,13-bis(triisopropylsilylethynyl)pentacene.

Although longer linear acenes (such as pentacenes, hexacenes and heptacenes) typically have lower HOMO-LUMO gaps and some excellent device properties, they are susceptible to oxidation and dimerisation. This can be rationalised that in increasing length of the linear poly aromatic, the HOMO-LUMO energy gap (or  $E_g$ ) is depressed, creating greater diradical character. Indeed, the rate of photooxidation of **3** is approximately 18 times greater than **2** (bimolecular rate constants  $k=23 \times 10^6 \text{ s}^{-1} \text{ M}^{-1}$  for **2** vs  $k=42 \times 10^7 \text{ s}^{-1} \text{ M}^{-1}$  for **3**) and require functionalisation (typically with 5,12-TIPS acetylenes such as **4**) to make them solvent processable.<sup>21</sup> While many impressive syntheses of higher acenes have been achieved, such as Miller *et al.* synthesis of a persistent nonacene<sup>22</sup> and Anthony *et al.* synthesis of hexacene and heptacene,<sup>23</sup> higher acenes require multiple synthetic steps and specific substitution to allow for synthetic tractability and stability. Furthermore, long

synthetic routes and prescribed substitution patterns limit rapid investigation of electronic properties and modification of the core polyaromatic, limiting the rate at which insights into developing better materials can be generated. While some longer quinone and tetracyanoquinone acenes and bent aromatic architectures have shown n-type semiconducting properties and resistance to oxidation,<sup>24-26</sup> tetracenes represent a better trade-off between stability and ease of synthesis. As they possess a greater resistance to oxidation they possess superior handling properties, making them attractive for simplified fabrication of devices. Similarly, tetracenes can be more concise to synthesise and can be more varied in substitution as they do not require as many blocking groups to prevent oxidation or dimerisation. Furthermore, high measured  $\sigma$  values have been observed in substituted tetracene derivatives, such as tetrathiotetracene (TTT) **4**. For example, some (TTT)<sub>2</sub>I<sub>3</sub> radical cation salts can have conductivities as high as  $4 \times 10^4 \Omega^{-1} \text{ cm}^{-1}$  predicted for pure crystals, roughly 8 times superior to Bi<sub>2</sub>Te<sub>3</sub>.<sup>27</sup>

Manipulations of the substitution of organic materials allows for the tuning of HOMO-LUMO gaps, but can also alter the crystal packing properties of organic materials. Crystalline tetracene adopts a herringbone stacking motif where each adjacent tetracene molecule orients perpendicularly, with minimal  $\pi$ -stacking in the unit cell (Figure 1.7, tetracene's packing from the CCD file TETCEN01).

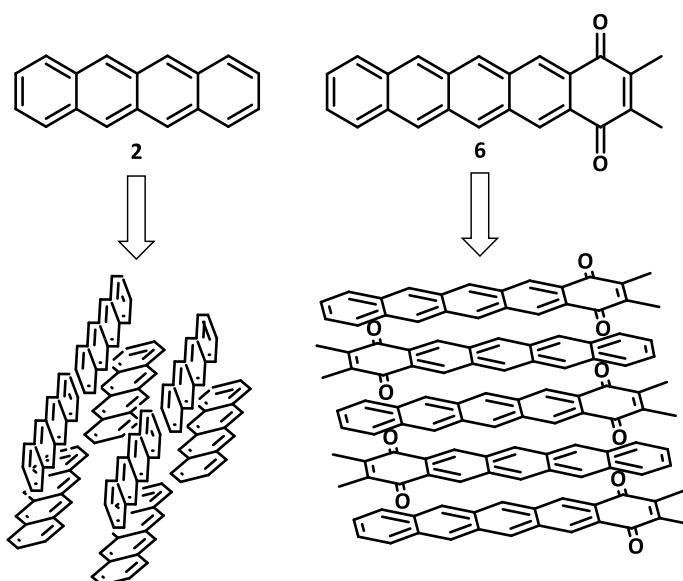


Figure 1.7 - Comparison of the stacking motifs in tetracene **2** and a quinone tetracene **6**.

Modification of supramolecular ordering in oligoacenes is regarded as key to optimal electron and hole transport for semiconducting properties. In oligoacenes, the predominant transport mechanism is still debated, however, there is a larger body of evidence for an intermolecular hopping mechanism above 100K.<sup>28-30</sup> Furthermore, tetracene **2** shows a significant conductivity anisotropy along the a-b axis, where  $\pi$ - $\pi$  contact is closer, resulting in a four-fold increase in conductivity.<sup>28</sup> Theoretical treatments have highlighted that increased  $\pi$ -facial stacking in organic oligomers increases electron mobility and conductivity.<sup>31-33</sup> The electrons from an excited molecule exchange with a neighbouring molecule, and this exchange is dependent on the overlap between the respective orbitals of the molecules. As such increased  $\pi$ - $\pi$  staking and decreased stacking distance are desirable, as increased overlap increases electronic coupling between the conducting molecules and as such lowers the energy barrier for exchange, allowing greater charge transport.<sup>31, 34, 35</sup>

Modification of supramolecular interactions can be accounted for by the 3 factors: steric repulsion of pendant groups altering the herringbone stacking motif, the introduction of electron-withdrawing or donating groups to create dipole interactions and intramolecular bonding interactions between pendant groups. This was hypothesised to be due to disruption of herringbone stacking and increased  $\pi$ -orbital overlap. For example, Moon *et al.* found that 5,11-dichlorotetracene adopted a  $\pi$ -stacking motif with a higher electron mobility (1.6 cm<sup>2</sup>/V.s vs 1.3 cm<sup>2</sup>/V.s) than unfunctionalised tetracene.<sup>36</sup>

The introduction of electron-withdrawing and releasing groups can therefore be factored into molecular design to generate desired  $\pi$ -overlap and reduced  $\pi$ - $\pi$  distance by altering the dipole of the aromatic molecule,<sup>37</sup> improving conductivity and electron mobility. For example, Nuckolls *et al.* increased end on end stacking by attaching acenes with electron rich quinones to achieve greater  $\pi$ -overlap (Figure 1.6, **6**).<sup>38</sup>

Furthermore, introducing sterically demanding groups onto the tetracene structure has been shown to modulate crystal packing by preventing herringbone stacking, such as in the case of the alkylated and carboxylate tetracenes studied by Kitamura *et al.*<sup>39</sup> Finally, Miao *et al.* found that the introduction of hydrogen bonding

moieties (in this case amides) interrupted herringbone stacking and increased  $\pi$ -stacking distance, which was found to alter the regioselectivity of photooxidation.<sup>40</sup> Therefore, the relative oxidative stability of tetracenes coupled with the ability to modify their electronic and crystal packing properties *via* modification of substitution makes them attractive to investigate for semiconducting applications.

Organic semiconductors therefore present an attractive, sustainable alternative to elemental semiconductors for thermoelectric applications and are a rapidly developing area in the literature, although they are not without drawbacks. The development of optimal organic devices requires the careful tuning of p- and n-type semiconductors, and although many new n-type organic materials have been developed, there are still relatively few of these in comparison to p-type organic semiconductors.<sup>33</sup>

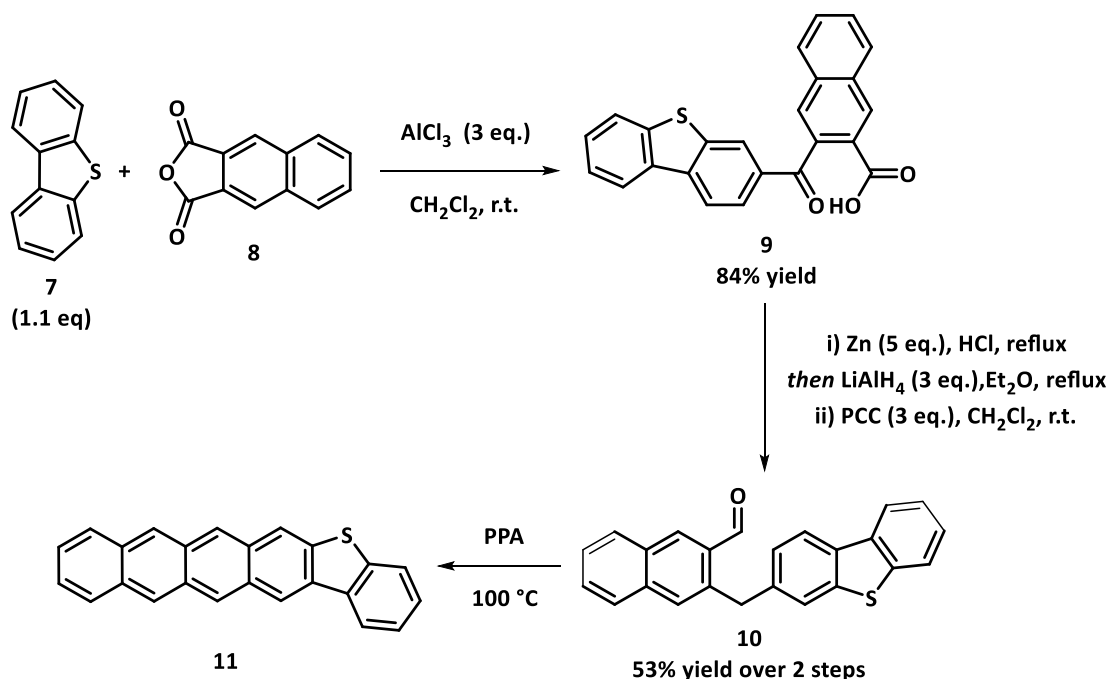
## 1.4. Synthesis of Tetracenes

Tetracenes may therefore present an excellent choice for the development of organic semiconductors for thermoelectric devices: while their band gaps and performance may be lower than that of pentacenes and longer polyacenes, they possess slower rate of dimerisation and oxidation, providing more stable materials. However, one drawback is that tetracene cannot be drawn from coal feedstocks unlike naphthalene and anthracene, but instead must be synthesised. A wide range of synthetic methods have been developed for the synthesis of tetracenes, including Friedel-Crafts acylations, aldol condensations, Diels-Alder cycloadditions, Bergman cyclisations and transition metal [2+2+2] co-trimerisations, [4+2] cyclisations and C-H activations and cross couplings and the relative merits of these are discussed below.<sup>41</sup>

### 1.4.1. Friedel-Crafts approaches

Utilising Friedel-Crafts acylations is one means to extend aromatic molecules (Scheme 1.1). Several groups have utilised simple Friedel-Crafts acylations between aromatic molecules and 2,3-naphthalic anhydrides. Typically, a primary Friedel-Crafts

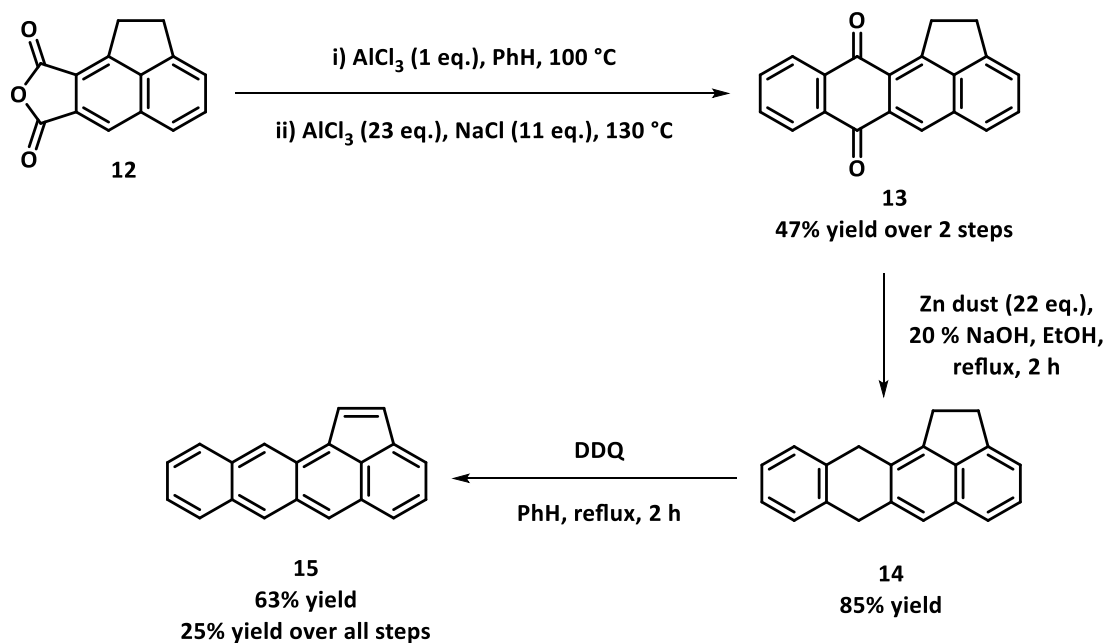
acylation forms the intermediate naphthyl keto acid followed by a second cyclisation step furnishing the desired fused ring system of tetracene. This approach has been utilised by many groups in the synthesis of terminally substituted tetracenes, for example in the synthesis of tetraceno-2,3-benzothiophene **11** by Du *et al.* (Scheme 1.1).<sup>42</sup>



Scheme 1.1 – Synthesis of a benzothiophenyl tetracene **11** via a Friedel-Crafts acylation.

The keto acid is formed *via* the facile Friedel-Crafts acylation between 2,3-naphthalic anhydride **8** and dibenzothiophene **7** in 84% yield with  $\text{AlCl}_3$ . To achieve the second closure the ketone **9** was reduced with  $\text{Zn}/\text{AcOH}$  and the carboxylic acid reduced to the alcohol with  $\text{LiAlH}_4$  and oxidised to the aldehyde **10** with PCC with a yield of 54% over the three steps. This allowed a final Bradsher cyclisation to be performed in PPA to yield the desired tetracene **11** with no reported yield. While the preceding steps were moderately high yielding, the multiple redox steps required highlights that the route is far from ideal.

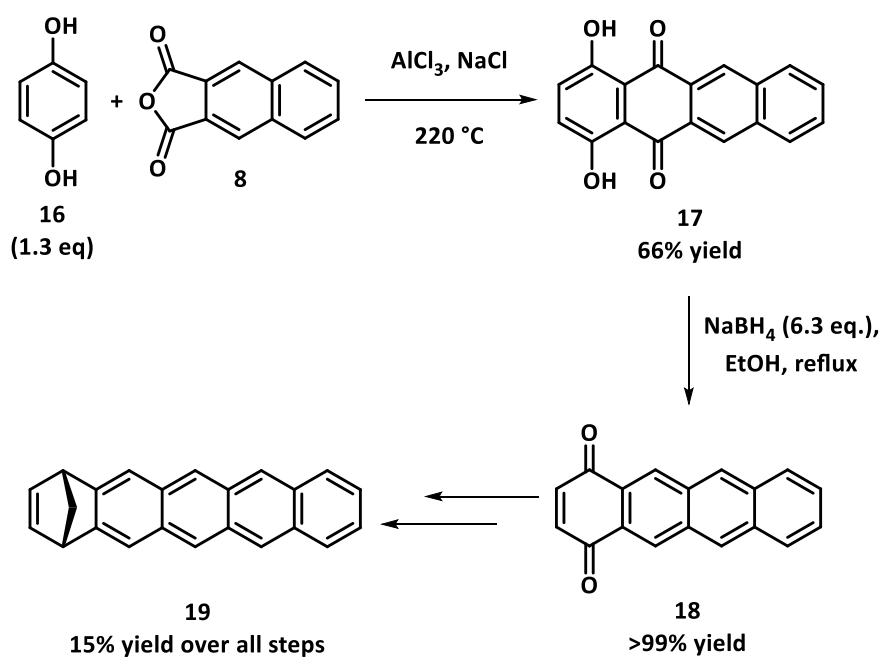
A similar approach was utilised by Gold and Sangaiah to synthesise benz[k]aceanthrylene **15** *via* a similar acylation with benzene to the substituted anhydride **12** with  $\text{AlCl}_3$ , giving a 85% yield of regioisomers (Scheme 1.2).<sup>43</sup>



Scheme 1.2 – Synthesis of benz[k]aceanthrylene **15** via a Friedel-Crafts acylation.

The tetracene quinone **13** was formed *via* a second acylation with  $\text{AlCl}_3$  in 55% yield. The desired tetracene **15** could then be formed *via* a Zn mediated reduction to the dihydrotetracene **14** and oxidation with DDQ under reflux. The route suffers from similar limitations: the naphthalene anhydride must be synthesised for the first acylation, and the fact that a second more forceful acylation is required to form the linear fused ring system along with the subsequent reductions and oxidation lowers the yield and step efficiency.

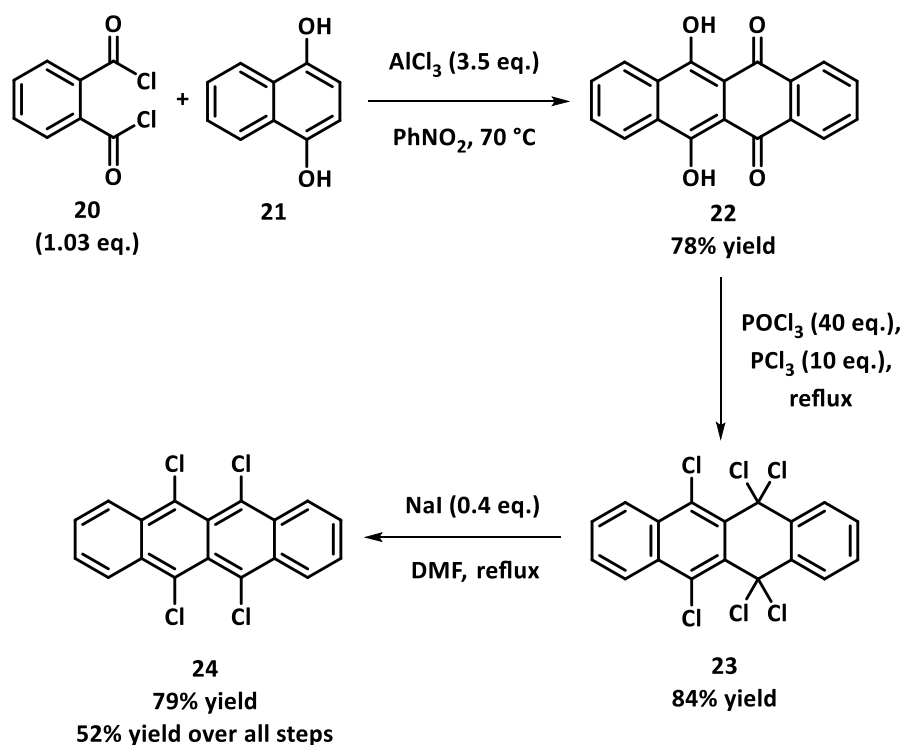
In the synthesis of 2,3-norbornadienonaphthacene **19**, the double Friedel-Crafts acylation of 1,4-hydroquinone **16** with 2,3-naphthalic anhydride **8** yielded the desired tetracene quinone in 66% yield using  $\text{AlCl}_3$  as the Lewis acid (Scheme 1.3).<sup>44</sup>



**Scheme 1.3** – Synthesis of 2,3-norbornadieneonaphthacene **19** via a Friedel-Crafts acylation.

After reducing the intermediate tetracene quinone **17** to the 1,4-tetracene quinone **18** in quantitative yield, the desired norbornyl **19** tetracene could be synthesised *via* a Diels-Alder cyclisation to cyclopentadiene and reduced to the tetracene *via* a LiAlH reduction and tosylation.

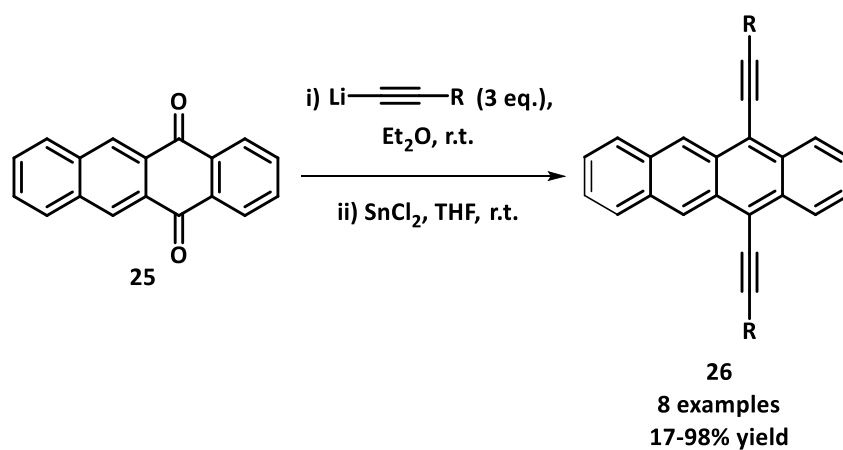
Douglas *et al.* synthesised 5,6,11,12-tetrachlorotetracene **24** *via* a Friedel-Crafts acylation of 1,4-dihydroxynaphthalene **21** with phthaloyl chloride **20** and subsequent treatment with POCl<sub>3</sub> and PCl<sub>5</sub> and NaI, with an overall yield of **24** in 52% over multiple steps (Scheme 1.4).<sup>45</sup>



**Scheme 1.4** – Synthesis of 5,6,11,12-tetrachlorotetracene **24** via a Friedel-Crafts acylation.

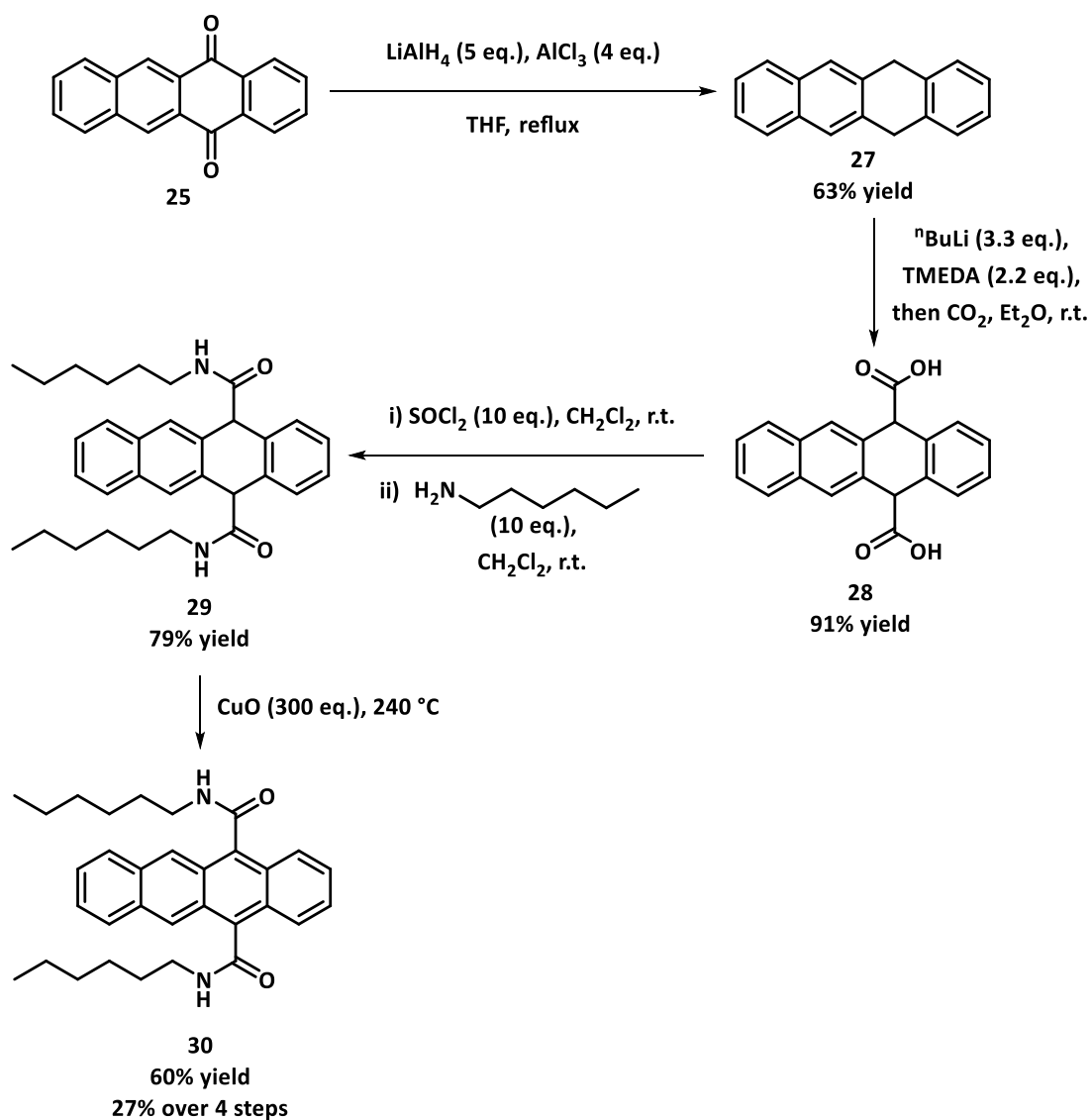
The incorporation of the chlorides at the 5, 6, 11 and 12 positions carry the advantage of allowing further substitution, *via* Kumada-Corriu cross-coupling/C-H activations with phenyl magnesium bromide or by  $\text{S}_{\text{N}}\text{Ar}$  reactions leading to electron rich chalcogen substituted tetracenes.<sup>46</sup>

A clear disadvantage to the Friedel-Crafts routes to tetracene is the common intermediate quinone structures formed in the transformation. This leaves the core at the incorrect oxidation state, necessitating further reactions to furnish the desired polyaromatic molecule. Several groups have exploited the carbonyl functionality to introduce further substitution to the central aromatic rings such as the Diels-Alder substitution shown above, increasing molecular complexity (Scheme 1.5). Anthony *et al.* utilised the addition of lithium acetylides to the quinone carbonyls of **25** and subsequent reduction with  $\text{SnCl}_2$  to synthesise a range of 5,12 - ethynyl tetracenes **26** in poor to excellent yield (Scheme 1.5).<sup>47</sup>



**Scheme 1.5** – Synthesis of a range of 5,12 – alkynyltetracenes **26** from tetracene dione **25**.

Miao *et al.* reduced the tetracene quinone **25** to the dihydrotetracene **27**, which could then be lithiated at the doubly benzylic  $\text{sp}^3$  centre and reacted with  $\text{CO}_2$  to form the dicarboxylate **28** (Scheme 1.6).<sup>40</sup>

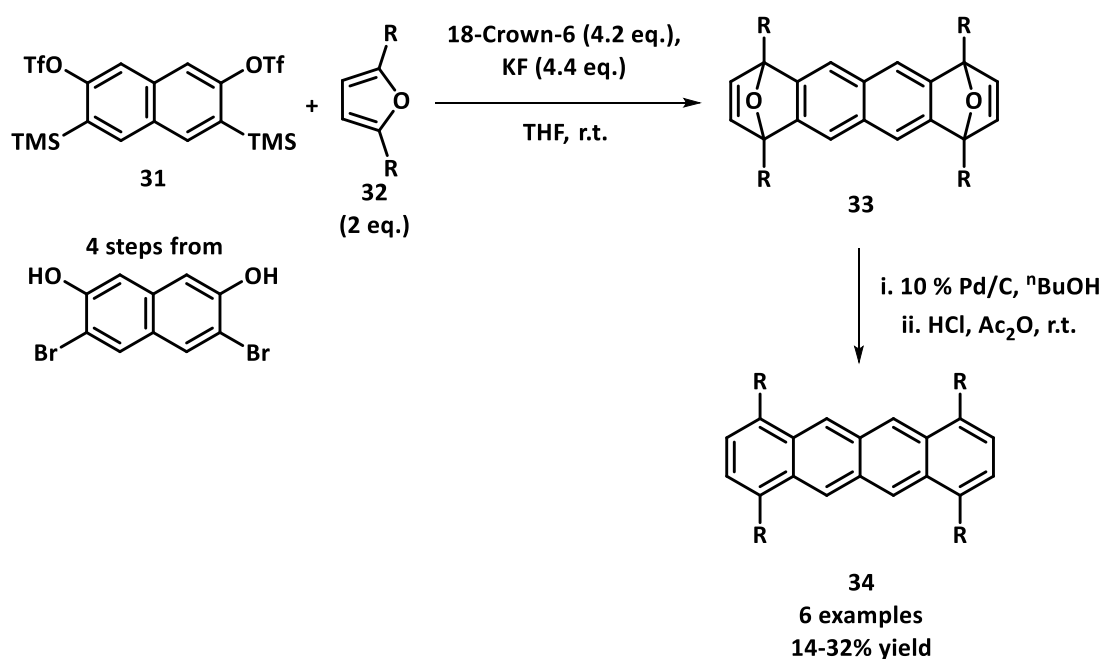


**Scheme 1.6** – Synthesis of a 5,12 – amidotetracene **30** utilising hydrotetracene **27** as an intermediate.

An amide formation (hydroacetone **29**) and oxidation with  $\text{Cu}^{\text{II}}\text{O}$  formed tetracene **30**. While the quinone can therefore be exploited to introduce further structural complexity to the core tetracene structure, these transformations are often multistep and can be low yielding. Furthermore, the oxidation of intermediates such as dihydrotetracene can take as many as 4 days to complete using 10 mol% to stoichiometric loadings of Pd/C, making them cumbersome intermediates.

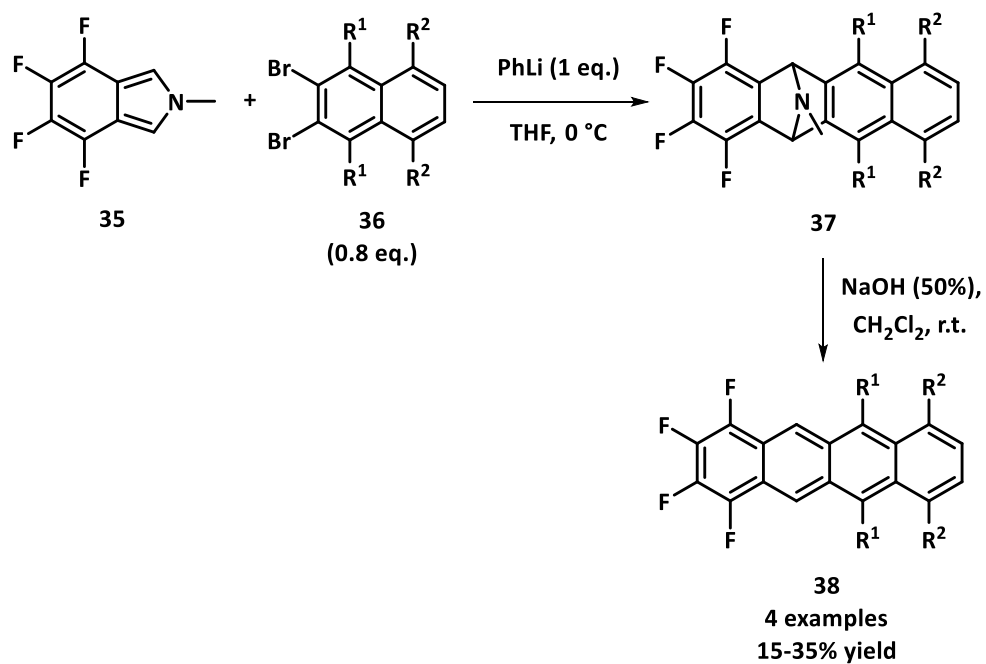
### 1.4.2 Diels-Alder Approaches to Tetracenes

Many literature methods utilise the Diels-Alder reaction with an aryne as the dienophile to homologate aromatic molecules over two steps. Representative approaches are shown in Scheme 1.7. Kitamura *et al.* synthesised a range of alkyl substituted tetracenes **34** from the bis aryne Diels-Alder cyclisation of 3,6,-dibromo-2,7-dihydroxynaphthalene **31** with alkyl substituted furans **32** similar to the method used by Gribble *et al.*,<sup>48</sup> however the method required several protection steps and further transformations to form the desired tetracene with low to moderate yields (Scheme 1.7).<sup>39</sup>



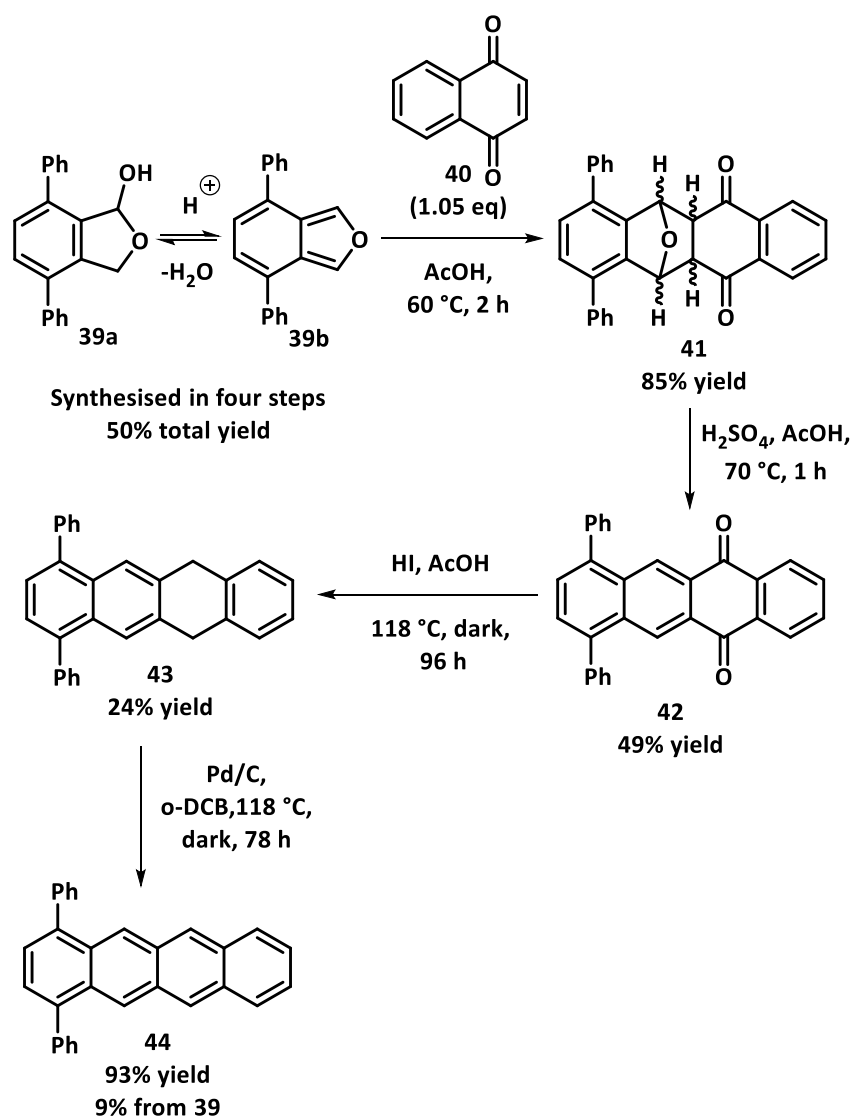
**Scheme 1.7** – Synthesis of tetracenes **34a-f** via Diels-Alder reactions with furans as the diene.

Swager *et al.* used a similar approach to the synthesis of fluorinated tetracenes **38** utilising fluorinated isoindole **35** and naphthalene arynes formed from naphthalenes **36**, but similarly over several steps only poor to modest yields are achieved (Scheme 1.8).<sup>49</sup>



**Scheme 1.8** – Synthesis of tetracenes **38** via Diels-Alder reactions with isoindoles as the diene.

Miller and Rainbolt similarly utilised isobenzofuran **39** to synthesise tetracenes and similar polyaromatic ring systems without utilising aryne intermediates (Scheme 1.9).

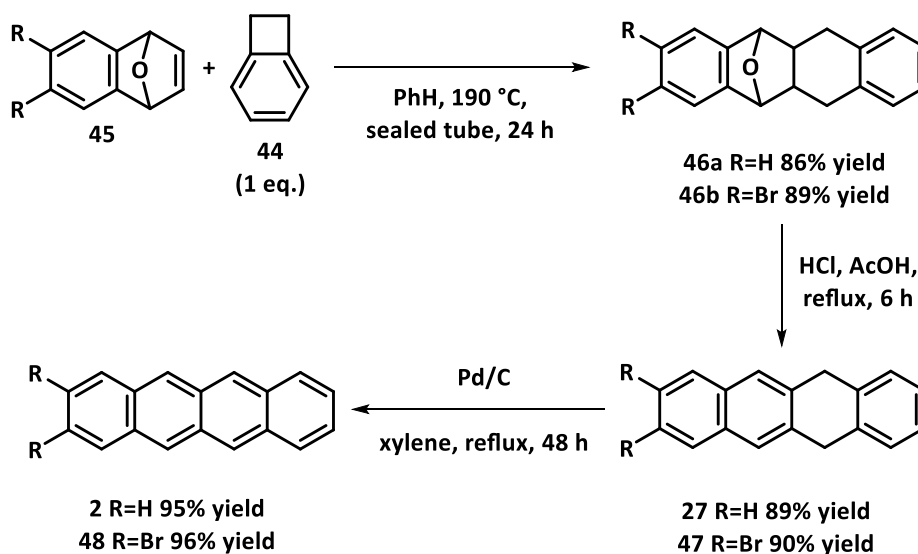


**Scheme 1.9** – Synthesis of tetracenes via Diels-Alder reactions with transiently generated isobenzofuran as the diene.

By treating the hemiacetal **39a** with AcOH, the desired isobenzofuran **39b** could be generated *in situ* and undergo a Diels alder cyclisation with 1,4-naphthoquinone **40** forming cycloadduct **41** in one-pot in good yield (85%).<sup>50</sup> However, two further reductions and a final oxidation are required to yield the final desired tetracene **44** in a low overall yield from the starting hemiacetal. Furthermore, four synthetic steps were required to furnish the requisite hemiacetal for the reaction illustrating the inefficiency of these routes to tetracene.

Reactive dienes can similarly be generated from the thermal retro-electrocyclisations of benzoncyclobutenes in the synthesis of polyaromatic molecules.

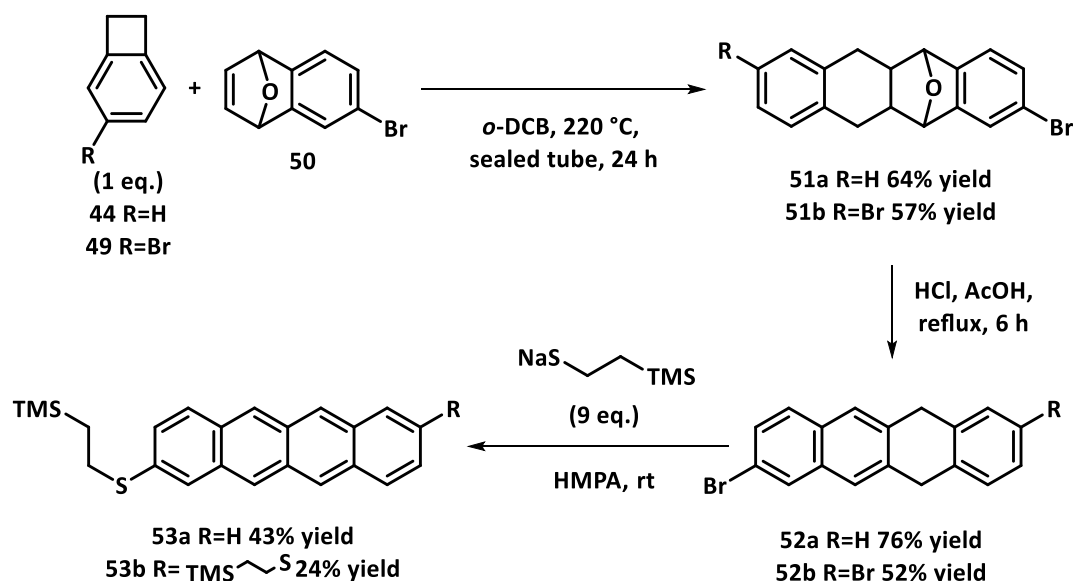
Luo and Hart utilised the cycloaddition of benzocyclobutene **44** and endoxides **45** as the dienophile (Scheme 1.10).<sup>51</sup>



**Scheme 1.10** – Synthesis of tetracenes **2** and **48** via Diels-Alder reactions with generation of diene via cyclobutene ring opening.

After 24 h in a sealed tube, both the unsubstituted and dibrominated cycloadducts **46a-b** were formed in excellent yield. A subsequent reduction of the bridgehead ester and oxidation of the formed dihydro-tetracene **27** and **47** yielded the two tetracenes in excellent yield (72% for **2**, 77% for **48**) in an attractive 4 step sequence. Some downsides are clear however: the oxidation of the dihydro-tetracenes take 2 days to complete and the initial endoxides must be synthesised adding further steps making the synthesis time and step inefficient.

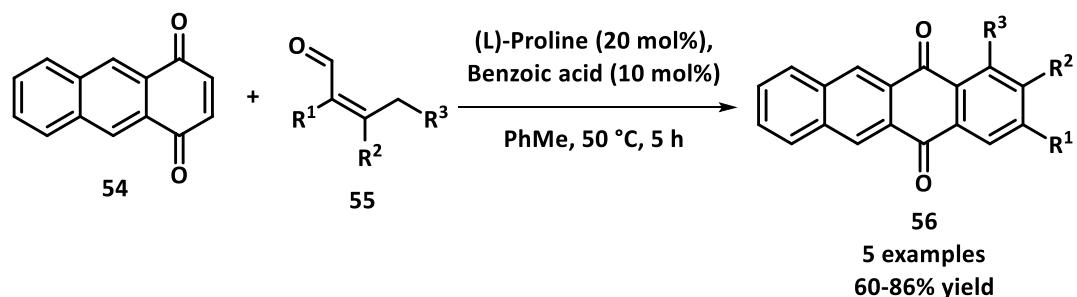
Frisbie utilised a similar synthetic strategy to form thioester substituted tetracenes **53a-b**, albeit with lower yields from the Diels-Alder reaction (Scheme 1.11).<sup>52</sup>



**Scheme 1.11** – Synthesis of thioether substituted tetracenes **53a-b** via Diels-Alder reactions with generation of diene via cyclobutene ring opening.

In addition, the route suffered from the same limitations: the synthesis of the brominated endoxide **50** and benzocyclobutene **44** and **49** are required for the route, and the subsequent reduction and oxidation/nucleophilic aromatic substitution steps are low yielding and erode the yield significantly.

Interestingly, organocatalytic Diels-Alder like cycloadditions have been utilised to form tetracenediones **56**. Lee *et al.* utilised catalytic amounts of L-proline to form azadienes from crotonaldehydes **55** which then went on to react with 1,4-anthracenedione **54** to form tetracene diones **56** (Scheme 1.12).<sup>53</sup>

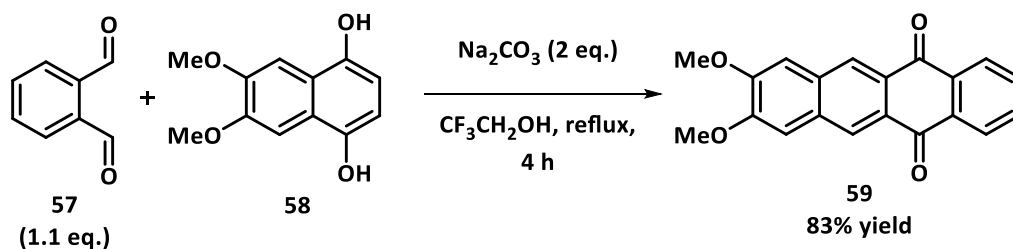


**Scheme 1.12** – Organocatalytic generation of tetracenediones **56**.

While an interesting disconnection, the lack of control over the regioselectivity of the cycloaddition and the need to subsequently reduce the molecule mars the disconnection.

### 1.4.3 Aldol Approaches to Tetracenes

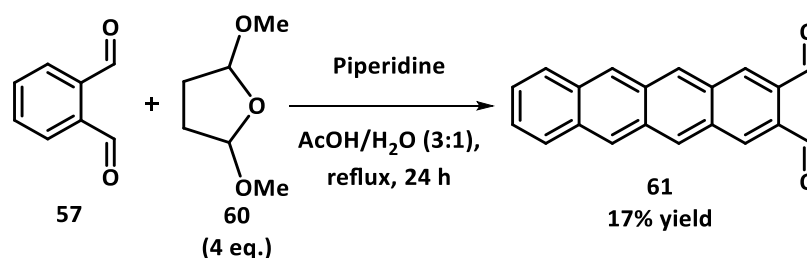
Aldol condensations have also been widely utilised in synthesising tetracenes. Desvergne *et al.* utilised an aldol condensation between phthalaldehyde **57** and 1,4-dihydroxy-6,7-dimethoxynaphthalene **58** in the presence of  $\text{Na}_2\text{CO}_3$  (Scheme 1.13).<sup>54</sup>



Scheme 1.13 – Synthesis of tetracene dione **59** via an aldol condensation.

This transformation had the advantage of being very high yielding in furnishing the desired tetracene dione **59**. However, disadvantages in this approach to the synthesis of tetracenes are clear in that further reductions (in this case a Meerwein-Ponndorf-Verley reduction) are necessary to provide the aromatic rings of tetracene.

The tetracene core has also been generated iteratively *via* the sequential aldol condensation of phthalaldehyde **57** with succinaldehyde **60** by Mallouli and Lepage, with the same methodology used by Nuckolls *et al.* to synthesise terminal quinone substituted polyacenes *via* a terminal aldol condensation of tetracene-2,3-dicarboxaldehyde with 2,3-dimethylhydroquinone (Scheme 1.14).<sup>38, 55</sup>

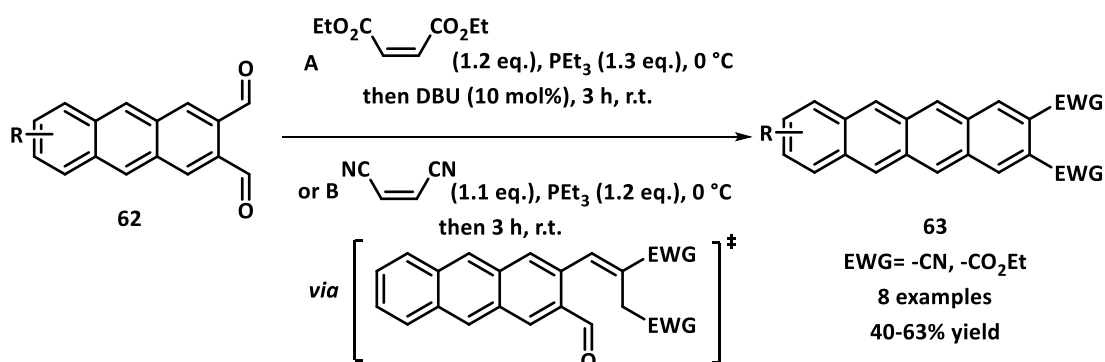


Scheme 1.14 – Synthesis of tetracene **61** via a one-pot sequential aldol condensation.

An attractive quality of the route is that the desired polyacene **61** can be made in one synthetic transformation by altering the stoichiometry of the acetal in relation to **57**. This route carries the advantage of utilising relatively inexpensive and commercially available starting materials with the potential to generate the desired

tetracene-2,3-dicarboxaldehyde in a step efficient manner. However, the condensations in the original iterative synthesis were poor (17-26%), limiting the applicability of the approach.

In a synthesis inspired by this iterative aldol condensation approach to polyacenes, Lin *et al.* synthesised a range of polyaromatics *via* the generation of a phosphine ylide from diethyl maleate and  $\text{PEt}_3$ , which subsequently participated in a Wittig reaction with dialdehydes **62** and a Knoevenagel condensation mediated by catalytic DBU to furnish a homologated polyaromatics **63** in a single step (Scheme 1.15).<sup>56</sup>

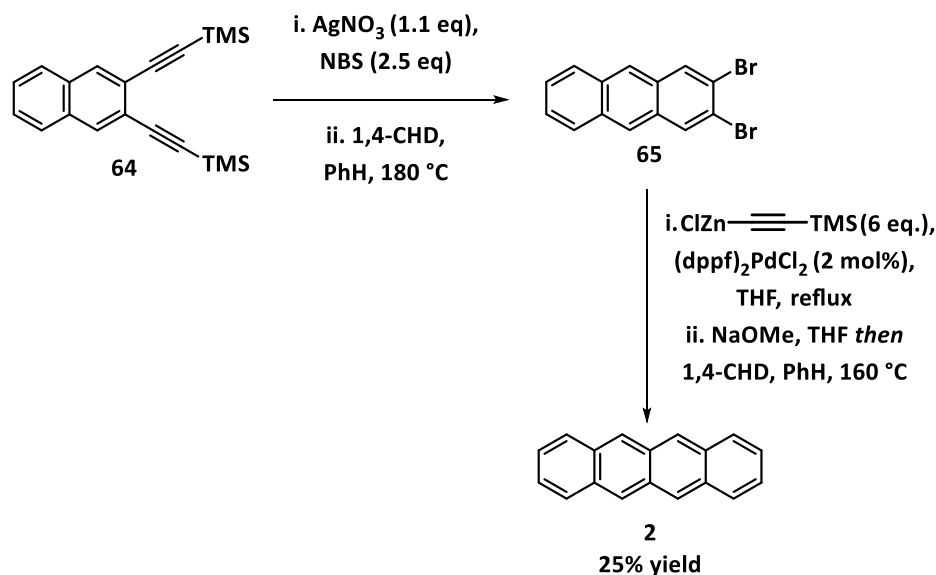


**Scheme 1.15** – Synthesis of tetracenes **63** via a cascade of a Wittig reaction and an aldol condensation.

This approach offers a greater scope of substitution on the synthesised polyaromatics. The reaction was also performed well when fumaryl nitrile is used as the Michael acceptor in the ylide generation with comparable yields as diethyl maleate without catalytic base. Furthermore, a modest scope of aromatic substitution on the parent dialdehyde is tolerated, generating some interesting “push-pull” motifs across the length of the molecule making it a more attractive route for synthesising polyaromatics to investigate for materials. However, there is a clear disadvantage in that the product from each homologation requires the diesters or dinitriles generated be reduced to the aldehyde to perform the next homologation. This introduces a further two synthetic steps: a DIBAL-H reduction and Swern oxidation which makes the route less efficient for the synthesis of higher polyacenes such as tetracene. Furthermore, the yields for tetracenes *via* this route, while generally moderate to good (40-63%) tend to be lower than their respective naphthalenes and anthracenes.

#### 1.4.4 Bergman Approach to Tetracenes

Further methods for the generation of linear aromatic rings can be found by utilising the Bergman cyclisation of ene-diyne (Scheme 1.16).<sup>57</sup> *naphthalene*



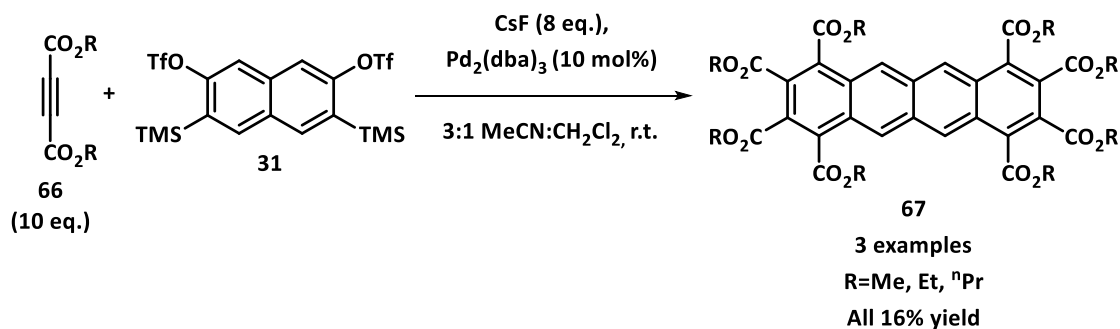
Scheme 1.16 - Iterative Bergman cyclisation of tetracene **2**.

Anthony *et al.* utilised an iterative method *via* the repeated halogenation of TMS acetylene **64**, followed by a radical cyclisation and a Negishi coupling ingeniously yielding the desired tetracene core **2**. This carries the same issues as the iterative *bis*-aldol condensation approaches, the intermediates require multiple time intensive synthetic steps for each benzannulation. This impacts atom efficiency and yield, in this case leading to a modest 25% yield over 8 total steps.

#### 1.4.5. Organometallic and Transition Metal-Catalysed Approaches to Tetracenes

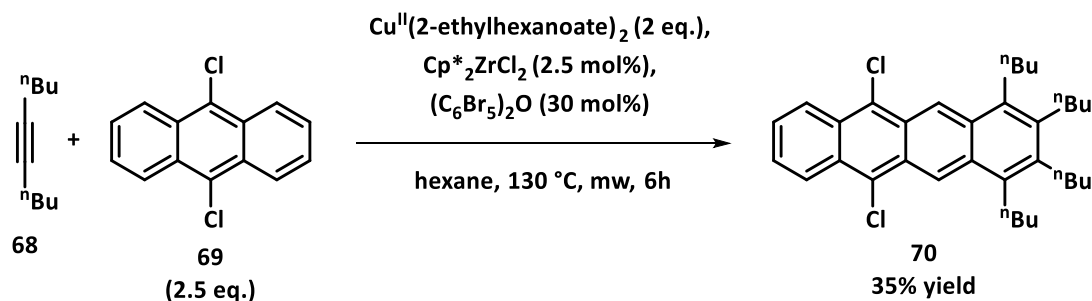
Recent oligoacene syntheses have used transition metal-catalysed [2+2+2] cotrimerisations and [4+2] cycloadditions to generate tetracenes by benzannulating smaller aromatic starting materials.

Kitamura *et al.* synthesised a range of octaalkoxy-substituted tetracenes **67** from the generation of a *bis*-aryne from **31** and subsequent Pd-catalysed [2+2+2] reaction in poor yield (Scheme 1.17).<sup>58</sup>



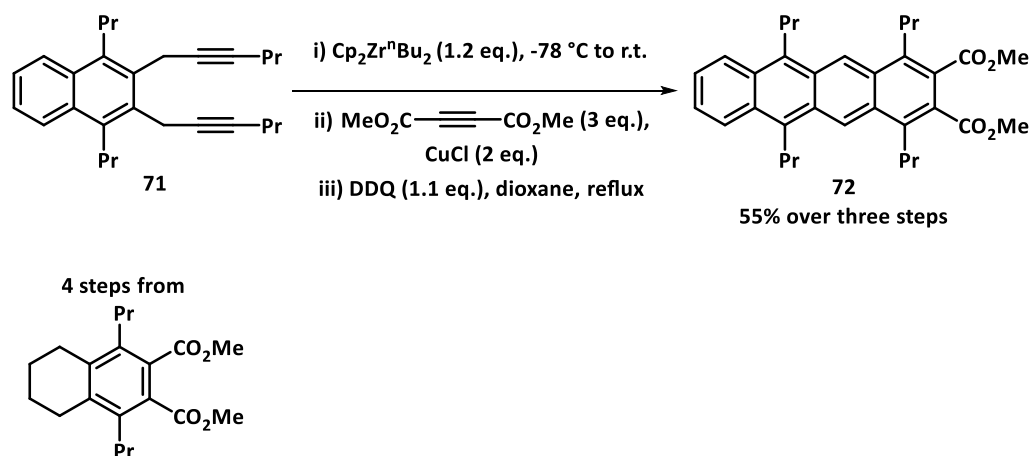
Scheme 1.17 –  $\text{Pd}_2(\text{dba})_3$ -catalysed [2+2+2] synthesis of tetracenes **67** via a transient aryne.

Cramer *et al.* used a similar [2+2+2] homologation to synthesise **70** from the C-H activation of chlorinated anthracene **69**, but again in low yield (Scheme 1.18).<sup>59</sup>



Scheme 1.18 – Zirconocene-catalysed [2+2+2] synthesis of tetracenes **70**.

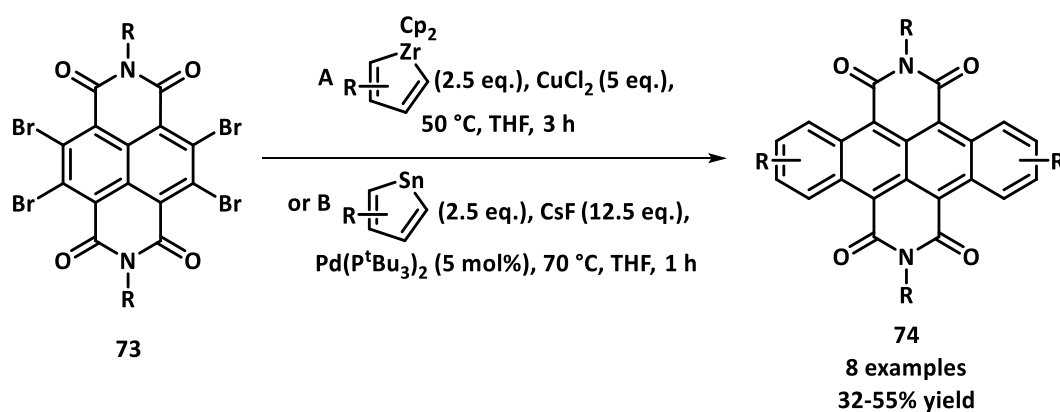
Takahashi *et al.* effected the synthesis of the alkyl substituted tetracene **72** via zirconocyclisation followed by coupling to DMAD and a final oxidation (Scheme 1.19).



Scheme 1.19 – A further zirconocene metal-catalysed [2+2+2] synthesis of tetracene **72**.

While this provided a route to alkylated polyacenes, it is still multistep and required the use of a stoichiometric bis(pentamethylcyclopentadienyl) zirconium reagent, as well as the multi-step synthesis of the starting diyne.<sup>60</sup>

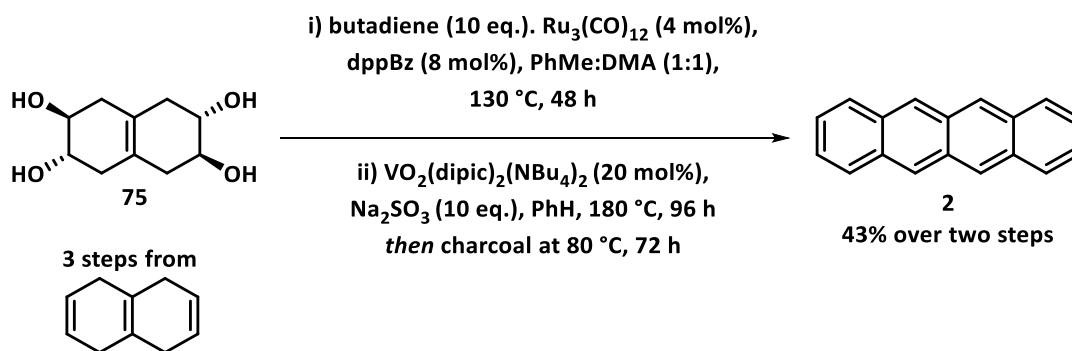
Wang *et al.* similarly synthesised 5,6,11,12-tetracene diimides **74** via a double cross-coupling reaction of 2,3,6,7-tetrabromo-1,4,5,8-naphthalene tetracarboxylic diimides **73** with a range of similar preformed zirconocyclopentadienes in poor to moderate yields (35-55%) (Scheme 1.20).



**Scheme 1.20** – Synthesis of a range of 5,6,11,12- tetracene diimides **74**.

A similar benzannulation could be effected with a double Stille-like coupling with stannylcyclopentadienes in moderate yield (32% and 42%).<sup>61</sup> While an interesting disconnection, the required tetrabromonaphthalene diimides must be synthesised, stoichiometric zirconocyclopentadienes and toxic stannanes required along with the moderate yield highlights the limitation of the approach.

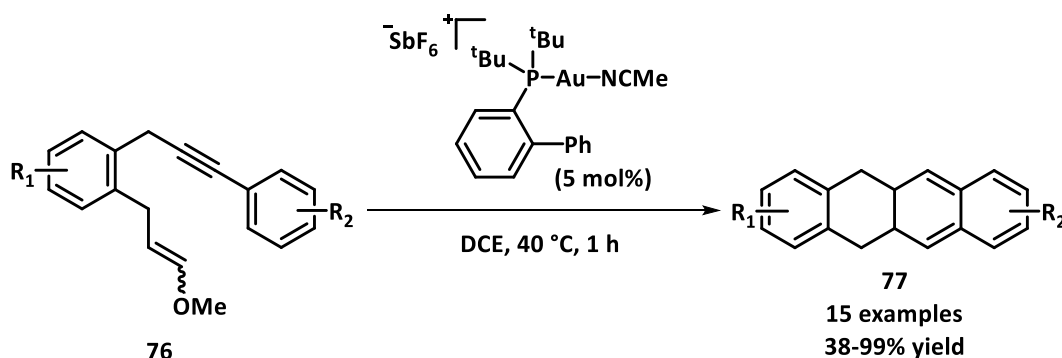
Krische *et al.* utilised a two-step procedure via a formal [4+2] cycloaddition catalysed by triruthenium dodecarbonyl followed by a vanadium catalysed dehydrogenation to give tetracene **2** from **75** (Scheme 1.21).<sup>62</sup>



Scheme 1.21 – Synthesis of tetracene **2** via a ruthenium catalysed formal [4+2] reaction.

While this may yield tetracene, the yield is modest, and the complicated, long and harsh reaction conditions would potentially render it an unsuitable method for the synthesis of substituted tetracenes.

Echavarren *et al.* provided an interesting route to hydro-tetracenes **27** and **77** and longer hydroacene derivatives *via* a  $\text{Au}^I$ -catalysed cyclisation of aryl tethered 1,7-eneynes **76** to furnish hydro tetracenes in moderate to excellent yields (Scheme 1.22).<sup>63</sup>

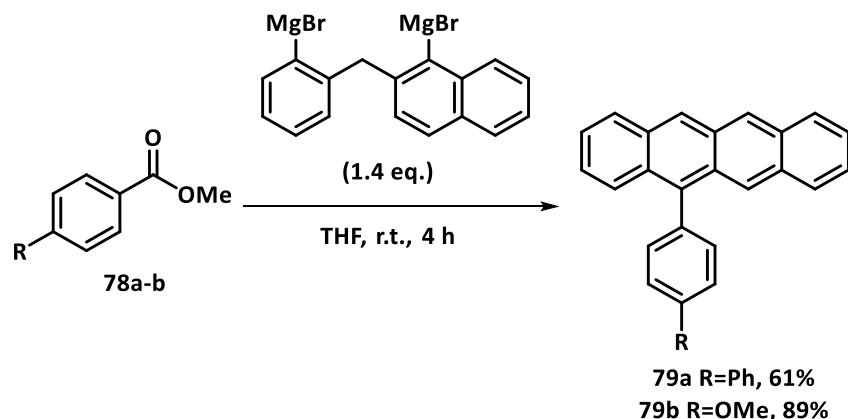


Scheme 1.22 – Synthesis of hydroacenes **27** and **77** via a gold catalysed cyclisation.

Furthermore, the Sonagashira coupling of various aryl iodides provides access various end substituted hydroacenes, creating substitution patterns hard to access due to the inherent reactivity of tetracene. However, it must be stated that the products require further oxidation of the hydroacenes as shown in previous examples, and the starting aryl enynes can only be accessed *via* multiple steps from aryl halides.

The unifying limitation of these metal-catalysed approaches to the tetracene core is that they rely on transition metal catalysis, which increase the cost of each

transformation. A novel method for the synthesis of benzene rings and higher acenes is the [5+1] benzannulation developed by Sparr *et al.* (Scheme 1.23).<sup>64</sup>

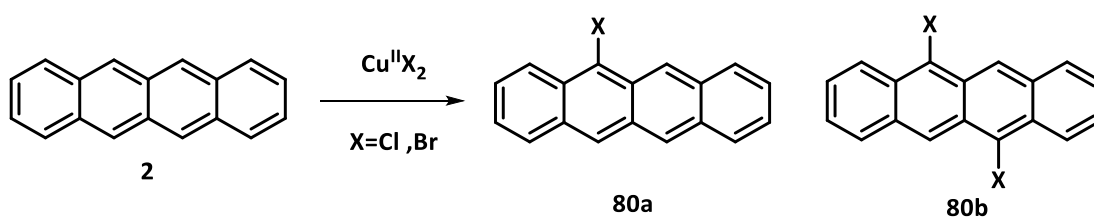


**Scheme 1.23** – Synthesis of tetracenes **79a** & **b** via a [5+1] Grignard benzannulation.

This takes advantage of the double Grignard addition to aromatic methoxy esters **78a-b** and 1,4 elimination of the magnesium alkoxide to form the aromatic ring of tetracenes **79a-b**. This method allows the synthesis of substituted benzenes, but more interestingly anthracenes, tetracenes and pentacenes in good to excellent yields. While this is an excellent disconnection which exploits the over-addition of Grignard reagents to esters, the formation of the Grignard reagents themselves are time consuming and multiple synthetic steps were required.

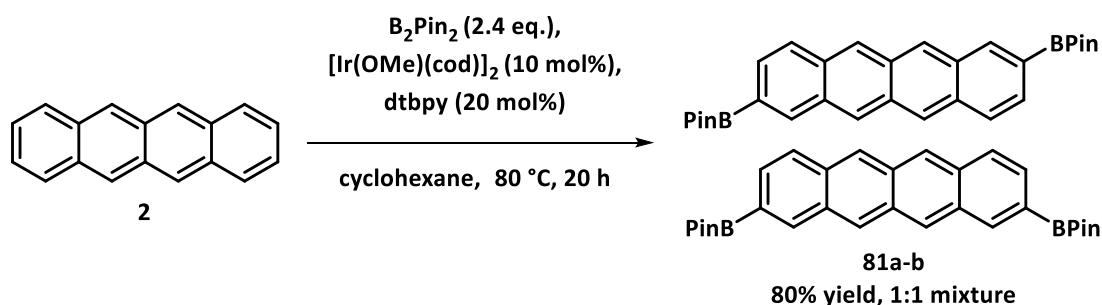
#### 1.4.6. Late-stage Modification of Tetracene

An argument could therefore be made that modification of the tetracene could be attempted *via* nucleophilic aromatic substitutions to furnish substituted tetracenes in a single step, instead of a multi-step synthetic route. Halogenations of tetracene have been performed using cupric halide sources to yield mono- and di-chlorinated and brominated tetracenes (Scheme 1.24).<sup>36</sup>



**Scheme 1.24** – Generalised substitution patterns in the halogenation of tetracene.

The introduction of halides provides a reactive handle on tetracene for further diverse elaboration *via* cross-couplings. However, there is the distinct disadvantage that substitution occurs solely on the central rings limiting substitution, owing to the largest LUMO orbitals being present on these rings. Limited examples of substitutions to the outermost rings exist, but they are marred by issues of selectivity. Kobayashi *et al.* found that tetracene **2** could be doubly borylated *via* iridium catalysis in high yield, but unfortunately in a 1:1 mixture of the 2,8- and 2,9- regioisomers **81a-b** (Scheme 1.25).<sup>65</sup>



**Scheme 1.25** – Synthesis of borylated tetracenes **81a-b** utilising iridium catalysis.

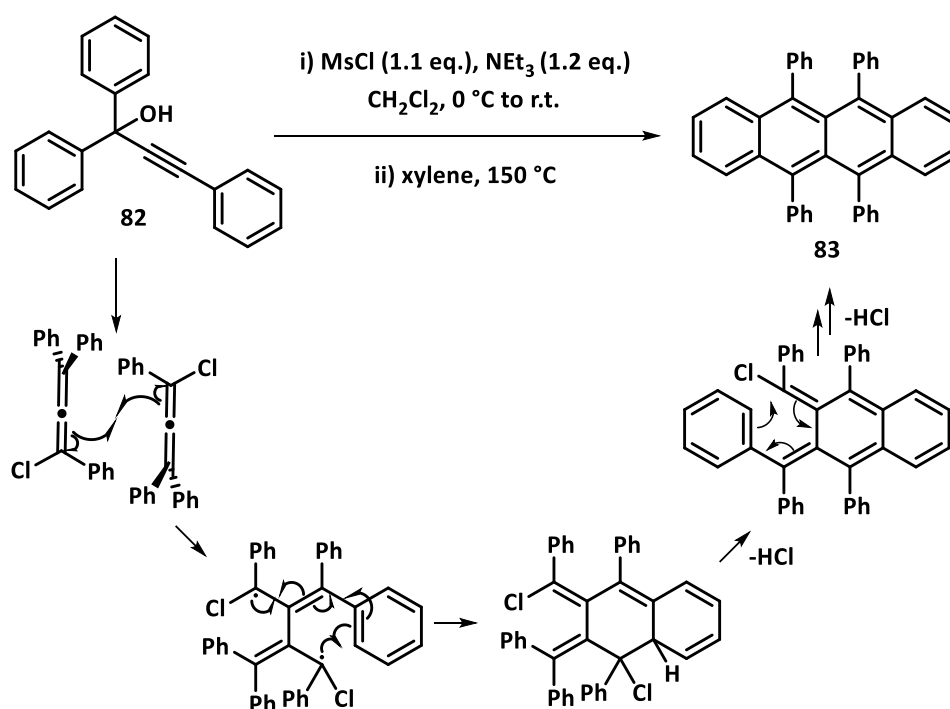
While this allowed access to multiple substituted tetracenes *via* Suzuki couplings, the lack of selectivity and the reliance on high loadings of iridium make this route less attractive.

One consistent feature of these methods is that the starting materials are generally not commercially available but must be prepared over several steps, all of which carry further steps to furnish the desired tetracene core. More specifically, the methods often yield intermediates which require time consuming and harsh reductions or oxidations to form the aromatic ring. This frequently leads to low overall yields, making current syntheses of tetracenes time consuming and inefficient. Furthermore, the use of expensive transition metal catalysts increases the cost of the synthesis and therefore limiting the wide application of any materials synthesised in general device applications. Therefore, short, operationally simple and substrate tolerant synthetic route would be a great boon to tetracene synthesis.

### 1.4.7. Sigmatropic routes to tetracenes

Novel approaches to the core fused ring structure of polyacenes have been designed to exploit pericyclic reactions in cascade reactions to achieve synthetic expediency. By designing the synthesis to incorporate multiple rearrangements in a single reactive step, the step and atom efficiency of the synthesis of tetracenes and other such polyaromatics can be drastically improved. Furthermore, the use of pericyclic reactions carries the added benefit of not requiring extensive modification of commercially available aromatic precursors, instead synthesising the aromatic rings in a single sigmatropic rearrangement and elimination in one synthetic step.

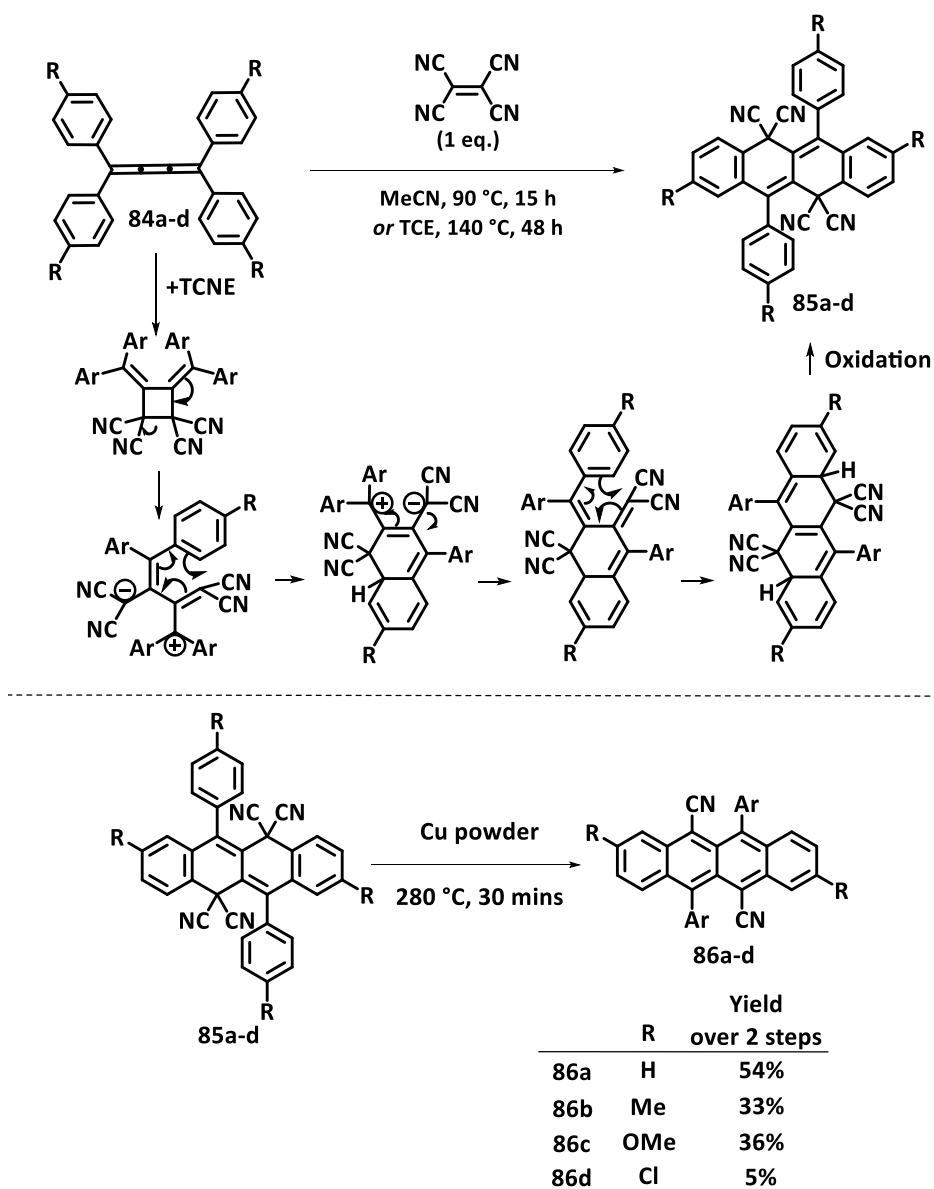
A simple and well-studied example would be the synthesis of rubrene **83** and substituted rubrene-like polyacenes *via* the dimerisation of allenes derived from propargylic alcohol **82**. The allenes can then be formed *via* mesylation and  $S_N2'$  with an adventitious chloride anion to the desired chloroallene<sup>66, 67</sup> or *via* a thermal rearrangement.<sup>68</sup> The mechanism is proposed to proceed *via* a radical dimerisation of the chloroallene and multiple rearrangements to yield rubrene **83** after the elimination of HCl (Scheme 1.26).



Scheme 1.26 - Proposed mechanism for the synthesis of rubrene **83** from propargylic alcohols **82**.

These reactions carry the distinct advantage of multiple bonds of the tetracene core being formed in a single synthetic step without the requirement of further reactions, achieving remarkable synthetic concision. Furthermore, the starting propargylic alcohols can be simply prepared *via* addition of lithium or magnesium acetylides to aromatic ketones or high yielding Sonagashira reactions, simplifying the synthesis of substituted tetracenes.

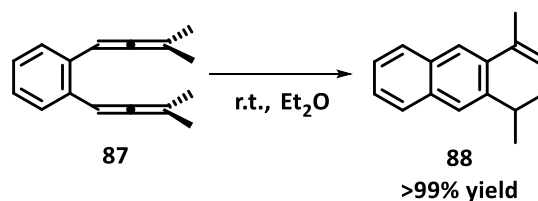
Diedrich *et al.* developed a two-step synthesis of a small library of 5,11-dicyano-6,12-diaryltetracenes **85a-d** utilising an interesting cascade reminiscent of the rubrenic synthesis above in the first step of the synthesis.<sup>69</sup> The reaction begins with the [2+2] addition of TCNE to a 3-cumulene **84a-d**, then a cyclobutane ring-opening to furnish the zwitterionic intermediate, which can then undergo two sequential electrocyclic rearrangements and oxidation to furnish the intermediate 5,5,11,11-tetracyano-5,11-dihydratetracenes **85a-d** (Scheme 1.27).



**Scheme 1.27** – Proposed mechanism and yields for the synthesis of 5,11-cyanotetracenes **86a-d**.

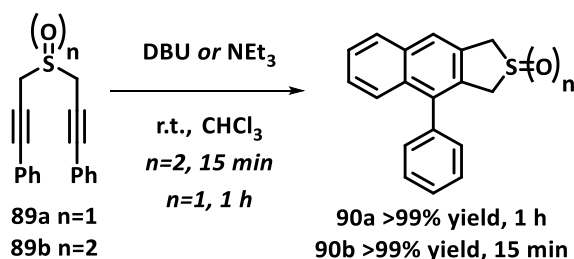
Subsequent elimination of two molecules of cyanide then provides the tetracene molecules **86a-d**. While this is certainly an interesting and rapid means of producing the tetracene core, there are noteworthy limitations to the method. The scope of the reaction is limited only to electron releasing substituents in the para position and the effect of the substitution seems to rapidly erode the yield considerably. It must also be mentioned that, while the cumulenes could be synthesised in high yields, they required a total of 4 synthetic steps to furnish the examples used in the study.

As can be seen from the previous examples, the design of reactions to form multiple bonds *via* cascades of sigmatropic rearrangements can form polyaromatic cores with remarkable concision, but often in poor yield. A frequently employed synthetic strategy for the synthesis of linearly fused aromatic architectures utilises the initiation of cascade reactions from the formation of allenes *ortho* to unsaturated aromatic alkynes which then undergo further radical or sigmatropic rearrangements to form aromatic rings. Braverman *et al.* demonstrated that alkyl substituted *ortho* *bis*-allene **87** underwent thermal electrocycloisatation and subsequent [1,5]-hydride shift to form vinyl naphthalene **88** in quantitative yield in diethyl ether at room temperature (Scheme 1.28).<sup>70</sup>



**Scheme 1.28** – Synthesis of naphthylene **88** via a  $6\pi$ -electrocyclisation tethered allene **87**.

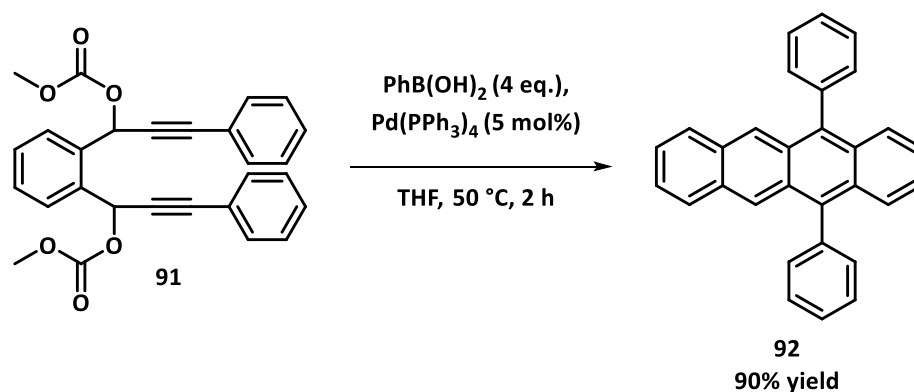
Furthermore, it was demonstrated by the same authors that extended aromatic architectures could be synthesised *via* the base mediated rearrangement of *bis*-propargylic sulfoxides and sulfones **89a-b** in quantitative yield (Scheme 1.29).<sup>71</sup> This was proposed to be *via* an intramolecular Diels-Alder cycloaddition of the *bis*-allene formed by the deprotonation  $\alpha$  to the sulfoxide or sulfone bridge in **89a-b**.



**Scheme 1.29** – Synthesis of a naphthylenes **89a-b** via an intramolecular Diels-Alder cycloaddition of allenes generated by deprotonation of alkynes **90a-b**.

It can be seen from these examples that this *bis*-allenic rearrangement strategy to furnish the core structure of tetracene can be utilised to generate substituted tetracenes in a small number of steps. A recently developed methodology developed based on this disconnection was utilised by Liu *et al.* to synthesise

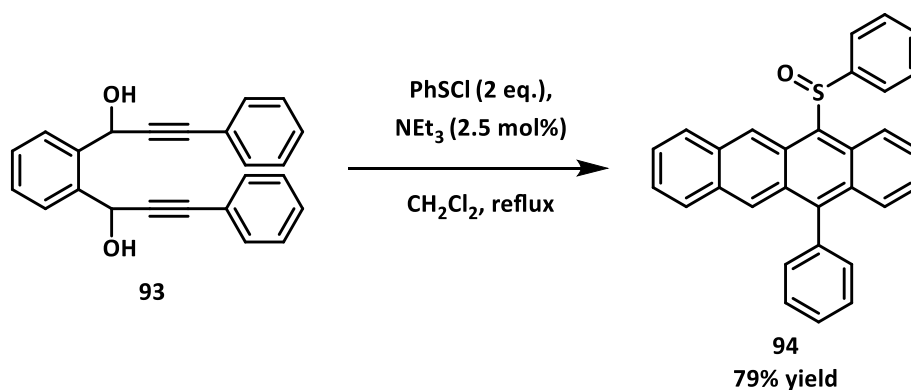
tetracenes and pentacenes from Pd<sup>0</sup>-catalysed rearrangement of propargyl carbonates such as **91** (Scheme 1.30).<sup>72</sup>



**Scheme 1.30** – Example of a tetracene **92** synthesised in one-pot via a Pd catalysed sigmatropic cascade.

This initiated two subsequent 6 $\pi$ -electrocyclic rearrangements terminating in a Suzuki coupling with boronic acids to synthesise a range of phenyl tetracenes. This method has the benefit of generation of the two of the central aromatic rings of tetracene in a single step. While this method is certainly attractive in yield (many tetracenes and pentacenes were synthesised between 45-98% yield), and step efficiency, the use of four equivalents of boronic acid and Pd catalysis reduces the atom efficiency of the method.

Kitagaki *et al.* found that the *bis*-sulfinyl allenes generated from [2,3]-rearrangements of sulfinyl esters derived from diols such as **93** gave the desired diene for further electrocyclic rearrangements.<sup>73</sup> This approach was utilised by Lin in order to form phenyl *bis*-allenes and two further 6 $\pi$ -electrocyclisations yielding a wide array of sulfoxide and sulfone substituted tetracenes, such as **94** (Scheme 1.31).<sup>74</sup>



**Scheme 1.31** – Examples of a tetracene **94** synthesised in one-pot via a sigmatropic cascade initiated by the rearrangement of propargyl sulfenyl esters derived from diol **93**.

This approach has the dual advantages of being tolerant to a wide array of substitution on the phenyl rings leading to increased structural variance in the resultant tetracene molecule.

### 1.5 Aims

In summary, it should be clear that while there are diverse routes for the synthesis of tetracenes, there are few concise and general methods for controlled synthesis of substituted polyacenes. Therefore, the aims of this project were to devise step and atom efficient methods to synthesise a range of substituted tetracenes and analyse their crystal structures, conductive and thermoelectric properties. This has been undertaken to a) improve step and cost efficiency in comparison to existing methods for creating polyacenes and b) to attain a better understanding of the structural features which will improve the behaviour of the molecules as semiconductors and as thermoelectric materials through further testing.

# Chapter Two

## *Propargyl Xanthate Cascade Approach to 5-Phenyl Tetracenes*

### Publications from this section

1. Anionic Sigmatropic-Electrocyclic-Chugaev Cascades: Accessing 12-aryl-5-(methylthio (carbonyl)thio)tetracenes and a Related Anthra[2,3-b]thiophene, L. Burroughs, J. Ritchie, M. Ngwenya, D. Khan, W. Lewis, S. Woodward, *Beilstein J. Org. Chem.* **2015**, *11*, 273-279
2. Understanding Anionic Chugaev Elimination in Pericyclic Tetracene Formation, L. Burroughs, J. Ritchie, S. Woodward, *Tetrahedron.* **2016**, *72*, 1686-1689.

### Acknowledgements

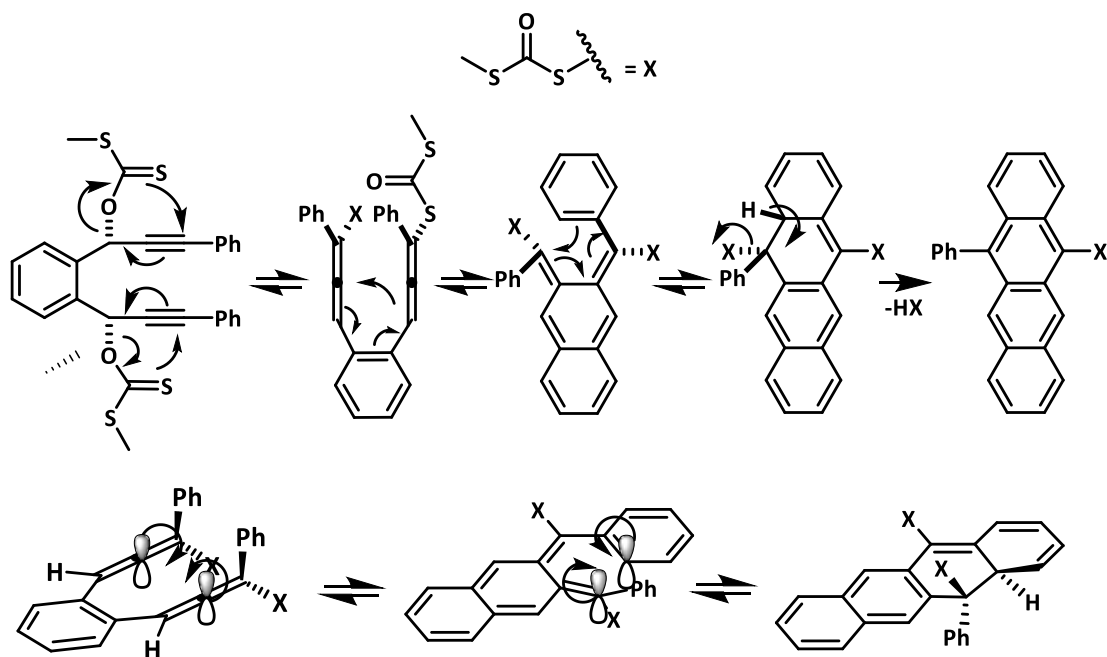
- Compounds **101** and **102** in Scheme 2.12 were synthesised and characterised by Mkethwa Ngwenya.
- Compound **103** in Scheme 2.12 was characterised by Dr Laurence Burroughs. Dr Burroughs also assisted in the computational studies of the mechanism of the reaction.

## 2.1. Results and discussion

### 2.1.1. Optimisation and Scope of the Sigmatropic Rearrangement Cascade

#### Cascade

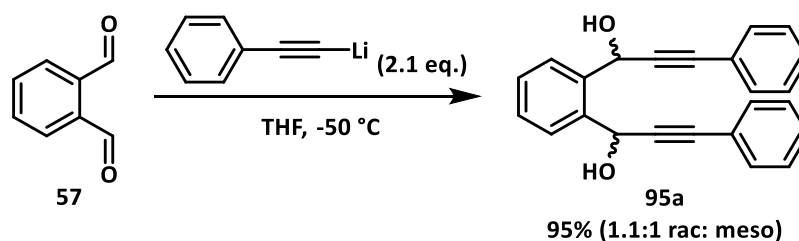
As stated in the previous chapter, various methods for the sigmatropic cascade synthesis terminated by a final irreversible reaction (such as sulfoxide elimination or C-C bond formation) of tetracenes exist within the literature, however the use of harsh reagents and conditions (such as PhSCl) or Pd catalysis and large excesses of boronic acids leaves room for improvement. Building upon these methods, a cascade to *bis*-allenes initiated *via* the [3,3]-sigmatropic rearrangement of propargyl xanthates was proposed (Scheme 2.1).



Scheme 2.1 – Proposed [3,3]-sigmatropic cascade reaction

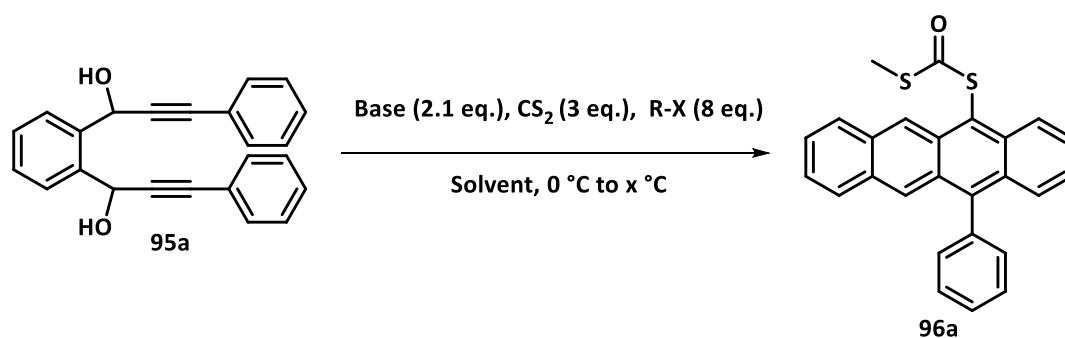
The thermal rearrangement of  $\alpha$ -propargyl methyl xanthate esters to the corresponding allenes is a known transformation.<sup>75</sup> Furthermore, the required propargyl xanthate esters can be prepared simply in one pot with the addition of base, CS<sub>2</sub> and a suitable alkylating agent.

An initial model synthesis began with the formation of *bis*-propargyl diol **95a** from the addition of lithium phenyl acetylide to phthalaldehyde **57**, furnishing the diol in 95% yield as a 1:1 ratio of diastereomers (Scheme 2.2).



**Scheme 2.2** – Synthesis of *bis*-propargyl diol **95a**

Diol **95a** was then deprotonated by LiHMDS at 0 °C, then reacted with CS<sub>2</sub> and MeI and immediately heated at variable temperatures in various solvents to yield the 5-phenyl tetracene **96a** (Scheme 2.3).



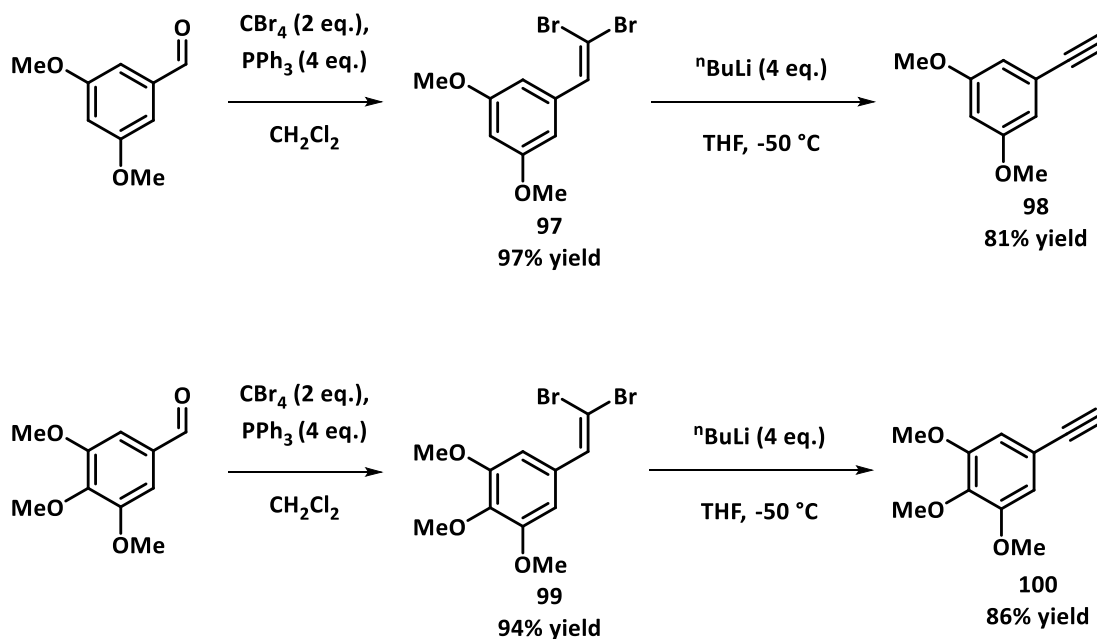
Temperature	Base	R-X	Solvent	Yield (%)
40 °C	LiHMDS	Mel	DME	41
60 °C	LiHMDS	Mel	DME	25
80 °C	LiHMDS	Mel	DME	32
40 °C	LiHMDS	Mel	THF	49
60 °C	LiHMDS	Mel	THF	60
60 °C	NaH	Mel	THF	43
60 °C	NaHMDS	Mel	THF	0
60 °C	KHMDS	Mel	THF	50
60 °C	LiHMDS	EtBr	THF	Trace <sup>a</sup>
60 °C	LiHMDS	BnBr	THF	Trace <sup>a</sup>

<sup>a</sup> Observed in the <sup>1</sup>H NMR spectrum of the crude reaction mixture

**Scheme 2.1** – Optimisation of synthesis of tetracene **96a**

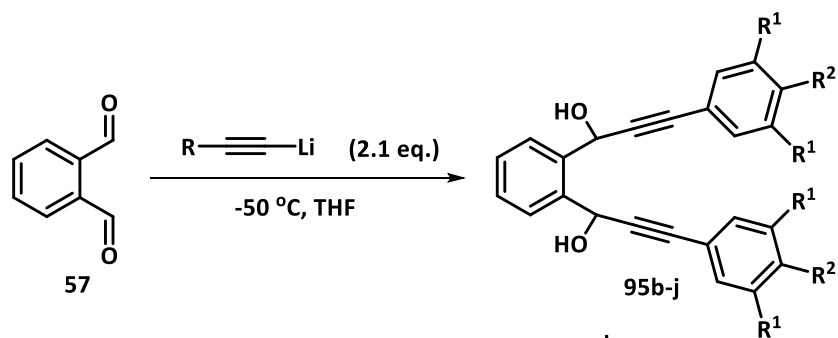
The highest yield of **96a** was found in THF at 60 °C, and as these conditions were kept constant across further reactions. Further optimisation was undertaken on the base used in the reaction, of which LiHMDS provided the highest yield of the desired tetracene over other alkali metal bases, with NaHMDS intriguingly not promoting the reaction at all. Other alkylating agents were also trialled, however, both benzyl bromide and bromoethane only returned traces of tetracene and this can most likely be attributed to the C-Br bonds in benzyl bromide and bromoethane being stronger than the C-I bond in MeI<sup>76</sup> and the increase in the steric bulk around the  $\sigma^*$  orbital preventing the S<sub>N</sub>2 reaction.

After the optimisation of the general method, several variously substituted diols were synthesised from the addition of a range of aromatic ring substituted alkynes to determine whether the method could be widely applicable to generate substituted tetracenes. The alkynes were predominantly commercially available or synthesised in high yield from a two-step Corey-Fuchs homologation (Scheme 2.4).<sup>77</sup>

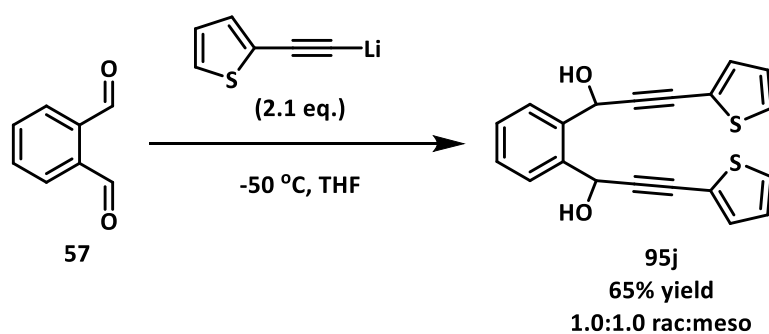


Scheme 2.4 – Synthesis of alkynes **98** and **100**

A family of propargyl diols **96b-j** was then synthesised from the addition of the corresponding lithium acetylide to phthalaldehyde **57** in moderate to excellent yield and in an array of diastereomeric ratios (Scheme 2.5).

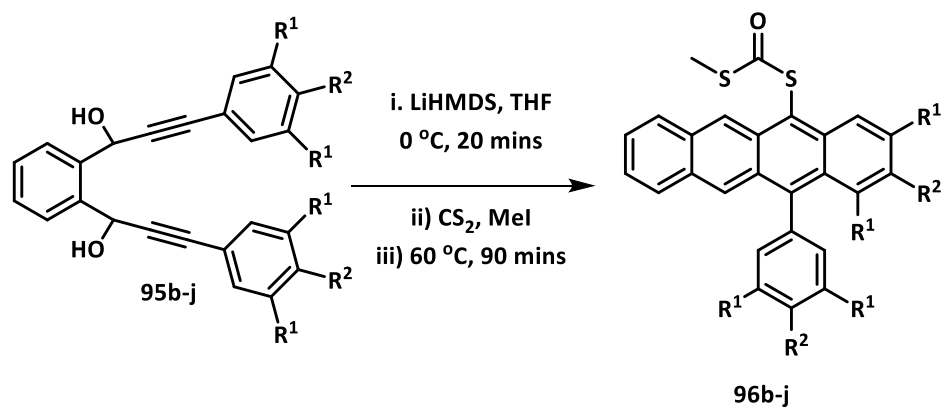


Compound	R <sup>1</sup>	R <sup>2</sup>	Yield (%)	d.r. ( <i>rac:meso</i> )
95b	OMe	OMe	74	1.9:1.0
95c	CF <sub>3</sub>	H	60	2.0:1.0
95d	OMe	H	70	1.8:1.0
95e	F	H	79	1.6:1.0
95f	H	CF <sub>3</sub>	86	1.0:1.2
95g	H	OMe	91	1.3:1.0
95h	H	<sup>t</sup> Bu	66	1.0:1.6
95i	H	Me	57	1.0:1.9

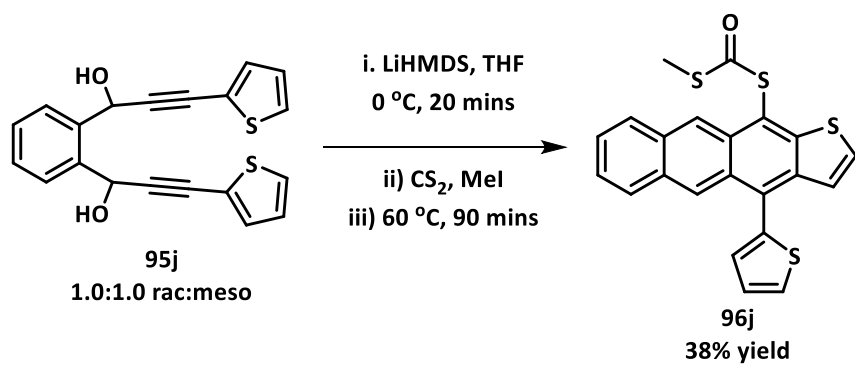


Scheme 2.5 – Synthesis of diols **95b-j**

The produced propargylic diols were then reacted in the established conditions to form the tetracenes **96b-i** and anthrothiophene **96j** in poor to quantitative yields (Scheme 2.6).



Diol	d.r. ( <i>rac:meso</i> )	R <sup>1</sup>	R <sup>2</sup>	Tetracene	Yield (%)
95b	1.9:1.0	OMe	OMe	96b	47
95c	2.0:1.0	CF <sub>3</sub>	H	96c	56
95d	1.8:1.0	OMe	H	96d	>99
95e	1.6:1.0	F	H	96e	29
95f	1.0:1.2	H	CF <sub>3</sub>	96f	44
95g	1.3:1.0	H	OMe	96g	38
95h	1.0:1.6	H	<sup>t</sup> Bu	96h	22
95i	1.0:1.9	H	Me	96i	32

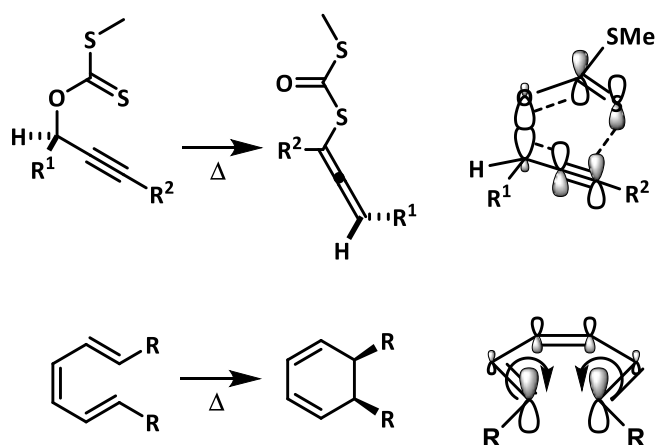


**Scheme 2.6** – Synthesis of tetracenes **96b-i** and anthrathiophene **96j**.

### 2.1.2. Mechanistic Investigation of the rearrangement cascade

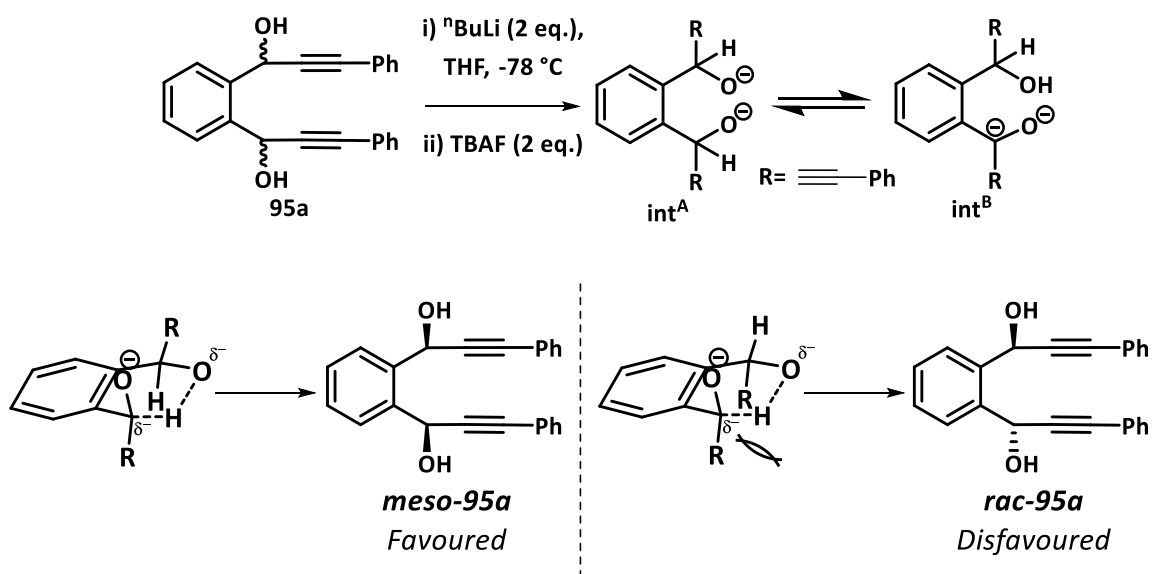
In an attempt to rationalise the yields of compounds **96a-j**, two factors were investigated: the effect of the diastereomeric ratio of the starting diol on yield and the substitution patterns of the aryl rings.

As is stipulated by the Woodward-Hofmann rules, the [3,3]-sigmatropic rearrangement must be suprafacial and the thermally allowed  $6\pi$ -electrocyclisations must be disrotatory, with the retention of stereochemistry (Scheme 2.5).<sup>48, 78</sup>



**Scheme 2.7** – An orbital treatment of a [3,3]-sigmatropic rearrangement and a  $6\pi$ -electrocyclisation.

Therefore, the initial stereochemistry of the diols is retained across all steps of the cascade, and therefore, different diastereomers provide different geometries for the final elimination. In the original mechanistic proposal, it was predicted that the *meso* would give a higher yield of tetracene as the abstracted proton and dithiocarbonate group would be antiperiplanar with respect to one another allowing an E2 elimination (as shown in Scheme 2.1), and so enriching mixtures of the *meso* was hypothesised to improve the yield. To enrich the *meso* enantiomer in the mixtures isolated, **95a** was deprotonated with 2 equivalents of <sup>n</sup>BuLi and addition of 2 equivalents of TBAF was found to enrich the *meso* diastereomer of **95a**, enriching the *rac*: *meso* ratio to 1:5 (Scheme 2.8).



**Scheme 2.8** – Enrichment of *meso* diastereomer, results obtained by Dr Laurence Burroughs.

This can be hypothesised to arise from the deprotonation of the propargylic alcoholic groups and the sequestration of lithium cations with TBAF forming the dialkoxide (**int<sup>A</sup>**). One alkoxide can subsequently deprotonate the alpha proton of the second alcohol, forming the benzylic anion (**int<sup>B</sup>**). These two anions exist in equilibrium, with the proton shifting between the oxygen and carbon atom. It is postulated that the *meso* diastereomer was formed preferentially due to the lessened steric interaction of the pendant alkyne groups in the transition state posited in Scheme 2.8.

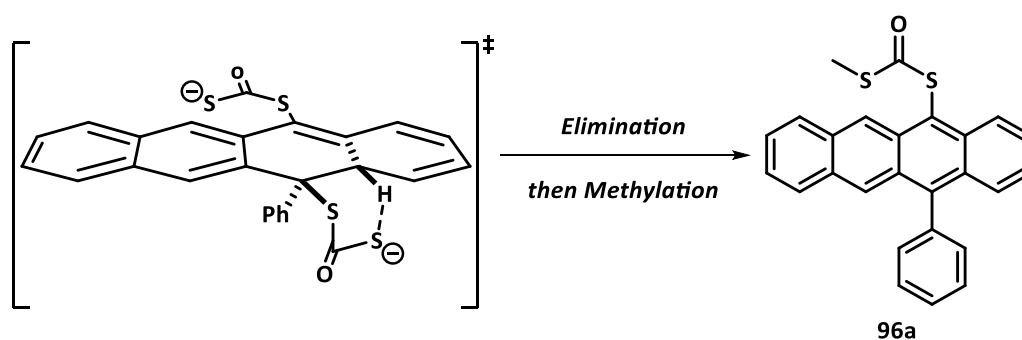
However, diol mixtures containing more of the *meso* diastereomer were found to give lower yields of the desired tetracenes under the optimised reaction conditions (Table 2.1).<sup>79</sup>

Diol	d.r. ( <i>rac</i> : <i>meso</i> )	Tetracene yield (%)	Diol	d.r. ( <i>rac</i> : <i>meso</i> )	Tetracene yield (%)
 <b>95a</b>	1.6:1.0	85	 <b>95c</b>	4.8:1.0	56
	1.1:1.0	60		1.0:4.8	26
	1.0:2.0	38			

**Table 2.1** – Effect of diastereomeric ratio of **95a** and **95c** upon yield of tetracene **96a** and **96c**.

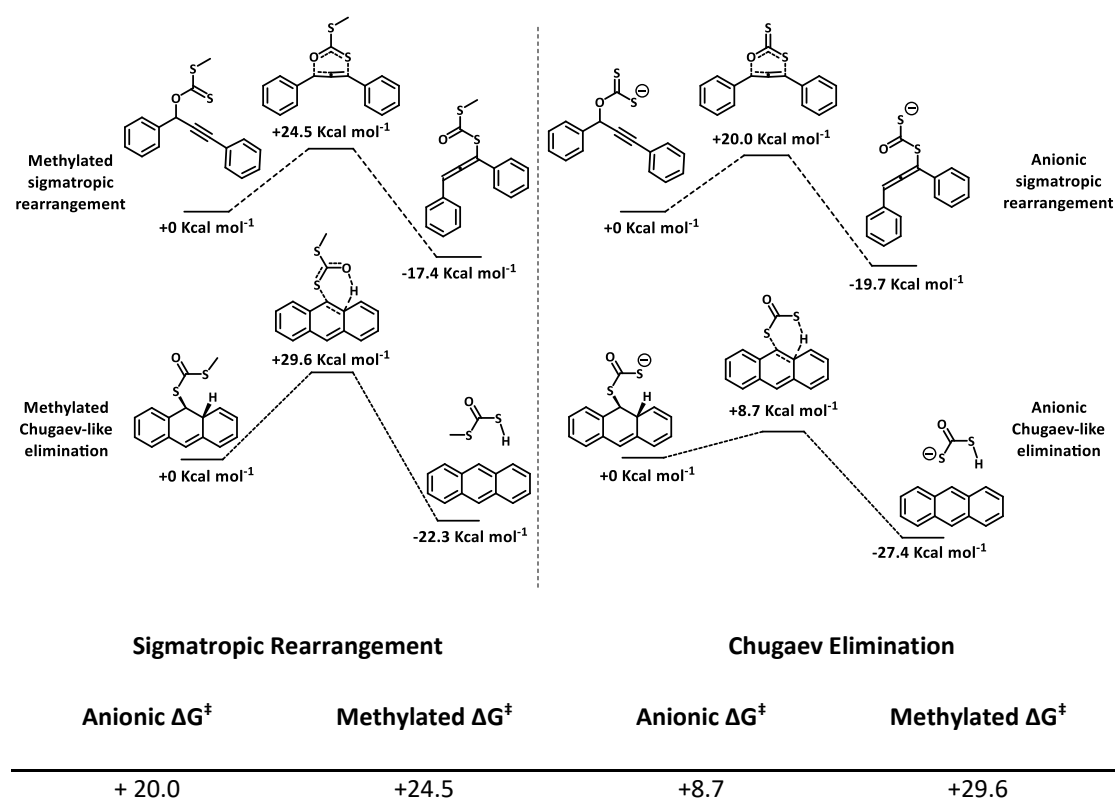
Separation by flash column chromatography was found to enrich earlier isolated fractions of **95a** with the *rac* diastereomer and upon subjecting the mixture to the reaction conditions a higher yield of 85% was observed. The *d.r.* was assessed *via* titration of NMR samples with Eu(facam)<sub>3</sub> utilised by Saa *et al.*<sup>80</sup> The diastereomers could be assigned due to the formation splitting of peaks corresponding to the *rac* diastereomer: the *rac* diastereomer could form in a mixture of 2 enantiomers, whereas the *meso* diol is  $\sigma$  symmetric, and therefore only one isomer exists. The interaction of the chiral europium salt causes the peak for the *rac* isomer to split, allowing for the peaks to be differentiated from the *meso* diastereomer (see NMR spectrum in appendix 1). Furthermore, recrystallization of **95c** from chloroform was found to enrich the *rac* enantiomer owing to comparative insolubility relative to the *meso* isomer. Subjecting the *rac* enriched and *meso* mixtures of **95c** to the optimised conditions provided the same result, with the *rac* enriched mixture furnishing a higher yield (Table 2.1).

This led to a revision of the proposed elimination to a hypothesised *syn* Chugaev-like elimination. However, Chugaev eliminations and similar *syn* pyrolytic eliminations classically proceed at high temperature (>150 °C), and therefore the comparatively mild reaction conditions should not effect the elimination.<sup>81</sup> In addition to this apparent paradox, if the intermediate xanthate was isolated and subsequently heated (>200 °C) in a separate synthetic procedure, no product tetracene was observed. Further attempting to force the rearrangement with UV light and Bauld's catalyst failed to initiate the reaction.<sup>82</sup> It was then hypothesised that the elimination proceeds anionically, with the alkylation of the pendant dithiocarbonate anion occurring after the formation of the tetracene core (Scheme 2.9).



**Scheme 2.9** – Proposed final transition state in the rearrangement cascade.

Furthermore, examples exist within the literature for the Chugaev elimination occurring at low temperatures (0 °C) without alkylating agents to “cap” the xanthate.<sup>83</sup> This lent credence to the hypothesis that the reaction must be anionically accelerated, with the alkylation of the dithiocarbonate as the final step. However, to what extent the anionic charge accelerated the reaction was unclear, as was which aspect of the cascade the negative charge had the greatest energetic effect on, as it has also been observed that anionic charge can accelerate various sigmatropic rearrangements.<sup>84-86</sup> Therefore, DFT calculations were undertaken at the CBS-QB3 level of theory,<sup>87, 88</sup> in a vacuum without metal ions, by optimising the geometries of our transition states shown in our proposed reaction mechanism and using the QST3 function to optimise the proposed transition states from the optimised starting molecule, final molecule and a proposed transition state. Unfortunately, attempts to model the entire reaction *via* the transition states hypothesised in Scheme 2.1 proved to be too computationally intensive. As such, the sigmatropic rearrangement was modelled on a simpler phenyl propargyl xanthate and the elimination was modelled on anthracene (Scheme 2.10).



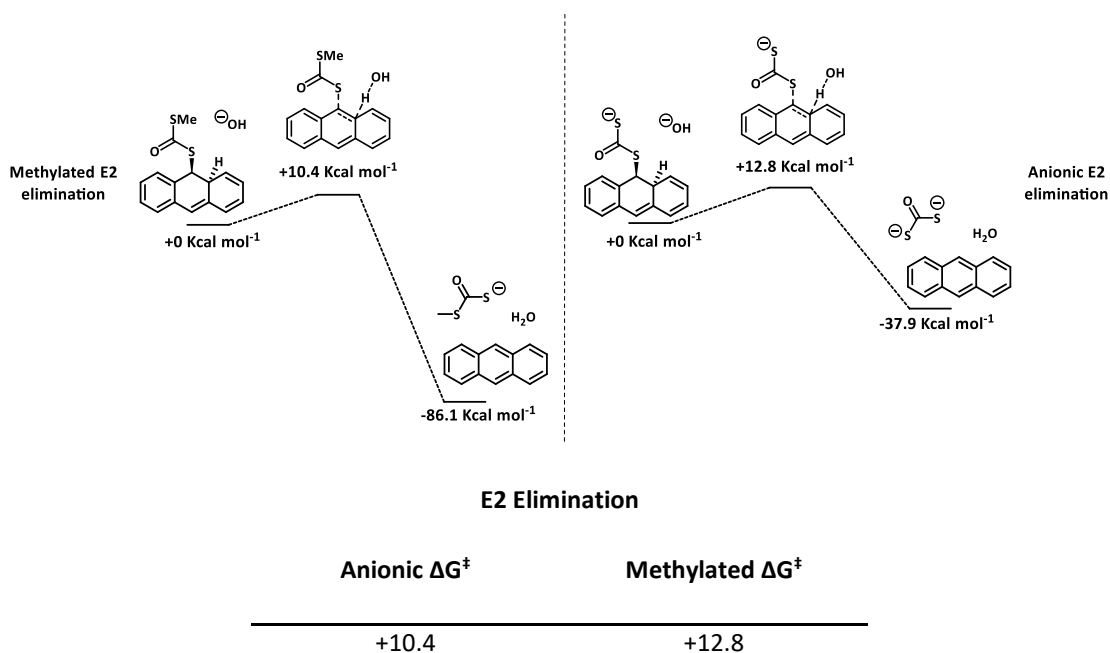
**Scheme 2.10** – Computed energies of anionic and methylated transition states.

Interestingly, it was found that the anionic analogues produced lower energy transition states, and that there was a massive reduction in  $\Delta G^\ddagger$  for the anionic Chugaev-like elimination (Scheme 2.11), implying that the greatest energetic contribution to the reaction came from the elimination. This is perhaps to be expected as the anionic charge on the dithiocarbonate facilitates the deprotonation. However, by substituting the computed energies into the Eyring equation (Equation 2.1,  $K_B$ =Boltzmann's constant,  $T$ =temperature,  $h$ =Planck's constant,  $\Delta G^\ddagger$ =Gibbs energy of activation,  $R$ =gas constant), it was found that the methylated Chugaev elimination would have been 0.13% complete over the 90 mins of the reaction at 60 °C, whereas the anionic elimination would have been 99% complete in 320 ns.

$$k = \frac{K_B T}{h} e^{-\frac{\Delta G^\ddagger}{RT}} \quad (2.1)$$

Conversely, the methylated sigmatropic rearrangement would be 87% complete over the 90 min reaction time, whereas the anionic case would be complete in 8.9 secs. This highlights the greater acceleration on the Chugaev elimination over the sigmatropic rearrangement.

Attempts to model the *anti* E2 elimination within the same parameters proved to be more troublesome. A simplified E2 elimination utilising hydroxide as the deprotonating anion was modelled at the B3LYP/6-31+G(d,p) level of theory, due to issues with getting the elimination to converge at the CBS-QB3 level of theory. The Gibbs energy of activation calculated at this level of theory proved to be very low, implying that the *anti* elimination was viable (Scheme 2.11).



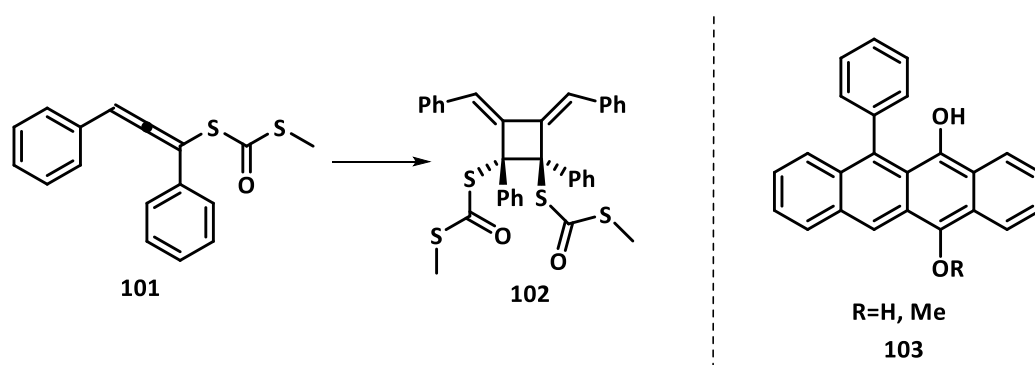
**Scheme 2.11** – Computed energies of anionic and methylated anti elimination transition states.

The methylated E2 elimination appears to be the far more thermodynamically favourable elimination, which can be accounted for by the generation of an anion as opposed to the dianion formed from the anionic equivalent. However, it can be considered that the energy barriers are close enough in energy that both are viable elimination pathways. However, care should be taken in assuming that the *anti* elimination is viable. Firstly, the calculation was performed within a vacuum, without specifying a solvent dipole moment, and it can be expected that the calculations will not describe the E2 elimination. The hydroxide will lower the energy due to charge-dipole interactions, therefore giving a lower energy result than would be expected in solvent due to the loss of this interactions. Secondly, the model is fairly removed from the reaction, and as such should be noted, but not treated as a reliable model for the elimination.

It could therefore be argued that the difference in energy of the anionic Chugaev and methylated Chugaev transition state was similarly overestimated. However, the CBS-QB3 level of theory is considered more accurate than B3LYP/6-31+G(d,p) and should there be a lowering of the energy barrier due to lessening of charge due to dipole interactions from the solvent, it is likely that the difference would

be significant to an intramolecular process (Chugaev elimination) vs an intermolecular process (E2 elimination).

The other explanation for the spread of yields is that they are due to the steric and electronic contributions from the aryl substitution. The general trend across the yields of tetracenes appears to be that *para* substitution negatively affects the yield of the final tetracene, as can be observed in the relative distribution of yields across the methoxy substituted tetracenes (yield = **95d** (>99%) >> **95b** (47%) > **95g** (38%)). Several publications in the synthesis of oligoacenes *via* allenic rearrangements report that the intermediate shown below (**102**, scheme 2.11) exists in equilibrium with the cyclobutene when the allene is tetrasubstituted, also stating that the intermediate in many *bis*-allenic rearrangements is due to a radical dimerisation of allenes (Scheme 2.12).<sup>60, 67, 70, 73</sup>



**Scheme 2.12** – Dimerisation of **101** to cyclobutane **102**, and unstable tetracene **103**. Compounds **101** and **102** were prepared by Mkethwa Ngenywa and compound **103** was isolated by Dr Laurence Burroughs.

Therefore, it can perhaps be speculated that the *para* substitution alters the cyclobutene: diene equilibrium by the stabilisation of radicals *via* an increased captodative effect, promoting the [2+2] cyclisation and reducing the amount of free allene left to undergo the  $6\pi$ -electrocyclisation, thus reducing the yield. This is corroborated by evidence within the literature. It was found in the allenic dimerisation of rubrene (Scheme 2.2) that electron-donating groups at *para* positions on the phenyl ring favoured the formation of the cyclobutene *via* a radical mechanism over rubrene.<sup>67</sup> Therefore, if the reversible cyclobutene formation is favoured, on quenching diminished yield of the tetracene would be observed. This theory is potentially corroborated by the isolated crystals of the cyclobutadiene **102** from the

rearrangement of the simple phenyl dithiocarbonate allene **101**, as well as a second tetracene molecule **103** which proved difficult to isolate due to its inherent instability (Scheme 2.12).

However, this does not account fully for the yield variance in the *meta* substituted cases, as the quantitative return of tetracene **96d** implies that the E2 elimination must be proceeding. It was therefore hypothesised that the increase in the steric bulk of the *meta* substituents was driving the increase in yield. As the calculated Van der Waals volume at the *meta* position increased, the yield also increased (OMe 33.32 Å<sup>3</sup> (**96d** = >99% yield), CF<sub>3</sub> 22.12 Å<sup>3</sup> (**96c** = 56% yield), F 3.59 Å<sup>3</sup>, (**96e** = 56% yield)),<sup>89</sup> perhaps implying that the extra steric bulk was forcing the E2 elimination. Some evidence of *trans* Chugaev eliminations exists within the literature, however, these are usually dependent upon groups which lower the pK<sub>a</sub> of the antiperiplanar proton.<sup>90</sup> However, the high yield of the parent phenyl tetracene **96a** implies that the true cause for the spread of yield in the transformation is a complicated combination of unknown factors and the factors discussed.

### 2.1.3. Density Functional Theory Calculations and Electrooptic properties

To develop a better working knowledge of which motifs produced more favourable HOMO and LUMO energies, computational calculations of the molecules were undertaken using Gaussian from the B3LYP/6-31G\*\* basis set (Table 2.2).

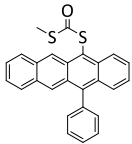
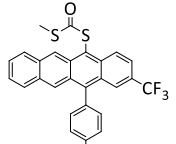
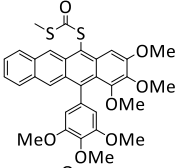
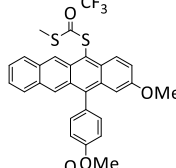
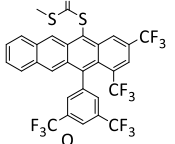
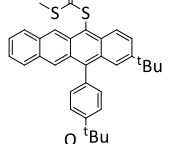
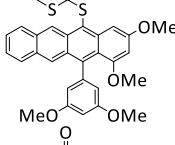
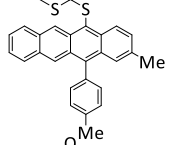
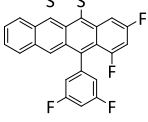
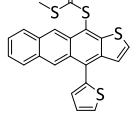
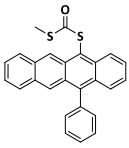
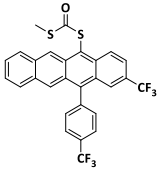
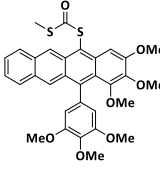
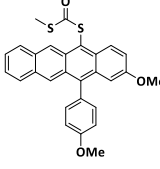
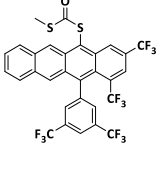
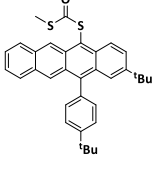
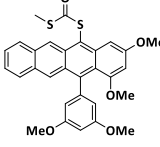
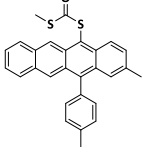
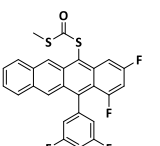
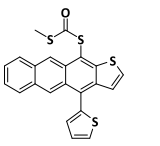
Tetracene	HOMO (eV)	LUMO (eV)	$E_g$	Tetracene	HOMO (eV)	LUMO (eV)	$E_g$
	-5.16	-2.51	2.65		-5.61	-2.98	2.63
	-5.21	-2.57	2.64		-5.20	-2.69	2.51
	-5.23	-2.93	2.60		-5.33	-2.69	2.65
	-4.89	-2.36	2.55		-5.31	-2.65	2.66
	-5.58	-2.96	2.62		-5.27	-2.32	2.95

Table 2.2 – HOMO and LUMO energies computed at the B3LYP/6-31\*\* level of theory

The variance in the HOMO-LUMO levels for the substituted tetracenes highlighted two important factors: a) electron-withdrawing groups largely lowered the HOMO and LUMO while electron-donating groups raised the HOMO and LUMO, and b) the tetracenes substituted derived from the diols with *para* substitution lowered the HOMO and LUMO energies, potentially highlighting that the location of substitution has a great effect on the electronics of the aromatic core. This is corroborated by the lowest LUMO in **96f** and highest HOMO in **98d** which is lowered by the introduction of a further methoxy group in **96b**. The wider HOMO-LUMO gap in anthrathiophene **96j** is perhaps to be expected due to the introduction of the thiophene interrupting the  $\pi$ -delocalisation across the aromatic rings.

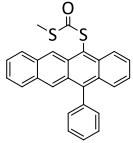
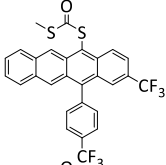
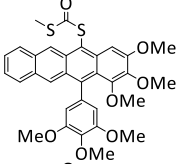
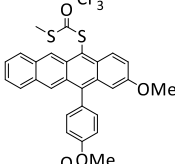
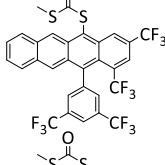
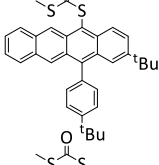
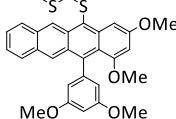
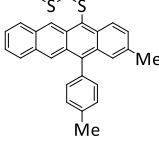
	Tetracene			Tetracene					
	$E^{1/2}$ (ox.) (V) <sup>a</sup>	$E_g$ opt (eV) <sup>b</sup>	$E_g$ opt (eV) <sup>c</sup>	$E^{1/2}$ (ox.) (V) <sup>a</sup>	$E_g$ opt (eV) <sup>b</sup>	$E_g$ opt (eV) <sup>c</sup>			
<b>96a</b>		+0.52	-4.82	2.27	<b>96f</b>		+0.76	-5.46	2.24
<b>96b</b>		+0.22	-4.62	2.23	<b>96g</b>		+0.43	-4.70	2.28
<b>96c</b>		+1.07	-5.14	2.18	<b>96h</b>		+0.55	-4.79	2.26
<b>96d</b>		+0.29	-4.65	2.09	<b>96i</b>		+0.41	-4.81	2.32
<b>96e</b>		+0.65	-5.04	2.27	<b>96j</b>		+0.60	-4.88	2.49

**Table 2.3** – Experimentally derived HOMO levels and HOMO-LUMO gap

Estimates of the optical bandgap  $E_g$  opt. were attained from the onset of the lowest energy band in the UV/vis spectrum as it corresponds to the HOMO-LUMO  $\pi$  to  $\pi^*$  transition (Table 2.3). It was observed that the general trend of the  $E_g$  measured by UV/vis matched the trend in the calculated  $E_g$ , showing that the calculated gap could be used moderately reliably for the prediction of the HOMO-LUMO gap. The HOMO gap could be derived experimentally from cyclic voltammetry measurements (supp info.). Estimation of the LUMO was difficult and in many cases, could not be attained, however, the calculated HOMO levels obtained corroborate the previously observed pattern that donating groups raise the HOMO and withdrawing groups lower it, and that *para* substitution depresses the energy levels.

It must be stressed however, that while these combined methods add insight into the electronic properties of the polyaromatics, the values measured differ in some fundamental ways. The calculated energy gap can be considered as an approximation of the fundamental gap ( $E_{\text{fund}}$ ), which is defined as the difference between the calculated ionisation potential and electron affinity of the molecule. The Tauc method for approximating the HOMO-LUMO gap ( $E_{\text{opt}}$  or the optic gap) is similarly not a perfect approximation of the fundamental gap.<sup>91</sup> The excitation of an electron *via* an absorbed photon to the lowest accessible electronic transition does not reflect the ionic method calculated by DFT. As the electron promoted and the hole generated remain electrostatically bound, the optical gap calculated from UV spectroscopy is often much lower than  $E_{\text{fund}}$ .

To probe the properties further, alternate DFT methods were employed to gain more accurate approximations of  $E_{\text{fund}}$ . Previous computational studies have shown that calculations of excitation of an electron to the first singlet state can be treated as an approximation of the HOMO-LUMO gap.<sup>92</sup> Furthermore, improved accuracy of the excitation energy has been described using time-dependent DFT at the CAM-B3LYP/6-31G(d,p) level of theory with the Tamm-Dancoff approximation. As such the tetracenes synthesised were assessed at this level of theory (Table 2.4).<sup>93</sup>

Tetracene	HOMO (eV)	LUMO (eV)	$E_g$	Tetracene	HOMO (eV)	LUMO (eV)	$E_g$
	-5.94	-3.29	2.65		-6.54	-3.80	2.74
	-5.90	-3.32	2.58		-6.17	-3.51	2.66
	-6.85	-3.91	2.94		-6.10	-3.38	2.72
	-6.04	-3.41	2.63		-6.03	-3.42	2.61

**Table 2.4** – Time dependent DFT calculations

As can be seen from table 2.4, the computational results generated from the CAM-B3LYP/6-31G(d,p) level of theory are not in agreement with the experimental values, with the HOMO and LUMO overestimated across the molecules studied. As such, it could be inferred that the B3LYP/6-31G(d,p) was sufficient in modelling the tetracenes.

#### 2.1.4. Crystal Structures of Dithiocarbamate Tetracenes

In analysing the crystal structures of the synthesised tetracenes, it was found that electronic and steric factors influenced the crystal packing to varying degrees. In the model 5-phenyl tetracene **96a** increased  $\pi$ -stacking was observed with a high degree of overlap compared with unsubstituted tetracene, which can probably be attributed to the increased steric bulk over the tetracenes interrupting the usual herringbone stacking of tetracenes, with a 3.68 Å C-C distance. Furthermore, the phenyl group introduced an edge-to-face interaction (C-H to C 2.89 Å) with a further molecule, creating columns of  $\pi$ -stacked tetracenes in the unit cell (Figure 2.1).

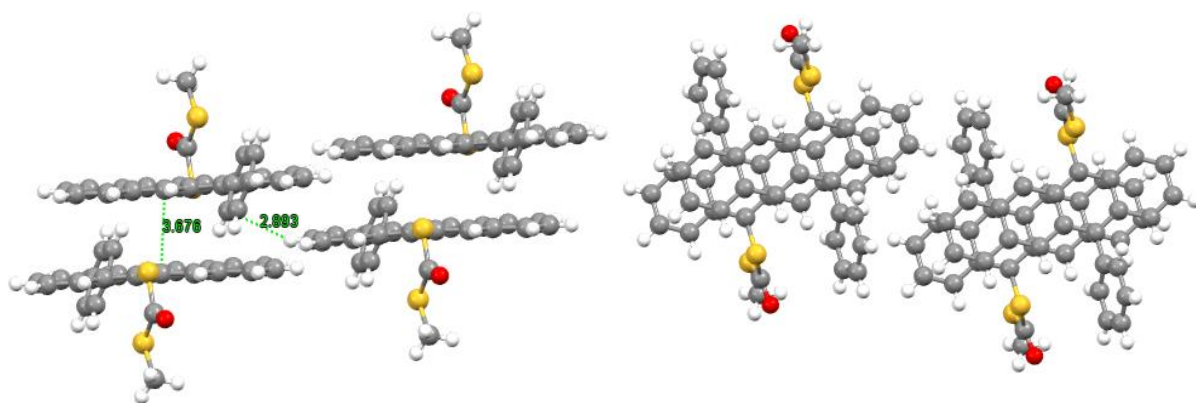


*Figure 2.1 –  $\pi$ -stacking behaviour in 96a.*

Nuckolls and Swager both found that introducing electron-withdrawing or releasing groups onto the acene structure on the peripheral rings created an electron rich and electron poor end, creating a greater dipole along the length of the molecule, and increasing the  $\pi$ -stacking within the crystal structure.<sup>38, 73,49,66</sup> This effect was observed in the unit cell of **96d**, where there was overlap on the methoxy substituted terminus of the molecule with the unsubstituted terminus of a second molecule, producing a large offset of roughly 7.35 Å and a  $\pi$ -stacking distance of 3.51 Å (Figure 2.2).

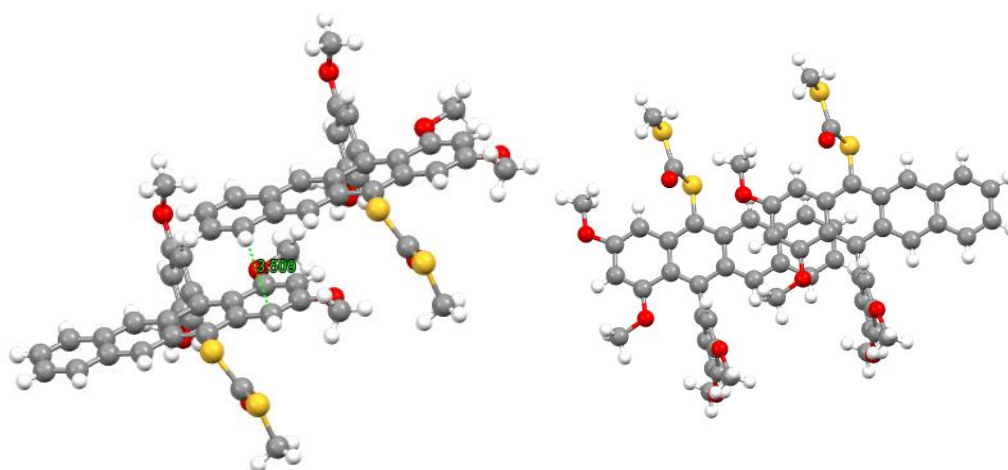
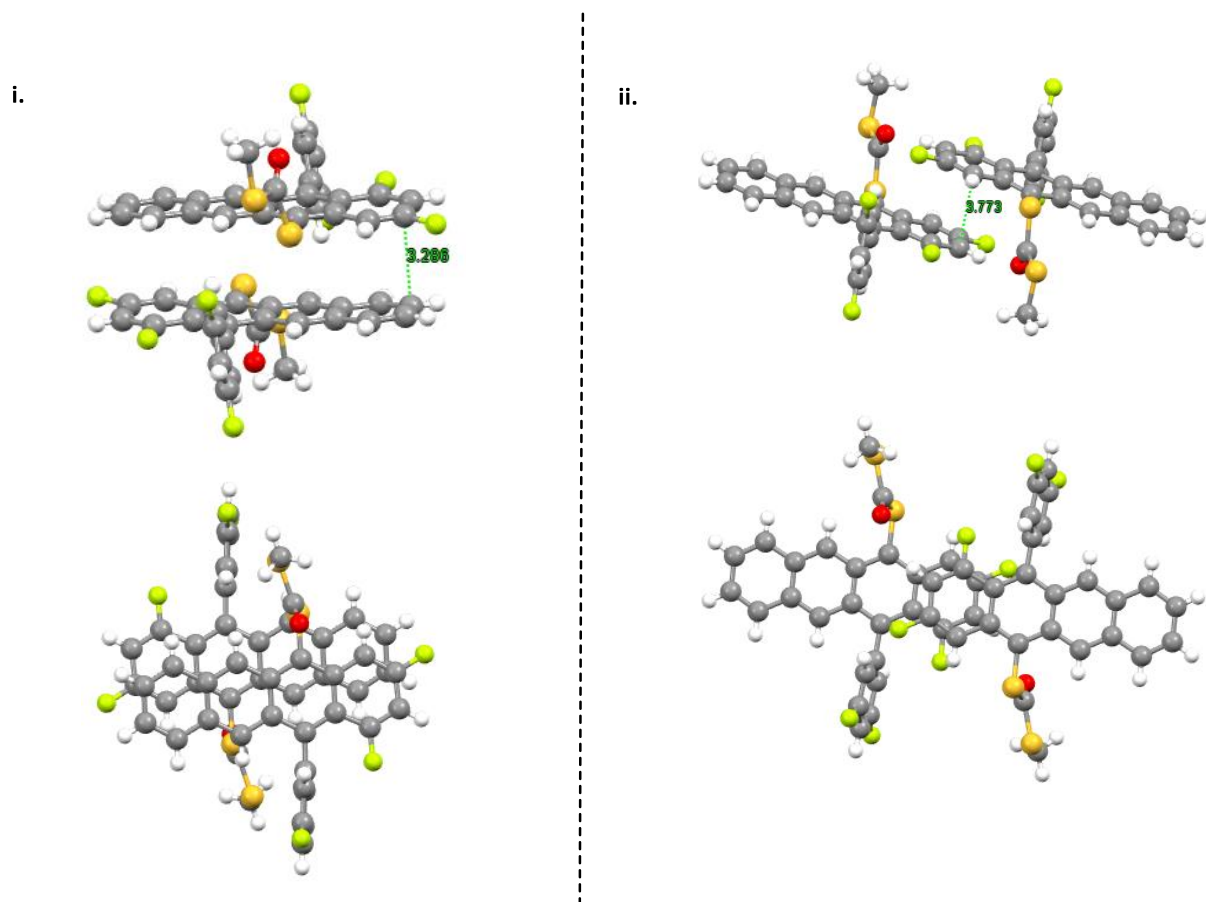


*Figure 2.2 –  $\pi$ -stacking behaviour in 96d*

This offset is also due to the 5-phenyl methoxy groups forming H-bonding interactions (2.48 Å) in the unit cell, reducing the  $\pi$ -overlap from that observed in **96a**.

Interestingly, the crystal packing in **96e** displays a similar overlap due to dipole as displayed in **26d** with two molecules orienting in reverse, as in **96a** (Figure 2.1 and

2.2), and a very reduced  $\pi$ -stacking distance (C to C 3.286 Å) (Figure 2.3.i) and a slight offset, but also forms a second overlap with another molecule of **96e** ( $\pi$ -stack distance, C to C 3.773 Å) (Figure 2.3.ii).



*Scheme 2.3 –  $\pi$ -stacking behaviour in 96e.*

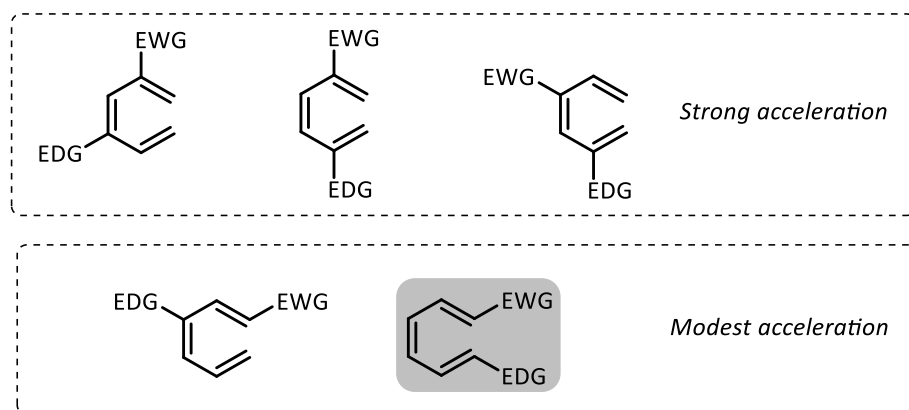
This implies that the introduction of a dipole along the molecule in the tetracenes induces greater  $\pi$ -stacking as might well be expected, but that the size of the attached groups limits the overlap of the acenes. This implies that for the greatest overlap of the molecules, modestly sterically demanding groups with high inductive withdrawing or releasing effects (such as fluorines or linear functional groups such as cyanides) are desired.

## 2.2. Conclusions and Future Work

To conclude, the xanthate rearrangement to substituted xanthate tetracenes is concise and mechanistically interesting, and furnishes insights into substitution

effects on crystal habits in the materials that can be synthesised by the method. However, the wide variation in the yield coupled with the erosion of yield on scale makes the method insufficient for generation of a wide range of tetracenes.

Mechanistic insight was gained through experimental observation and computational investigation. While the calculations do indicate a significant anionic rate acceleration in the final elimination step, this insight comes with distinct caveats. The full reaction coordinate proved to be too computationally intensive to model, and so the transition states do not necessarily represent the actual progression of the reaction. Furthermore, separately modelling the sigmatropic rearrangement and the final *syn* elimination means that there is little insight into how the  $6\pi$ -electrocyclisations are affected by the presence of the charge on the dithiocarbonate. Computational analysis of electrocyclization of hexatrienes has shown that altering substitution around the chain accelerates the cyclisation *via* captodative effects.<sup>94</sup> Donating groups at the 2 position and withdrawing groups at the 3 position have been shown to accelerate electrocyclisations, with evidence from Magomedov *et al.* that anionic groups are sufficiently activating (Scheme 2.13).<sup>95, 96</sup>



**Scheme 2.13** – Known accelerating substitution patterns in  $6\pi$ -electrocyclisations.

Substitution at the 1 and 6 positions was also found to be moderately activating, as such an argument could be made that the substitution of the allenes affects the course of the reaction. Therefore, attempts to model the cyclisation computationally would no doubt be worthwhile to gain greater insight into the reaction.

## Chapter 3

### *Synthesis of 8-membered rings via a [1,5]-hydride rearrangement-propargyl Michael addition cascade*

#### Publications from this section

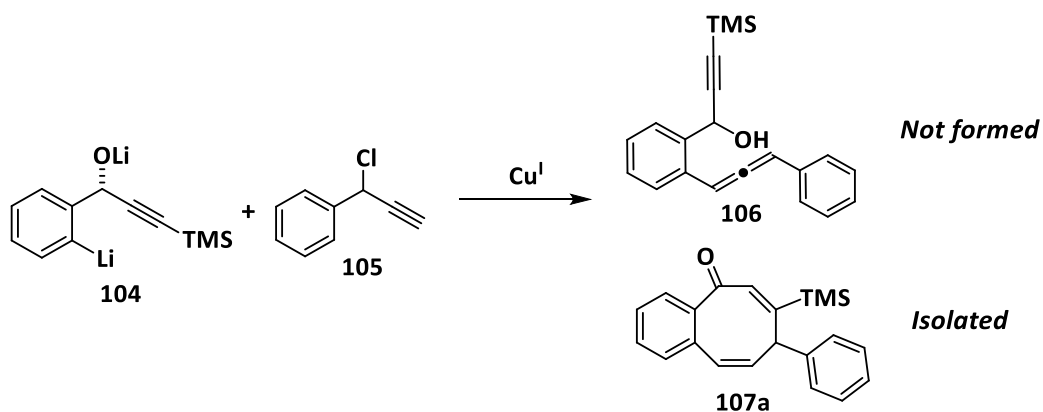
1. One-Pot Cannizzaro Cascade Synthesis of *ortho*-Fused Cycloocta-2,5-dien-1-ones from 2-Bromo(hetero)aryl Aldehydes, L. Burroughs, L. Eccleshare, J. Ritchie, O. Kulkarni, B. Lygo, S. Woodward, W. Lewis, *Angew. Chem. Int. Ed.* **2015**, *54*, 10648-10651.
2. Diversification of *ortho*-Fused Cycloocta-2,5-dien-1-one Cores and 8 to 6-Ring Conversion by Sigma Bond C-C Cleavage, L. Eccleshare, L. Lozada-Rodríguez, P. Cooper, L. Burroughs, J. Ritchie, W. Lewis, S. Woodward, *Chem. Eur. J.* **2016**, *22*, 12542-12547.

#### Acknowledgements

- Compounds **107e-f** were synthesised and characterised by Dr Lee Eccleshare. Compound **175** was synthesised by Dr Laurence Burroughs.
- Entries **1-4** in Scheme 3.12 were attained by Omkar Kulkarni and Dr Laurence Burroughs.

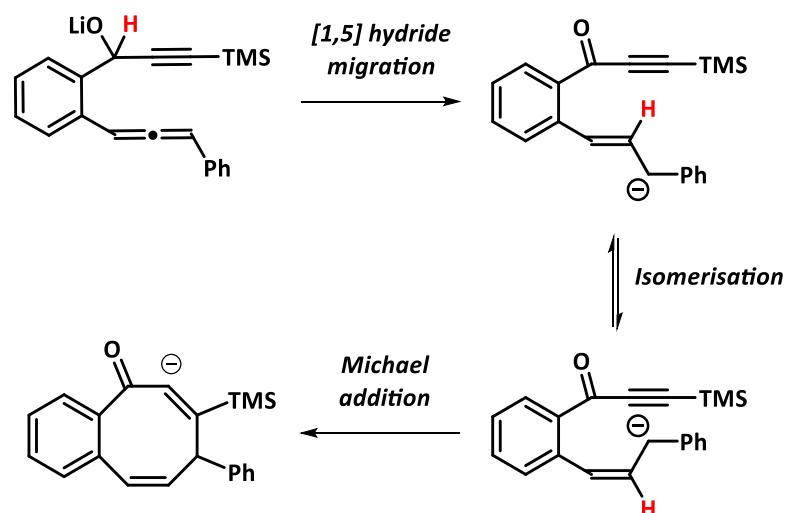
### 3.1. Introduction

Over the course of investigating the *bis*-allenenic rearrangement route to form tetracene, attempts were made to synthesise compound **106** *via* a Cu<sup>I</sup>-mediated S<sub>N</sub>2' addition of the intermediate aryl lithium **104** to  $\alpha$ -phenyl propargyl chloride **105** (Scheme 3.1).



*Scheme 3.1 – An unexpected 8-membered ring.*

It was intended that **106** would then be converted into the propargyl xanthate to effect the rearrangement cascade discussed in Chapter 2. However, this transformation was unsuccessful, and an unexpected 8-membered carbocycle **107a** was isolated from the reaction mixture in very low yield. It was speculated that the intermediate allene was formed, however, the anomeric donation of charge from the propargyl alkoxide to the  $\sigma^*$  orbital was sufficient to accelerate the [1,5]-migration of the  $\alpha$ -proton. The subsequent allylic anion formed was then sufficiently nucleophilic to undergo a Michael addition to the pendant ynone formed by the rearrangement, and on quenching the reaction, form the carbocyclic enone **107** (Scheme 3.2).



Scheme 3.2 – Putative mechanism for 8-ring formation.

Though formed in a low yield, this reaction was sufficiently mechanistically interesting to warrant further investigation. 8-membered rings pose a synthetic challenge owing to their inherent strain due to conformation and transannular interactions across the ring, and conformational interactions on 8-membered rings can have profound and unexpected effects on further reactions to the carbocycle.<sup>97</sup> However, in spite of these difficulties in synthesising 8-membered rings, they are a common motif in natural products with interesting biological properties (Figure 3.1), and so efficient synthesis of challenging medium sized rings creates a clear boon to medicinal and natural product chemistry.<sup>98-103</sup>

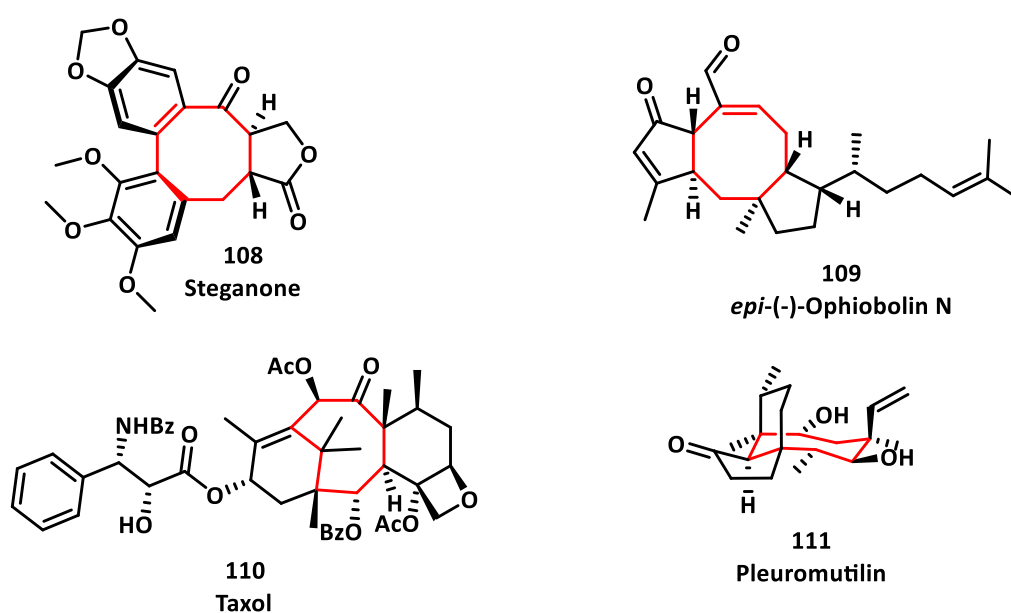


Figure 3.1 – A number of 8-membered ring containing natural products.

A brief survey of synthetic methods employed in 8-membered ring synthesis (primarily metathesis, ring expansions, metal-catalysed additions, aldol reactions and rearrangements) and their limitations are discussed below.

### 3.1.1. Ring Closing Metathesis (RCM) Approaches to 8-Membered Rings

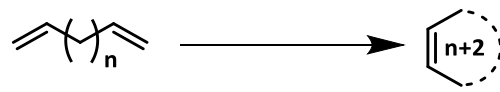
One of the most common synthetic strategies for accessing medium sized rings utilises ring closing metathesis (RCM). While RCM has proven a great boon to synthesis of small rings and indeed large rings, such as in the 16-membered ring systems in epothilones,<sup>104</sup> entropic and enthalpic factors make the synthesis of 8-membered rings challenging. As studied by Hillier *et al.*, the high ring strain of 8-membered rings creates a strong enthalpic barrier to formation, and the entropic barrier due to loss of bond rotors in the fused ring being far less favourable to intermolecular polymerisation.<sup>105</sup>

The metric used for the comparison of the favourability of various ring sizes was the thermodynamic effective molarity ( $EM_T$ ).  $EM_T$  is a measure of the favourability of ring closure over dimerisation and is calculated from the intramolecular cyclisation equilibrium constant and the intermolecular dimerisation equilibrium constant (Equation 3.1).

$$EM_T = \frac{K_{intra}}{K_{inter}} = e^{\frac{(\Delta G_{intra}^\ddagger - \Delta G_{inter}^\ddagger)}{RT}} \quad (3.1)$$

Effectively it is a metric for determining the concentration at which cyclisation out-competes dimerisation. Hence an increase in effective molarity signifies a more favourable cyclisation. As can be seen above, the 6-membered ring closure is favoured over the competing polymerisation, with 9-membered ring formation strongly disfavoured over polymerisation (Scheme 3.3).

n	Log <sub>10</sub> (EM <sub>T</sub> )
3	-0.64
4	1.52
5	-2.51
6	-3.31
7	-9.24
8	-3.48

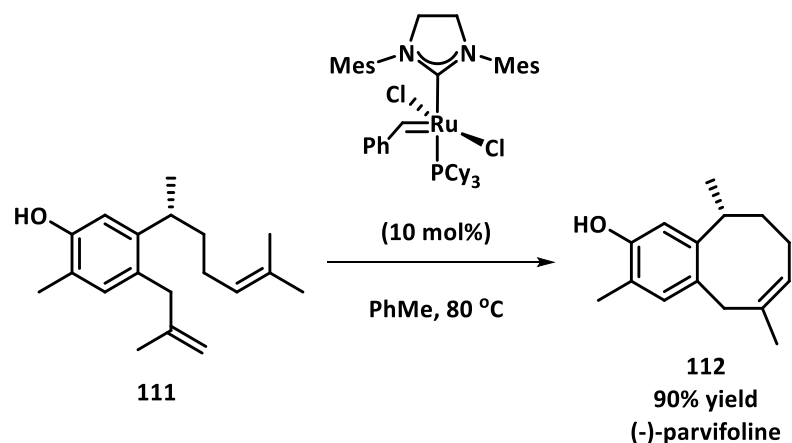


**Scheme 3.3** – Thermodynamic effective molarity as a factor of chain length calculated by Hillier *et al.*

While the 8-membered ring closure is more favourable than the analogous 9-membered closure, to attain the same ring closure: polymerisation (EM ratio for a 6 membered ring in 1 ml, the corresponding molar concentration for the 8-membered ring formation would require dilution in 100 L of solvent. This makes it clear that the ring closing event is highly disfavoured.

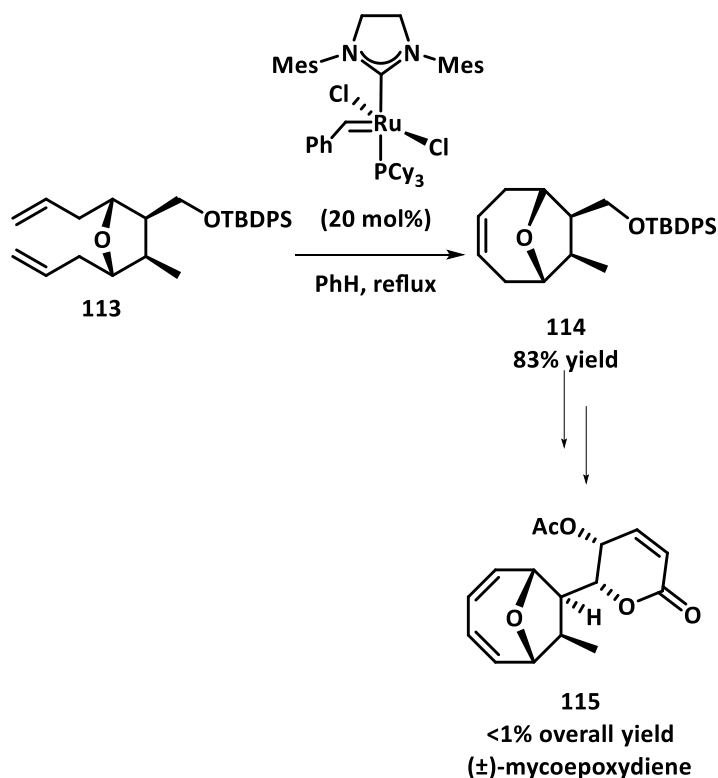
This result is in close agreement with experimental evidence. Grubbs *et al.* discovered success in the metathesis of 8-membered rings was usually only successful in the introduction of geometric constraints in the diene to effect ring closure.<sup>106</sup> When groups incapable of rotation were introduced, the cyclisation became relatively high yielding: as an example, the introduction of a *trans*-cyclohexene unit actively favours the ring closure due to the reduction of bond rotors.

This has been exploited in many natural product syntheses. Chavan *et al.* synthesised the carbocyclic natural product (-)-parvifolene **112** over 8 steps from (R)-(+)-citronellal with a high yielding RCM of **111** as the final step (Scheme 3.4).<sup>107</sup>



**Scheme 3.4** – Application of RCM to the synthesis of 8-membered rings in total synthesis of (-)-parvifolene **112**.

While this transformation furnished an excellent yield of the final product, it must be highlighted a high catalyst loading of Grubbs 2<sup>nd</sup> generation catalyst was required in addition to the conformational restraint of the phenyl ring. Tadano *et al.* similarly utilised conformational restraints inherent in the structure of ( $\pm$ )-mycoepoxydiene **115** (Scheme 3.5).<sup>108</sup>

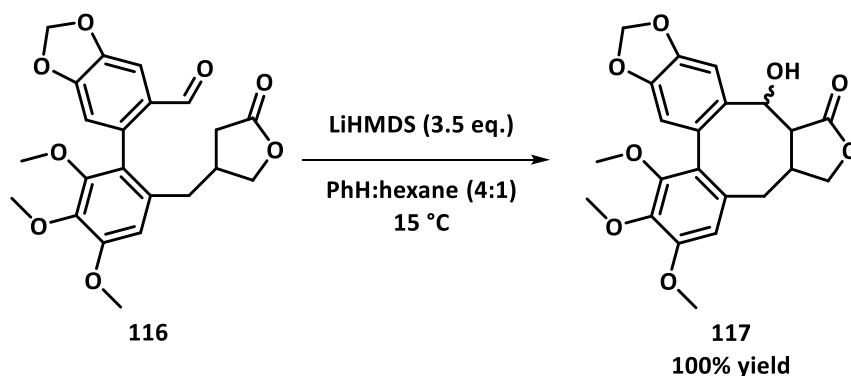


**Scheme 3.5** – Application of RCM to the synthesis of 8-membered rings in total synthesis of ( $\pm$ )-mycoepoxydiene **115**.

A high yield of the desired cyclooctene **114** could be effected due to the bridging ether in the resultant structure: the RCM was enhanced due to the two allyl groups being syn to one another on the tetrahydrofuran ring in **113**, again reducing the entropic barrier to the reaction. However, this similarly required high catalyst loadings in order to effect the reaction. As such, while it has been employed to good effect, metathesis often requires geometric constraint and high loadings to effect efficient closure, limiting wide applicability to medium sized ring synthesis.

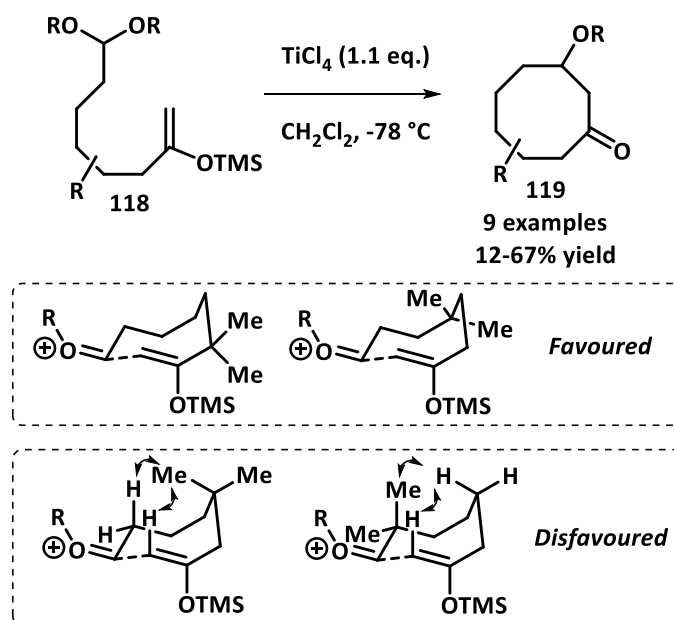
### 3.1.2. Aldol Approaches to 8-Membered Rings

Attempts toward aldol closure for 8-membered rings have also been reported. Robin *et al.* utilised an intramolecular aldol addition to an aromatic aldehyde **116** to excellent effect in their studies toward the synthesis of steganone **108** (Scheme 3.5).<sup>109</sup>



Scheme 3.5 – Aldol ring closure en route to steganone **108**

Treadgold *et al.* reported a Mukaiyama aldol annulation to form a variety of rings **119** (Scheme 3.6).<sup>110</sup>



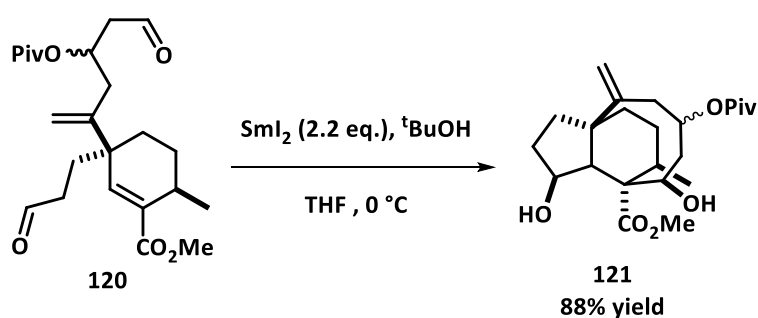
Scheme 3.6 - Mukaiyama aldol ring closure and proposed transannular interactions promoting or disfavoring ring formation.

However, the yields for this transformation were typically low. This again highlights that geometric constraint are generally key in forming 8-membered rings

to lower the entropic barrier to ring closure, an issue not present in Robin *et al.* synthesis due to the rings in **116**. There are also geometric constraints to Mukaiyama annulation: eclipsing interactions in a proposed chair boat transition state could disfavour the aldol closure (Scheme 3.6). In many substrates *gem*-dimethyl substituted carbons, most likely implemented to accelerate ring closure *via* the Thorpe-Ingold effect, either promoted or disfavoured the closure. In the case of the neopentyl TMS-enol ether, there was no eclipsing interaction, whereas in the neopentyl acetal case, this lead to eclipsing interactions, disfavoured closure. This shows that utilising an aldol method requires judicious choice of substitution to favour the desired ring closure.

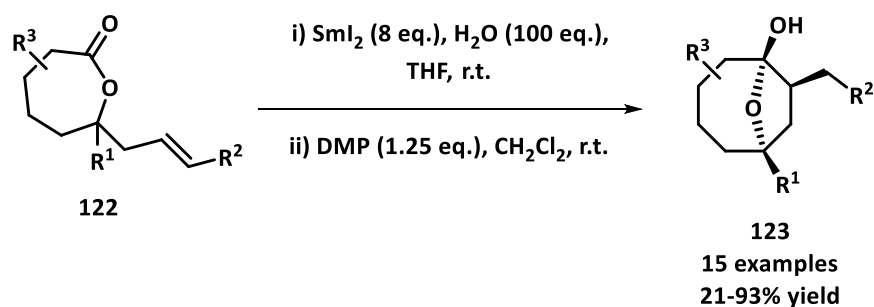
### 3.1.3. Radical Approaches to 8-Membered rings

A range of radical methods have been used to synthesise 8-membered rings. Using  $\text{SmI}_2$  in order to form ketyl radicals in order to effect ring closure is a well-studied method within the literature, having been utilised in model systems and applied to the synthesis of natural products.<sup>111, 112</sup> Procter *et al.* utilised the radical ketyl forming and Lewis acid activity of  $\text{SmI}_2$  to effect an impressive cascade to form the 8-membered ring of the pleuromutilin skeleton **121** in excellent yield (Scheme 3.7).<sup>111</sup>



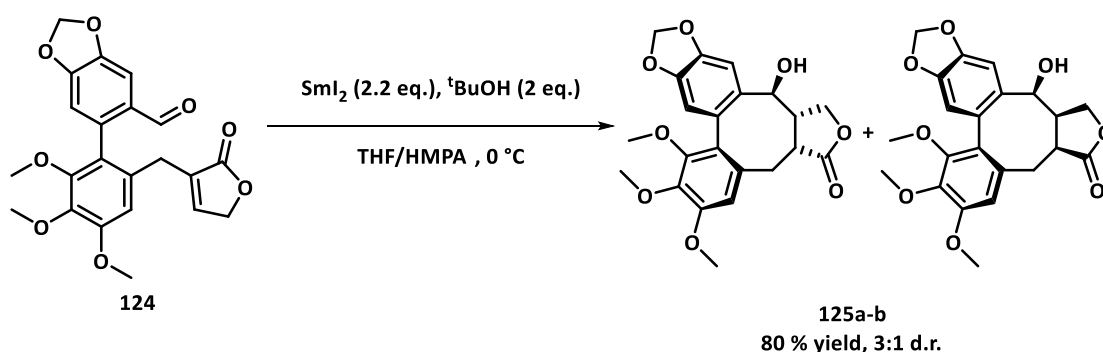
**Scheme 3.7** – Application of  $\text{SmI}_2$  mediated radical ketal addition to the synthesis of (+)-pleuromutilin **111**.

In further model systems however, limitations of the radical cyclisation become apparent. In the 5-exo-trig cyclisations of  $\delta$ -lactones **122** to form 8-membered rings **123** (Scheme 3.8),<sup>112</sup> yield seems to be severely eroded if the radical formed by the cyclisation is not stabilised by an aromatic group, perhaps highlighting the limited scope of such transformations.



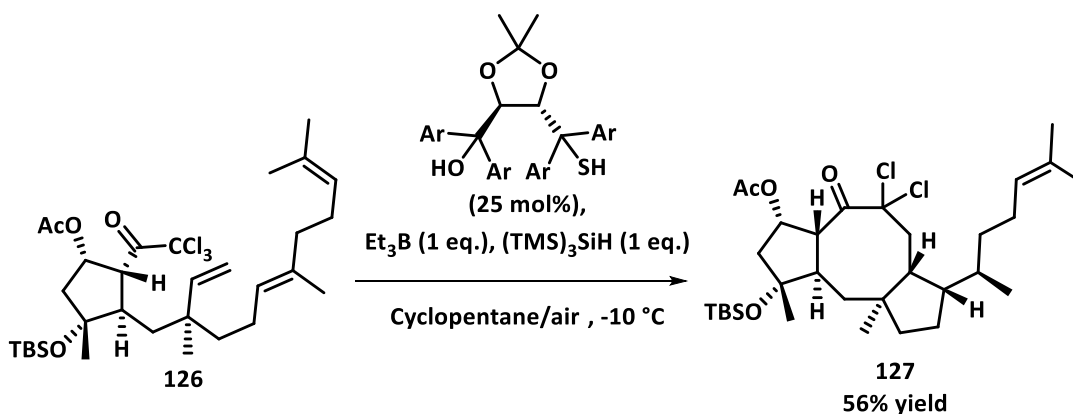
**Scheme 3.8** – Application of  $Sml_2$  mediated radical ketal conversion of 7-membered lactones **122a-o** to 8-rings **123**.

Molander *et al.* utilised the same reactivity to synthesise the 8-membered ring of steganone **125a-b** in good yield (Scheme 3.9).<sup>113</sup> However, the 8-ring formed a mixture of diastereomers **125a-b** which required epimerisation of the carbon  $\alpha$  to the ester carbonyl with base to furnish the desired stereochemistry. Additionally, this cyclisation proves to be highly yielding, but this again is likely due to the geometric constraints due to the  $sp_2$  hybridised carbons on the ring removing bond rotors and favouring ring closure.



**Scheme 3.9** –  $Sml_2$  radical ketal approach to steganone.

In a highly inventive cascade disconnection, Maimone *et al.* facilitated the synthesis of the fused 5,8,5 ring system of (-)-*epi*-opiobolin-N **127** in a single step in 56% yield (Scheme 3.10).<sup>99</sup>

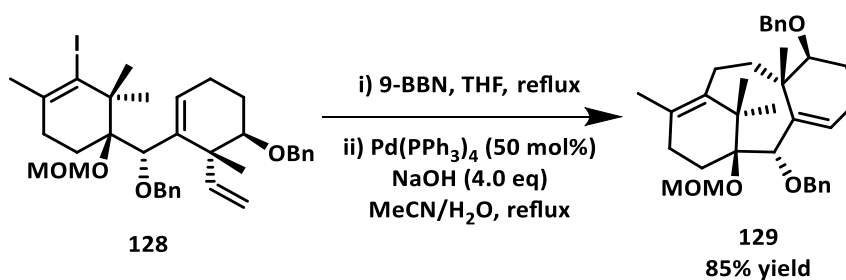


Scheme 3.10 – Radical cascade approach to (-)-epi-ophiobolin-N **109**.

The reductive formation of an electrophilic radical  $\alpha$ -to the ketone then underwent an 8-endo-trig addition followed by a 5-exo-trig cyclisation, and terminated with a hydrogen atom transfer (HAT) from a chiral thiol catalyst. While impressive, it must be stated that the yield and *d.r.* of the final product were poor across a range of HAT catalysts, most likely due to epimerisation of the epimerisation of the tertiary radical formed at the end of the cascade being faster than the hydrogen atom transfer that ends the cascade.

### 3.1.4. Transition Metal-catalysed Approaches to 8-Membered Rings

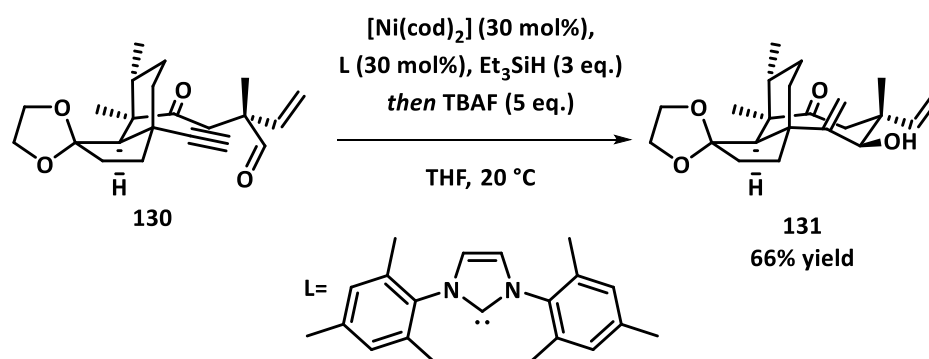
Transition metal-catalysed transformations have been employed to great effect in the synthesis of 8-membered rings, both in the synthesis of natural products and in general methodologies. In the synthesis of the 8-membered ring of a taxane, Nakada utilised a Suzuki-Miyaura cross coupling between a vinyl iodide **128** tethered to an alkyl borane derived from a hydroboration to furnish the taxane skeleton **129** in a high yield (Scheme 3.11).<sup>114</sup>



Scheme 3.11 – Alkyl Suzuki cross-coupling approach to Taxane ring system **129**.

However, it must be noted that the reaction conditions are long (72 h) and the palladium loading is also incredibly high (50 mol%). Furthermore, in extending the methodology to the synthesis of a simple fused carbocycle, yield proved to be low in most instances, but could be improved with addition of CsF as the base. No doubt the entropic loss of bond rotors sufficiently disfavoured the cross-coupling, but the addition of a more activating base began to favour transmetalation of the boronate. This no doubt highlights the difficulty in overcoming the enthalpic and entropic barriers in developing a general tolerant route to 8-membered rings *via* cross-coupling.

Herzon *et al.* utilised a  $[\text{Ni}(\text{cod})_2]$  catalysed reductive cyclisation of **130** to furnish the 8-membered ring system of pleuromutilin **131** in good yield (Scheme 3.12).<sup>98</sup>



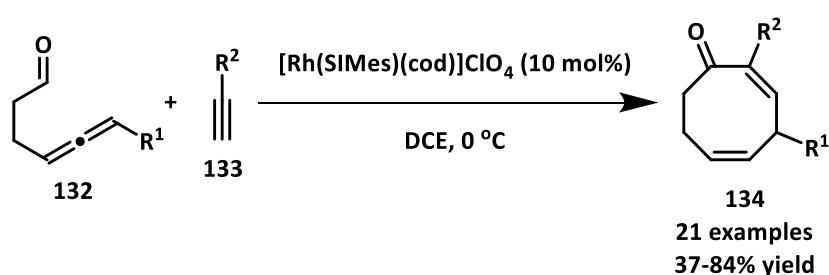
**Scheme 3.12** – Reductive Ni cyclisation en route to pleuromutilin **111**.

While this ring formation was successful in high yield, as is noted in the paper, it is the sole instance of a nickel reductive coupling known in the literature, and the reasons given for the favourable result are the reduced number of bond rotors due to the bicyclic rings in the starting material **130** and the  $\text{sp}^2$  hybridisation inherent to the molecule lowering the transannular interactions, rendering the ring formation favourable. Furthermore, the high loading of the nickel catalyst further mars the transformation. As this is in keeping with the current wisdom concerning 8-ring formation, it can be inferred the strategy could not be utilised widely for ring formation without similar constraints.

One of the common themes of the carbocyclisations discussed above is that the cyclisation step forms only one bond, and that multistep syntheses are required

to form the intermediates for the ring forming event. As such, metal-catalysed transformations creating multiple bonds in a single transformation are appealing as they circumvent the requirement of long syntheses to form 8-membered rings.

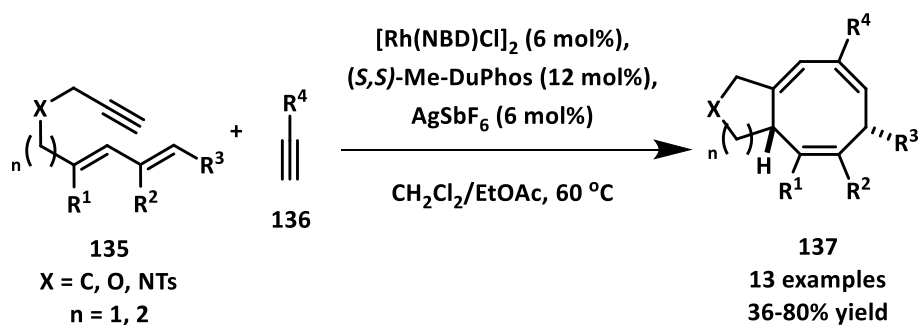
Rhodium catalysis has been exploited to good effect in the synthesis of fused 8-membered rings *via* [4+2+2] and [6+2] cyclisations.<sup>115-117</sup> Sato *et al.* reported a Rh catalysed [6+2] addition of alkynes **133** to allenals **132** in poor to excellent yield, with the addition tolerant to alkyl, phenyl, esters, alcohols, amines and acetylene gas (Scheme 3.13).<sup>118</sup>



Scheme 3.13 – Rh catalysed [6+2] cyclisation of allenals **132**.

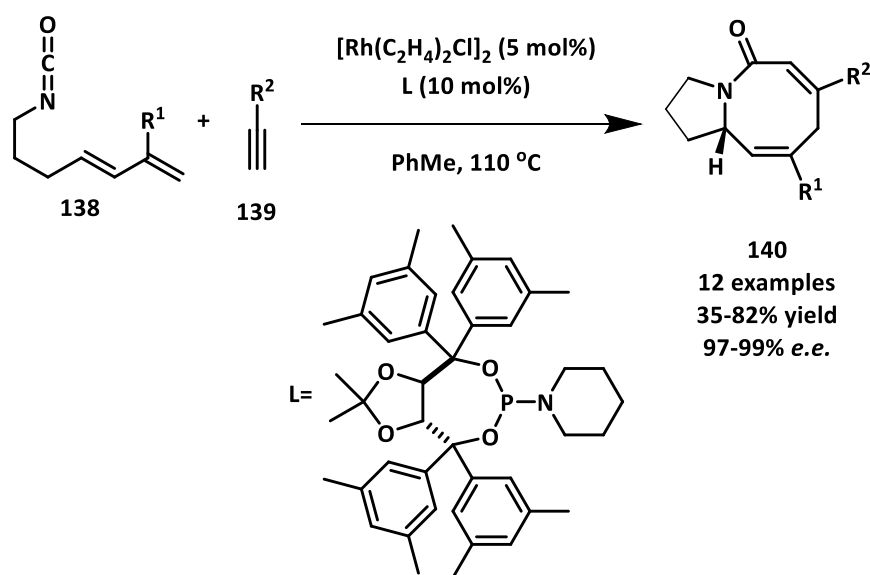
However, regioselectivity of the alkyne addition was adversely affected by substitution upon the alkyne, and *gem*-dimethyl substituted allenals favoured the formation of cyclohexenes. Furthermore, the loadings of the Rh catalyst were high (10 mol%) and the allenals required multiple steps to access, generally between 4-7 steps, limiting the applicability of the method.

Rhodium catalysis has also been applied to [4+2+2] ring forming reactions with tethered dienes and alkynes. DeBoef *et al.* synthesised a range of fused 8-membered rings **137** from the [4+2+2] condensation between alkynes **136** and tethered alkynyl dienes **135** in poor to excellent yields (Scheme 3.14).<sup>115</sup>



Scheme 3.14 – Rh catalysed [4+2+2] cyclisation.

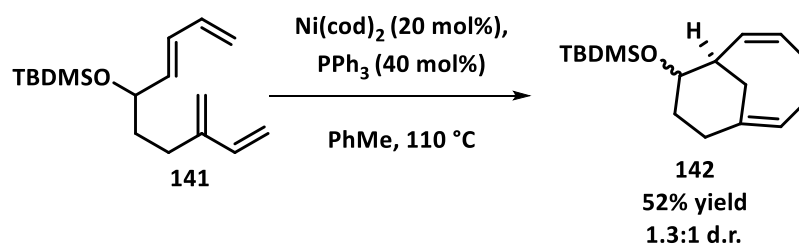
However, the diene substitution proved to be key for regioselectivity: if the terminal alkene was unsubstituted, the 8-rings were formed in a mixture of regioisomers. Furthermore, the desired tethered alkynyl diene starting materials needed to be synthesised, and a route to access them was not discussed. Rovis *et al.* synthesised a range of unsaturated azocanes **140** in poor to excellent yields with excellent e.e. with chiral phosphoramidate ligands, *via* the [4+2+2] condensation of dienyl isocyanates **138** and alkynes **139** (Scheme 3.15).<sup>116</sup>



Scheme 3.15 – Enantioselective Rh catalysed [4+2+2] cyclisation.

However, as is the case with most of these Rh catalysed reactions, the isocyanates were non-commercial, and synthesised over multiple steps.

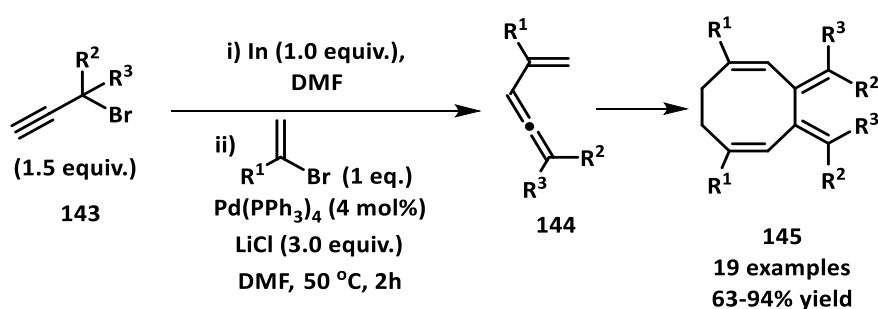
Wender *et al.* developed a  $\text{Ni}(\text{cod})_2$ , catalysed [4+4] cycloaddition of tethered dienes **141** in high yield and deployed the methodology to good effect toward the synthesis of the fused taxane ring system **142** (Scheme 3.16).<sup>119, 120</sup>



Scheme 3.16 – Ni catalysed [4+4] cycloaddition to Taxane-like fused ring system **142**.

While this generates two new bonds in high yield, the loadings of Ni(cod)<sub>2</sub> are high (10-22 mol%) and diastereoselectivity in the bicycles formed was sensitive to substitution.

The methodology developed by Kang *et al.* is therefore an attractive one. A palladium cross-coupling between variously substituted vinyl bromides and propargyl halides and pseudohalides, generating a transient vinyl allene **144** which then undergoes a Pd catalysed [4+4] reaction to generate a series of 8-membered ring **145** (Scheme 3.17).<sup>121</sup>

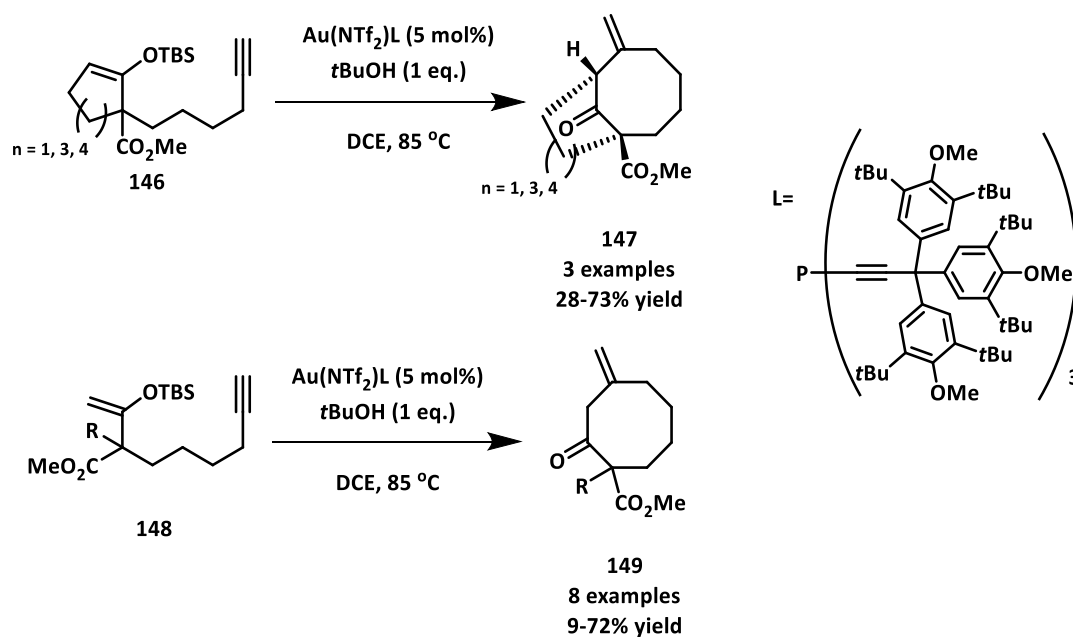


Scheme 3.17 – Pd catalysed [4+4] cycloaddition developed by Kang *et al.*

Impressively, this generates the carbocycle from simple starting materials (bromostyrenes and propargylic halides **143**) in good yields, and the methodology can be expanded to do a further [4+2] reaction to form fused rings in a simple, one pot transformation. Where the methodology suffers however is in the scope. When the vinyl bromide bears an alkyl substituent, a [4+2] cyclisation predominates and little variation to the substitution on the propargyl fragments is poor (H and Me only).

### 3.1.5. Gold Catalysed Approaches to 8-Membered Rings

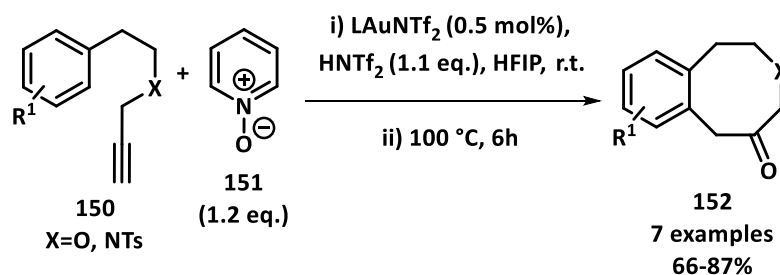
A number of groups have exploited gold catalysis in order to effect the ring closure of 8-membered rings. This is typically effected *via* the catalytic use of Au<sup>I</sup> acting as  $\pi$ -acids on terminal alkynes,<sup>122</sup> allowing for nucleophilic addition to form the ring. Sawamura *et al.* effected the 8-exo-dig cyclisation of silyl enol ethers **146** through the judicious usage of large encumbering alkyne ligands (Scheme 3.18).<sup>123</sup>



Scheme 3.18 – Au catalysed ring closure effected by large phosphine ligands.

This allowed access to a number of fused bicyclic 8 membered rings **147**, and a number of 8-membered rings **149** from linear enol ethers **148**. It was theorised that the increase of steric bulk created a “semi-hollow” steric environment with forced the 8-membered ring into a reactive conformation, overcoming entropic factors disfavouring cyclisation. However, while impressive it must be noted that to achieve high yields catalyst loadings were somewhat high (5 mol%) and in the absence of *gem*-disubstitution on the ring further favouring ring closure *via* the Thorpe-Ingold effect yield was much lower (9-22%).

While the methodology was more successful in 7-membered rings, Zhang *et al.* utilised one-pot umpolung cyclisation utilising pyridine *N*-oxide **151** insertion into alkynes **150**, followed by an electrophilic aromatic substitution to furnish 8-membered ketones **152** (Scheme 3.19).<sup>124</sup>

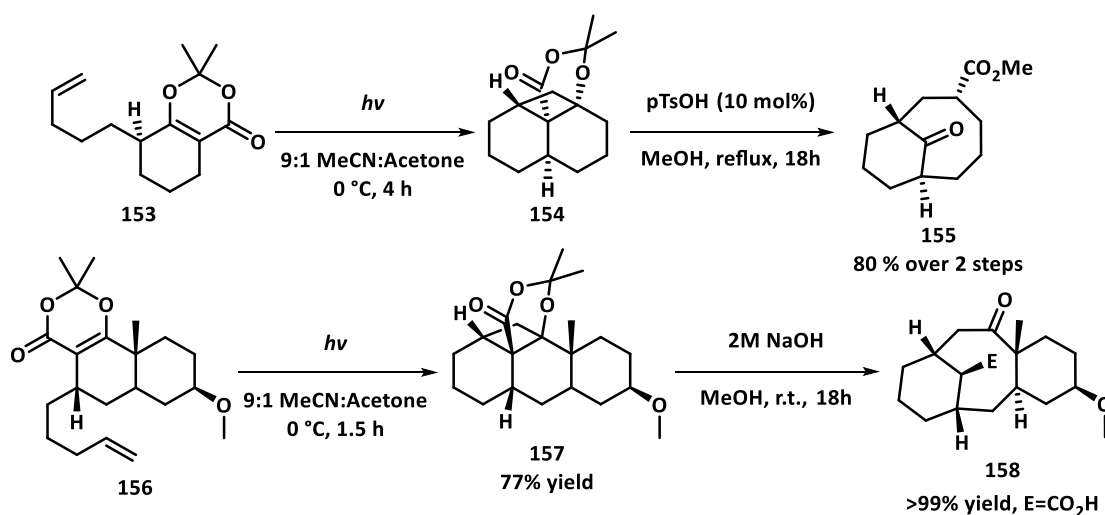


Scheme 3.19 – Au catalysed ring closure via a formal umpolung aldol reaction.

While yields attained were good to excellent and the transformation was mechanistically interesting due to the electrophilic aromatic ring closure mimicking an umpolung enolate disconnection, the scope for this transformation in 8-membered rings is limited to 8 examples and generally in a mixture of isomers. This was posited to arise from *spiro* intermediates rearranging, and as such limits the efficacy of the method.

### 3.1.6. Synthesis of 8-Membered Rings via Ring expansions, Fragmentations and Rearrangements

Many interesting syntheses of 8-membered rings arise from ring expansions and rearrangements. This can circumvent many of the issues associated with the methods disclosed above. The DeMayo reaction has been exploited in multiple examples to synthesise 8-membered carbocycles and 8-membered natural product like fragments, such as **155** and **158**. The carbocyclic fragment is formed *via* a photochemical [2+2] and basic ring opening of the cyclobutanyl intermediate, such as **154** and **157** and has been exploited in high yield (Scheme 3.20).<sup>125, 126</sup>

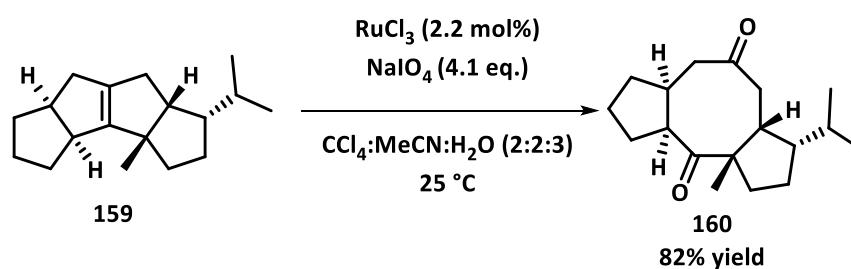


**Scheme 3.20** – DeMayo ring expansions forming taxane-like fused ring structures **155** and **158**.

Frequently, the starting materials for these reactions are easily accessed cyclohexenones or unsaturated ketone and ester molecules, and in intramolecular ring closures can access complex carbocyclic ring structures. However, the generality of the method can be called into question. Intermolecular [2+2] reactions are far less

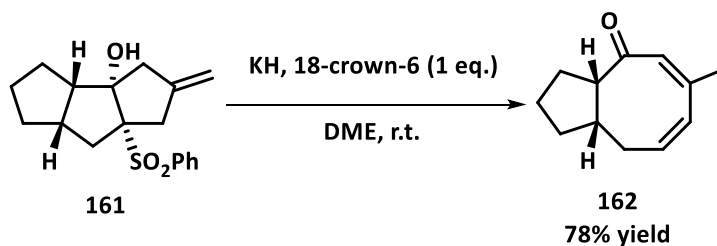
efficient,<sup>127, 128</sup> and substrates for the intermolecular ring expansion must be accessed over multiple synthetic steps.

Fragmentations of other ring systems have also been exploited to great effect. Mehta *et al.* synthesised an 8-membered ring **160** *via* a Lemieux-Johnson reaction to effect ring opening of a tetrasubstituted double bond in **159** (Scheme 3.21).<sup>129, 130</sup>



Scheme 3.21 – Formation of **157** via a Lemieux-Johnson ring fragmentation of **156**.

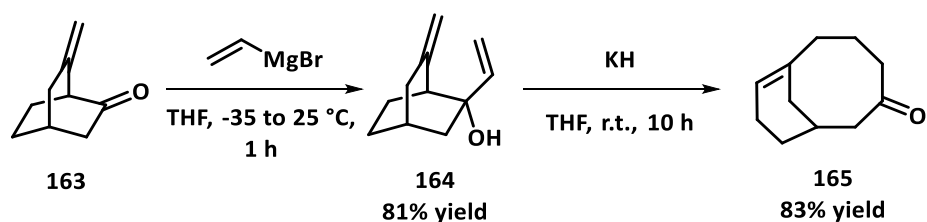
Furthermore, Trost *et al.* utilised the anion stabilising character of sulfones in **161** to effect a basic ring opening in good yield (Scheme 3.22).<sup>131</sup>



Scheme 3.22 – Grob fragmentation of **161** to an 8-membered enone **162**.

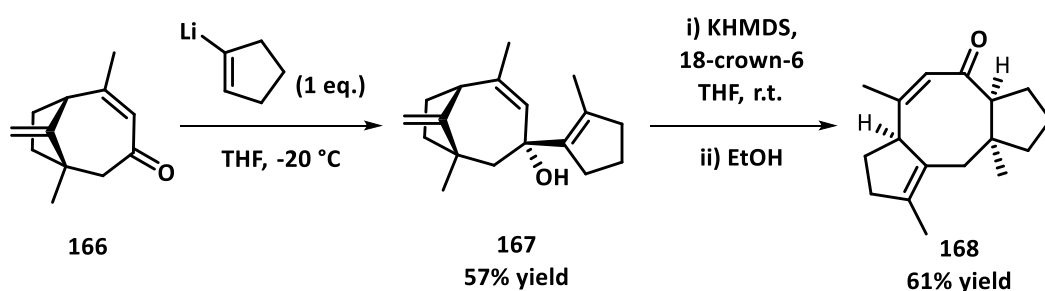
These methods are, like the DeMayo ring expansion, marred by the number of synthetic steps required to synthesise the desired starting materials.

Rearrangements have been applied to medium ring synthesis with some success. The appeal of utilising sigmatropic rearrangements for 8-rings is akin to the appeal of their deployment in tetracene synthesis (see Chapter 2): the concision of making and forming multiple bonds in a single step shortens the route to the desired molecule. For example, Martin *et al.* demonstrated that the carbocyclic taxane ring system **165** could be simply accessed *via* an oxy anionic Cope rearrangement of **164** through the simple addition of vinyl magnesium bromide to the ketone **163**, in good yield (Scheme 3.23).<sup>85, 132</sup>



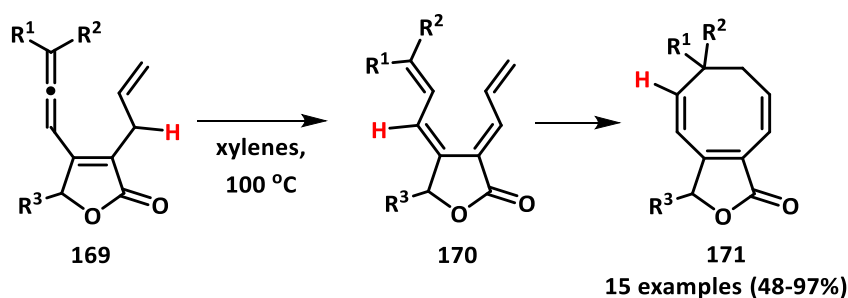
Scheme 3.23 – Taxane 8-ring system **165** formed via an oxyanionic Cope rearrangement

Similarly, Paquette *et al.* exploited the same reactivity and the stereoretentive nature of the sigmatropic rearrangement to achieve the synthesis of more complex carbocycle **168** with complete diastereocontrol (Scheme 3.24).<sup>133</sup>



Scheme 3.24 – Ophiobolin-like 8-ring system **168** formed via an oxyanionic Cope rearrangement

Ma and Gu report a fascinating cascade of rearrangements to form a range of cyclooctatrienes **171** (Scheme 3.25).<sup>134</sup>



Scheme 3.25 – Pericyclic cascade approach to cyclooctatrienes **171** initiated by a [1,5]-hydride migration.

The putative mechanism involves a [1,5]-hydride shift to form a tetraene intermediate **170** which then undergoes a thermal  $8\pi$ -electrocyclisation. The transformation was appealingly tolerant of substitution, required no catalysts or other reagents and was entirely atom efficient. However, the starting allene required multiple synthetic steps to access.

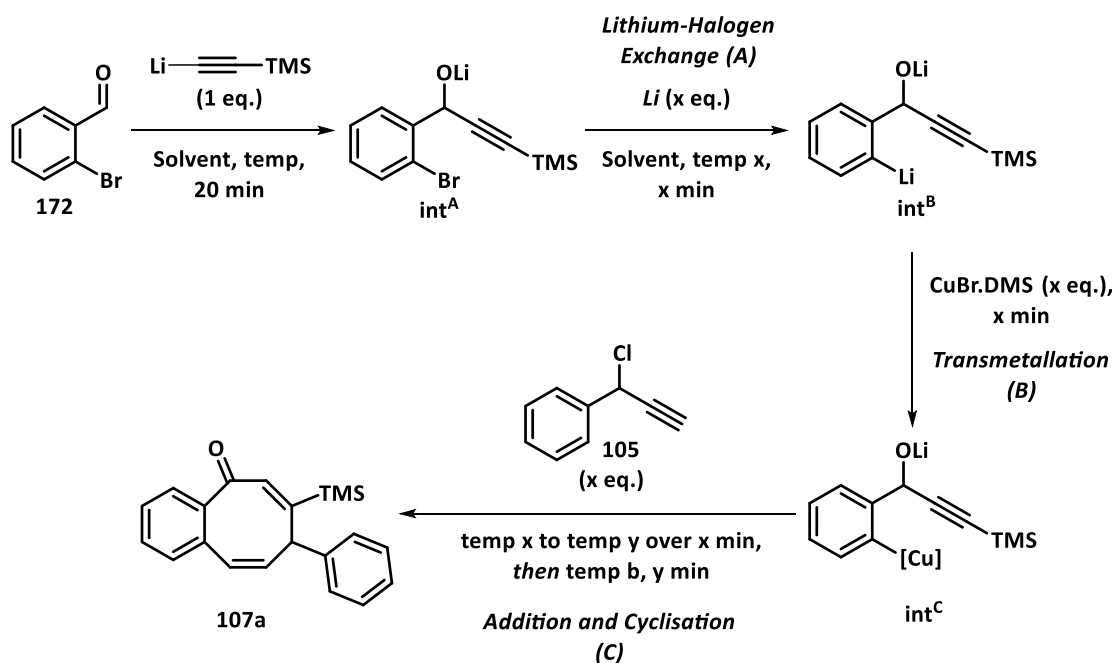
While there are multiple variants of these kinds of transformations well studied within the literature, they are typical of the drawbacks associated with these transformations. They require multiple steps to synthesise the required intermediates and are often limited to specific substitution patterns.

While many more diverse variations upon these reactions exist for the synthesis of 8-membered rings,<sup>135</sup> the brief survey above should make clear some common limitations: a) many of the routes suffer from multiple synthetic steps to access 8-membered rings, b) in different ways, many of the routes can be limited in scope by meagre tolerance to substitution and c) expensive metal catalysts and/or high catalyst loadings are required. As such, a one-pot, multicomponent reaction furnishing 8-membered rings would likely avoid the shortfalls of the methods disclosed above.

## *3.2. Results and Discussion*

### *3.2.1. Optimisation and Mechanistic Investigation*

With the initial result in hand, efforts were directed toward the optimisation of the reaction conditions (Scheme 3.26).



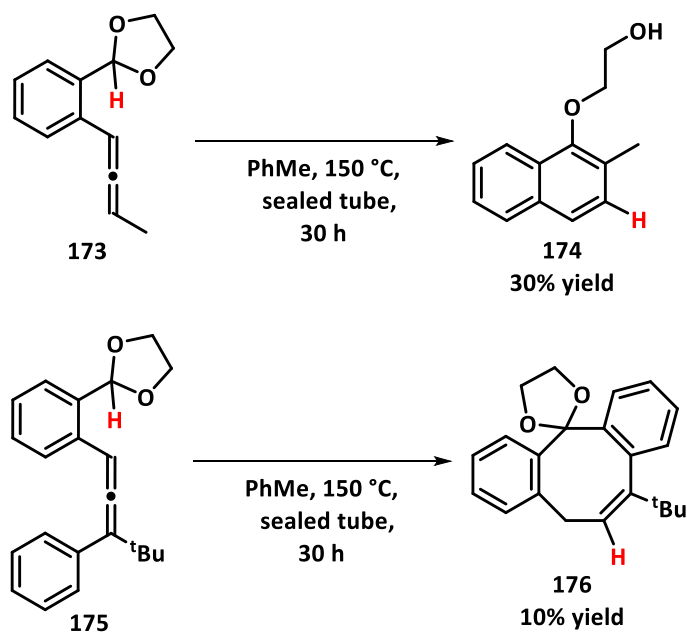
Entry	Solvent	Li-Halogen Exchange Conditions (A)	Transmetallation Conditions (B)	Addition-Cyclisation Conditions (C)	Yield (%)
1	Et <sub>2</sub> O	<sup>t</sup> BuLi (2 eq.), -50 °C, 20 min	(1 eq.), -50 °C, 20 min	(1 eq.), -50 °C to r.t. over 300 min	>10
2	Et <sub>2</sub> O	<sup>n</sup> BuLi (1 eq.), 0 °C, 10 min	(0.5 eq.), -50 °C, 5 min	(0.5 eq.), -50 °C to 10 °C over 72 min	14
3	THF	<sup>n</sup> BuLi (1 eq.), 0 °C, 15 min	(0.5 eq.), -50 °C, 10 min	(0.5 eq.), -50 °C to 10 °C over 72 min	53
4	THF	<sup>n</sup> BuLi (1 eq.), 0 °C, 15 min	(0.5 eq.), -50 °C, 60 min	(0.5 eq.), -50 °C to -10 °C over 90 min; kept at -10 °C for 60 min	70
5	THF	<sup>n</sup> BuLi (1 eq.), 0 °C, 15 min	(0.5 eq.), -50 °C, 60 min	(0.5 eq.), -50 °C to -10 °C over 90 min; kept at -10 °C for 120 min	35

**Scheme 3.26** – Optimisation of the 8-ring cascade. Entries 1-4 were obtained by Dr Laurence Burroughs and Omkar Kulkarni.

The initial intermediate A was formed via the addition of TMS-acetylene to bromoaldehyde **172**, followed by a subsequent lithium halogen exchange to give intermediate B. The organolithium intermediate is transformed to the copper intermediate C via transmetallation, and finally propargyl chloride **105** is added (Scheme 3.27). Alteration of the solvent from Et<sub>2</sub>O to THF resulted in a marked improvement in the yield. Furthermore, forming the organocuprate instead of the organocopper intermediate by reducing the equivalents of CuBr.DMS to 0.5 with respect to the aryllithium intermediate further improved the yield. Interestingly, increasing the transmetallation time also improved the yield considerably, and

warming the reaction from -50 °C to -10 °C over 1 h, then holding the temperature at -10 °C returned a 70% yield as assessed by GC. As such these conditions were carried forward as the standard reaction conditions.

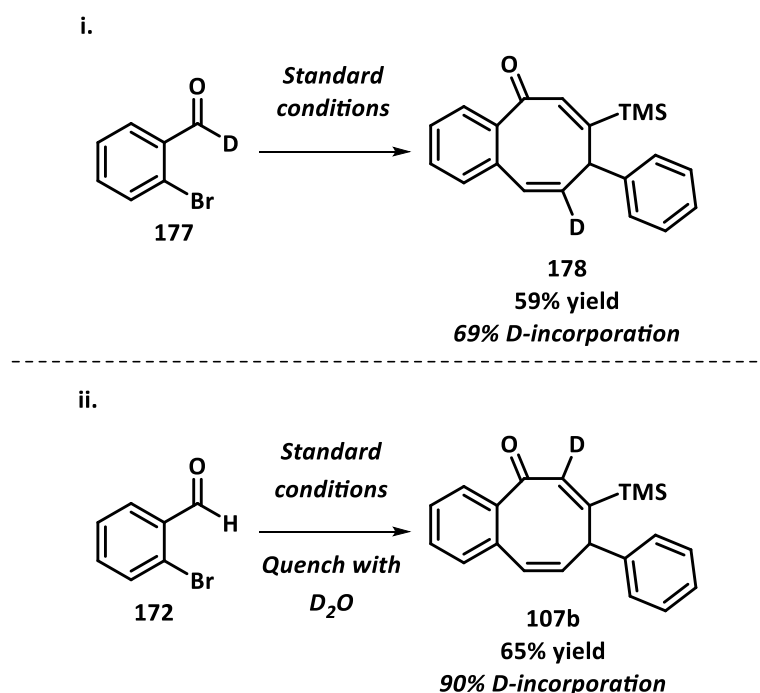
With an optimised procedure in hand, efforts were then directed toward establishing the mechanism of the reaction. As stated in the introduction, it was posited that the propargyl alcohol formed *via* a Cannizzaro-like displacement of a hydride alpha to oxygen, subsequently undergoing a nucleophilic attack on the allene, or *via* a [1,5]-hydride shift. The allylic anion subsequently generated then attacks the pendant ynone in a Michael addition, generating a allenolate anion, which upon quenching the reaction forms the 8-membered carbocycle **107a**. [1,5]-hydride migration to an *o*-allene is preceded within the literature. Vidal *et al.* utilised the migration initiate a  $6\pi$ -electrocyclisation reaction from the initial acetal **173** to form naphthalene **174**, and in the case of aryl substituted allene **175** an 8-membered ring **176** in low yield *via* an  $8\pi$ -electrocyclisation (Scheme 3.27).



**Scheme 3.27** – Synthesis of naphthalene **174** and 8-membered ring **176** initiated by a [1,5]-hydride shift.

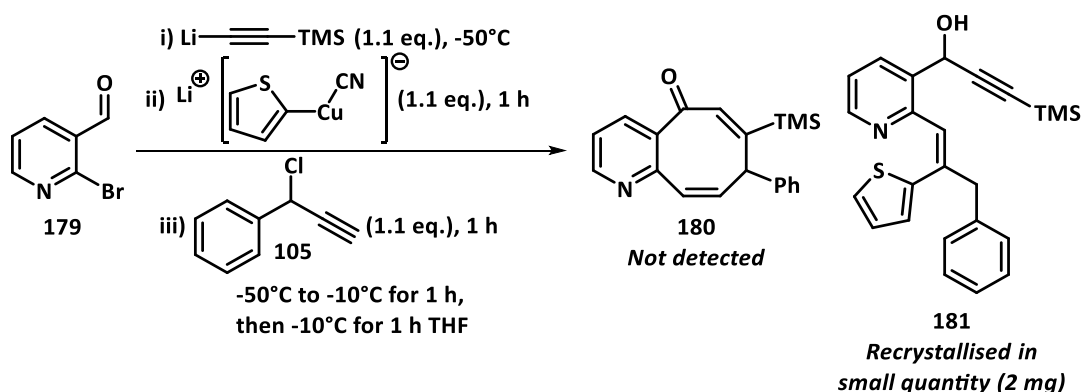
Furthermore, the reaction disclosed in Scheme 3.25 utilises the same hydride shift to initiate the formation of a series of 8-membered rings **171**. Where these differ from the organocuprate method discussed here is that the allenes must be synthesised and isolated, unlike the one pot method discussed herein.

To probe this, the D-aldehyde **177** was submitted to the reaction conditions to assess whether the deuterium would be retained in the reaction. It was observed that the expected deuterated 8-ring **178** was formed in 59% yield and with 69% deuterium incorporation, strongly implying an intramolecular displacement of hydride is in operation in the putative mechanism. Furthermore, evidence for the Michael addition of an allyl anion was given from quenching the reaction with D<sub>2</sub>O, which gave the deuterated **107b** in 65% yield and with 90% D-incorporation, strongly implying that the final intermediate was the allenolate anion posited (Scheme 3.28).



**Scheme 3.28** – Experimental corroboration of the putative 8-ring cascade mechanism via deuterium labelling.

Further experimental evidence for the mechanism was gathered from attempts to improve the reaction conditions. It must be noted that the generation of the cuprate in the reaction meant that for every reductive elimination of the aryl group to the propargyl chlorides, one equivalent of the propargyl alcohol is unreacted, meaning that the transformation is quite atom poor. Therefore, an attempt was made to form the higher order organocuprate from lithium 2-thienylcyanocuprate (Scheme 3.29).<sup>136</sup>

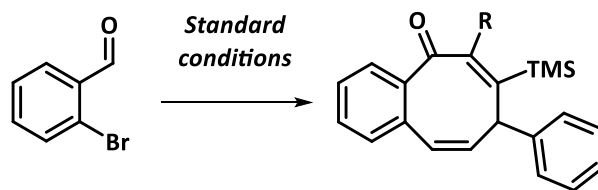


Scheme 3.29 – Formation of an unexpected alkene **181**.

Instead of the expected pyridyl 8-ring **180**, a 2 mg quantity of the propargylic alcohol **181** was recrystallised from the reaction mixture. This unexpected product can be assumed to have been formed by the reductive elimination of the 2-thienyl group to the allene over the migration of the hydride, which supports the mechanism stated above. Furthermore, the double bond geometry of **181** implies that the allenyl anion isomerises to the required geometry for the Michael addition. The alkene geometry formed in the transfer of the thiophene would be expected to be the (*E*)-alkene, however, the isolation of the (*Z*)-alkene shown above implies isomerisation does occur.

### 3.2.2. Diversification of the 8-Ring Structure

The scope of trapping the 8-ring with electrophiles was further investigated. Various electrophiles were successfully reacted with the allenolate (Scheme 3.30).



8-ring	Electrophile	R	Yield (%)
<b>107a</b>	H		72
<b>107b</b>	D		65
<b>107c</b>	Allyl Br		17 (61)
<b>107d</b>	SMe		52
<b>107e</b>	I		58
<b>107f</b>	CO <sub>2</sub> H		49
<b>107g</b>	DEAD		0
<b>107h</b>	ClSn(Bu) <sub>3</sub>		0

**Scheme 3.30** – Synthesis of a range of substituted 8-rings **107a-h**. Compounds **107e** & **f** were obtained by Dr Lee Eccleshare.

However, reacting larger electrophiles such as DEAD and ClSn(Bu)<sub>3</sub> gave no yield of the desired 8-ring. However, trapping with other nucleophiles tended to give good yields of the products. Where poor yields were reported, increasing the equivalents allowed for a higher yield to be obtained (upon increasing the number of equivalents of allyl bromide from 2.5 to 4, the yield of **107c** improved dramatically, see Scheme 3.31). Reacting the 8-ring with I<sub>2</sub> and CO<sub>2</sub> allows for the further diversification of the 8-ring *via* Suzuki cross couplings and amide couplings.<sup>137</sup>

### 3.3. Further Work

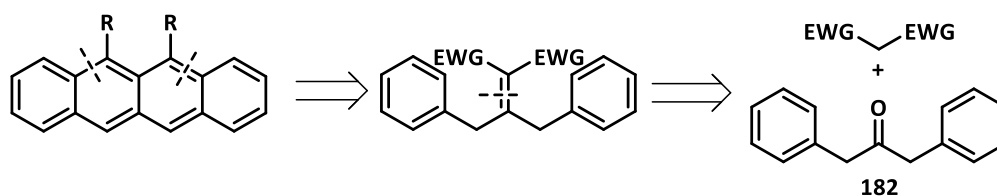
Further work into the scope of the reaction in the varying of the alkyne and propargyl chloride has been published, along with further diversification of the 8-membered enone structures.<sup>137, 138</sup>

# Chapter 4

## *Knoevanagel Cyclisation Approach to Tetracenes*

## 4.1. Introduction

A clear drawback to the sigmatropic cascade reaction is the stereochemical requirement to generate higher yields of tetracene, and currently no method exists enriching the *rac* diastereomer in the diols made. Future investigations were undertaken into other methods which could generate the tetracene core from achiral starting materials. By a series of disconnections about the double bond in the centre of the tetracene rings, it was hypothesised that the molecule could be generated in two steps from the Knoevenagel condensation of a reactive methylene compound and 1,3-diphenyl ketone **182**, followed by a Friedel-Crafts acylation (Scheme 4.1).



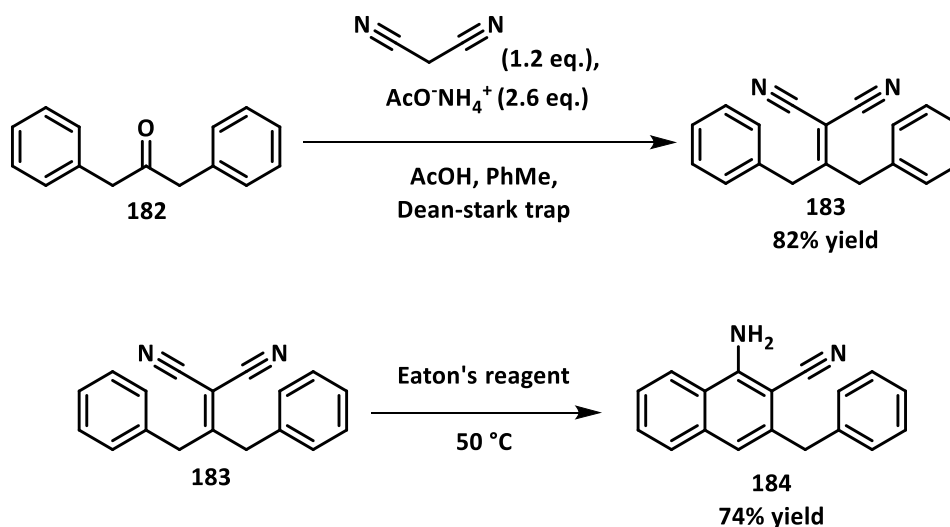
**Scheme 4.1** – Proposed disconnection of tetracene from 1,3-diphenyl propanone **182**.

This method is attractive as evidenced by the large number of reported facile methods for Knoevenagel condensations in the literature,<sup>139-141</sup> and that the cyclisation of aromatic rings and 2-methylenemalononitrile moieties is well known.<sup>142</sup> This method could therefore be a highly yielding and rapid synthesis of tetracene. Indeed, this transformation has been reported in a series of papers by Duffraise *et al.*<sup>143</sup> by the generation of 2-(1,3-diphenylpropan-2-ylidene)malononitrile and a subsequent cyclisation to form the 5,6-perdiamine tetracene *via* two sequential cyclisations. Furthermore, calculations using the same basis set above predicted that the tetracene would possess a lower HOMO-LUMO gap (2.42 eV) compared with the other tetracenes made by the sigmatropic cascade reaction.

## 4.2 Results and discussion

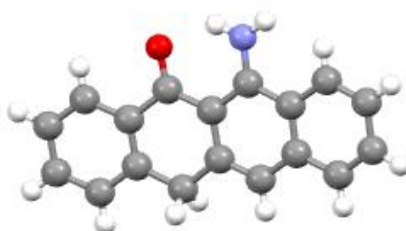
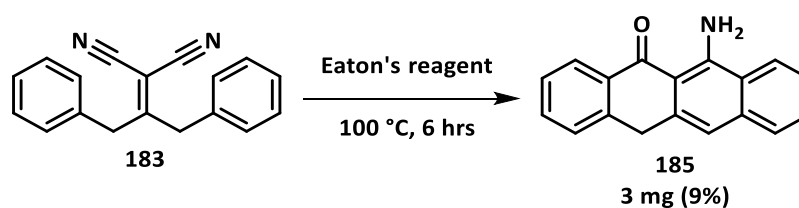
The desired alkene was synthesised *via* a Knoevenagel condensation with **182** and azeotropic removal of water *via* a Dean-Stark trap in good yield. On treating **183**

with Eaton's reagent and heating to 50 °C for 90 mins, the major product was the mono-ring closure product **181** in good yield (Scheme 4.2).



**Scheme 4.2** – Synthesis of **183** and **184**.

Further attempts at these conditions to force the second cyclisation in **184** only returned the naphthalene **184**. Attempting more forcing conditions to promote the double closure of **183** were then attempted, including higher temperatures in Eaton's reagent, resulting in a large loss of material, and the formation of small amounts of the oxidised *peri*-aminotetracene **185**, similarly to that reported by Dufraise and observed in the crystal structure of the isolated product (Scheme 4.3).

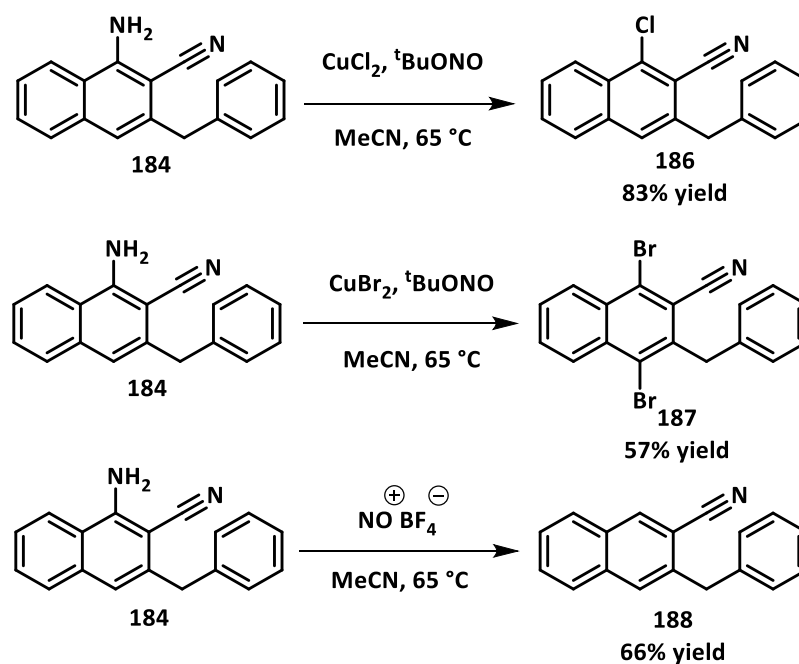


**Scheme 4.3** – Formation of by-product **185**.

Furthermore, attempts to cyclise using PPA produced no cyclisation in the starting alkene, and attempts with sulfuric acid produced large volumes of insoluble

red salts. This minor product may have been the only product detected due to the greater stability of the mono ring closure product compared with the desired 5,6-diamine tetracene: the  $\text{-NH}_2$   $\sigma_{\text{para}}=-0.66$  making the acene structure very electron rich and therefore reactive and hard to isolate.<sup>144</sup> Indeed, the high lying HOMO (-4.68 eV) calculated at the B3LYP/6-31+G(d,p) level of theory agrees with the level at which oxidation is highly likely due to inductive elevation as evaluated by Nakano *et al.*<sup>10</sup> Furthermore, it was found that the rate of oxidation of the aromatic amine to the carbonyl was accelerated by the lack of steric substitution *ortho* to the amine group. Attempts to remove the amines from the final tetracene product were then attempted. As might be expected, attempts to reduce the *bis*-nitrile to the aldehyde using DIBAL-H resulted in complex mixtures, most likely due to the conjugate addition of the hydride to the alkene which probably acts as an excellent Michael acceptor.

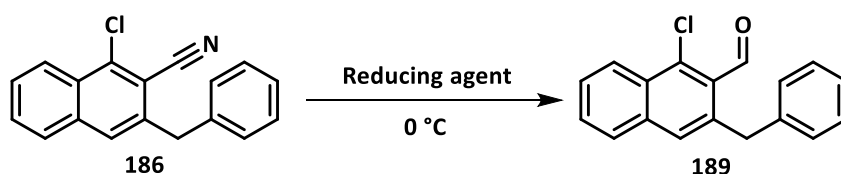
To improve the processability of the tetracene core derived from the second cyclisation, it was envisaged that the aromatic amine could be removed from the intermediate naphthalene **184** through a Sandmeyer reaction to introduce various halide groups, and reduce the nitrile to the corresponding aldehyde and effect a Friedel-Crafts cyclisation with a suitable Lewis acid. Fortunately, in preliminary reactions, the amine could be halogenated in good yield utilising variations upon Doyle *et al.* one-pot Sandmeyer conditions with cupric halides and <sup>t</sup>BuONO (Scheme 4.4).<sup>145</sup>



*Scheme 4.4 – Syntheses of 186-188.*

Interestingly, the  $\text{CuBr}_2$  brominated the naphthalene *para* to the amine as well as replacing the nitrogen group, which can perhaps be rationalised as a SET halogenation due to the use of a cupric halide (Scheme 4.4).<sup>146</sup> Attempts to form the fluoride *via* a Balz-Schiemann reaction with nitrosonium tetrafluoroborate deaminated the naphthylamine in good yield.

Attempts were then made to reduce the nitrile of **186** to naphthaldehyde **189**. It was envisaged that the nitrile could be reduced selectively to the aldehyde using an aluminium hydride.<sup>147</sup> Unfortunately, when  $\text{LiAlH}_4$ , DIBAL-H and Superhydride were trialled as reducing agents, the formation of the aldehyde was nil or was very poorly yielding (Scheme 4.5).



Reducing agent	Yield (%)
LiAlH <sub>4</sub>	0
DIBAL-H	16
LiBHET <sub>3</sub>	18

**Scheme 4.5** – Attempted reductions of **186**.

Furthermore, when the modest amount of aldehyde was heated with BF<sub>3</sub>.OEt, no cyclisation to the desired 5-chlorotetracene was observed. In addition to these methods attempts were made to effect the cyclisation *via* reduction to the nitrile to the more reactive imine using Raney Nickel, however this attempt returned the starting material with no tetracene observed. Furthermore, an envisaged anionic cyclisation of the starting naphthalene was attempted with LDA, although again this did not yield any of the desired product. The failure of all these approaches may be attributed to the naphthyl ring: the  $\pi$  to  $\pi^*$  donation from the naphthylene to the nitrile deactivating it toward addition of nucleophiles, hence the difficulty of the reduction.

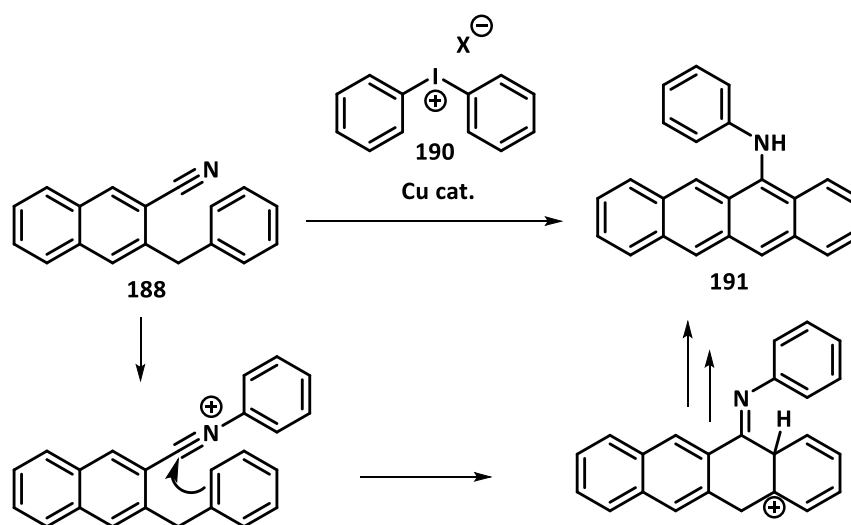
### 4.3 Future Work

The primary issue from these preliminary studies toward aminotetracenes has therefore yielded two observations. Firstly, that the free amine may be too electron-donating to the tetracene, making it more sensitive to oxidation and decomposition, and secondly that the second nitrile closure requires more forcing conditions due to the electronic deactivation of the nitrile. As such a proposed future route to the aminated tetracenes may be to utilise synthetic conditions which activate the nitrile and deactivate the amine on the aromatic ring formed.

An excellent candidate for this could be the formation of an intermediate aryl nitrilium species *via* arylation. Multiple heterocycles have been accessed *via*

transiently generated aryl and vinyl nitrilium species generated from aryliodonium salts **190**. The aryl nitrilium is much more electrophilic than the parent nitrile, and as a result more rapidly undergoes nucleophilic attack, and this reactivity has been exploited to generate a variety of heterocycles in copper catalysed [2+2+2] additions.<sup>148-150</sup>

It could therefore be proposed that arylation of the deaminated naphthalene **190** could react in a similar manner, furnishing the 6-exo dig cyclised product and rearomatizing to the desired tetracene **191** (Scheme 4.6).



*Scheme 4.6 – Proposed nitrilium cyclisation of 188.*

Furthermore, ability to introduce electron-poor aromatic rings on the amine will temper the mesomeric donation to the core of the tetracene allowing for potential tuning of the electronics for stability.

# Chapter 5

## *Carbometallation Approach to Tetracenes*

### Publications from this section

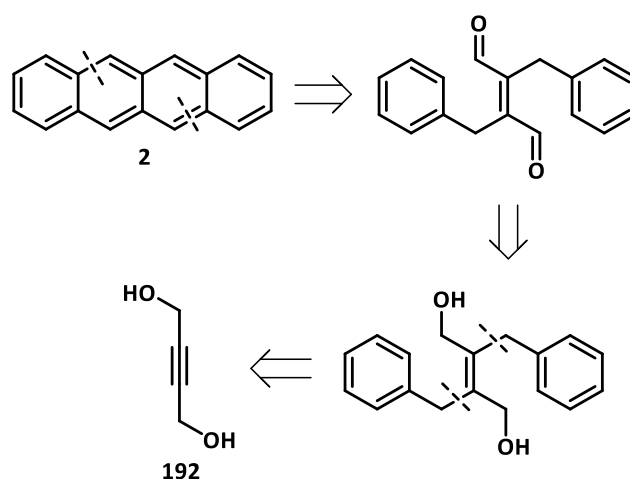
1. Straightforward Synthesis of 2- and 2,8-Substituted Tetracenes, S. Woodward, M. Ackermann, S. Ahirwar L. Burroughs, M. R. Garrett, J. Ritchie, J. Shine, B. Tyril, K. Simpson, P. Woodward *Chem. Eur. J.* **2016**, *23*, 7819-7824.

### Acknowledgements

- The results disclosed in Scheme 5.11 were attained by Dr Laurence Burroughs.
- Compounds **197d**, **203c-l** and **202 b, f & m** were synthesised by Dr Mary-Robert Garrett.
- Compounds **199g** and **201g** were synthesised by Miriam Ackerman.
- Compound **199i** was synthesised by Saurabh Ariwar.

## 5.1. Introduction

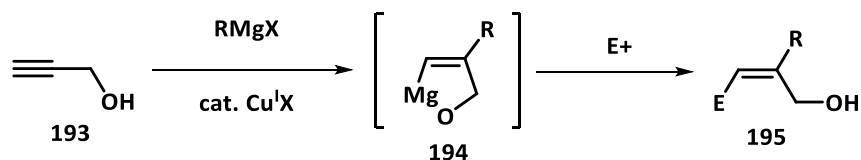
Owing to the lack of success from the sigmatropic rearrangement and Knoevenagel cyclisation routes a novel disconnection was sought. As stated in chapter 1, many of the synthetic routes reported within the literature depend upon Lewis acid-mediated Friedel-Crafts acylations. As previously discussed, these approaches typically involve a single ring closure, and multiple steps to install the pertinent functional groups. It was envisaged that a double ring closure from  $C_2$  symmetric **x** would instead limit the number of synthetic steps required to furnish tetracene *via* a ring closing method by forming the two central tetracene rings *via* a double Bradsher closure in a single step (Scheme 5.1).



**Scheme 5.1** – Proposed disconnection of tetracene **2** to 1,4-butyne diol **192**.

The synthesis of tetrasubstituted alkenes is a well-studied synthetic challenge. One of the favoured routes is carbometallation of alkynes followed by electrophile trapping, providing a reactive handle for further elaboration.<sup>151</sup> This method presents two issues. Firstly, regioselectivity and secondly stereoselectivity of the alkenes formed. Many groups have studied the use of directing groups for carbometallation in a regiocontrolled manner, utilising pyridines,<sup>152</sup> carbamates,<sup>153</sup> ethers<sup>154</sup> and unprotected alcohols.<sup>154, 155</sup> Unfortunately, within the multitudinal carbometallations studied within the literature, the majority exhibit *cis* regioselectivities.<sup>156</sup> Pleasingly, there are many carbometallations of alkynes which display the desired regioselectivity and (*E*)- stereoselectivity from organomagnesium and organozinc reagents in the presence of unprotected alcohols<sup>22, 157-160</sup> or esters.<sup>161</sup> This is putatively explained by

the formation of a 5-membered chelate **194** from the alcohol to the formed vinyl magnesium reagent formed, ensuring anti-selectivity and regioselectivity in the product alkene **195** (Scheme 5.2).



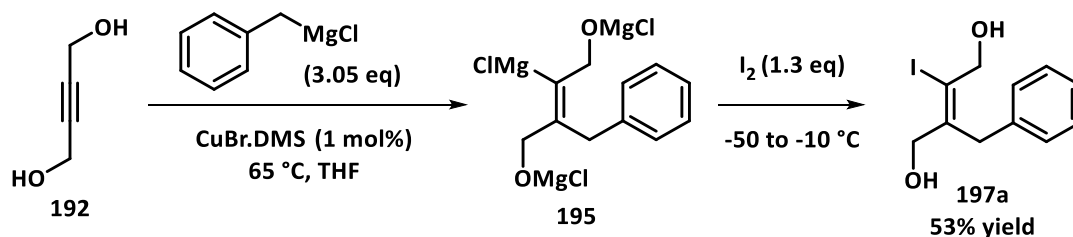
**Scheme 5.2** – Proposed *trans*-selective carbometallation of propargyl alcohol **193**.

This is corroborated by some experimental evidence that indicates that increasing the alkyl chain distance between the alcohol and alkyne of propargyl alcohols severely erodes the yield as the chelate is less entropically favoured to form.<sup>22</sup> Furthermore, utilising unprotected alcohols as directing groups allows for the oxidation to the desired aldehyde for the Bradsher closure.

## 5.2. Results and Discussion

### 5.2.1. Carbometallation and Negishi Cross-Coupling of Vinyl Iodides

As such a carbometallation of but-2-yne-1,4-diol **192** with benzylmagnesium chloride was envisaged to test the viability of the proposed disconnection (Scheme 5.3).

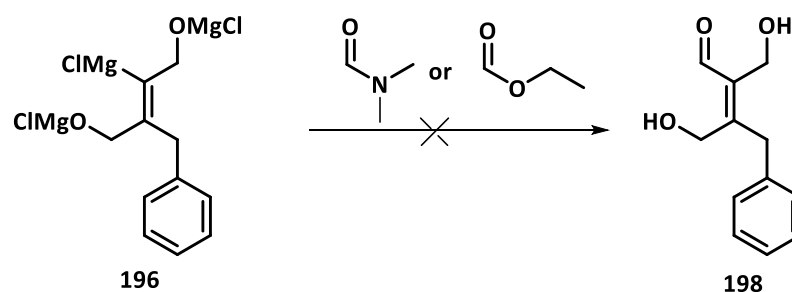


**Scheme 5.3** – Proposed *cis*-selective carbometallation of propargyl alcohol **189** and synthesis of vinyl iodide **49**.

The carbometallation was attempted and formed the desired trisubstituted alkene upon quenching with  $\text{NH}_4\text{Cl}$  in 74% yield. Initial attempts were then made to form the desired diol in one step with the addition of benzyl chloride and  $\text{Co}(\text{Acac})_2$  to effect an alkylation with the intermediate vinylmagnesium chloride **195**.<sup>162</sup> However, this proved to be fairly capricious and low yielding, and attempts were made to trap

the intermediate vinylmagnesium with electrophiles to effect a two-step synthesis of the desired C<sub>2</sub>-symmetric synthon.

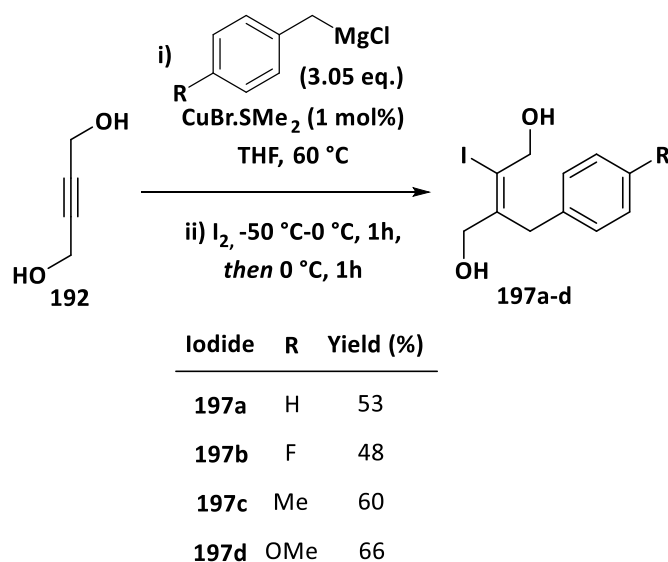
Considering the difficulty of cross coupling the vinyl iodides, efforts then turned toward the use of other electrophile substituents that could be cross coupled. The cross-couplings of tosylhydrazones with transition metal catalysts are well developed reactions,<sup>163</sup> and one pot formations of tosylhydrazones from aldehydes and subsequent metal free couplings to boronic acids are known and would be an excellent and general alternatives to transition metal-catalysed cross couplings.<sup>164</sup> However, attempts to trap the Grignard intermediate with DMF and ethyl formate did not return the desired  $\alpha,\beta$ -unsaturated aldehyde (Scheme 5.4).



*Scheme 5.4 – Failed synthesis of 198.*

Attempts to form the vinyl boronic acid *via* trapping of the intermediate Grignard with (iPrO)<sub>3</sub>B were made to form the cyclic hemi-boronic ester to attempt the reverse coupling to phenyltosylhydrazone. Similar cyclic borates have been synthesised and have shown to be competent reactants which have been utilised in Suzuki and Chan-Lam cross couplings, Petasis reactions and oxidations.<sup>165-169</sup> Unfortunately, it proved similarly difficult to form the cyclic hemi-boronic acid, with no product observed. Attempts to form the vinyl sulphide by trapping with (PhS)<sub>2</sub> also failed, and as such new electrophiles were sought.

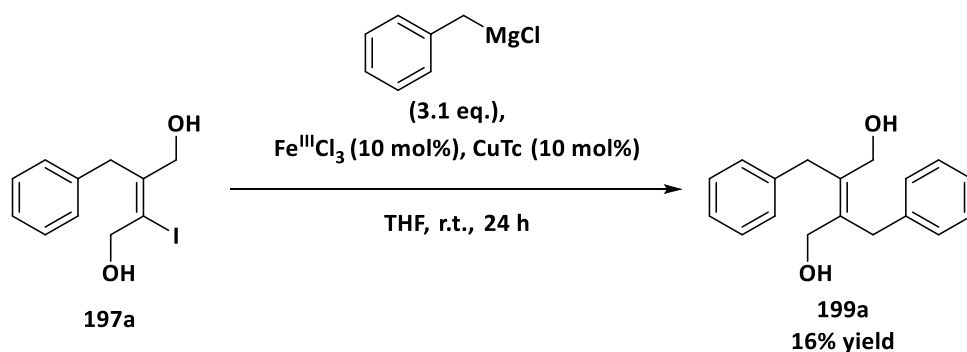
Pleasingly, the desired iodide **194a** could be synthesised in a modest yield of 53% (Scheme 5.5).



*Scheme 5.5 – Synthesis of vinyl iodides 197a-d*

Similarly substituted iodides **197a-d** could be synthesised in moderate to good yield by trapping with iodine, offering a range of substituted lynchpin vinyl iodides. The issues with the trapping of various electrophiles could perhaps be rationalised as a function of the pKa of the conjugate bases formed, with more stable anionic leaving groups facilitating the nucleophilic attack of the vinyl Grignard intermediate. The values pKa values for the halogens are many orders of magnitude lower in comparison the alcohols and thiols that would be displaced in using the electrophile trapping attempts above (pKa  $^-I = -8.56$  vs  $^-SPh = 6.50$  in water at 25°C).<sup>170</sup>

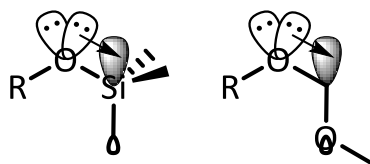
Initial attempts with Pd and Ni catalysis to couple the vinyl iodide to benzyl halides had returned no yield of the desired diol. Consequently, efforts were turned toward the use of iron catalysis, which confers the benefit of general mild conditions, less toxic reactants and a well-studied array of  $sp^2$ - $sp^3$  couplings.<sup>171</sup> The  $Fe^{III}Cl_3/CuTc$  cross coupling developed by Hamze *et al.* was attempted, which pleasingly returned the desired diol **199a**, but in an unsatisfactory yield of 16% (Scheme 5.6).<sup>172</sup>



**Scheme 5.6** –  $\text{Fe}^{\text{III}}\text{Cl}_3/\text{CuTc}$  catalysed cross-coupling of vinyl iodide **194a** with benzylmagnesium chloride.

As such attempts to improve the yield through introduction of ligands and additives were undertaken. Changing the iron catalyst to  $\text{Fe}^{\text{III}}(\text{Acac})_3$  had a deleterious effect on the yield, and introduction of various phosphine ligands also had little effect upon the cross coupling with only  $\text{PCy}_3$  matching the yield of the initial conditions. Changing the stoichiometry of the copper and iron also had a modest beneficial effect. Doubling both led to an increase in yield, but individually increasing the CuTc to 20 mol% had a greater effect on the yield over increasing the  $\text{Fe}^{\text{III}}\text{Cl}_3$ . The addition of LiBr increased the formation of the homocoupled dibenzyl product. The addition of NMP also led to a reduction in yield, and TMEDA prevented the formation of the diol entirely (on addition of TMEDA the reaction mixture rapidly formed a solid gel). Across all the reactions, there was a moderate yield of the unreacted iodide, which coupled with the modest increase in the yield of the diol led to the postulate that the benzyl Grignard reagent was reacting too rapidly with the  $\text{Fe}^{\text{III}}\text{Cl}_3$  and deactivating the catalyst.

It was also hypothesised that the primary alcohols were interfering with the cross-coupling reaction, and that by protecting them yield could be maximised, and fewer equivalents of Grignard reagent would be needed. As such, the starting propargyl diol was protected with TMSCl and MOMCl and the transmetalation reattempted. Unfortunately, the reacted diols were completely inert under the carbometallation conditions over 24 h, which can be rationalised by the inductive removal of the lone pair electron density by the Si  $\sigma^*$  orbital and by the C-O  $\sigma^*$  orbital by the anomeric effect, preventing the directing effect and limiting the rate of the reaction, if not preventing it completely (Scheme 5.7).



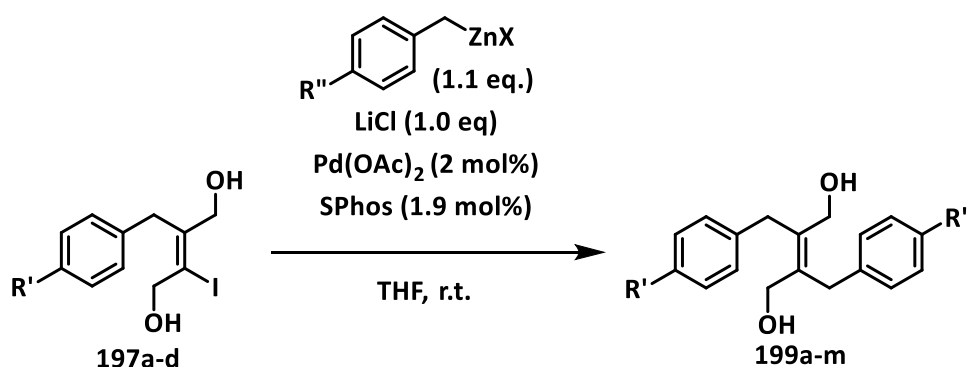
**Scheme 5.7** – Electronic deactivation of protected alcohols

Upon difficulty of the optimisation of the cross-coupling of **197a** using Hamze's conditions and the relative lack of reactivity of the Grignard to various electrophiles, new means of coupling benzyl electrophiles to **199a** were sought. The usage of benzyl zinc halides in  $sp^3$ - $sp^2$  as electrophiles in cross couplings has been reported within the literature in excellent yield and with the presence of unprotected alcohols and amines by Knochel *et al.*<sup>173, 174</sup> High yield of the cross coupled product versus the protonation of the active lithium organozincate halides was rationalised *via* competitive protonation studies with  $i$ PrOH. It was found that the benzyl organozinc halides were less basic than the corresponding alkyl and aryl zinc halides. The aryl and alkyl organozinc halides were chemoselectively protonated, with the benzylzinc halide almost unreacted. This could likely be attributed to the resonance stabilisation of the negative charge on the benzylic position by the benzene ring. As such, the limited basicity of the benzylorganozinc chloride may mean that the transmetallation to palladium is faster than the deprotonation of the diol **197a**.

Pleasingly, performing the reaction with a 1 mol% Pd(OAc)<sub>2</sub>/ 2 mol% SPhos catalyst loading at room temperature in under 30 minutes yielded a 94% return of desired diol **199a** without the need of further purification. However, on repeating the procedure, conversion proved to be capricious. Full conversion could be ensured by reducing the ligand loading to 1 mol% with no erosion of yield and excellent reproducibility. This may offer insight into the mechanism of the cross coupling. The steric bulk of SPhos may well be limiting the oxidative addition to the palladium: the  $14e^-$  complex of the (SPhos)<sub>2</sub>Pd<sup>0</sup> generally considered necessary to participate in a catalytic cycle might be too sterically encumbered. Therefore, the oxidative addition of the vinyl iodide to the (SPhos)<sub>2</sub>Pd<sup>0</sup> might well be inhibited, hence the inconsistency of the 2:1 SPhos: Pd(OAc)<sub>2</sub> stoichiometry.

The reduction of Pd(OAc)<sub>2</sub> can most likely be attributed to the benzylorgano zinc halide, as two equivalents of phosphine to palladium is usually required to reduce Pd<sup>II</sup> to Pd<sup>0</sup> and allow the cross coupling to occur.<sup>175</sup> If this were the case, an excess of SPhos would be required to reduce Pd<sup>II</sup>, which is absent in the reaction conditions. The absence of any oxidant within the relatively mild reaction conditions perhaps precludes the presence of a Pd<sup>II</sup>/Pd<sup>IV</sup> catalytic cycle,<sup>176</sup> however further investigation is required.

Pleasingly, the Negishi cross-coupling conditions proved relatively general, cross coupling with various substituted benzyl zinc halide and heterocyclic equivalents, yielding a wide range of substituted *trans*-benzyl diols (Scheme 5.8).



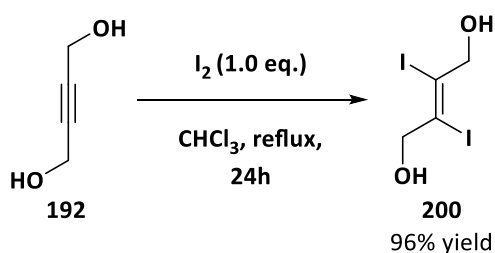
Compound	R'	R''	X	Yield (%)	Compound	R'	R''	X	Yield (%)
199a	H	H	Cl	87	199h	Me	Me	Cl	93
199b	H	F	Cl	96	199i	Me	iPr	Cl	87
199c	H	Ph	Cl	94	199j	Me	Br	Cl	92
199d	H	OMe	Br	82	199k	OMe	OMe	Br	85
199e	H	Me	Cl	84	199l	OMe	Me	Cl	93
199f	F	F	Cl	82	199m	OMe	F	Cl	85
199g	Me	Vinyl	Cl	96					

**Scheme 5.8** – Synthesis of a range of diols **199a-m**. Compound **199g** was synthesised by Miriam Ackermann, compound **199i** was synthesised by Saurabh Ariwhar and compound **199m** was synthesised by Simon Woodward.

Unfortunately, the vinyl bromide was not a competent reaction partner within the established conditions. Given the exemplary ease and celerity of the Negishi cross-

coupling, rapid access to a range of substituted diols offers large scope to the synthesis of a wide range of variably substituted polyaromatic molecules *via* the subsequent oxidation and ring closure.

While the carbomagnesiation of 2-butyne-1,4-diol proved to be general, it must be noted that the synthesis of a symmetrically substituted diol requires large quantities of benzyl organometallic reagents over two steps, and with moderate yields in the carbomagnesiation. As such, it was posited that the (*E*)-diiodide could be a competent partner in a double cross coupling with similar conditions to the monocoupling. Pleasingly, the synthesis of the diiodide is known, although attempts to emulate the literature conditions provided low yields of the desired diiodide **200**.<sup>177</sup> However, stirring 2-butyne-1,4-diol with iodine in chloroform at reflux for 24 h provided the desired *trans*-diiodide **200** in excellent yield (Scheme 5.9).

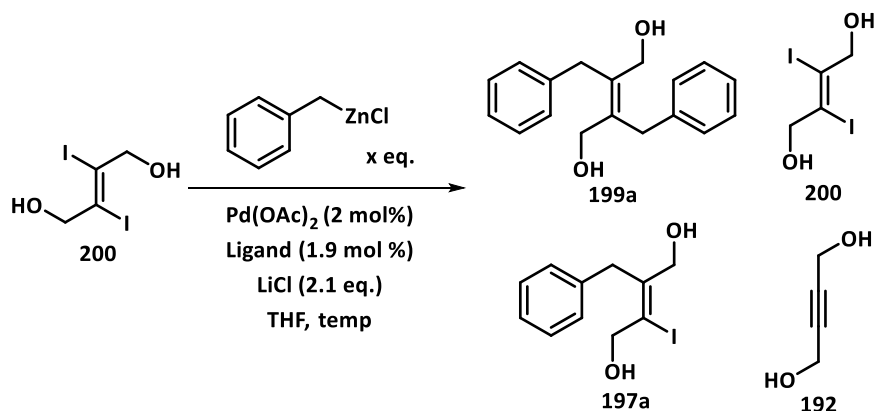


*Scheme 5.9* – Synthesis of a range of diiodide **200**.

Furthermore, the insolubility of the product allowed for the material to be simply filtered and washed with chloroform to provide the desired product in sufficient purity.

The disubstitution was then investigated. Initial runs emulating the reaction conditions using SPhos provided a 34% yield of the product and a larger 66% yield of the diiodinated 2-butyne-1,4-diol. Changing the ligand to Cy<sub>3</sub>P provided a similar but marginally superior yield by NMR in the conditions, and as such was the ligand carried forward across further runs. Attempts with PPh<sub>3</sub> provided a mixture of desired product, diiodinated alkyne and unreacted diiodide, but interestingly the highest yield was of the monocoupled product. Increasing the reaction temperature had the effect of incrementally improving the conversion to the desired product. Furthermore, increasing the number of equivalents of the benzylzinc chloride had a positive effect

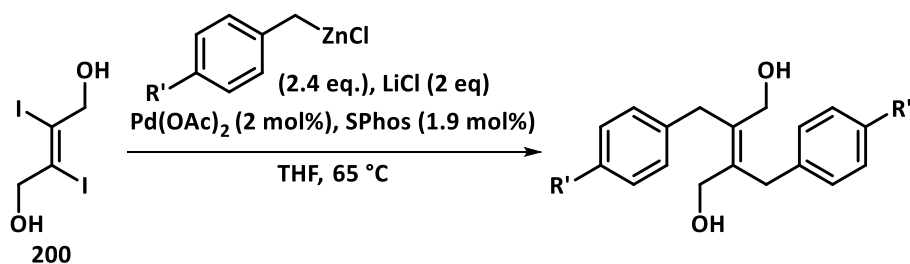
upon the yield, however increasing beyond 2.4 equivalents ceased to favour the cross-coupling. 2.4 equivalents of benzylzinc chloride at 65 °C in THF were therefore selected as the general conditions for the reaction (Scheme 5.10).



Temp (°C)	BzZnCl (eq.)	Ligand	199a:200:197a:193
rt	2.1 eq.	$\text{Ph}_3\text{P}$	24:32:13:31
rt	2.1 eq.	$\text{Cy}_3\text{P}$	34:0:0:66
rt	2.1 eq.	SPhos	35:0:0:65
rt	2.1 eq.	$\text{Cy}_3\text{P}$	37:0:0:63
45	2.1 eq.	$\text{Cy}_3\text{P}$	53:0:0:47
55	2.1 eq.	$\text{Cy}_3\text{P}$	60:0:0:40
55	2.4 eq.	$\text{Cy}_3\text{P}$	67:0:0:33
65	2.4 eq.	$\text{Cy}_3\text{P}$	80:0:0:20

**Scheme 5.10** – Optimisation of a Negishi di-coupling.

With these conditions in hand the scope of the di-coupling was investigated. The conditions produced the desired parent diol in 72% isolated yield (Scheme 5.11).



Compound	R'	Yield (%)
<b>199a</b>	H	72
<b>199h</b>	Me	33
<b>199n</b>	Br	65

*Scheme 5.11 – Synthesis of a range of diols 195a, h & n via a Pd-catalysed decoupling.*

Attempts with other organozinc halides produced only poor to moderate yields, and proved to be less general than the monocoupling. While it provided access to the doubly bromoarylated diol **199n** in good yield (which could not be made *via* the carbometallation due to the 4-Br benzylmagnesium organometallic being inaccessible synthetically), the erosion of yield in changing the substitution made it far less general than the mono coupling.

### 5.2.2. Oxidation of the Diols

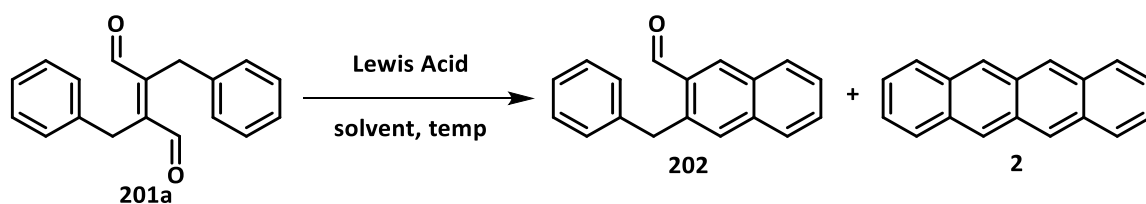
With the desired diols in hand, attention then turned to oxidation conditions to furnish the desired dialdehydes. Of the plethora of oxidation conditions available, the O<sub>2</sub>/Cu<sup>I</sup>/TEMPO catalysed conditions developed by Stahl *et al.* appealed due to the generality of the scope of the reaction in primary alcohols and the catalytic quantities of the reagents necessary for the oxidation.<sup>178</sup> Upon testing these conditions upon the starting material, it was found that the oxidation proceeded almost quantitatively within 1 h. Furthermore, they proved to be quite general, furnishing high to quantitative yields of diols **201a-n** for most of the diols reacted (Scheme 5.12).



to see if similar yields could be attained.<sup>179</sup> This appeared to be the case as similarly high yields of the desired aldehyde could be isolated from this reaction, however, the results could be far more capricious, often requiring repeated redosing of the copper and TEMPO to effect full conversion. Furthermore, attempts to perform a Swern oxidation on the products were low yielding and difficult to purify.

### *5.2.3. Cyclisation of the Dialdehydes*

At this point with multiple aldehydes in hand, attempts to perform the cyclisation were undertaken. Multiple Lewis acids were screened to attain optimal conditions for the reaction (Table 5.1).



Solvent	T (°C)	Lewis Acid	Lewis Acid (Mol %)	Time (h)	<b>2</b> yield (%)	<b>198</b> yield (%)
DCE	83	Ag(OTf)	60	5	0	0
DCE	83	Al(OTf) <sub>3</sub>	60	5	0	0
DCE	83	FeCl <sub>3</sub>	60	5	0	0
DCE	83	La(OTf) <sub>3</sub>	60	5	0	0
DCE	83	Sc(OTf) <sub>3</sub>	60	5	0	0
DCE	83	Sn(OTf) <sub>2</sub>	60	5	0	0
DCE	83	Ti(O <sup>i</sup> Pr) <sub>4</sub>	60	5	0	0
DCE	83	Yb(OTf) <sub>3</sub>	60	5	0	0
DCE	83	Zn(OTf) <sub>2</sub>	60	5	0	0
DCE	83	Pyridine	200	5	0	0
DCE	83	AlCl <sub>3</sub>	60	5	3	8
DCE	83	Cu(OTf) <sub>2</sub>	60	5	10	19
DCE	83	In(OTf) <sub>3</sub>	60	5	43	40
DCE	83	BF <sub>3</sub> .OEt <sub>2</sub>	200	5	84	0
DCE	115 (μw)	In(OTf) <sub>3</sub>	60	3	79	0
PhCF <sub>3</sub>	103	BF <sub>3</sub> .OEt <sub>2</sub>	60	5	88	0
CyH	80	BF <sub>3</sub> .OEt <sub>2</sub>	200	5	79	0
DCE	115 (μw)	ZnCl <sub>2</sub>	200	5	65	23
Neat	120	ZnCl <sub>2</sub>	60	1.5	56	0

**Table 5.1** – A range of trialled Lewis acid mediated Bradsher closures. Results obtained by Dr Laurence Burroughs

At 83 °C, the majority of the Lewis acids screened were ineffective in effecting the closure, with the exception of In(OTf)<sub>3</sub>, BF<sub>3</sub>.OEt<sub>2</sub> and ZnCl<sub>2</sub>. Higher loadings of the Lewis acids and solvents which allowed access to higher temperatures were found to favour the formation of tetracene. As the improvement in yield was minor upon the increase of temperature of change of Lewis acid from BF<sub>3</sub>.OEt<sub>2</sub>, 2 equivalents of BF<sub>3</sub>.OEt<sub>2</sub> at 83 °C in DCE were the conditions taken forward. On limiting the BF<sub>3</sub>.OEt<sub>2</sub> to 1 eq., the monoclosure product **202** could be effected cleanly in DCE in 82% yield under the same conditions.

While this reaction was favourable on small scale, upon repeating the conditions on larger scales, difficulties were encountered in reproducing the yield. Interestingly, attempts to force the second closure proved to be difficult, providing no yield of the tetracene, but instead forming dihydrotetracene **27** in a modest yield (51%). To probe this transformation,  $^1\text{H}$  NMR spectra of the reaction mixture were taken at intervals to monitor the course of the reaction (Figure 5.1).

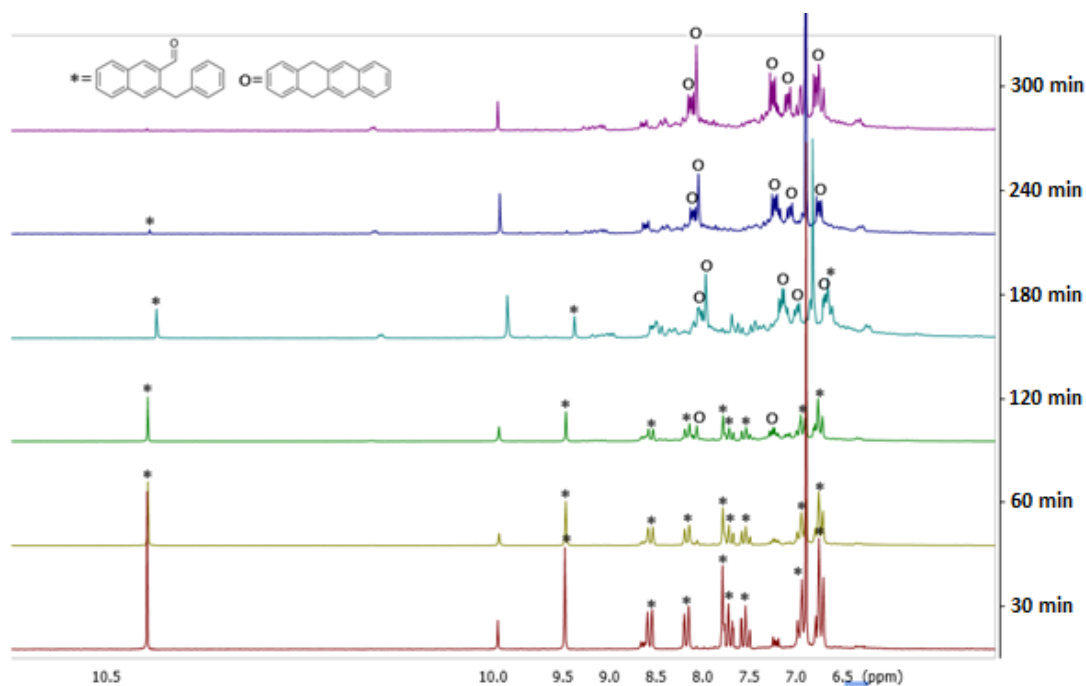


Figure 5.1 –  $^1\text{H}$  NMR of formation of dihydrotetracene **27**.

By taking the integrals of the peaks in the reaction mixture, a rough kinetic assessment of the reactions could be made *via* the graphical method described by Mata-Perez and Perez-Bonito.<sup>180</sup> Through this NMR analysis it was shown that the formation of the monoclosure is rapid and at 30 mins, the major product. However, as the reaction proceeds this is rapidly overtaken by **27**, and by 2.5 h was effectively the sole product (Figure 5.2).

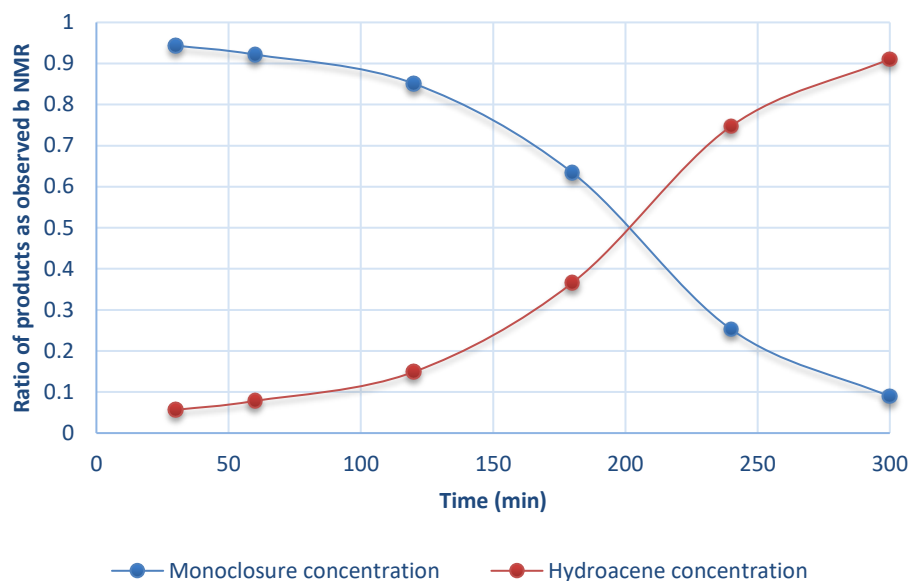


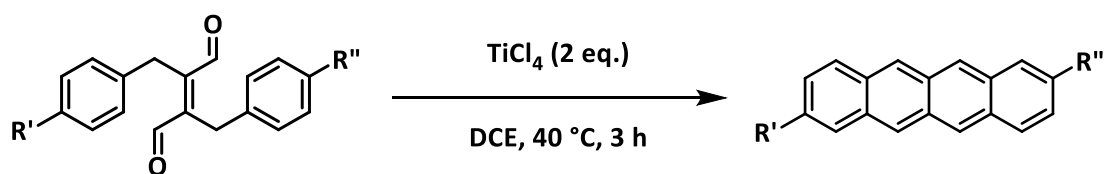
Figure 5.2 – Observed change in ratio of aldehyde **198** to dihydrotetracene **27**.

This is intriguing as after 30 mins there does appear to be a small quantity of tetracene has been formed, implying that the cyclisation was initially proceeding but was then superseded by a second reaction. Due to the formation of H<sub>2</sub>O from the Bradsher closure, it could be posited that the use of the molecular sieves in the reaction were not removing the adventitious water efficiently.

This would therefore mean that the increasing concentration of water in combination with the stoichiometric amounts of BF<sub>3</sub>.OEt<sub>2</sub>, that BF<sub>3</sub>.OH<sub>2</sub> may begin to form, potentially catalysing the rapid reduction of the desired tetracene. Formally, on the completion of a single Bradsher closure one equivalent of water is formed. As such this would explain the roughly autocatalytic reaction kinetics observed in the reaction: complexation of the BF<sub>3</sub> to water decreases the pK<sub>a</sub> of water significantly *via* the formation of a species with acidity akin to concentrated sulfuric acid (approx. H<sub>0</sub> = -12).<sup>181</sup> This is due to the oxophilic nature of BF<sub>3</sub> (BDE B-O ΔH<sub>f298</sub> = 806 kJ/mol).<sup>170</sup> This rapidly leads to the dissociation of a proton from water to form the boronate species [BF<sub>3</sub>OH]<sup>-</sup>H<sup>+</sup>. This has been exploited synthetically to effect S<sub>N</sub>Ar reactions of benzylic chlorides, benzylic alcohols and aldehydes.<sup>182-184</sup> Furthermore, the reduction of acenes by strongly acidic conditions is precedented within the literature, with tetracene reduced to hydrotetracene **27** by HI/AcOH.<sup>185</sup> It could therefore be hypothesised that the increasing acidic conditions caused by the formation of [BF<sub>3</sub>OH]<sup>-</sup>

H<sup>+</sup> are catalysing the formation of the tetracene radical cation. Traditional means of accessing the species utilise strong acids such as H<sub>2</sub>SO<sub>4</sub> and methanesulfonic acid, which have similar pK<sub>a</sub> values to the proposed boronate species.<sup>186, 187</sup> It must however be noted that if indeed the hydroacene **27** is formed *via* a radical cation intermediate, it is currently unclear what species acts as a reductant (in this instance, a hydride source). It could be proposed that the 53% yield is due to a disproportionation of the radical cationic intermediate, however, further investigation is necessary for mechanism to be inferred than the more general assessment described above.

Alternate Lewis acids were then trialled due to the instability of tetracene within the previously established conditions. TiCl<sub>4</sub> has been utilised in the Bradsher closure of benzyl groups has been employed in the synthesis of naphthalenes.<sup>188</sup> As such it was utilised in the double closure of dial **201a**. This was found to synthesis the desired tetracene in high yield with 2 equivalents of TiCl<sub>4</sub> in DCE at 0 °C, then heating at 40 °C for 5 h (80%). Furthermore, the reaction conditions proved to be far more general when compared to the use of BF<sub>3</sub>.OEt<sub>2</sub>. The reaction mixture could be left for 22 h with no degradation of the tetracene products by NMR. This can most likely be attributed to the high oxophilicity of titanium double bond formed facilitating the removal of the oxygen formed in the ring closure and the absence of a background reaction as observed in the BF<sub>3</sub>.OEt<sub>2</sub> mediated closure. These conditions proved to be general across the dials substituted with electron-donating groups (Scheme 5.14).

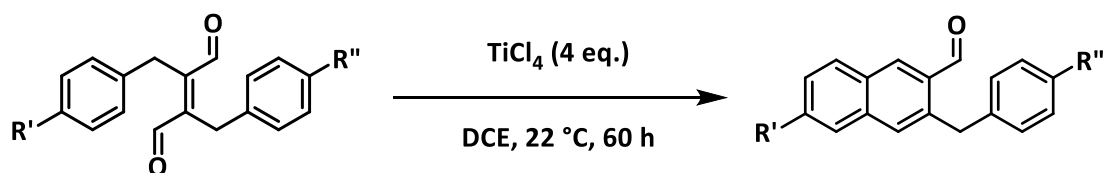


Compound	R'	R''	Yield (%)	Compound	R'	R''	Yield (%)
Tetracene (2)	H	H	80	203h	Me	Me	86
203c	H	Ph	71	203i	Me	<sup>i</sup> Pr	82
203d	H	OMe	56	203k	OMe	OMe	86
203e	H	Me	87	203l	OMe	Me	81

**Scheme 5.14** – Cyclisation yields of tetracene **2** and substituted tetracenes **203c, d, e, h, l, k & i**. Compounds **203c-l** were synthesised by Dr Mary-Robert Garrett.

As is clear from the entries in Scheme 5.14, the presence of electron-donating groups was key to force the reaction. What is interesting is that the Hammett parameter for the *meta* position is positive, denoting inductive electron withdrawal by the methoxy group, which (as it lowers electron density), should disfavour cyclisation.<sup>189</sup> However, the general trend holds that the presence of electron-donating groups favour the ring closure.

Cyclisation attempts with dials with electron-withdrawing substituents proved difficult, with most examples forming the aldehyde from the single Bradsher closure (Scheme 5.15).

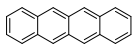
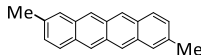
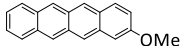
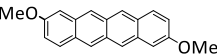
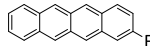
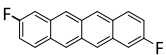
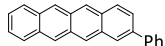
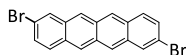
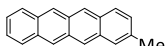


Compound	R'	R''	Yield (%)
202b	H	F	37
202f	F	F	63
202m	OMe	F	39

**Scheme 5.15** – Attempted cyclisations of substrates bearing electron-withdrawing groups. Results attained by Dr Mary-Robert Garrett.

Attempts to force the closure using the conditions established in Scheme 5.13 proved to not force the Bradsher closure of rings bearing electron-withdrawing groups, as such additional equivalents of  $\text{TiCl}_4$  and longer reaction times were attempted. However, the alterations to the conditions still resisted the double closure, instead forming the aldehydes **202b**, **202f** and **202m**. This is to be expected as the electron-withdrawing groups would naturally lower the electron density at the meta position, preventing the closure. As such, new cyclisation conditions for these substrates must be sought.

#### 5.2.4. Calculated and Electrooptic properties

Tetracene	HOMO (eV)	LUMO (eV)	$E_g$	Tetracene	HOMO (eV)	LUMO (eV)	$E_g$
	-5.67	-3.29	2.75		-5.93	-3.20	2.72
	-5.70	-2.60	3.10		-5.75	-3.19	2.56
	-5.84	-2.63	3.21		-6.24	-3.51	2.73
	-5.72	-2.58	3.14		-6.40	-3.54	2.86
	-5.98	-3.22	2.76				

**Scheme 5.12** –  $^1\text{H}$  NMR of formation of dihydrotetracene **5.16**.

Employing the same basis set and TDDFT method utilising the Tam-Dancoff modification as discussed in the second chapter, the HOMO and singlet excited states for various substituted tetracenes were investigated. As was stated in Chapter 2, the method proved not to be an accurate system for the dithiocarbonate tetracenes **96a-j**. However, the calculation for tetracene **2** proved to be more accurate as an assessment of  $E_g$  in agreement with computational and experimentally derived results.<sup>190</sup>

### 5.3. Conclusions and Future Work

In conclusion, a general method for the synthesis of tetracenes over 4 steps was developed, with varying substitution attained from simple *para* substituted benzylorganometallic reagents. As such, no synthetic effort has currently been dedicated to varying the substitution of the starting organometallic reagents, with substitution at the *meta* or *ortho* positions of the aromatic rings, or attempts with heteroatomic rings.

Furthermore, the synthesis of the brominated diols and diols **199n** and **201n** offers an ancillary approach to substitution. As reactive handles, they offer opportunities *via* cross coupling to new substitution patterns should the initial benzylzinc halide or chloride not be available commercially. As such investigations into cross-coupling conditions with these substrates would no doubt be worthwhile in further developing the synthetic route to allow for the design of substituted tetracenes.

The difficulty in forcing the Bradsher closure in diols with electron-withdrawing groups must also be addressed.

# Appendices

## Appendix 1 – Experimental Data for Chapter 2

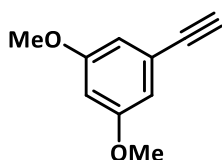
### General information

All reactions were carried under argon atmospheres using flame-dried Schlenk apparatus. Dichloromethane, toluene and acetonitrile were used distilled from calcium hydride; dimethoxyethane and tetrahydrofuran were used distilled from sodium/benzophenone ketyl.<sup>191</sup> Alkynes were purchased from Sigma-Aldrich, Alfa-Aesar and Maybridge and were distilled under reduced pressure before use. High cost alkynes were also prepared by Corey-Fuchs procedures.<sup>77</sup> Phthalaldehyde was purchased from Alfa-Aesar; hexamethyl disilazane, allyl bromide, diphenyl carbon disulfide and iodomethane were purchased from Sigma-Aldrich and were dried (4Å sieves) as necessary. 1,3-Dibenzylketone, methanesulfonic acid, ammonium acetate and malonitrile were purchased from Sigma-Aldrich; <sup>t</sup>BuONO was purchased from Fischer Scientific and all were utilised with no further purification. CuTc, FeCl<sub>3</sub>, CuCl<sub>2</sub>, CuBr<sub>2</sub> and CuBr.DMS were purchased from Sigma Aldrich and Fischer Scientific and were dried *in vacuo* before use and stored under an atmosphere of argon before use and when not in use. Eaton's reagent was prepared by a literature procedure.<sup>192</sup> Benzyl halides purchased from Sigma Aldrich and distilled before use. Reducing reagents were assayed *via* a gas evolution. Organolithium reagents were Gilman double titrated before use. All temperatures referred to those of the external oil baths used. Thin layer chromatography was performed on foil-backed plates coated with Merck Silica gel 60 F<sub>254</sub>. The plates were developed using ultraviolet light and basic aqueous potassium permanganate. Preparative thin layer chromatography was performed using Analtech 1000 µm UV254 pre-coated plates. Liquid chromatography was performed using forced flow (flash column) with the solvent systems indicated. The stationary phase used was silica gel 60 (220–240 mesh) supplied by Fluorochem. Infrared spectra were recorded on a Bruker Tensor 27 FT-IR spectrometer using NaCl plates (films were formed by evaporation of chloroform) or a Perkin–Elmer 1600 FT-IR in solution cells. Solution UV-vis spectra were recorded on a Bruker Lambda 25

instrument. Nuclear magnetic resonance spectra were recorded on Bruker DPX-400 (400.2 MHz), AV400 (400.1 MHz), AV(III)400 (400.1 MHz) or AV(III)500 (500.1 MHz) spectrometers at ambient temperature. Chemical shifts are quoted in parts per million (ppm) and were referenced as follows: chloroform-d, 7.26 ppm, methanol-d<sub>4</sub>, 4.87 ppm for <sup>1</sup>H NMR data; and for <sup>13</sup>C NMR data: chloroform-d, 77.16 ppm, methanol-d<sub>4</sub>, 49.00.<sup>193</sup> Coupling constants (*J*) are quoted in Hertz and coupling correlations were based on standard COSY, DEPT, HMQC, HMBC experiments. Mass spectrometry was performed using a VG Micromass AutoSpec spectrometer (EI) or Bruker MicroTOF (ESI) as noted. Melting points were determined with a Stuart Scientific SMP3 melting point apparatus.

### Preparation of diol starting materials **98** and **100**

#### *3,5-Dimethoxyphenylacetylene* **98**

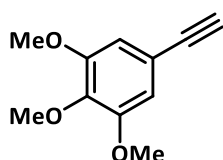


(i) Preparation of dibromoalkene. Freshly sublimed CBr<sub>4</sub> (6.39 g, 19.3 mmol, 2 equiv.) was dissolved in dry CH<sub>2</sub>Cl<sub>2</sub> (20 ml) and cooled to 0 °C. Triphenylphosphine (10.1 g, 38.5 mmol, 4 equiv.) in dry CH<sub>2</sub>Cl<sub>2</sub> (20 ml) was added and the mixture left stirring for 30 min. Solid 3,5-methoxybenzaldehyde (1.61 g, 9.69 mmol, 1 equiv.) dissolved in CH<sub>2</sub>Cl<sub>2</sub> (20 ml) was added dropwise and the reaction monitored by TLC indicated completion (product *R<sub>f</sub>* 0.74, 7:3 pentane:Et<sub>2</sub>O). The resultant mixture was quenched with a 1:1 mixture of CH<sub>2</sub>Cl<sub>2</sub>:H<sub>2</sub>O (75 ml), extracted with CH<sub>2</sub>Cl<sub>2</sub> (3 x 30 ml), dried (MgSO<sub>4</sub>), filtered and reduced *in vacuo*, giving a solid yellow crude (16.4 g). Purification by flash column chromatography (1:9 CH<sub>2</sub>Cl<sub>2</sub>:pentane) give a colourless powder **97** (2.99 g, 97%), *R<sub>f</sub>* = 0.74 (7:3 pentane:ether), m.p. 74-75 °C. <sup>1</sup>H NMR (400.1 MHz, CDCl<sub>3</sub>): δ 7.45 (s, 1H, CCH), 6.72 (d, *J* = 2.1 Hz, 2H, ArH), 6.49 (t, *J* = 2.1 Hz, 1H, ArH), 3.83 (s, 6H, OCH<sub>3</sub>). <sup>13</sup>C NMR (100.6 MHz, CDCl<sub>3</sub>): δ 160.7 (C), 137.0 (C), 136.9 (CH), 106.5 (CH), 100.9 (CH), 90.0 (C), 55.4 (CH<sub>3</sub>). MS ESI calcd. for C<sub>10</sub>H<sub>10</sub>O<sub>2</sub>Br<sub>2</sub> *m/z* expected 320.9120 (M+H), *m/z* found 320.9110 (M+H).

(ii) Corey-Fuchs procedure. **97** (2.99 g, 9.28 mmol, 1 equiv.) was dissolved in dry THF (50 ml) under argon with stirring at -50 °C (dry ice/acetonitrile bath). A solution of <sup>n</sup>BuLi (24.0 ml, 1.6 M in hexanes, 38.4 mmol, 4.1 equiv.) was added dropwise after

which TLC indicated completion of the reaction. The mixture was quenched with saturated ammonium chloride (40 ml), extracted with CH<sub>2</sub>Cl<sub>2</sub> (3 x 20 ml), dried (NaSO<sub>4</sub>), filtered and evaporated, giving an orange brown oil (1.61 g). Purification by flash column chromatography (pure pentane, followed by 19:1 pentane: Et<sub>2</sub>O) gave a pure colourless crystalline solid **98** (1.22 g, 81%), *R<sub>f</sub>* = 0.24 (pentane), m.p. 46-47 °C with literature properties.<sup>i</sup> <sup>1</sup>H NMR (400.1 MHz, CDCl<sub>3</sub>): δ 6.72 (d, *J* = 2.3 Hz, 2H, *ArH*), 6.50 (t, *J* = 2.3 Hz, 1H, *ArH*), 3.76 (s, 6H, OCH<sub>3</sub>), 3.15 (s, 1H, CCH). <sup>13</sup>C NMR (100.6 MHz, CDCl<sub>3</sub>): δ 160.6 (C), 123.4 (C), 110.0 (CH), 102.3 (CH), 83.7 (C), 76.9 (CH), 55.4 (CH<sub>3</sub>).

#### 1-Ethynyl-3,4,5-trimethoxybenzene **100**



i) Sublimed CBr<sub>4</sub> (6.43g, 19.4 mmol) was added to a flame dried Schlenk flask of dry dichloromethane (67 ml) and stirred at 0 °C. Triphenylphosphine (10.47 g, 39.9 mmol) was then added and stirred for 30 minutes. 3,4,5-trimethoxybenzaldehyde was then added in one portion and stirred. When TLC indicated completion, the reaction was quenched with 1:1 dichloromethane: water, extracted with dichloromethane, dried with MgSO<sub>4</sub>, filtered and concentrated under reduced pressure giving a crude yellow solid (19.6 g). The crude was purified by flash column chromatography (7:3 pentane:diethyl ether) giving a colourless crystalline solid **99** (3.30g, 94%). *R<sub>f</sub>* = 0.31 (7:3 pentane:diethyl ether), m.p. 60 - 62 °C. ), IR (CHCl<sub>3</sub>) *v*<sub>max</sub>/cm<sup>-1</sup> 3011, 2965, 2940, 2916, 2839. <sup>1</sup>H NMR (400.2 MHz): δ 7.36 (s, 1H, C=CH), 6.76 (s, 2H, *ArH*), 3.83 (s, 3H, OCH<sub>3</sub>), 3.80 (s, 6H, OCH<sub>3</sub>). <sup>13</sup>C NMR (100.6 MHz, CDCl<sub>3</sub>) δ 152.7 (C), 138.1 (C), 136.4 (CH), 130.1 (C), 105.5 (C), 88.2 (CH), 60.4 (CH<sub>3</sub>), 55.8 (CH<sub>3</sub>). MS (+ESI) calcd. for C<sub>11</sub>H<sub>12</sub>O<sub>3</sub>Br<sub>2</sub> *m/z* 350.9226 (M+H), found *m/z* 350.9239 (M+H).

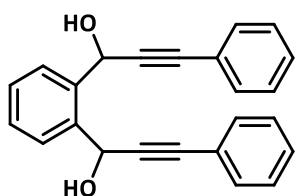
ii) <sup>n</sup>Butyllithium (22.5 ml, 1.6 M in hexanes, 36 mmol) was added dropwise to a stirred solution of 5-(2,2-dibromovinyl)-1,2,3-trimethoxybenzene **99** (3.06g, 8.69 mmol) in dry THF (45ml) under argon at -48 °C. On indication of completion by TLC, the mixture was quenched with saturated ammonium chloride, extracted with dichloromethane (3 x 20 ml), the organic washings dried with MgSO<sub>4</sub>, filtered and concentrated under reduced pressure giving a crude brown oil (1.82 g). The crude oil was then filtered through a pad of silica with 4:1 pentane ether, and reduced under pressure giving a colourless solid **100** (1.44 g, 86%). *R<sub>f</sub>* = 0.29 (4:1 pentane:diethyl ether), m.p. 74 - 75

°C. **IR** (CHCl<sub>3</sub>)  $\nu_{\max}/\text{cm}^{-1}$  3690, 3607, 3305, 3011, 2967, 2942, 2839, 2361, 2341, 2112, 1601, 1580, 1504, 1465, 1451, 1433, 1413, 1335, 1241, 1132, 1000, 957, 924, 839. **<sup>1</sup>H NMR** (400.2 MHz, CDCl<sub>3</sub>)  $\delta$  6.67 (s, 2H, ArH), 3.79 (s, 3H, OCH<sub>3</sub>), 3.78 (s, 6H, OCH<sub>3</sub>), 3.00 (s, 1H, C $\equiv$ CH). **<sup>13</sup>C NMR** (100.6 MHz, CDCl<sub>3</sub>)  $\delta$  153.2 (C), 139.4 (C), 117.1 (C), 109.5 (CH), 83.8 (C), 76.3 (CH), 61.0 (CH<sub>3</sub>), 56.2 (CH<sub>3</sub>). **MS** (+ESI) calcd. for C<sub>11</sub>H<sub>12</sub>O<sub>3</sub>  $m/z$  192.0786 (M), found 192.0780 (M)

### General procedure for preparation of the 1,4-diols **95a-j**

A solution of <sup>n</sup>BuLi (7.6 ml of 1.6 M hexane solution, 12.2 mmol, 2.1 equiv.) was added to a stirred solution of arylacetylene (12.2 mmol, 2.1 equiv.) in dry THF (25 ml) under argon in Schlenk tube at -50 °C (dry ice/acetonitrile bath). Once the lithium acetylide had formed (typically 20 min), phthalaldehyde (6.1 mmol, 1 equiv.) was then added as a solid and the mixture allowed to come to room temperature (typically 3 h) until TLC showed formation of the diol **95a**. The reaction mixture was quenched with saturated ammonium chloride (25 ml) and extracted with ether (3 x 20 ml). The organic washings were combined, dried (MgSO<sub>4</sub>), filtered, and evaporated to the crude product. Purification was achieved by flash column chromatography (3:2 pentane:diethyl ether). Generally, the *rac:meso* diastereomers (1:2 to 1.9:1 mixtures) proved essentially inseparable.

#### 1,1'-(1,2-Phenylene)bis(3-phenylprop-2-yn-1-ol) **95a**



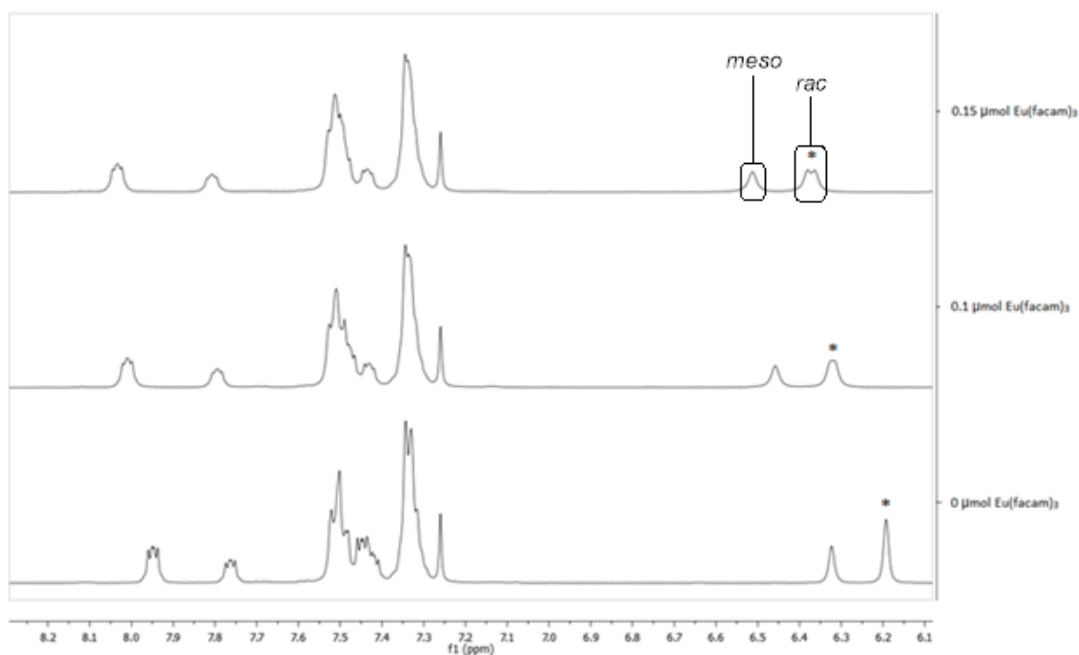
From phenylacetylene (1.3 mL, 1.2 g, 11.8 mmol), <sup>n</sup>BuLi (7.3 mL, 1.55 M in hexanes, 11.3 mmol) and phthalaldehyde (0.75 g, 5.60 mmol) to yield **95a** as a pale yellow oil 1.89 g, 99% (*rac:meso* 1.2:1.0) with literature properties.  $R_f$  = 0.15

(3:2 pentane:diethyl ether). **IR** (film):  $\nu_{\max}/\text{cm}^{-1}$  3691, 3587, 3008, 2928, 2856, 2361, 2230, 1601, 1491, 1455, 1444, 1375, 1242, 1070, 1031, 1015. **<sup>1</sup>H NMR** (400.1 MHz, CDCl<sub>3</sub>):  $\delta$ (*rac*) 7.96-7.93 (m, 2H, ArH), 7.52-7.29 (m, 12H, ArH), 6.20 (d,  $J$  = 4.7 Hz, 2H, ArCHOH), 3.50 (d,  $J$  = 4.7 Hz, 2H, OH);  $\delta$ (*meso*): 7.78-7.76 (m, 2H, ArH), 7.52-7.29 (m, 12H, ArH), 6.33 (d,  $J$  = 6.0 Hz, 2H, ArCHOH), 3.50 (d,  $J$  = 6.0 Hz, 2H, OH). **<sup>13</sup>C NMR** (100.6 MHz, CDCl<sub>3</sub>):  $\delta$ (*rac*) 138.0 (C), 131.9 (CH), 129.3 (CH), 128.8 (CH), 128.5 (CH), 128.2 (CH), 122.4 (C), 87.9 (C), 87.8 (C), 62.5 (CH);  $\delta$ (*meso*) 138.4 (C), 131.9 (CH), 129.4 (CH),

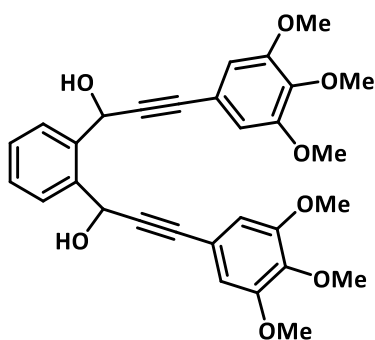
128.8 (CH), 128.4 (CH), 128.2 (CH), 122.5 (C), 88.2 (C), 87.5 (C), 64.0 (CH). **MS** (+ESI) calcd. for C<sub>24</sub>H<sub>18</sub>NaO<sub>2</sub> *m/z* 361.1199 (M+Na), found *m/z* 361.1191 (M+Na). The *rac/meso* stereochemical assignments were confirmed using the procedure of Saá<sup>80</sup>; which are in agreement both with the literature and across the family of diols we have prepared.

### Stereochemical enrichment of 1,1'-(1,2-phenylene)bis(3-phenylprop-2-yn-1-ol) **95a**

A sample of **95a** (*rac:meso* 5.0:1.0) could be prepared by addition of dry tetrabutylammonium fluoride (3.21 g, 12.3 mmol, 2.2 equiv.) to the reaction mixture immediately after the addition of phthalaldehyde.<sup>194</sup> The reaction mixture was then subsequently warmed to room temperature over 1 h. It was quenched and worked up in the normal way to provide *meso* enriched **95a**. No direct synthetic procedure to prepare *rac* enriched **95a** could be found. In all cases, the diastereomers were identified with the addition of sufficient mol equivalents of Eu(facam)<sub>3</sub> to show splitting of the *rac* benzyl peak. All the upfield benzyl signals correlated to the *rac* diastereomer, and the remaining peaks were assigned to each diastereomer with <sup>1</sup>H:<sup>1</sup>H COSY, HMBC and HMQC NMR techniques. Representative <sup>1</sup>H NMR spectra of Eu(facam)<sub>3</sub> shifted **95a** are shown below:



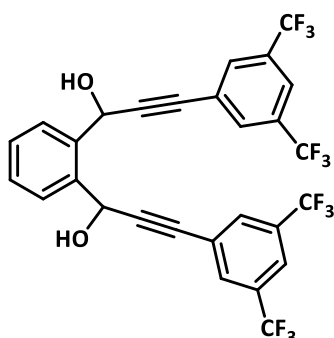
1,1'-(1,2-phenylene)bis(3-(3,4,5-trimethoxyphenyl)prop-2-yn-1-ol) **95b**



From 3,4,5-tris(methoxy)phenylacetylene (1.12 g, 5.83 mmol), <sup>n</sup>BuLi (3.64 mL, 1.60 M in hexanes, 4.2 mmol) and phthalaldehyde (372 mg, 2.78 mmol) to yield novel **95b** as a colourless solid 1.13 g, 74% (*rac:meso* 1.9:1.0). *R<sub>f</sub>* = 0.14 (7:3 pentane:diethyl ether), **m.p.** 64-65 °C. IR (film):  $\nu_{\text{max}}/\text{cm}^{-1}$  3583, 3011, 2967, 2941,

2841, 2232, 1580, 1464, 1454, 1433, 1413, 1242, 1187, 1166, 1132, 1059, 1032, 998, 953, 892, 837. <sup>1</sup>H NMR (400.2 MHz, CDCl<sub>3</sub>) *rac*  $\delta$  7.88 (dd, *J* = 5.7, 3.5 Hz, 2H, ArH), 7.39 (dd, *J* = 5.7, 3.4 Hz, 2H, ArH), 6.69 (s, 4H, ArH), 6.14 (s, 2H, ArCHOH), 3.97 (s, 2H, OH), 3.81 (s, 3H, OCH<sub>3</sub>), 3.78 (s, 6H, OCH<sub>3</sub>), *meso*  $\delta$  7.69 (dd, *J* = 5.7, 3.4 Hz, 2H, ArH), 7.36 (dd, *J* = 5.7, 3.4 Hz, 2H, ArH), 6.66 (s, 4H, ArH), 6.27 (s, 2H, ArCHOH), 4.43 (s, 2H, OH), 3.80 (s, 3H, OCH<sub>3</sub>), 3.75 (s, 6H, OCH<sub>3</sub>). <sup>13</sup>C NMR (100.6 MHz, CDCl<sub>3</sub>) *rac*  $\delta$  153.0 (C), 139.1 (C), 138.0 (C), 129.1 (CH), 128.1 (CH), 117.4 (C), 109.0 (CH), 87.4 (C), 87.0 (C), 62.3 (CH), 60.9 (CH<sub>3</sub>), 56.2 (CH<sub>3</sub>), *meso*  $\delta$  153.0 (C), 139.0 (C), 138.5 (CH), 129.2 (CH), 129.1 (CH), 117.4 (C), 109.0 (CH), 87.4 (C), 87.2 (C), 63.8 (CH), 60.9 (CH<sub>3</sub>), 56.1 (CH<sub>3</sub>). MS (+ESI) calcd. for C<sub>30</sub>H<sub>30</sub>O<sub>8</sub> *m/z* 541.1833 (M+Na), found *m/z* 541.1845 (M+Na).

1,1'-(1,2-Phenylene)bis(3-(3,5-bis(trifluoromethyl)phenyl)prop-2-yn-1-ol) **95c**



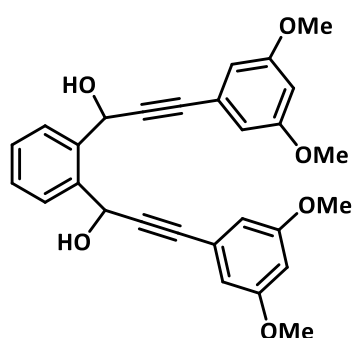
From 3,5-bis(trifluoromethyl)phenylacetylene (743  $\mu$ L, 1.00 g, 4.20 mmol), <sup>n</sup>BuLi (2.7 mL, 1.56 M in hexanes, 4.2 mmol) and phthalaldehyde (268 mg, 2.00 mmol) to yield novel **95c** as a colourless solid 1.03 g, 84% (*rac:meso* 1.9:1.0). *R<sub>f</sub>* = 0.14 (7:3 pentane:diethyl ether), **m.p.** 164-165 °C. IR (film):  $\nu_{\text{max}}/\text{cm}^{-1}$  3693, 3583, 3438, 3085, 3008,

2924, 2232, 1814, 1614, 1603, 1488, 1463, 1382, 1280, 1184, 1145, 1108, 1032, 989, 951, 900, 849. <sup>1</sup>H NMR (400.2 MHz, MeOD):  $\delta$ (*rac*) 7.97-7.83 (m, 6H, ArH), 7.77 (dd, *J* = 5.8, 3.5 Hz, 2H, ArH), 7.43 (dd, *J* = 5.8, 3.4 Hz, 2H, ArH), 6.20 (s, 2H, ArCHOH);  $\delta$ (*meso*) 7.97-7.83 (m, 6H, ArH), 7.73 (dd, *J* = 5.8, 3.4 Hz, 2H, ArH), 7.43 (dd, *J* = 5.8, 3.4 Hz, 2H, ArH), 6.23 (s, 2H, ArCHOH); OH signals not detected due to exchange. <sup>13</sup>C NMR (100.6 MHz, MeOD):  $\delta$ (*rac*) 139.5 (C), 133.1 (C, d, *J<sub>CF</sub>* = 33.7 Hz), 132.7 (CH, q, *J<sub>CF</sub>* = 3.0 Hz), 129.8 (CH), 128.5 (C), 126.7 (C), 124.3 (C, q, *J<sub>CF</sub>* = 272.1 Hz), 122.8 (m, CH), 94.7 (C),

83.5 (C), 62.2 (CH);  $\delta(\text{meso})$  139.8 (C), 133.1 (C, d,  $J_{CF} = 33.7$  Hz), 131.2 (CH, q,  $J_{CF} = 3.1$  Hz), 130.0 (CH), 129.5 (CH), 126.7 (C), 124.2 (q,  $J_{CF} = 272.2$  Hz), 122.8 (s), 94.8 (s), 84.0 (s), 63.0 (s),  $^{19}\text{F NMR}$  (376.6 MHz,  $\text{CD}_3\text{OD}$ ):  $\delta(\text{rac}/\text{meso})$  -64.69 (s), -64.72 (s). **MS** (-ESI): calcd. for  $\text{C}_{22426}\text{O}_2\text{F}_{12}$   $m/z$  609.0729 (M-H), found  $m/z$  609.0714 (M-H).

Diastereomeric ratios of up to 4.8:1.0 (*rac*:*meso*) could be achieved *via* the addition of  $\text{CHCl}_3$ , as the *rac* diastereomer of **95c** is nearly insoluble in this solvent.

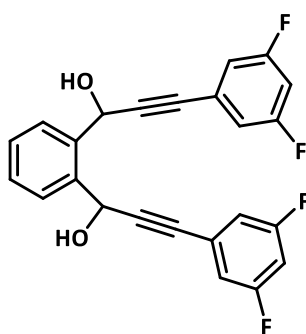
*1,1'-(1,2-Phenylene)bis(3-(3,5-dimethoxyphenyl)prop-2-yn-1-ol)* **95d**



From 3,5-bis(methoxy)phenylacetylene (1.00 g, 6.17 mmol),  $n\text{BuLi}$  (3.9 mL, 1.68 M in hexanes, 6.55 mmol) and phthalaldehyde (375 mg, 2.79 mmol) to yield **95d** as an off-white solid 0.88 g, 69% (*rac*:*meso* 1.8:1.0).  $R_f = 0.12$  (7:3 pentane:diethyl ether), **m.p.** 73-74 °C. **IR** (thin film):  $\nu_{\text{max}}/\text{cm}^{-1}$  3693, 3603, 3011, 2963, 2940, 2842, 2360,

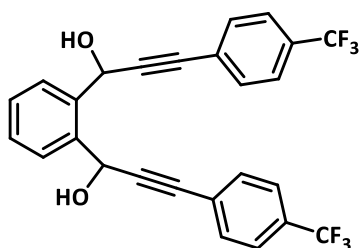
2342, 2229, 1708, 1598, 1518, 1458, 1422, 1350, 1301, 1193, 1157, 1121, 1065, 1032, 990, 952, 923, 852, 837.  $^1\text{H NMR}$  (400.1 MHz,  $\text{CDCl}_3$ ):  $\delta(\text{rac})$  7.91 (dd,  $J = 5.7, 3.4$  Hz, 2H, ArH), 7.41 (dd,  $J = 5.7, 3.4$  Hz, 2H, ArH), 6.64 (d,  $J = 2.3$  Hz, 4H, ArH), 6.44 (t,  $J = 2.3$  Hz, 2H, ArH), 6.14 (s, 2H, ArCHOH), 3.74 (s, 12H, MeH);  $\delta(\text{meso})$  7.71 (dd,  $J = 5.7, 3.4$  Hz, 2H, ArH), 7.38 (dd,  $J = 5.7, 3.4$  Hz, 2H, ArH), 6.62 (d,  $J = 2.3$  Hz, 4H, ArH), 6.43 (d,  $J = 2.3$  Hz, 2H, ArH), 6.29 (s, 2H, ArCHOH), 3.72 (s, 12H, OCH<sub>3</sub>); OH signals not detected due to exchange.  $^{13}\text{C NMR}$  (100.6 MHz,  $\text{CDCl}_3$ ):  $\delta(\text{rac})$  160.5 (C), 138.0 (C), 129.2 (CH), 128.1 (CH), 123.7 (C), 109.6 (CH), 102.1 (CH), 87.6 (C), 87.5 (C), 62.4 (CH), 55.5 (CH<sub>3</sub>);  $\delta(\text{meso})$  160.5 (C), 138.4 (C), 129.3 (CH), 128.1 (C), 123.7 (C), 109.6 (CH), 102.1 (CH), 87.9 (C), 87.2 (C), 63.9 (CH), 55.4 (CH<sub>3</sub>). **MS** (+ESI): calcd. for  $\text{C}_{22}\text{H}_{26}\text{O}_6$   $m/z$  expected 481.1622 (M+Na), found  $m/z$  481.1612 (M+Na).

*1,1'-(1,2-Phenylene)bis(3-(3,5-difluorophenyl)prop-2-yn-1-ol) 95e*



From 1-ethynyl-3,5-difluorobenzene (599  $\mu$ L, 5.04 mmol),  $n$ BuLi (3.2 mL, 1.68 M in hexanes, 4.7 mmol) and phthalaldehyde (322 mg, 2.40 mmol) to yield novel **95e** as a 774 mg, 79% (*rac:meso* 1.6:1.0)  $R_f$  = 0.29 (6:4 pentane: ether), **m.p.** 110-112  $^{\circ}$ C. **IR** (film):  $\nu_{\max}/\text{cm}^{-1}$  3583, 3090, 3012, 2458, 2242, 1705, 1618, 1590, 1514, 1502, 1474, 1456, 1431, 1378, 1338, 1260, 1241, 1166, 1123, 1094, 1044, 991, 954, 909, 860.  **$^1\text{H}$  NMR** (400.2 MHz,  $\text{CDCl}_3$ )  $\delta$  (*rac*) 7.85 (dd,  $J$  = 5.7, 3.4 Hz, 2H, ArH), 7.44 (dd,  $J$  = 5.8, 3.4 Hz, 2H, ArH), 7.02 – 6.91 (m, 4H, ArH), 6.85 – 6.74 (m, 2H, ArH), 6.10 (s, 2H, ArCHOH), 3.77 (s, 2H, OH);  $\delta$  (*meso*) 7.67 (dd,  $J$  = 5.5, 3.4 Hz, 2H, ArH), 7.41 (dd,  $J$  = 5.6, 3.4 Hz, 2H, ArH), 7.02 – 6.91 (m, 4H, ArH), 6.85 – 6.74 (m, 2H, ArH), 6.21 (s, 2H, ArCHOH), 4.12 (s, 2H, OH).  **$^{19}\text{F}$  NMR** (376.6 MHz,  $\text{CDCl}_3$ )  $\delta$  (*rac*) -109.21 (s);  $\delta$  (*meso*) -109.25 (s).  **$^{13}\text{C}$  NMR** (100.6 MHz,  $\text{CDCl}_3$ )  $\delta$  (*rac*) 161.5 (d,  $J$  = 13.4 Hz, C), 137.5 (C), 129.6 (CH), 128.2 (CH), 124.9 (dd,  $J$  = 11.7, 2.8 Hz, C), 114.8 (dd,  $J$  = 11.6, 2.8 Hz, CH), 105.2 (dd,  $J$  = 25.3, 4.4 Hz, CH), 89.7 (C), 85.5 (t,  $J$  = 3.9 Hz, C), 62.3 (CH);  $\delta$  (*meso*) 164.1 (d,  $J$  = 13.3 Hz, C), 138.0 (C), 129.6 (CH), 129.4 (CH), 124.9 (dd,  $J$  = 11.8, 2.8 Hz, C), 114.9 (dd,  $J$  = 26.9, 2.8 Hz, CH), 105.0 (dd,  $J$  = 25.3, 4.5 Hz, CH), 90.1 (C), 85.3 (t,  $J$  = 3.9 Hz, C), 63.8 (CH). **MS** (+ESI) calcd. for  $\text{C}_{24}\text{H}_{14}\text{O}_2\text{F}_4$   $m/z$  433.0822 (M+Na), found 433.0812 (M+Na).

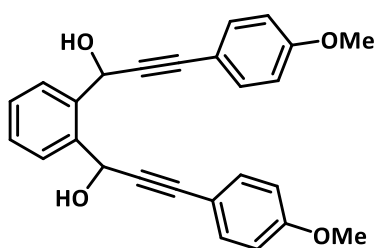
*1,1'-(1,2-Phenylene)bis(3-(4-(trifluoromethyl)phenyl)prop-2-yn-1-ol) 95f*



From 4-(trifluoromethyl)phenylacetylene (103  $\mu$ L, 1.07 g, 6.30 mmol),  $n$ BuLi (4.1 mL, 1.54 M in hexanes, 6.3 mmol) and phthalaldehyde (402 mg, 3.00 mmol) to yield **95f** as an off-white solid 1.24 g, 89% (*rac:meso* 1.0:1.1) with literature properties.<sup>72</sup>  $R_f$  = 0.28 (1:1 pentane:diethyl ether), **m.p.** 53-54  $^{\circ}$ C. **IR** (thin film):  $\nu_{\max}/\text{cm}^{-1}$  3690, 3586, 3009, 2960, 2929, 2873, 2359, 1922, 1700, 1615, 1516, 1488, 1455, 1405, 1374, 1324, 1265, 1172, 1134, 1107, 1068, 1018, 951, 844.  **$^1\text{H}$  NMR** (400.1 MHz,  $\text{CDCl}_3$ ):  $\delta$  7.90 (dd,  $J$  = 5.7, 3.5 Hz, 2H, ArH), 7.57 (s, 4H, ArH), 7.55 (s, 4H, ArH), 7.46 (dd,  $J$  = 5.7, 3.5 Hz, 2H, ArH), 6.17 (s, 2H, ArCHOH), 3.39 (s, 2H, OH);  $\delta$  (*meso*) 7.73 (dd,  $J$  = 5.7, 3.5 Hz, 2H, ArH), 7.57 (s, 4H, ArH), 7.55 (s, 4H, ArH), 7.44 (dd,  $J$  = 5.7, 3.5 Hz, 2H, ArH), 6.29 (s, 2H, ArCHOH),

3.77 (s, 2H, OH).  $^{13}\text{C NMR}$  (100.6 MHz,  $\text{CDCl}_3$ ):  $\delta(\text{rac})$  137.7 (C), 132.1 (CH), 130.7 (C, q,  $J_{\text{CF}} = 32.8$  Hz), 129.6 (CH), 128.5 (CH), 126.3-126.0 (m, C), 125.6-125.3 (CH, m), 123.9 (C, q,  $J_{\text{CF}} = 272.1$  Hz), 90.1 (C), 86.5 (C), 62.6 (CH);  $\delta(\text{meso})$  138.1 (C), 132.2 (CH), 130.7 (C, q,  $J_{\text{CF}} = 32.8$  Hz), 129.6 (CH), 129.4 (CH), 126.3-126.0 (m, C), 125.6-125.3 (CH, m), 123.92 (C, q,  $J_{\text{CF}} = 272.1$  Hz), 90.5 (C), 86.2 (C), 64.0 (CH). Multiple  $J_{\text{CF}}$  couplings prevent complete assignments being made.  $^{19}\text{F NMR}$  (376.6 MHz,  $\text{CD}_3\text{OD}$ ):  $\delta(\text{rac/meso})$  -62.92 (s), -62.93 (s). **MS** (+ESI): calcd. for  $\text{C}_{26}\text{H}_{16}\text{O}_2\text{F}_6$   $m/z$  expected 497.0947(M+Na), found  $m/z$  497.0942 (M+Na).

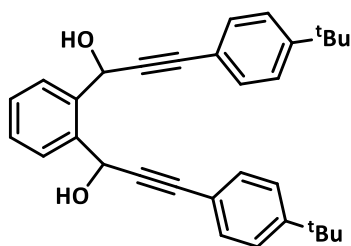
**1,1'-(1,2-Phenylene)bis(3-(4-methoxyphenyl)prop-2-yn-1-ol) 95g**



From 4-methoxyphenylacetylene (0.8 mL, 6.2 mmol),  $n\text{BuLi}$  (4.1 mL, 1.54 M in hexanes, 6.3 mmol) and phthalaldehyde (402 mg, 3.00 mmol) to yield **95g** as an off-white solid 0.98 g, 82% (*rac:meso* 1.3:1.0) with literature properties.<sup>72</sup>  $R_f = 0.12$  (1:1 pentane:diethyl

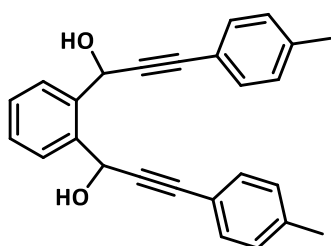
ether), m.p. 48-49 °C. **IR** (thin film):  $\nu_{\text{max}}/\text{cm}^{-1}$  3691, 3587, 3008, 2928, 2856, 2361, 2230, 1601, 1491, 1455, 1444, 1375, 1242, 1070, 1031, 1015, 998, 950, 922, 843.  $^1\text{H NMR}$  (400.2 MHz,  $\text{CDCl}_3$ ):  $\delta(\text{rac})$  7.93 (dd,  $J = 5.7, 3.5$  Hz, 2H, ArH), 7.49-7.35 (m, 6H, ArH), 6.88-6.74 (m, 4H, ArH), 6.15 (d,  $J = 4.4$  Hz, 2H, ArCHOH), 3.80 (s, 6H, MeH);  $\delta(\text{meso})$  7.74 (dd,  $J = 5.6, 3.5$  Hz, 2H, ArH), 7.49-7.35 (m, 6H, ArH), 6.88-6.74 (m, 4H, ArH), 6.29 (d,  $J = 5.6$  Hz, 2H, ArCHOH); 3.80 (s, 6H, OCH<sub>3</sub>); OH signals not detected due to exchange.  $^{13}\text{C NMR}$  (100.6 MHz,  $\text{CDCl}_3$ ):  $\delta(\text{rac})$  160.0 (C), 138.3 (C), 133.4 (CH), 129.2 (CH), 128.2 (CH), 114.5 (C), 114.1 (CH), 87.8 (C), 86.5 (C), 62.7 (CH), 55.4 (CH<sub>3</sub>);  $\delta(\text{meso})$  160.0 (C), 138.6 (C), 133.4 (CH), 129.3 (CH), 129.2 (CH), 114.6 (C), 114.1 (CH), 87.4 (C), 86.9 (C), 64.1 (CH), 55.4 (CH<sub>3</sub>). The signal at 129.2 is formed from a *meso* CH and *rac* CH signal overlapping (as confirmed by HMBC spectral data). **MS** (+ESI) calcd. for  $\text{C}_{26}\text{H}_{16}\text{O}_4$   $m/z$  497.0947(M+Na), found  $m/z$  497.0942 (M+Na).

*1,1'-(1,2-Phenylene)bis(3-(4-(tert-butyl)phenyl)prop-2-yn-1-ol) 95h*



From 4-(*tert*-butyl)phenylacetylene (2.1 mL, 11.6 mmol), <sup>n</sup>BuLi (6.8 mL, 1.7 M in hexanes, 11.5 mmol) and phthalaldehyde (0.77 g, 5.74 mmol) to yield **95h** as a colourless solid 1.71 g, 66% (*rac:meso* 1.0:1.6) with literature properties.<sup>74</sup>  $R_f = 0.11$  (7:3 pentane:diethyl ether), m.p. 78-79 °C. **IR** (thin film):  $\nu_{\max}/\text{cm}^{-1}$  3690, 3602, 3451, 3075, 3011, 2970, 2360, 2342, 2230, 1603, 1505, 1408, 1397, 1365, 965, 948, 837. **<sup>1</sup>H NMR** (400.2 MHz, CDCl<sub>3</sub>):  $\delta(\text{rac})$  8.00 (dd,  $J = 5.7, 3.4$  Hz, 2H, ArH), 7.54-7.47 (m, 4H, ArH), 7.43 (dd,  $J = 5.8, 3.4$  Hz, 2H, ArH), 7.39-7.34 (m, 4H, ArH), 6.15 (s, 2H, ArCHOH), 4.14 (s, 2H, OH), 1.36 (s, 12H, <sup>t</sup>BuH);  $\delta(\text{meso})$  7.77 (dd,  $J = 5.6, 3.4$  Hz, 2H, ArH), 7.54-7.47 (m, 4H, ArH), 7.40 (dd,  $J = 5.6, 3.4$  Hz, 2H, ArH), 7.39-7.34 (m, 4H, ArH), 6.35 (s, 2H, ArCHOH), 4.54 (s, 2H, OH), 1.35 (s, 12H, <sup>t</sup>BuH). **<sup>13</sup>C NMR** (100.6 MHz, CDCl<sub>3</sub>):  $\delta(\text{rac})$  151.8 (C), 138.0 (C), 131.7 (CH), 129.3 (CH), 128.1 (CH), 125.3 (CH), 119.5 (C), 87.7 (C), 87.4 (C), 62.3 (CH), 34.8 (C), 31.2 (CH<sub>3</sub>);  $\delta(\text{meso})$  151.8 (C), 138.6 (C), 131.6 (CH), 129.1 (CH), 128.1 (CH), 125.2 (CH), 119.5 (C), 87.8 (C), 87.4 (C), 63.9 (CH), 34.8 (C), 31.2 (CH<sub>3</sub>). **MS** (+ESI) calcd. for C<sub>32</sub>H<sub>34</sub>O<sub>2</sub>  $m/z$  473.2451 (M+Na), found  $m/z$  473.2448 (M+Na).

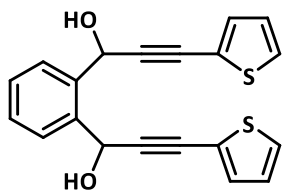
*1,1'-(1,2-phenylene)bis(3-(*p*-tolyl)prop-2-yn-1-ol) 95i*



From 4-ethynyltoluene (1.33 mL, 10.5 mmol), <sup>n</sup>BuLi (6.8 mL, 1.5 M in hexanes, 10.5 mmol) and phthalaldehyde (671 mg, 5.00 mmol) to yield **95i** as a colourless solid 1.08 g, 57% (*rac:meso* 1.0:1.9),  $R_f = 0.12$  (7:3 pentane:diethyl ether), m.p. 52-53 °C. **<sup>1</sup>H NMR** (400.1 MHz, CDCl<sub>3</sub>):  $\delta(\text{rac})$  7.94 (dd,  $J = 5.7, 3.5$  Hz, 2H, ArH), 7.44 (dd,  $J = 5.7, 3.4$  Hz, 2H, ArH), 7.40 (d,  $J = 7.8$  Hz, 4H, ArH), 7.14 (d,  $J = 7.7$  Hz, 4H, ArH), 6.18 (d,  $J = 4.7$  Hz, 2H, ArCHOH), 3.14 (d,  $J = 4.7$  Hz, 2H, OH), 2.36 (s, 6H, MeH);  $\delta(\text{meso})$   $\delta$  7.76 (dd,  $J = 5.6, 3.5$  Hz, 2H, ArH), 7.41 (dd,  $J = 5.6, 3.5$  Hz, 2H, ArH), 7.38 (d,  $J = 8.0$  Hz, 4H, ArH), 7.13 (d,  $J = 8.0$  Hz, 4H, ArH), 6.31 (d,  $J = 6.1$  Hz, 2H, ArCHOH), 3.53 (d,  $J = 6.1$  Hz, 1H, OH), 2.35 (s, 6H, MeH); **<sup>13</sup>C NMR** (100.6 MHz, CDCl<sub>3</sub>):  $\delta(\text{rac})$  139.1 (C), 138.2 (C), 131.9 (CH), 129.3 (CH), 129.2 (CH), 128.3 (CH), 119.3 (C), 88.1 (C), 87.1 (C), 62.8 (CH), 21.7 (CH<sub>3</sub>);  $\delta(\text{meso})$  139.0 (C), 138.5 (C), 131.8 (CH), 129.4 (CH), 129.3 (CH), 129.2 (CH), 119.4 (C), 87.7 (C), 87.5 (C), 64.16

(CH), 21.65 (CH<sub>3</sub>); **MS** (+ESI) calcd. for C<sub>26</sub>H<sub>22</sub>O<sub>2</sub> *m/z* 389.1512 (M+Na), found *m/z* 389.1505 (M+Na).

*1,1'-(1,2-Phenylene)bis(3-(thiophen-2-yl)prop-2-yn-1-ol) 95j*



From 3-(thiophen-2-yl)acetylene (500 mg, 4.62 mmol), <sup>n</sup>BuLi (2.8 mL, 1.68 M in hexanes, 4.7 mmol) and phthalaldehyde (310 mg, 2.31 mmol) to yield novel **95j** as a low melting yellow solid 529 mg, 65% (*rac:meso* 1.0:1.0), *R<sub>f</sub>* = 0.30 (1:1 pentane:diethyl ether). **IR** (thin film):  $\nu_{\text{max}}/\text{cm}^{-1}$  3691, 3676, 3583, 3438, 3113, 3079, 3011, 2878, 2360, 2340, 2224, 1801. 1669, 1603, 1559, 1540, 1519, 1487, 1454, 1425, 1408, 1373, 1269, 1191, 1109, 1081, 1046, 1004, 935, 852, 834. **<sup>1</sup>H NMR** (400.2 MHz, CDCl<sub>3</sub>):  $\delta$ (*rac*) 7.89 (dd, *J* = 5.7, 3.4 Hz, 2H, ArH), 7.46 (dd, *J* = 5.7, 3.4 Hz, 2H, ArH), 7.31-7.26 (m, 4H, ArH), 7.00 (dd, *J* = 3.4, 1.7 Hz, 2H, ArH), 6.20 (d, *J* = 4.8 Hz, 2H, ArCHOH), 2.95 (d, *J* = 4.8 Hz, 2H, OH);  $\delta$ (*meso*) 7.73 (dd, *J* = 5.6, 3.4 Hz, 2H, ArH), 7.43 (dd, *J* = 5.7, 3.4 Hz, 2H, ArH), 7.31-7.26 (m, 4H, ArH), 6.98 (dd, *J* = 3.4, 1.9 Hz, 2H, ArH), 6.98 (d, *J* = 6.3 Hz, 2H, ArCHOH), 3.35 (d, *J* = 6.3 Hz, 2H, OH). **<sup>13</sup>C NMR** (100.6 MHz, CDCl<sub>3</sub>):  $\delta$ (*rac*) 137.5 (C), 132.7 (CH), 129.1 (CH), 128.0 (CH), 127.6 (CH), 126.9 (CH), 122.2 (C), 91.8 (C), 80.8 (C), 62.8 (CH);  $\delta$ (*meso*) 138.0 (C), 132.7 (CH), 129.2 (CH), 129.2 (CH), 127.6 (CH), 127.0 (CH), 122.2 (C), 92.0 (C), 80.6 (C), 63.8 (CH). **MS** (+ESI) calcd. for C<sub>20</sub>H<sub>14</sub>S<sub>2</sub>O<sub>2</sub> *m/z* 373.0319 (M+Na), found *m/z* 373.0327 (M+Na).

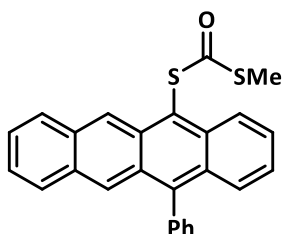
### Preparation of Tetracenes

*General procedure for formation of tetracenes 96a-i and antrathiophene 96j.*

Acenes **7** could be prepared *via* deprotonation *via* addition of LiHMDS (370  $\mu$ L of 1.0 M tetrahydrofuran solution, 0.37 mmol) of stirred solutions of diols **95a-j** (0.18 mmol) in tetrahydrofuran (4 mL) at 0 °C under an argon atmosphere. After 20 mins, CS<sub>2</sub> (32  $\mu$ L, 0.53 mmol) and iodomethane (88  $\mu$ L, 1.42 mmol) were added, and the reaction vessel transferred to an oil bath preheated to 60 °C and stirred for 90 mins. This was usually accompanied by a bright orange or red colour developing within 5-15 mins. The reaction was quenched with water (4 mL), extracted with dichloromethane (3 x 4 mL) and dried with MgSO<sub>4</sub>. The reaction mixture could then be purified *via* preparative TLC (7:3 pentane: diethyl ether for **96a-g** & **96i-j**; 6:1 pentane:CH<sub>2</sub>Cl<sub>2</sub> for **96h**). The

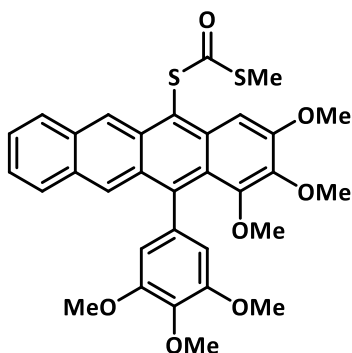
moderately soluble acenes could then be recrystallised either by liquid layering of pentane:diethyl ether and cooling from r.t. to 5 °C, or from stepwise cooling of refluxing acetonitrile solutions first to ambient temperature then to -24 °C.

*5-(((Methylthio)carbonyl)thio)-12-phenyltetracene 96a*



From diol **95a** (62 mg, 0.15 mmol), LiHDMS (0.35 mL, 1.0 M in THF, 0.35 mmol), CS<sub>2</sub> (32 μL, 40.6 mg, 0.53 mmol) and iodomethane (88 μL, 202 mg, 1.42 mmol) to yield **96a** as an orange solid 64 mg, 85% that could be recrystallised from by liquid layering (pentane:ether, 5°C). *R<sub>f</sub>* = 0.76 (3:2 pentane:ether), *m.p.* 166-167 °C. **IR** (CHCl<sub>3</sub>):  $\nu_{\max}/\text{cm}^{-1}$  3692, 3060, 3003, 2979, 2930, 2873, 2361, 2341, 1639, 1602, 1491, 1462, 1491, 1462, 1442, 1384, 1344, 1319, 1261, 1110, 1024, 909, 881, 854, 660. **<sup>1</sup>H NMR** (400.1 MHz, CDCl<sub>3</sub>):  $\delta$  9.38 (s, 1H, *ArH*), 8.72 (d, *J* = 9.0 Hz, 1H, *ArH*), 8.32 (s, 1H, *ArH*), 8.09 (d, *J* = 8.5 Hz, 1H, *ArH*), 7.81 (d, *J* = 8.5 Hz, 1H, *ArH*), 7.70-7.62 (m, 4H, *ArH*), 7.56 (ddd, *J* = 9.0, 6.4, 1.2 Hz, 2H, *ArH*), 7.53 (broad, s, 2H), 7.47-7.42 (m, 1H, *ArH*), 7.39-7.34 (m, 1H, *ArH*), 7.32 (ddd, *J* = 9.0, 6.4, 1.2 Hz, 1H, *ArH*), 2.31 (s, 3H, SCH<sub>3</sub>). **<sup>13</sup>C NMR** (100.6 MHz, CDCl<sub>3</sub>):  $\delta$  190.3 (C), 142.6 (C), 138.6 (C), 135.3 (C), 132.4 (C), 132.4 (C), 131.3 (C), 131.2 (CH), 130.0 (C), 129.7 (C), 128.6 (2 overlapping signals, both CH), 128.5 (CH), 128.1 (CH), 127.9 (CH), 127.5 (CH), 127.1 (CH), 126.3 (CH), 126.3 (CH), 125.7 (CH), 125.1 (CH), 124.9 (CH), 120.2 (C), 13.7 (CH<sub>3</sub>); UV-vis (CHCl<sub>3</sub>):  $\lambda_{\max}$  286.8 nm. MS (+ESI) calcd. for C<sub>26</sub>H<sub>18</sub>OS<sub>2</sub> *m/z* 433.0691 (M+Na), found *m/z* 433.0702 (M+Na). **CHN Anal.** calcd. for C<sub>26</sub>H<sub>18</sub>OS<sub>2</sub> C: 76.06, H: 4.42; found C: 76.01, H: 4.58%.

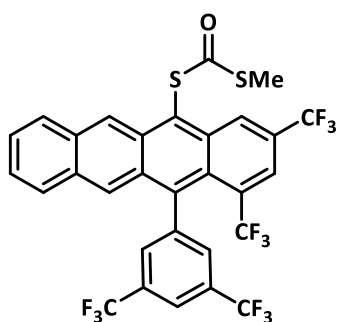
*5-(((Methylthio)carbonyl)thio)-1,2,3-trimethoxy-12-(1,2,3-trimethoxyphenyl)-tetracene 96b*



From diol **95b** (93 mg, 0.16 mmol), LiHDMS (0.35 mL, 1.0 M in THF, 0.35 mmol), CS<sub>2</sub> (32 μL, 40.6 mg, 0.53 mmol) and iodomethane (88 μL, 202 mg, 1.42 mmol) to yield **96b** as an orange solid 49 mg, 47% that could be recrystallised from by liquid layering (pentane:ether, 5°C). *R<sub>f</sub>* = 0.14 (7:3 pentane:ether), *m.p.* 214-216. **IR**

(CHCl<sub>3</sub>):  $\nu_{\max}/\text{cm}^{-1}$  3690, 3059, 3045, 3006, 2966, 2938, 2838, 2422, 1717, 1635, 1618, 1601, 1584, 1544, 1525, 1509, 1464, 1421, 1414, 1379, 1350, 1313, 1297, 1254, 1164, 1129, 1105, 1053, 1006, 964, 938, 896, 880, 854. **<sup>1</sup>H NMR** (500.1 MHz, CDCl<sub>3</sub>)  $\delta$  9.20 (s, 1H), 8.20 (s, 1H), 8.04 (d,  $J = 8.5$  Hz, 1H), 7.82 (d,  $J = 8.5$  Hz, 1H), 7.80 (s, 1H), 7.45 – 7.40 (m, 1H), 7.38 – 7.33 (m, 1H), 6.67 (s, broad, 2H), 4.09 (s, 3H), 4.04 (s, 3H), 3.92 (s, 3H), 3.85 (s, 6H), 3.46 (s, 3H), 2.33 (s, 3H). **<sup>13</sup>C NMR** (125.8 MHz, CDCl<sub>3</sub>)  $\delta$  190.5 (C), 154.7 (C), 152.5 (C), 149.3 (C), 142.4 (C), 139.9 (C), 137.9 (C), 136.7 (C), 134.6 (C), 132.5 (C), 132.1 (C), 130.8 (C), 130.1 (C), 128.9 (CH), 128.4 (CH), 127.7 (CH), 126.5 (CH), 125.4 (CH), 123.9 (CH), 123.2 (C), 117.6 (C), 107.1 (CH), 99.3 (CH), 61.4 (CH<sub>3</sub>), 61.0 (CH<sub>3</sub>), 60.9 (CH<sub>3</sub>), 56.3 (CH<sub>3</sub>), 56.1 (CH<sub>3</sub>), 13.8 (CH<sub>3</sub>), **UV-vis** (CH<sub>2</sub>Cl<sub>2</sub>):  $\lambda_{\max}$  297.3 nm. **MS** (+ESI) calcd. for C<sub>32</sub>H<sub>30</sub>O<sub>7</sub>S<sub>2</sub>  $m/z$  613.1325 (M+Na), found  $m/z$  613.1313 (M+Na).

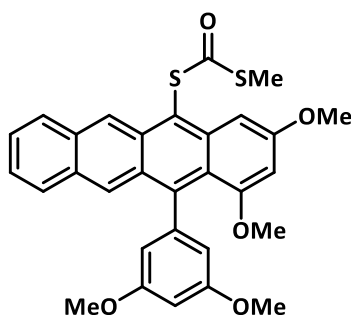
*1,3-Bis(trifluoromethyl)-12-((3,5-bis(trifluoromethyl)phenyl)-5-(((methylthio)carbonyl)thio)-tetracene* **96c**



From diol **95c** (109 mg, 0.18 mmol), LiHDMS (0.35 mL, 1.0 M in THF, 0.35 mmol), CS<sub>2</sub> (32  $\mu$ L, 40.6 mg, 0.53 mmol) and iodomethane (88  $\mu$ L, 202 mg, 1.42 mmol) to yield **96c** as an orange solid 60.1 mg, 56% that could be recrystallised from acetonitrile at -24 °C.  $R_f = 0.72$  (7:3 pentane:ether), **m.p.** 226-228 °C. **IR** (CHCl<sub>3</sub>):  $\nu_{\max}/\text{cm}^{-1}$  3696, 3089, 3054, 2928, 2856, 2361, 1719, 1648, 1587, 1542, 1458, 1420, 1396, 1367, 1345, 1314, 1279, 1266, 1246, 1176, 1142, 1108, 1006, 956, 902, 880, 871, 850, 640. **<sup>1</sup>H NMR** (400.1 MHz, CDCl<sub>3</sub>):  $\delta$  9.45 (s, 1H, ArH), 9.36 (s, 1H, ArH), 8.15 (s, 1H, ArH), 8.14 (d,  $J = 8.4$  Hz, 1H, ArH), 8.07 (s, 1H, ArH), 7.98 (s, 1H, ArH), 7.96 (s, 2H, ArH), 7.83 (d,  $J = 8.5$  Hz, 1H, ArH), 7.60-7.54 (m, 1H, ArH), 7.51 (m, 1H, ArH), 2.41 (s, 3H, SCH<sub>3</sub>). **<sup>13</sup>C NMR** (125.8 MHz, CDCl<sub>3</sub>): Extensive  $J_{CF}$  couplings prevented complete assignment of the spectrum, **<sup>19</sup>F NMR** (376.5 MHz, CDCl<sub>3</sub>):  $\delta$  -53.5 (s, 3F), -62.8 (s, 6F), -63.6 (s, 3F). **UV-vis** (CHCl<sub>3</sub>):  $\lambda_{\max}$  297.2 nm. **MS** (+ESI) calcd. for C<sub>30</sub>H<sub>14</sub>F<sub>12</sub>OS<sub>2</sub>  $m/z$  705.0194 (M+Na), found  $m/z$  705.0187 (M+Na).

1,3-Dimethoxy-12-(3,5-dimethoxyphenyl)-5-(((methylthio)carbonyl)thio)-tetracene

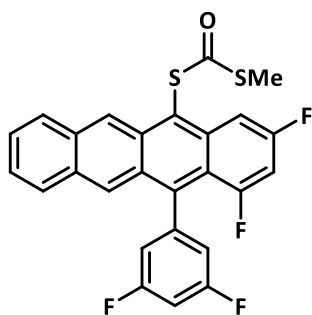
96d



From diol **95d** (84.6 mg, 0.18 mmol), LiHDMS (0.35 mL, 1.0 M in THF, 0.35 mmol), CS<sub>2</sub> (32 μL, 40.6 mg, 0.53 mmol) and iodomethane (88 μL, 202 mg, 1.42 mmol) to provide a quantitative yield of **96d** as a red solid (96.3 mg) that could be recrystallised from liquid layering (2:1 pentane ether, 5°C). *R<sub>f</sub>* = 0.43 (7:3 pentane:ether), m.p.

220-221 °C. IR (CHCl<sub>3</sub>):  $\nu_{\max}/\text{cm}^{-1}$  3691, 3604, 3011, 2963, 2938, 2840, 1766, 1720, 1696, 1633, 1624, 1591, 1558, 1527, 1504, 1465, 1455, 1422, 1382, 1347, 1324, 1280, 1265, 1241, 1165, 1156, 1113, 1061, 1014, 992, 969, 946, 927, 893, 880, 856, 827. <sup>1</sup>H NMR (400.1 MHz, CDCl<sub>3</sub>):  $\delta$  9.19 (s, 1H, ArH), 8.27 (s, 1H, ArH), 8.03 (d, *J* = 8.5 Hz, 1H, ArH), 7.81 (d, *J* = 8.5 Hz, 1H, ArH), 7.57 (d, *J* = 2.3 Hz, 1H, ArH), 7.45-7.40 (m, 1H, ArH), 7.35-7.30 (broad, s, 1H, ArH), 6.62 (dd, *J* = 2.3, 2.2 Hz, 1H, ArH), 6.32 (d, *J* = 2.2 Hz, 1H, ArH), 4.02 (s, 3H, MeH), 3.83 (s, 6H, MeH), 3.51 (s, 3H, MeH), 2.29 (s, 3H, SCH<sub>3</sub>). <sup>13</sup>C NMR (125.8 MHz, CDCl<sub>3</sub>): 191.2 (C), 160.0 (2C, C), 159.5 (C), 158.9 (C), 144.8 (C), 141.8 (C), 138.3 (C), 132.9 (C), 132.8 (C), 130.6 (C), 129.4 (C), 129.0 (CH), 128.4 (CH), 128.3 (CH), 126.6 (CH), 125.1 (CH), 123.5 (CH), 120.8 (C), 116.7 (C), 99.2 (CH), 98.9 (CH), 94.9 (CH), 55.9 (CH<sub>3</sub>), 55.7 (CH<sub>3</sub>), 55.6 (CH<sub>3</sub>), 13.8 (CH<sub>3</sub>). UV-vis (CH<sub>2</sub>Cl<sub>2</sub>):  $\lambda_{\max}$  296.4 nm. MS (+ESI) calcd. for C<sub>30</sub>H<sub>26</sub>O<sub>5</sub>S<sub>2</sub> *m/z* 531.1294 (M+H), found *m/z* 531.1305 (M+H). CHN Anal. calcd. for C<sub>30</sub>H<sub>26</sub>O<sub>5</sub>S<sub>2</sub> C: 67.90, H: 4.94; found C: 67.86, H: 5.01%.

1,3-Difluoro-12-(3,5-difluorophenyl)-5-(((methylthio)carbonyl)thio)-tetracene 96e

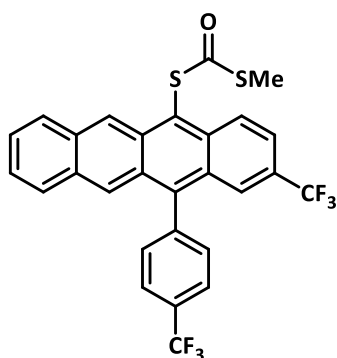


From diol **95e** (69.9 mg, 0.170 mmol), LiHDMS (0.35 mL, 1.0 M in THF, 0.35 mmol), CS<sub>2</sub> (31 μL, 38.9 mg, 0.51 mmol) and iodomethane (85 μL, 193 mg, 1.36 mmol) to yield **96e** as an orange solid 23.9 mg, 29% that could be recrystallised from liquid layering (2:1 pentane:ether) at 5 °C. *R<sub>f</sub>* = 0.67 (7:3 pentane:ether), m.p. 224-226 °C. IR (CHCl<sub>3</sub>):  $\nu_{\max}/\text{cm}^{-1}$  3691,

3606, 3045, 3009, 2933, 2419, 1720, 1648, 1622, 1594, 1600, 1459, 1432, 1386, 1370, 1348, 1320, 1283, 1256, 1193, 1150, 1133, 1121, 1074, 1004, 989, 942, 881, 857, 831. <sup>1</sup>H NMR (500.1 Hz, CDCl<sub>3</sub>)  $\delta$  9.30 (s, 1H, ArH), 8.21 (ddd, *J* = 11.2, 2.3, 1.4 Hz, 1H, ArH),

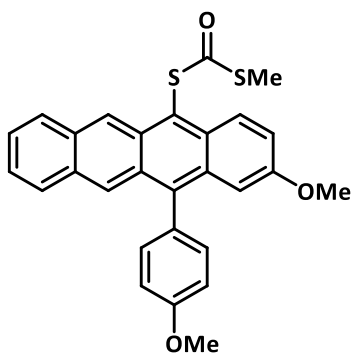
8.16 (s, 1H, ArH), 8.08 (d,  $J = 8.6$  Hz, 1H, ArH), 7.83 (d,  $J = 8.6$  Hz, 1H, ArH), 7.53-7.48 (m, 1H, ArH), 7.45-7.40 (m, 1H, ArH), 7.09 – 7.03 (m, 1H, ArH), 7.03 (broad, s, 2H, ArH), 6.92 (ddd,  $J = 12.4, 8.0, 2.4$  Hz, 1H, ArH), 2.37 (s, 3H, MeH).  $^{13}\text{C NMR}$  (125.8 Hz,  $\text{CDCl}_3$ ):  $\delta$  189.0 (C), 133.3 (C), 132.8 (C), 131.8 (C), 129.3 (C), 128.7 (CH), 128.6 (CH), 127.4 (s), 127.2 (s), 126.55 (s), 125.05 (s), 13.83 ( $\text{CH}_3$ ).  $^{19}\text{F NMR}$  (376.5 MHz,  $\text{CDCl}_3$ )  $\delta$  -98.93 (d,  $J = 9.0$  Hz, 1F), -107.28 (d,  $J = 9.0$  Hz, 1F), -110.00 to -110.28 (m, 2F). **UV-vis** ( $\text{CH}_2\text{Cl}_2$ ):  $\lambda_{\text{max}}$  286.3 nm. **MS** (+ESI) calcd. for  $\text{C}_{26}\text{H}_{14}\text{OS}_2\text{F}_4$   $m/z$  482.0422 (M), found  $m/z$  482.0434 (M).

*5-(((Methylthio)carbonyl)thio)-2-(trifluoromethyl)-12-(4-(trifluoromethyl)phenyl)-tetracene 96f*



From diol **95f** (167 mg, 0.36 mmol), LiHDMS (0.71 mL, 1.0 M in THF, 0.71 mmol),  $\text{CS}_2$  (64  $\mu\text{L}$ , 81.2 mg, 1.07 mmol) and iodomethane (177  $\mu\text{L}$ , 404 mg, 2.84 mmol) to yield **96f** as an orange solid 86.0 mg, 44% that could be recrystallised from liquid layering (pentane:ether) 5 °C.  $R_f = 0.72$  (3:2 pentane:ether), **m.p.** 225-226 °C. **IR** ( $\text{CHCl}_3$ ):  $\nu_{\text{max}}/\text{cm}^{-1}$  2928, 2856, 1721, 1645, 1456, 1406, 1386, 1363, 1347, 1325, 1300, 1278, 1263, 1168, 1131, 1108, 1068, 1020, 975, 882, 847, 821, 638, 609.  $^1\text{H NMR}$  (500.1 MHz,  $\text{CDCl}_3$ ):  $\delta$  9.42 (s, 1H, ArH), 8.84 (d,  $J = 9.4$  Hz, 1H, ArH), 8.23 (s, 1H, ArH), 8.12 (d,  $J = 8.6$  Hz, 1H, ArH), 7.98 (d,  $J = 8.2$  Hz, 2H, ArH), 7.91 (s, 1H, ArH), 7.89 (d,  $J = 8.5$  Hz, 1H, ArH), 7.68 (dd,  $J = 9.4, 1.7$  Hz, 1H, ArH), 7.66 (broad, s, 2H, ArH), 7.57-7.48 (m, 1H, ArH), 7.48-7.39 (m, 1H, ArH), 2.36 (s, 3H,  $\text{SCH}_3$ ).  $^{13}\text{C NMR}$  (125.8 MHz,  $\text{CDCl}_3$ ):  $\delta$  189.3 (C), 142.6 (C), 141.5 (C), 135.0 (C), 133.2 (C), 133.0 (C), 132.0 (C), 131.6 (CH), 131.1 (C, q,  $J_{\text{CF}} = 32.7$  Hz), 129.7 (C), 128.7 (CH), 128.6 (CH), 128.4 (CH), 128.1 (C), 127.4 (C, q,  $J_{\text{CF}} = 32.3$  Hz), 127.3 (CH), 127.1 (CH), 126.7 (CH), 126.1 (CH, dd,  $J_{\text{CF}} = 7.2, 3.6$  Hz), 125.6 (CH), 125.5 (CH, q,  $J_{\text{CF}} = 5.1$  Hz), 125.3 (C, q,  $J_{\text{CF}} = 27.3$  Hz), 123.1 (C, q,  $J_{\text{CF}} = 27.0$  Hz), 122.4 (CH, q,  $J_{\text{CF}} = 2.7$  Hz), 122.4 (C), 13.8 ( $\text{CH}_3$ ).  $^{19}\text{F NMR}$  (376.6 MHz,  $\text{CDCl}_3$ ):  $\delta$  -62.4 (s), -63.3 (s). **UV-vis** ( $\text{CH}_2\text{Cl}_2$ ):  $\lambda_{\text{max}}$  290.9 nm. **MS** (+ESI) calcd. for  $\text{C}_{30}\text{H}_{16}\text{OS}_2\text{F}_6$   $m/z$  547.0620 (M+H), found  $m/z$  547.0625 (M+H).

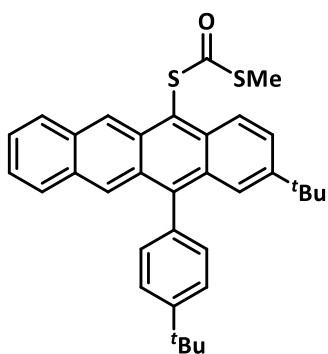
*2-Methoxy-12-(4-methoxyphenyl)-5-(((methylthio)carbonyl)thio)-tetracene 96g*



From diol **95g** (70.8 mg, 0.18 mmol), LiHDMS (0.35 mL, 1.0 M in THF, 0.35 mmol), CS<sub>2</sub> (32 μL, 40.6 mg, 0.53 mmol) and iodomethane (88 μL, 202 mg, 1.42 mmol) to yield **96g** as an orange solid 32 mg, 38% that could be recrystallised from hot acetonitrile subsequently chilled to -28 °C. *R<sub>f</sub>* = 0.41 (7:3 pentane:ether). **m.p.** 176-178 °C. **IR** (CHCl<sub>3</sub>):  $\nu_{\max}/\text{cm}^{-1}$  3607, 3489, 3045, 2928, 2854, 2359,

2338, 1718, 1648, 1602, 1506, 1457, 1396, 1368, 1345, 1314, 1279, 1176, 1142, 1107, 1106, 956, 902, 880, 871, 850. **<sup>1</sup>H NMR** (500.1 MHz, CDCl<sub>3</sub>):  $\delta$  9.32 (s, 1H, ArH), 8.64 (d, *J* = 9.6 Hz, 1H, ArH), 8.28 (s, 1H, ArH), 8.06 (d, *J* = 8.5 Hz, 1H, ArH), 7.81 (d, *J* = 8.5 Hz, 1H, ArH), 7.44 (s, broad, 2H, ArH), 7.43-7.39 (m, 2H, ArH), 7.37-7.33 (m, 2H, ArH), 7.28 (d, *J* = 2.5 Hz, 1H, ArH), 7.20 (d, *J* = 8.8 Hz, 2H, ArH), 6.87 (d, *J* = 2.5 Hz, 1H, ArH), 4.01 (s, 3H, OCH<sub>3</sub>), 3.73 (s, 3H, OCH<sub>3</sub>), 2.30 (s, 3H, SCH<sub>3</sub>); **<sup>13</sup>C NMR** (125.8 MHz, CDCl<sub>3</sub>):  $\delta$  190.6 (C), 159.4 (C), 156.6 (C), 139.8 (C), 132.7 (C), 132.3 (CH), 131.9 (C), 131.5 (C), 131.4 (C), 131.4 (C), 131.1 (C), 130.6 (C), 128.7 (CH), 128.5 (CH), 128.3 (CH), 126.4 (CH), 125.9 (CH), 125.7 (CH), 125.0 (CH), 123.2 (CH), 120.2 (C), 114.3 (CH), 103.0 (CH), 55.6 (CH<sub>3</sub>), 55.3 (CH<sub>3</sub>), 13.8 (CH<sub>3</sub>). **UV-vis** (CHCl<sub>3</sub>):  $\lambda_{\max}$  290.0 nm. **MS** (+ESI) calcd. for C<sub>30</sub>H<sub>22</sub>O<sub>3</sub>S<sub>2</sub> *m/z* 471.1083 (M+H), found *m/z* 471.1100 (M+H).

#### 2-(tert-Butyl)-12-(4-(tert-butyl)phenyl)-5-(((methylthio)carbonyl)thio)-tetracene **96h**

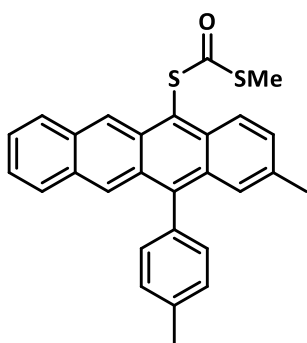


From diol **95h** (80 mg, 0.18 mmol), LiHDMS (0.35 mL, 1.0 M in THF, 0.35 mmol), CS<sub>2</sub> (32 μL, 40.6 mg, 0.53 mmol) and iodomethane (88 μL, 202 mg, 1.42 mmol) to yield **96h** as an orange solid 20.3 mg, 22% that could be recrystallised by liquid layering (pentane:ether). *R<sub>f</sub>* = 0.58 (7:3 pentane:ether), **m.p.** 255-256 °C. **IR** (CHCl<sub>3</sub>):  $\nu_{\max}/\text{cm}^{-1}$  3092, 3871, 3853, 3838, 3821, 3802, 3691, 3676, 3649,

3608, 3080, 3057, 2966, 2931, 2870, 2377, 2337, 2229, 1734, 1699, 1684, 1636, 1602, 1559, 1541, 1490, 1457, 1396, 1365, 1341, 1314, 1263, 1248, 1190, 1128, 1107, 1019, 998, 979, 956, 923, 881, 852. **<sup>1</sup>H NMR** (500.1 MHz, CDCl<sub>3</sub>):  $\delta$  9.33 (s, 1H), 8.64 (d, *J* = 9.4 Hz, 1H), 8.39 (s, 1H), 8.07 (d, *J* = 8.6 Hz, 1H), 7.84 (d, *J* = 8.6 Hz, 1H), 7.69-7.64 (m, 3H), 7.56 (d, *J* = 1.6 Hz, 1H), 7.45 (s, broad 2H), 7.44-7.40 (m, 1H), 7.37-7.33 (m, 1H),

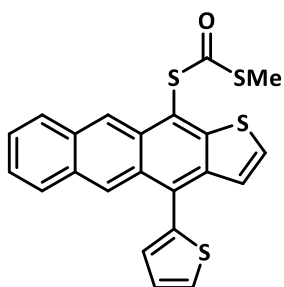
2.31 (s, 3H, SCH<sub>3</sub>), 1.52 (s, 9H, <sup>t</sup>BuH), 1.28 (s, 9H, <sup>t</sup>BuH). <sup>13</sup>C NMR (125.8 MHz, CDCl<sub>3</sub>): δ 190.8 (C), 151.0 (C), 147.1 (C), 142.6 (C), 135.6 (C), 134.4 (C), 132.3 (C), 132.2 (C), 131.2 (CH), 131.0 (C), 130.4 (C), 130.1 (C), 128.7 (CH), 128.6 (CH), 127.4 (CH), 127.2 (CH), 126.2 (CH), 126.0 (CH), 125.5 (CH), 125.4 (CH), 124.7 (CH), 122.1 (CH), 119.2 (C), 35.0 (C), 35.0 (C), 31.7 (CH<sub>3</sub>), 30.6 (CH<sub>3</sub>), 13.8 (CH<sub>3</sub>). **UV-vis** (CH<sub>2</sub>Cl<sub>2</sub>): λ<sub>max</sub> 289.0 nm. **MS** (+ESI) calcd. for C<sub>34</sub>H<sub>34</sub>OS<sub>2</sub> *m/z* 545.1943 (M+Na), found *m/z* 545.1968 (M+Na).

*2-(tert-Butyl)-12-(4-(tert-butyl)phenyl)-5-(((methylthio)carbonyl)thio)-tetracene 96i*



From diol **95i** (80 mg, 0.18 mmol), LiHDMS (0.35 mL, 1.0 M in THF, 0.35 mmol), CS<sub>2</sub> (32 μL, 40.6 mg, 0.53 mmol) and iodomethane (88 μL, 202 mg, 1.42 mmol) to yield **96i** as an orange solid 20.5 mg, 26% that could be recrystallised by liquid layering (pentane:ether). *R<sub>f</sub>* = 0.71 (7:3 pentane:ether). **m.p.** 136-138 °C **IR** (CHCl<sub>3</sub>): ν<sub>max</sub>/cm<sup>-1</sup> 3690, 3051, 3009, 2958, 2927, 2857, 2735, 1720, 1638, 1604, 1536, 1514, 1494, 1465, 1420, 1380, 1341, 1312, 1284, 1262, 1243, 11182, 1124, 1107, 1038, 1022, 972, 907, 881, 853, 823, <sup>1</sup>H NMR (500.1 MHz, CDCl<sub>3</sub>): δ 9.34 (s, 1H), 8.63 (d, *J* = 9.1 Hz, 1H), 8.31 (s, 1H), 8.07 (d, *J* = 8.6 Hz, 1H), 7.81 (d, *J* = 8.6 Hz, 1H), 7.49 – 7.44 (m, 2H), 7.42 (ddd, *J* = 8.6, 6.4, 0.9 Hz, 1H, *ArH*), 7.40 (dd, *J* = 9.1, 1.6 Hz, 2H), 7.37 – 7.32 (ddd, *J* = 8.6, 6.4, 0.9 Hz, 1H, *ArH*), 2.60 (s, CH<sub>3</sub>), 2.41 (s, 3H, CH<sub>3</sub>), 2.29 (s, 3H, SCH<sub>3</sub>), remaining signals could not be assigned due to extensive overlap of signals in the <sup>1</sup>H NMR, but were observed in COSY spectrum. <sup>13</sup>C NMR (125.8 MHz, CDCl<sub>3</sub>): δ 190.8 (C), 141.7 (C), 137.7 (C), 135.7 (C), 134.7 (C), 134.4 (C), 132.2 (C), 132.1 (C), 131.3 (C), 131.2 (CH), 130.6 (CH), 130.5 (C), 130.1 (C), 129.4 (CH), 128.7 (CH), 128.6 (CH), 127.1 (CH), 126.2 (CH), 126.2 (CH), 125.9 (CH), 125.6 (CH), 124.8 (CH), 119.7 (C), 22.1 (CH<sub>3</sub>), 21.7 (CH<sub>3</sub>), 13.8 (CH<sub>3</sub>). **UV-vis** (CH<sub>2</sub>Cl<sub>2</sub>): λ<sub>max</sub> 288.3 nm. **MS** (+ESI) calcd. for C<sub>28</sub>H<sub>22</sub>OS<sub>2</sub> *m/z* 439.1185 (M+H), found *m/z* 439.1197 (M+H).

### 11-(((Methylthio)carbonyl)thio)-4-(thiophen-2-yl)anthra[2,3-b]thiophene **96j**



From diol **95j** (82.9 mg, 0.24 mmol), LiHDMS (0.35 mL, 1.0 M in THF, 0.35 mmol), CS<sub>2</sub> (43 μL, 54.1 mg, 0.71 mmol) and iodomethane (88 μL, 298 mg, 1.89 mmol) to yield **96j** as a yellow-orange solid 38.3 mg, 38% that could be recrystallised from liquid layering (2:1 pentane:ether) at 5°C. *R<sub>f</sub>* = 0.65 (7:3 pentane:ether), **m.p.** 209-210 °C. **IR** (CHCl<sub>3</sub>):  $\nu_{\max}/\text{cm}^{-1}$  3692, 3058, 3007, 2692, 2932, 1719, 1648, 1502, 1460, 1432, 1413, 1369, 1321, 1290, 1262, 1176, 1115, 1091, 1045, 1028, 973, 909, 882, 853, 821. **<sup>1</sup>H NMR** (400.1 MHz, CDCl<sub>3</sub>):  $\delta$  9.06 (s, 1H), 8.69 (s, 1H), 8.10 (d, *J* = 8.4 Hz, 1H), 7.93 (d, *J* = 8.4 Hz, 1H), 7.66 (dd, *J* = 4.1, 2.2 Hz, 1H), 7.53-7.47 (m, 1H), 7.47-7.42 (m, 1H), 7.44 (d, *J* = 5.8 Hz, 1H), 7.36 (s, 1H), 7.35 (d, *J* = 2.0 Hz, 1H), 7.33 (d, *J* = 5.8 Hz, 1H), 2.35 (s, 3H, SCH<sub>3</sub>). **<sup>13</sup>C NMR** (125.8 MHz, CDCl<sub>3</sub>):  $\delta$  188.8 (C), 149.0 (C), 138.9 (C), 138.3 (C), 132.1 (C), 131.3 (C), 130.8 (C), 130.5 (C), 130.2 (C), 129.6 (CH), 129.3 (CH), 128.5 (CH), 128.5 (CH), 127.5 (CH), 127.2 (CH), 126.6 (CH), 126.4 (CH), 125.8 (CH), 124.8 (CH), 123.0 (CH), 116.6 (C), 13.8 (CH<sub>3</sub>). **UV-vis** (CH<sub>2</sub>Cl<sub>2</sub>):  $\lambda_{\max}$  283.7 nm. **MS** (+ESI) calcd. for C<sub>22</sub>H<sub>14</sub>OS<sub>4</sub> *m/z* 444.9820 (M+Na), found *m/z* 444.9811 (M+Na). **CHN** Anal. calcd. for C<sub>22</sub>H<sub>14</sub>OS<sub>4</sub> C: 62.53, H: 3.34%, found C: 62.67, H: 3.44%.

### Characterisation of electro-optic properties of acenes **96a-j**

#### Cyclic voltammetry studies

Cyclic voltammetry measurements were carried out in a three electrode cell under an argon atmosphere using 0.30 M TBAPF<sub>6</sub> in dry CH<sub>2</sub>Cl<sub>2</sub> as the supporting electrolyte. Typical concentrations of the tetracene analytes **96a-j** ranged from 2 mM to 5 mM. Cyclic voltammograms were recorded using a CH instruments CHI700D potentiostat. Curves were referenced from the Ag reference electrode calibrated using the ferrocene/ferrocinium (Fc/Fc<sup>+</sup>) redox couple as an internal standard, the halfwave potential (*E*<sub>1/2</sub>) of which was found to be 0.44-0.47 V relative to the reference electrode. Estimates of the HOMO levels could be attained by taking the onset of the oxidation peak and the known HOMO of Ferrocene (-4.4 eV) using the formula  $\text{HOMO} = -[E^{\text{OnsetOx}} + 4.4]\text{eV}$ .<sup>195</sup>

## Optical studies

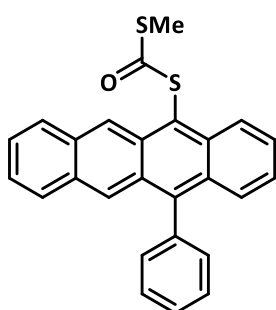
Estimates of the optical bandgap  $E_g$  opt. were attained from the onset of the lowest energy band in the UV visible spectrum. The method of Tauc was used: plots of  $(ah\nu)^{1/2}$  as a function of  $h\nu$  from the primary A vs. wavelength (converted into eV).<sup>196</sup> The UV/vis was collected from  $10^{-4}$  M solutions of the molecules in  $\text{CH}_2\text{Cl}_2$ .

## Computational Calculations

All calculations were carried out using Gaussian 09, Revision D.01<sup>197</sup> with default settings. Initial structure searches for mapping of the reaction coordinate were run at the B3LYP/6-31+G(d,p)<sup>ii198-202</sup> level of theory, and the resulting structures further optimized using CBS-QB3<sup>iii</sup> with 'tight' convergence and 'UltraFine' integration grid keywords specified. Transition-state structures were all characterized by a single imaginary vibrational frequency and IRC calculations were run at the B3LYP/6-31+G(d,p) level of theory to confirm all transition-states. All energies are listed in Hartrees and were converted to eV (1 Hartree = 27.2114 eV). Approximations for the HOMO eigenvalues of all tetracenes were calculated at the CAM-B3LYP/6-31G(d,p)<sup>202</sup> level of theory. Values for the vertical excitation energies of the first singlet and triplet excited states of all tetracenes were calculated using TD-SCF CAM-B3LYP/6-31G(d,p)<sup>202</sup> with the tda (Tamm-Dancoff Approximation)<sup>93</sup> keyword. The excitation energy of the first singlet excited state can be taken as a reasonable estimate of the HOMO-LUMO gap.<sup>92</sup>

### CAM-B3LYP/6-31G(d,p) HOMO Eigenvalues and TD-DFT Calculations:

96a:

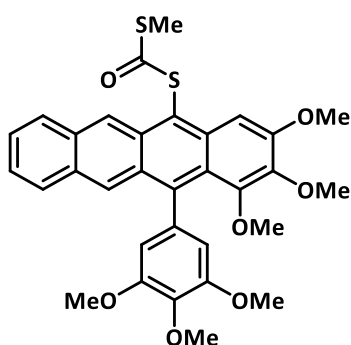


Highest alpha occupied eigenvalue: -0.21832

Triplet-A      0.9353 eV      1325.68 nm      f=0.0000      S<sup>2</sup>=2.000

Singlet-A 2.6475 eV 468.30 nm f=0.2654 S<sup>2</sup>=0.000

**96b:**

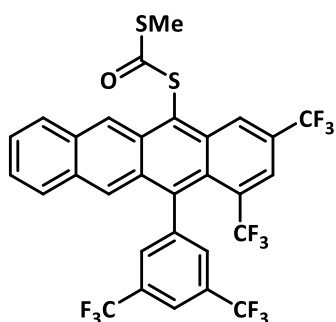


Highest alpha occupied eigenvalue: -0.21666

Triplet-A 1.0083 eV 1229.61 nm f=0.0000 S<sup>2</sup>=2.000

Singlet-A 2.5800 eV 480.56 nm f=0.2566 S<sup>2</sup>=0.000

**96c:**

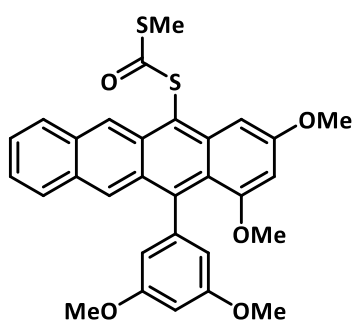


Highest alpha occupied eigenvalue: -0.25161

Triplet-A 1.5301 eV 810.30 nm f=0.0000 S<sup>2</sup>=2.000

Singlet-A 2.9359 eV 422.30 nm f=0.1978 S<sup>2</sup>=0.000

**96d:**

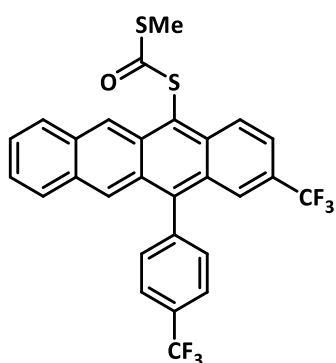


Highest alpha occupied eigenvalue: -0.22231

Triplet-A 1.5300 eV 810.36 nm f=0.0000 S<sup>2</sup>=2.000

Singlet-A 2.6274 eV 471.89 nm f=0.2523 S<sup>2</sup>=0.000

**96f:**

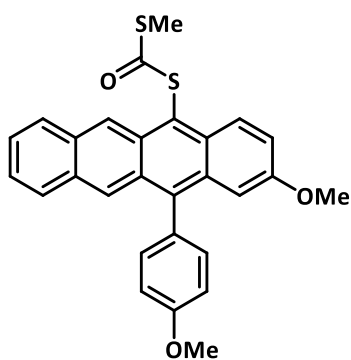


Highest alpha occupied eigenvalue: -0.24042

Triplet-A 1.1137 eV 1113.29 nm f=0.0000 S<sup>2</sup>=2.000

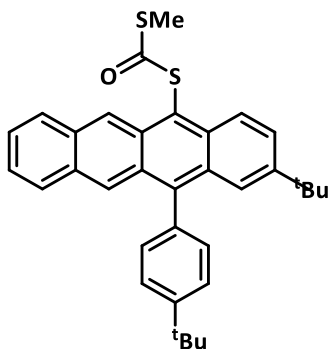
Singlet-A 2.7441 eV 451.82 nm f=0.2301 S<sup>2</sup>=0.000

**96g:**



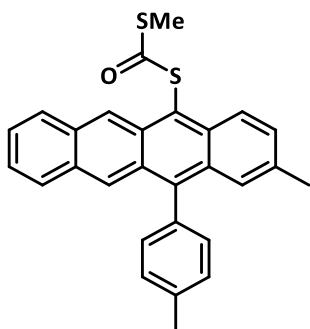
Highest alpha occupied eigenvalue:				-0.22696
Triplet-A	1.0196 eV	1216.04 nm	f=0.0000	S <sup>2</sup> =2.000
Singlet-A	2.6630 eV	465.57 nm	f=0.2604	S <sup>2</sup> =0.000

**96h:**



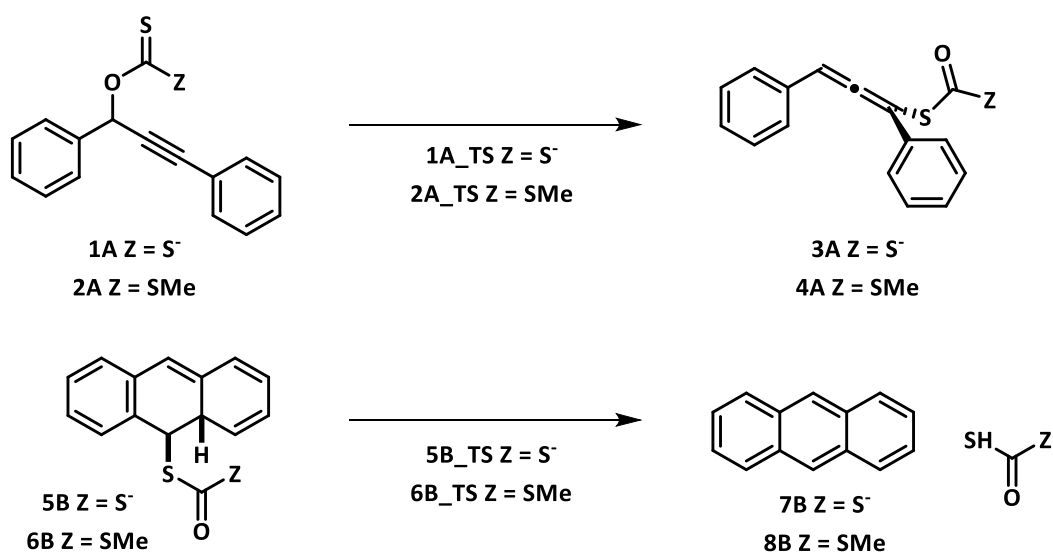
Highest alpha occupied eigenvalue:				-0.22404
Triplet-A	0.9054 eV	1369.32 nm	f=0.0000	S <sup>2</sup> =2.000
Singlet-A	2.7248 eV	455.02 nm	f=0.2512	S <sup>2</sup> =0.000

**96i:**



Highest alpha occupied eigenvalue:				-0.22169
Triplet-A	0.9494 eV	1305.87 nm	f=0.0000	S <sup>2</sup> =2.000
Singlet-A	2.6067 eV	475.64 nm	f=0.2797	S <sup>2</sup> =0.000

Calculated CBS-QB3 Reaction Coordinates:



**1A**

CBS-QB3 (0 K)	=	-1485.830076
CBS-QB3 Energy	=	-1485.813171
CBS-QB3 Enthalpy	=	-1485.812227
CBS-QB3 Free Energy	=	-1485.880809

**1A\_TS**

CBS-QB3 (0 K)	=	-1485.802680
CBS-QB3 Energy	=	-1485.786783
CBS-QB3 Enthalpy	=	-1485.785839
CBS-QB3 Free Energy	=	-1485.849362

**3A**

CBS-QB3 (0 K)	=	-1485.864139
CBS-QB3 Energy	=	-1485.846678
CBS-QB3 Enthalpy	=	-1485.845733
CBS-QB3 Free Energy	=	-1485.913747

**2A**

CBS-QB3 (0 K)	=	-1525.562823
CBS-QB3 Energy	=	-1525.543625
CBS-QB3 Enthalpy	=	-1525.542681

CBS-QB3 Free Energy = -1525.616606

#### **2A\_TS**

CBS-QB3 (0 K) = -1525.529429

CBS-QB3 Energy = -1525.510062

CBS-QB3 Enthalpy = -1525.509118

CBS-QB3 Free Energy = -1525.581858

#### **4A**

CBS-QB3 (0 K) = -1525.595445

CBS-QB3 Energy = -1525.576006

CBS-QB3 Enthalpy = -1525.575062

CBS-QB3 Free Energy = -1525.648302

#### **5B**

CBS-QB3 (0 K) = -1447.846103

CBS-QB3 Energy = -1447.830859

CBS-QB3 Enthalpy = -1447.829915

CBS-QB3 Free Energy = -1447.890516

#### **5B\_TS**

CBS-QB3 (0 K) = -1447.829880

CBS-QB3 Energy = -1447.815192

CBS-QB3 Enthalpy = -1447.814248

CBS-QB3 Free Energy = -1447.872339

#### **7B**

CBS-QB3 (0 K) = -1447.882665

CBS-QB3 Energy = -1447.865989

CBS-QB3 Enthalpy = -1447.865045

CBS-QB3 Free Energy = -1447.934064

#### **6B**

CBS-QB3 (0 K) = -1487.580076

CBS-QB3 Energy = -1487.562671

CBS-QB3 Enthalpy = -1487.561727

CBS-QB3 Free Energy = -1487.627737

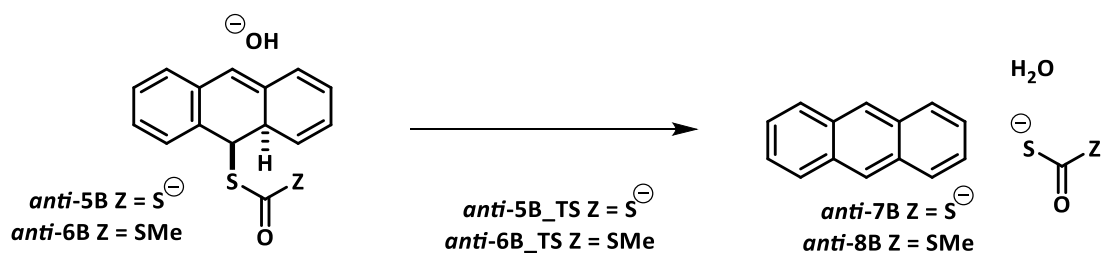
## 6B\_TS

CBS-QB3 (0 K)	=	-1487.536578
CBS-QB3 Energy	=	-1487.519477
CBS-QB3 Enthalpy	=	-1487.518533
CBS-QB3 Free Energy	=	-1487.583964

## 8B

CBS-QB3 (0 K)	=	-1487.615634
CBS-QB3 Energy	=	-1487.597063
CBS-QB3 Enthalpy	=	-1487.596118
CBS-QB3 Free Energy	=	-1487.668699

## Calculated B3LYP/6-31+G(d,p) E2 *anti*-Elimination Reaction Coordinates



## *anti*-5B

Sum of electronic and zero-point Energies	=	-1525.465788
Sum of electronic and thermal Energies	=	-1525.447515
Sum of electronic and thermal Enthalpies	=	-1525.446571
Sum of electronic and thermal Free Energies	=	-1525.513827

## *anti*-5B\_TS

Sum of electronic and zero-point Energies	=	-1525.443890
Sum of electronic and thermal Energies	=	-1525.425780
Sum of electronic and thermal Enthalpies	=	-1525.424836
Sum of electronic and thermal Free Energies	=	-1525.493486

## *anti*-7B

Sum of electronic and zero-point Energies	=	-1525.519176
---	---	--------------

Sum of electronic and thermal Energies	=	-1525.499379
Sum of electronic and thermal Enthalpies	=	-1525.498435
Sum of electronic and thermal Free Energies	=	-1525.574353

***anti-6B***

Sum of electronic and zero-point Energies	=	-1565.340391
Sum of electronic and thermal Energies	=	-1565.319916
Sum of electronic and thermal Enthalpies	=	-1565.318972
Sum of electronic and thermal Free Energies	=	-1565.391585

***anti-6B\_TS***

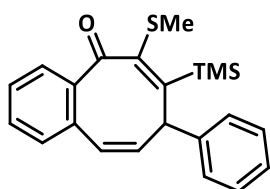
Sum of electronic and zero-point Energies	=	-1565.325260
Sum of electronic and thermal Energies	=	-1565.305601
Sum of electronic and thermal Enthalpies	=	-1565.304657
Sum of electronic and thermal Free Energies	=	-1565.375003

***anti-8B***

Sum of electronic and zero-point Energies	=	-1565.469114
Sum of electronic and thermal Energies	=	-1565.446931
Sum of electronic and thermal Enthalpies	=	-1565.445987
Sum of electronic and thermal Free Energies	=	-1565.528734

## Appendix 2 – Experimental Data for Chapter 3

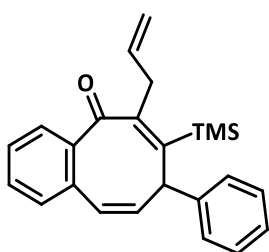
*Synthesis of (6Z,9Z)-6-(methylthio)-8-phenyl-7-(trimethylsilyl)benzo[8]annulen-5(8H)-one 107d*



<sup>n</sup>BuLi (1.0 mL, 1.58 M in hexanes, 1.62 mmol) was added to a stirred solution of trimethylsilylacetylene (229  $\mu$ L, 1.62 mmol) in THF (2 ml) at -50 °C. After 30 min, 2- bromobenzaldehyde (189  $\mu$ L, 1.62 mmol), was and stirred until TLC indicated the consumption of the aldehyde. <sup>n</sup>BuLi (1.0 mL, 1.58 M in hexanes, 1.62 mmol) was then added and stirred for 10 minutes. CuBr·SMe<sub>2</sub> (167 mg, 0.81 mmol) was then added as a solid and stirred for 1 h. (1- chloroprop-2-yn-1-yl)benzene (119 mg, 0.79 mmol) was

then added and warmed to  $-10\text{ }^{\circ}\text{C}$ . Dimethyldisulfide ( $374\text{ }\mu\text{L}$ ,  $3.97\text{ mmol}$ ) was added and stirred for 30 mins at  $-10\text{ }^{\circ}\text{C}$ , then allowed to warm to room temperature over 30 minutes and stirring for 30 minutes more, followed by quenching with buffered ammonia:ammonium chloride. The organic layer was extracted with EtOAc ( $3 \times 10\text{ ml}$ ) and the combined organic fractions dried over  $\text{MgSO}_4$ . and flash column chromatography (19:1 pentane:diethyl ether) afforded ( $151.2\text{ mg}$ ,  $0.41\text{ mmol}$ ) giving **107d** in 52% yield as a low melting solid.  $R_f = 0.37$  (9:1 Pentane:Et<sub>2</sub>O), IR (NaCl, film):  $\nu_{\text{max}}$  3062, 3031, 3017, 1650, 1590, 1496, 1434, 1250, 1194, 1023, 905, 840, 684  $\text{cm}^{-1}$ ;  $^1\text{H NMR}$  (400.2 MHz,  $\text{CDCl}_3$ ):  $\delta$  7.98 (app dt,  $J = 7.8, 1.4$ , 1H, ArH), 7.59 (app ddt,  $J = 7.8, 7.6, 1.4$ , 1H, ArH), 7.47 (app ddt,  $J = 8.2, 7.6, 1.4$ , 1H, ArH), 7.44 (d with unresolved long range couplings,  $J = 8.2\text{ Hz}$ , 1H, ArH), 7.38 – 7.23 (m, 5H, ArH), 6.76 (d with unresolved long range couplings,  $J = 11.4\text{ Hz}$ , 1H, CCHCH), 6.64 (ddd,  $J = 11.4\text{ Hz}, 8.5, 0.5\text{ Hz}$ , 1H, CCHCH), 4.76 (d,  $J = 8.5\text{ Hz}$ , 1H, CHPh), 2.21 (s, 3H, SCH<sub>3</sub>), 0.06 (s, 9H, Si(CH<sub>3</sub>)<sub>3</sub>);  $^{13}\text{C NMR}$  (100.6 MHz,  $\text{CDCl}_3$ ):  $\delta$  199.6 (C), 148.9 (C), 141.2 (C), 140.1 (C), 138.8 (C), 135.8 (CH), 135.0 (C), 134.3 (CH), 132.3 (CH), 131.7 (CH), 131.4 (CH), 128.5 (CH), 128.1 (CH), 126.9 (CH), 128.8 (CH), 49.1 (CH), 18.0 (SCH<sub>3</sub>), 1.5 (CH<sub>3</sub>); HRMS (+ESI) calcd. for  $\text{C}_{22}\text{H}_{24}\text{OSSi}$   $m/z$  365.1390 (M+H), found  $m/z$  365.1393 (M+H).

*Synthesis of (6E,9Z)-6-allyl-8-phenyl-7-(trimethylsilyl)benzo[8]annulen-5(8H)-one* **107c**

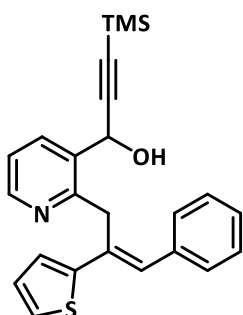


$^n\text{BuLi}$  ( $1.0\text{ mL}$ ,  $1.58\text{ M}$  in hexanes,  $1.62\text{ mmol}$ ) was added to a stirred solution of trimethylsilylacetylene ( $229\text{ }\mu\text{L}$ ,  $1.62\text{ mmol}$ ) in THF ( $2\text{ ml}$ ) at  $-50\text{ }^{\circ}\text{C}$ . After 30 min, 2-bromobenzaldehyde ( $189\text{ }\mu\text{L}$ ,  $1.62\text{ mmol}$ ), was and stirred until TLC indicated the consumption of the aldehyde.  $^n\text{BuLi}$  ( $1.0\text{ mL}$ ,  $1.58\text{ M}$  in hexanes,  $1.62\text{ mmol}$ ) was then added and stirred for 10 minutes.  $\text{CuBr}\cdot\text{SMe}_2$  ( $167\text{ mg}$ ,  $0.81\text{ mmol}$ ) was then added as a solid and stirred for 1 h. (1-chloroprop-2-yn-1-yl)benzene ( $119\text{ mg}$ ,  $0.79\text{ mmol}$ ) was then added and warmed to  $-10\text{ }^{\circ}\text{C}$ . Allyl bromide ( $170\text{ }\mu\text{L}$ ,  $1.98\text{ mmol}$ ) was added and stirred for 30 mins at  $-10\text{ }^{\circ}\text{C}$ , then allowed to warm to room temperature over 30 minutes and stirring for 30 minutes more, followed by quenching with buffered ammonia:ammonium chloride. The organic layer was extracted with EtOAc ( $3 \times 10\text{ ml}$ ) and the combined organic fractions dried over  $\text{MgSO}_4$ . and flash column chromatography (19:1 pentane:diethyl ether) afforded **107c** ( $49.1\text{ mg}$ ,  $0.136$

mmol 17%),  $R_f$  (9:1 pentane:diethyl ether): 0.60; mp: 88-90 °C; IR (NaCl, film):  $\nu_{max}$  3037, 3024, 3013, 1649, 1593, 1496, 1252, 963, 909, 843  $cm^{-1}$ ;  $^1H$  NMR (400.2 MHz,  $CDCl_3$ ):  $\delta$  7.90 – 7.86 (m, 1H, ArH), 7.53 – 7.47 (m, 2H, ArH), 7.30 – 7.23 (m, 4H, ArH), 7.21 – 7.16 (m, 1H, ArH), 6.74 (d,  $J = 11.3$  Hz, 1H, CCHCH), 6.66 (dd,  $J = 11.3$  Hz, 8.2 Hz, 1H, CCHCH), 5.48 (dddd,  $J = 17.1, 10.1, 7.4, 5.3$  Hz, 1H,  $CH_2CH$ ), 4.85 (app dq,  $J = 17.1, 1.4$  Hz, 1H, =CHtrans), 4.77 (app dq,  $J = 10.1, 1.4$  Hz, 1H, =CHcis), 4.56 (d,  $J = 8.2$  Hz, 1H, CHPh), 3.34 (app ddt,  $J = 15.3, 7.4, 1.4$  Hz, 1H,  $CH_2\alpha$ ), 3.11 (app ddt,  $J = 15.3, 5.3, 1.4$  Hz, 1H,  $CH_2\beta$ ), -0.04 (m, 9H,  $Si(CH_3)_3$ );  $^{13}C$  NMR (100.6 MHz,  $CDCl_3$ ):  $\delta$  206.2 (C), 147.4 (C), 143.8 (C), 141.5 (C), 139.8 (C), 137.1 (CH), 135.4 (C), 134.6 (CH), 133.9 (CH), 131.9 (CH), 131.6 (CH), 131.5 (CH), 128.4 (CH), 127.9 (CH), 127.0 (CH), 126.6 (CH), 116.9 (CH<sub>2</sub>), 48.1 (CH), 37.8 (CH<sub>2</sub>), 1.8 (CH<sub>3</sub>); HRMS (+ESI) calc. for  $C_{24}H_{26}OSi$   $m/z$  381.1645 (M+H), : found  $m/z$  381.1648 (M+H).

*(E)-1-(2-(3-Phenyl-2-(thiophen-2-yl)allyl)pyridin-3-yl)-3-(trimethylsilyl)prop-2-yn-1-ol*

**181**

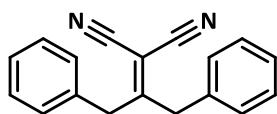


Recrystallised by liquid layering (2:1 pentane:Et<sub>2</sub>O) from the crude reaction mixture.

**m.p.** 148-149 °C; **IR** (NaCl,  $CHCl_3$ )  $\nu_{max}/cm^{-1}$  3691, 3597, 3062, 3010, 2965, 2173, 1600, 1587, 1574, 1492, 1432, 1367, 1252, 1040, 974, 921, 848  $cm^{-1}$ ;  $^1H$  NMR (400.2 MHz,  $CDCl_3$ )  $\delta$  8.54 (dd,  $J = 4.8, 1.7$  Hz, 1H, ArH), 7.97 (dd,  $J = 7.8, 1.7$  Hz, 1H, ArH), 7.40 – 7.35 (m, 3H, ArH), 7.31 – 7.24 (m, 2H, ArH), 7.25 – 7.17 (m, 2H, ArH), 7.09 (dd,  $J = 5.1, 1.1$  Hz, 1H, ArH), 6.93 (dd,  $J = 3.6, 1.1$  Hz, 1H, ArH), 6.85 (m, 1H, PhCHC), 5.66 (d,  $J = 4.9$  Hz, 1H, ArCHOH), 4.37 (s, 2H, ArCH<sub>2</sub>C), 2.24 (d,  $J = 4.9$  Hz, 1H, OH), 0.14 (s, 9H,  $Si(CH_3)_3$ );  $^{13}C$  NMR (100.6 MHz,  $CDCl_3$ )  $\delta$  157.4 (C), 149.3 (CH), 146.7 (C), 137.4 (C), 134.5 (CH), 133.6 (C), 132.2 (C), 128.8 (CH), 128.7 (CH), 128.4 (CH), 127.4 (CH), 127.1 (CH), 124.3 (CH), 123.8 (CH), 121.7 (CH), 103.4 (C), 92.8 (C), 62.1 (CH), 36.6 (CH<sub>2</sub>), -0.2 (CH<sub>3</sub>); **MS** (ESI+):  $m/z$  404 [M+H]<sup>+</sup>; **HRMS**:  $C_{24}H_{26}NOSSi$ + Calc. 404.1499 found 404.1522. Xray data at: CCDC 1405855.

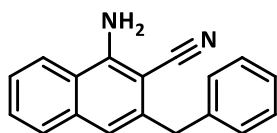
## Appendix 3 – Experimental Data for Chapter 4

### Synthesis of 2-(1,3-diphenylpropan-2-ylidene)malononitrile **183**



1,3-Diphenylketone **182** (11.5 g, 54.7 mmol) was added to a flame-dried 500 ml round bottom flask equipped with a Dean-Stark trap and condenser along with malonitrile (4.32 g, 65.4 mmol), ammonium acetate (11 g, 143 mmol), acetic acid (66ml) and dry toluene (438 ml). The mixture was heated on an oil bath at 85 °C until TLC indicated completion. The reaction mixture was cooled, quenched slowly with 2M NaOH and extracted with dichloromethane. The organic washings were then dried with MgSO<sub>4</sub> and reduced in vacuo giving a thick brown oil (12.1 g). The crude oil was passed through a short silica column with diethyl ether, reduced and recrystallised from methanol to give a light tan crystalline solid **183** (11.6 g, 82%), m.p. 53-54 °C, *R<sub>f</sub>* = 0.60 (1:1 hexane:ethyl acetate), IR (CHCl<sub>3</sub>)  $\nu_{\text{max}}/\text{cm}^{-1}$  3695, 3089, 3068, 3006, 2932, 2234, 1952, 1880, 1807, 1595, 1581, 1496, 1455, 1340, 1291, 1246, 1183, 1079, 1030, 994, 914, 646, <sup>1</sup>H NMR (400.2 MHz, CDCl<sub>3</sub>)  $\delta$  7.44 – 7.30 (m, 6H), 7.21 – 7.13 (m, 4H), 3.77 (s, 4H), <sup>13</sup>C NMR (100.6 MHz, CDCl<sub>3</sub>)  $\delta$  180.8 (C), 134.5 (C), 129.5 (CH), 129.1 (CH), 128.2 (CH), 112.3 (C), 86.9 (C), 40.5 (CH<sub>2</sub>). MS (+EI) calcd. *m/z* C<sub>12</sub>H<sub>14</sub>N<sub>2</sub> 258.1160 (M), found *m/z* 258.1151 (M).

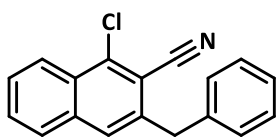
### Synthesis of 1-amino-3-benzyl-2-naphthonitrile **184**



**183** (200 mg) was added in one portion to a stirred solution of Eaton's reagent (12 ml) in a flame dried Schlenk tube under argon in a preheated oil bath at 60 °C. The resultant solution was left stirring until TLC indicated completion (N.B. the TLC spot for the forming naphthylamine is a bright electric blue under UV and highly indicative of formation of product). The reaction was then removed from the oil bath and allowed to cool before quenching with copious water and extracting with dichloromethane. The organic washings were then dried with MgSO<sub>4</sub> and reduced *in vacuo*, giving a brown solid (350 mg). The crude was then purified by flash column chromatography (1:1 hexane:ethyl acetate) giving an off white crystalline product **184** (149 mg, 74%), m.p. 78-79 °C, *R<sub>f</sub>* = 0.50 (1:1 hexane:ethyl acetate), IR (CHCl<sub>3</sub>)  $\nu_{\text{max}}/\text{cm}^{-1}$  3641, 3507, 3410, 3066, 3052, 3011, 2927, 2855, 2206, 1627, 1569, 1504, 1454, 1422, 1385, 1348, 1285, 1193, 1157,

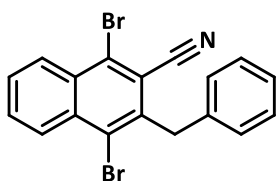
1109, 1076, 1030, 871, <sup>1</sup>H NMR (400 MHz, CDCl<sub>3</sub>) δ 7.75 (d, *J* = 8.4 Hz, 1H), 7.68 (d, *J* = 8.1 Hz, 1H), 7.59 – 7.51 (m, 1H), 7.51 – 7.43 (m, 1H), 7.35 – 7.28 (m, 4H), 7.28 – 7.21 (m, 1H), 6.98 (s, 1H), 5.11 (s, 2H), 4.20 (s, 2H), <sup>13</sup>C NMR (100.6 MHz, CDCl<sub>3</sub>) δ 149.2 (C), 139.2 (C), 138.4 (C), 135.8 (C), 129.4 (CH), 129.2 (CH), 128.8 (CH), 128.7 (CH), 126.7 (CH), 125.9 (CH), 121.1 (CH), 120.7 (C), 118.4 (CH), 118.0 (C), 91.4 (C), 40.9 (CH<sub>2</sub>). MS (+EI) calcd. *m/z* C<sub>12</sub>H<sub>14</sub>N<sub>2</sub> 258.1160 (M), found *m/z* 258.1151 (M).

#### Synthesis of 3-benzyl-1-chloro-2-naphthonitrile **186**



Copper (II) chloride (308 mg) and tert-butyl nitrite (341 μl) were added to dry acetonitrile (7.6 ml) in a flame dried Schlenk tube under argon with stirring in an oil bath at 65 °C. **184** (493 mg) was added to the resultant solution in portions and stirred (N.B. there is some gas evolution after addition as N<sub>2</sub> is formed) until TLC indicated completion. The reaction mixture was then removed from the oil bath and allowed to cool, then quenched with 1M HCl. Mixture was washed with dichloromethane (3x4 ml), the combined organic washings dried with MgSO<sub>4</sub> and then filtered and concentrated in vacuo giving a brown solid (543 mg). The crude product could be recrystallised from methanol, giving off-white crystals **186** (1.43 g, 75%), m.p. 111-112 °C, *R<sub>f</sub>* = 0.59 (3:2 hexane: ethyl acetate), IR (CHCl<sub>3</sub>) *v*<sub>max</sub>/cm<sup>-1</sup> 3691, 3606, 3065, 3012, 2930, 2858, 2229, 1718, 1625, 1601, 1560, 1494, 1455, 1379, 1358, 1331, 1260, 1239, 1152, 1075, 1029, 959, 939, 909, 893, 854, 821, 644, <sup>1</sup>H NMR (400.1 MHz, CDCl<sub>3</sub>) δ 8.32 – 8.25 (m, 1H), 7.82 – 7.75 (m, 1H), 7.68 – 7.61 (m, 2H), 7.57 (s, 1H), 7.39 – 7.26 (m, 5H), 4.36 (s, 2H), <sup>13</sup>C NMR (100.6 MHz, CDCl<sub>3</sub>) δ 139.6 (C), 138.3 (C), 138.2 (C) 135.5 (C), 129.9 (CH), 129.4 (CH), 129.1 (C), 128.9 (CH), 128.3 (CH), 128.2 (CH), 127.7 (CH), 127.1 (CH), 125.4 (CH), 116.0 (C), 112.0 (C), 40.7 (CH<sub>2</sub>), MS (+ESI) calcd. *m/z* C<sub>12</sub>H<sub>12</sub>Cl<sub>1</sub>N<sub>1</sub> 300.0550 (M+Na), found *m/z* 300.0542 (M+Na).

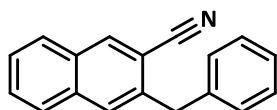
#### Synthesis of 3-benzyl-1,4-dibromo-2-naphthonitrile **187**



Copper (II) bromide (134 mg) and tert-butyl nitrite (87 μl) were added to dry acetonitrile (4 ml) in a flame dried Schlenk tube under argon with stirring in an oil bath at 65 °C. **184** (129 mg) was added to the resultant solution in portions and stirred

(N.B. there is some gas evolution after addition as N<sub>2</sub> is formed) until TLC indicated completion. The reaction mixture was then removed from the oil bath and allowed to cool, then quenched with 1M HCl. Mixture was washed with dichloromethane (3x4 ml), the combined organic washings dried with MgSO<sub>4</sub> and then filtered and concentrated in vacuo giving a brown solid (138 mg). The crude product could be recrystallised from methanol, giving tan crystalline **187** (114 mg, 57%), m.p. 111-112 °C, *R<sub>f</sub>* = 0.80 (3:2 hexane: ethyl acetate), IR (CHCl<sub>3</sub>)  $\nu_{\text{max}}/\text{cm}^{-1}$  3691, 3606, 3065, 3012, 2930, 2858, 2229, 1718, 1625, 1601, 1560, 1494, 1455, 1379, 1358, 1331, 1260, 1239, 1152, 1075, 1029, 959, 939, 909, 893, 854, 821, 644, <sup>1</sup>H NMR (400.1 MHz, CDCl<sub>3</sub>)  $\delta$  8.43 – 8.37 (m, 1H, ArH), 8.30 (dd, *J* = 8.4, 0.6 Hz, 1H, ArH), 7.76 (ddd, *J* = 8.4, 7.0, 1.2 Hz, 1H, ArH), 7.69 (ddd, *J* = 8.1, 7.0, 1.1 Hz, 1H, ArH), 7.34 – 7.17 (m, 5H, ArH), 4.66 (s, 2H, CH<sub>2</sub>), <sup>13</sup>C NMR (100.6 MHz, CDCl<sub>3</sub>)  $\delta$  139.3 (C), 137.1 (C), 134.7 (C), 131.4 (CH), 131.2 (C), 129.8 (C), 129.2 (CH), 129.2 (CH), 128.8 (CH), 128.7 (CH), 128.7 (CH), 126.9 (CH), 126.1 (C), 117.0 (C), 116.1 (C), 42.0 (CH<sub>2</sub>), MS (+ESI) calcd. *m/z* C<sub>12</sub>H<sub>12</sub>Cl<sub>1</sub>N<sub>1</sub> 424.0908 (M+Na), found *m/z* 423.9126 (M+Na).

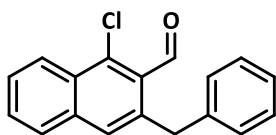
#### Synthesis of 3-benzyl-2-naphthonitrile **188**



Nitrosonium tetrafluoroborate (70 mg) was added to dry acetonitrile (2 ml) in a flame dried Schlenk tube under argon with stirring in an oil bath at 65 °C. **184** (129 mg) was added to the resultant solution in portions and stirred (N.B. there is some gas evolution after addition as N<sub>2</sub> is formed) until TLC indicated completion. The reaction mixture was then removed from the oil bath and allowed to cool, then quenched with 1M HCl. Mixture was washed with dichloromethane (3x4 ml), the combined organic washings dried with Na<sub>2</sub>SO<sub>4</sub> and then filtered and concentrated in vacuo giving a brown solid (139 mg). The crude product could be recrystallised from methanol, giving tan crystalline **188** (80.3 g, 66%), m.p. 111-112 °C, *R<sub>f</sub>* = 0.59 (3:2 hexane: ethyl acetate), IR (CHCl<sub>3</sub>)  $\nu_{\text{max}}/\text{cm}^{-1}$  3691, 3606, 3065, 3012, 2930, 2858, 2229, 1718, 1625, 1601, 1560, 1494, 1455, 1379, 1358, 1331, 1260, 1239, 1152, 1075, 1029, 959, 939, 909, 893, 854, 821, 644, <sup>1</sup>H NMR (400.1 MHz, CDCl<sub>3</sub>)  $\delta$  8.23 (s, 1H, ArH), 7.85 (dd, *J* = 8.1, 1.4 Hz, 1H, ArH), 7.79 – 7.76 (dd, *J* = 8.1, 1.4 Hz, 1H, ArH), 7.66 (s, 1H, ArH), 7.60 (ddd, *J* = 8.1, 6.9, 1.4 Hz, 1H, ArH), 7.54 (ddd, *J* = 8.1, 6.9, 1.4 Hz, 1H, ArH), 7.37 – 7.22 (m, 5H, ArH), 4.34

(s, 2H, CH<sub>2</sub>), <sup>13</sup>C NMR (100.6 MHz, CDCl<sub>3</sub>) δ 138.9 (C), 138.7 (C), 135.3 (CH), 135.1 (C), 131.1 (C), 129.3 (CH), 129.3 (CH), 128.9 (CH), 128.8 (CH), 128.2 (CH), 127.9 (CH), 127.2 (CH), 126.8 (CH), 118.5 (C), 111.0 (C), 40.3 (CH<sub>2</sub>), MS (+ESI) calcd. m/z C<sub>13</sub>H<sub>18</sub>N<sub>1</sub> 266.0940 (M+Na), found m/z 266.0940 (M+Na).

#### Synthesis of 3-benzyl-1-chloro-2-naphthaldehyde **189**

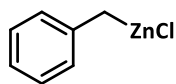


**186** (70 mg) was added to dry THF (2 ml) in a flame dried Schlenck tube under argon with stirring at 0 °C. LiBHET<sub>3</sub> (144 μl) was added to the resultant solution in portions and stirred (N.B. there is some gas evolution after addition as N<sub>2</sub> is formed) until TLC indicated completion. The reaction mixture was then quenched with 1M HCl, washed with diethyl ether (3x2 ml), the combined organic washings dried with MgSO<sub>4</sub> and then filtered and concentrated in vacuo giving a yellow oil (19.6 mg). The crude product was purified by flash column chromatography (7:3 pentane:diethyl ether), giving white solid **189** (7.3 g, 18%), R<sub>f</sub> = 0.60 (7:3 pentane: ether). <sup>1</sup>H NMR (400.2 MHz, CDCl<sub>3</sub>) δ 10.79 (s, 1H, O=CH), 8.46 – 8.40 (m, 1H, ArH), 7.80 – 7.76 (m, 1H, ArH), 7.67 – 7.64 (m, 1H, ArH), 7.64 – 7.61 (m, 1H, ArH), 7.31 – 7.26 (m, 2H, ArH), 7.23 – 7.20 (m, 1H, ArH), 7.17 (m, 2H, ArH), 4.49 (s, 2H, CH<sub>2</sub>). MS (+ESI) calcd. m/z C<sub>18</sub>H<sub>13</sub>Cl<sub>1</sub>O<sub>1</sub> 303.0547 (M+Na), found m/z 303.0539 (M+Na).

### Appendix 4 – Experimental Data for Chapter 5

#### Arylzinc chloride reagent preparation, representative examples: PhCH<sub>2</sub>ZnX (X = Cl,

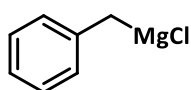
#### Br) Chloride reagents:



Zinc dust (5-9 μm, 52.4 g, 0.801 mol) was dried under vacuum at >200 °C (2-5 mins), then cooled to room temperature under an atmosphere of argon. Tetrahydrofuran (400 mL) was then added, forming a grey suspension. The reaction mixture was cooled to 0 °C and trimethylsilyl chloride (2.05 mL, 16.1 mmol) was added in one portion and the mixture stirred (0.5 h). Freshly distilled benzyl chloride (46.1 mL, 0.401 mol) was subsequently added over a period of 10 minutes. After addition of the PhCH<sub>2</sub>Cl was complete the reaction mixture was warmed to 40 °C and stirred (4 h). Cooling to room temperature provided a turbid white suspension over the remaining residual zinc powder. The supernatant solution

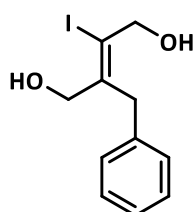
could be stored for at least one week at 4 °C (resulting in clear or pale yellow supernatants), but typically the organometallic was used within 48 h. Bromide reagents: were prepared from ArCH<sub>2</sub>Br and elemental zinc in THF at 0 °C using the method described by Shannon *et al.*<sup>203</sup>

### Grignard reagent preparation, representative example: PhCH<sub>2</sub>MgCl



Grignard quality magnesium turnings (55.0 g, 2.26 mol) were activated by mechanical stirring<sup>204</sup> under argon (20 °C, 14 h) until black in colour. Tetrahydrofuran (1.00 L) was then added, forming a suspension of activated magnesium. Distilled benzyl chloride (250 mL, 2.17 mol) was then added dropwise to the reaction mixture at a rate of ca. 0.2 mL min<sup>-1</sup>. After completion of the addition the reaction mixture was filtered through a sinter under argon to provide the desired Grignard reagent as a dark grey solution (on small scales the reagent could be simply syringed off). The solutions should be used within 48 h. N.B. Use of undistilled benzyl chloride can result in delayed vigorous exotherms that are potentially explosive at large scale. This is attributed to the propylene oxide commonly present in commercial PhCH<sub>2</sub>Cl (as supplied) as a radical inhibitor. This appears to delay initiation of Grignard formation resulting in a build-up of unreacted benzyl chloride. When the reaction does initiate uncontrolled exotherms result. Thus, all commercial benzyl chlorides were distilled before use, especially at larger scales.

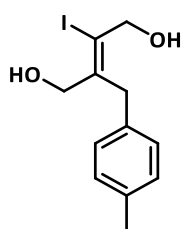
### Synthesis of (Z)-2-benzyl-3-iodobut-2-ene-1,4-diol **197a**



Benzylmagnesium chloride (7.6 ml, 2 M, 15.3 mmol) was added to a stirred solution of 1,4-but-2-yne diol **192** (436 mg, 5 mmol) in dry THF (20 ml) with rapid stirring in schlenk tube in an oil bath at 65 °C under an Ar atmosphere. After addition of the Grignard reagent, CuBr.DMS (11 mg, 0.05 mmol) was added in one portion and the reaction mixture was diluted with further dry THF (5 ml). When TLC showed the disappearance of the 1,4-butyne diol, the reaction mixture was chilled to -78 °C with a dry ice/acetone bath, and I<sub>2</sub> (1.52g, 6 mmol) was added in one portion. When TLC indicated completion, the reaction was quenched with saturated ammonium chloride,

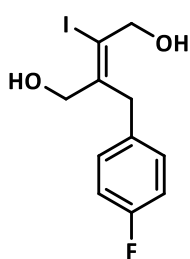
and washed with metabisulfite until the solution was a pale yellow. The aqueous layer was extracted with EtOAc (3 x 15 ml), the organic fractions combined and dried with Na<sub>2</sub>SO<sub>4</sub>, filtered and reduced under reduced pressure, giving a crude white crystalline solid with some yellow oil (1.29 g). The crude was then recrystallised from hot toluene, and the solid washed with toluene and dried in vacuo, giving a white crystalline solid **197a** (809 mg, 53%), *R<sub>f</sub>* = 0.57 (EtOAc), <sup>1</sup>H NMR (400.2 MHz, CDCl<sub>3</sub>) δ 7.34 – 7.28 (m, 2H), 7.25 – 7.22 (m, 1H), 7.21 – 7.17 (m, 2H), 4.50 (d, *J* = 6.6 Hz, 2H), 4.24 (d, *J* = 6.5 Hz, 2H), 1.98 (d, *J* = 6.6 Hz, 1H), 1.61 (t, *J* = 6.5 Hz, 1H), <sup>13</sup>C NMR (100.6 MHz, CDCl<sub>3</sub>) δ 144.6 (C), 138.0 (C), 128.9 (CH), 128.5 (CH), 126.8 (CH), 106.6 (CH), 71.1 (CH<sub>2</sub>), 67.8 (CH<sub>2</sub>), 36.0 (CH<sub>2</sub>). MS (+ESI) calcd. *m/z* C<sub>11</sub>H<sub>13</sub>O<sub>2</sub>I 326.9852 (M+Na), found *m/z* 326.9842 (M+Na).

*Synthesis of (Z)-2-iodo-3-(4-methylbenzyl)but-2-ene-1,4-diol 197b*



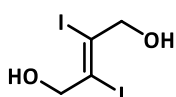
4-Methylbenzylmagnesium chloride (57.9 ml, 1.0 M) was added *via* cannula to a stirred solution of but-2-yne, 1,4- diol (1.64 g, 19.0 mmol) in THF (20 ml) heated to 60 °C over 15 minutes. After complete addition of the Grignard solution, solid CuBr.DMS (39.0 mg, 0.190 mmol) was added in a single portion. When TLC indicated that the starting diol had been consumed (1 h), the reaction flask was cooled to -40 °C, and solid I<sub>2</sub> (6.27g, 24.7 mmol, 1.30 eq.), and allowed to warm to -5 °C over 1h, at which point there was no spot for the carbomagnesium product or starting diol. The reaction mixture was then quenched with saturated sodium metabisulphite (100 ml) and the organic extracted with EtOAc (3 x 100ml). The organic fractions were then washed with water (50 ml), the combined organic fractions dried with MgSO<sub>4</sub>, filtered and concentrated in vacuo (9.48 g). The crude residue was then purified by flash column chromatography (CH<sub>2</sub>Cl<sub>2</sub>, then 9:1 DCM:EtOAc) giving the product **197b** as a white solid (4.24 g, 67%), *R<sub>f</sub>* = 0.64 (EtOAc), <sup>1</sup>H NMR (400.1 MHz, Chloroform-*d*) δ 7.12 (d, *J* = 7.9 Hz, 2H), 7.07 (d, *J* = 8.1 Hz, 2H), 4.50 (d, *J* = 6.6 Hz, 2H), 4.23 (d, *J* = 6.6 Hz, 2H), 3.76 (s, 2H), 2.32 (s, 3H), 1.95 (t, *J* = 6.6 Hz, 1H), 1.59 (t, *J* = 6.6 Hz, 1H), <sup>13</sup>C NMR (100.6 MHz, Chloroform-*d*) δ 144.9 (C), 136.5 (C), 134.8 (CH), 129.7 (CH), 128.4 (C), 106.5 (C), 71.3 (CH<sub>2</sub>), 67.8 (CH<sub>2</sub>), 35.8 (CH<sub>2</sub>), 21.2 (CH<sub>3</sub>).

*Synthesis of (Z)-2-(4-fluorobenzyl)-3-iodobut-2-ene-1,4-diol 197c*



4-Fluorobenzylmagnesium chloride (140 ml, 0.5 M) was added *via* cannula to a stirred solution of but-2-yne, 1,4- diol (1.86 g, 21.6 mmol) in THF (20 ml) heated to 60 °C over 15 minutes. After complete addition of the Grignard solution, solid CuBr.DMS (90.0 mg, 0.438 mmol) was added in a single portion. When TLC indicated that the starting diol had been consumed (1 h), the reaction flask was cooled to -40 °C, and solid I<sub>2</sub> (7.72 g, 30.4 mmol), and allowed to warm to -5 °C over 1h, at which point there was no spot for the carbomagnesium product or starting diol. The reaction mixture was then quenched with saturated sodium metabisulphite (100 ml) and the organic extracted with EtOAc (3 x 100ml). The organic fractions were then washed with water (50 ml), the combined organic fractions dried with MgSO<sub>4</sub>, filtered and concentrated in vacuo (9.48 g). The crude residue was then purified by flash column chromatography (CH<sub>2</sub>Cl<sub>2</sub>, then 9:1 DCM:EtOAc) giving the product **197c** as a white solid (3.36 g, 48%). *R<sub>f</sub>* = 0.43 (2:1 EtOAc:Hexane), *m.p.* 114-115 °C, **IR** (Solid ATR)  $\nu_{\text{max}}/\text{cm}^{-1}$  3251, 2947, 2928, 2874, 2844, 1626, 1600, 1506, 1477, 1462, 1439, 1414, 1317, 1295, 1244, 1222, 1160, 1099, 1071, 1021, 993, 962, 920, 841, 812, 760, 697, 660, 551, 497, 452, 439; **<sup>1</sup>H NMR** (400.2 MHz, D<sub>4</sub>-MeOD)  $\delta$  7.24 – 7.18 (m, 2H, H-7), 7.03 – 6.96 (m, 2H, H-8), 4.45 (s, 2H, H-4), 4.16 (s, 2H, H-1), 3.79 (s, 2H, H-5); **<sup>19</sup>F NMR** (100.6 MHz, MeOD)  $\delta$  -119.22 **<sup>13</sup>C NMR** (100.6 MHz, D<sub>4</sub>-MeOD):  $\delta$  163.0 (d, *J* = 243.0 Hz, C, C-9), 145.6 (C, C-2), 135.9 (d, *J* = 3.0 Hz, C, C-6), 131.2 (d, *J* = 8.4 Hz, CH, C-7), 116.0 (d, *J* = 21.5 Hz, CH, C-8), 106.5 (C, C-3), 71.1 (CH<sub>2</sub>, C-1), 68.1 (CH<sub>2</sub>, C-4), 34.8 (CH<sub>2</sub>, C-5); **HRMS** (+ESI) calcd. for C<sub>11</sub>H<sub>12</sub>IFO<sub>2</sub> *m/z* 344.9758 (M+Na), found *m/z* 344.9756 (M+Na).

#### Synthesis of (*E*)-2,3-diiodobut-2-ene-1,4-diol **200**

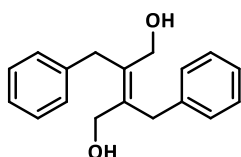


Granular solid iodine (9.00 g, 35.5 mmol) was suspended in CHCl<sub>3</sub> (120 mL) and a large (50 mm long x 15 mm wide) egg-shaped stir bar added. The stirred mixture was brought to reflux briefly, effecting I<sub>2</sub> dissolution, and then re-cooled to ambient temperature. Finely ground 2-butyne-1,4-diol **192** (3.11 g, 36.1 mmol) was added. The mixture was refluxed and stirred for 22h during which time it became almost colorless. Heating was stopped and the mixture allowed to come to room temperature. Any large masses of 4 or residual solid iodine were gently broken

up with a glass rod and the suspension gently warmed to ca. 40 °C. Diiodide **200** was isolated by filtration and washed with chloroform (2 × 30 mL) and Et<sub>2</sub>O (2 × 30 mL). Drying afforded **4** as a colourless powder 10.94 g (90%). This procedure gives much improved yields over those described in the literature and identical spectroscopic data.<sup>177</sup>  $R_f$  = 0.55 (1:1 EtOAc/hexane), <sup>1</sup>H NMR (400.1 MHz, DMSO-*d*<sub>6</sub>) δ 5.54 (t, *J* = 6.1 Hz, 1H), 4.23 (d, *J* = 6.1 Hz, 1H), <sup>13</sup>C NMR (100.6 MHz, DMSO-*d*<sub>6</sub>) δ 105.2 (C), 73.9 (CH<sub>2</sub>).

#### Synthesis of (*E*)-2,3-dibenzylbut-2-ene-1,4-diol **199a**

##### Method A - Fe<sup>III</sup>Cl<sub>3</sub>/CuTc catalysed Kumada coupling



CuTc (32 mg, 0.12 mmol) and FeCl<sub>3</sub> (19 mg, 0.12 mmol) were added to a flame dried Schlenk flask diluted with dry THF (4ml), and stirred rapidly under an atmosphere of argon. **197a** (360 mg 1.18 mmol) was added to the stirred mixture in one portion, and benzylmagnesium chloride (2 M, 1.8 ml, 3.67 mmol) was added rapidly in one portion and left for 24 h. The reaction was quenched with 1 M HCl, extracted with EtOAc (3 x 4 ml), dried with MgSO<sub>4</sub>, filtered and concentrated under reduced pressure to give a yellow solid (494 mg). The solid was then recrystallised from hot acetone, washed with acetone and dried *in vacuo*, giving a clear crystalline solid product **199a** (50mg, 16%),  $R_f$  = 0.18 (1:1 Hexane:EtOAc), <sup>1</sup>H NMR (400.2 MHz, CDCl<sub>3</sub>) δ 7.35 – 7.28 (m, 4H), 7.25 – 7.19 (m, 6H), 4.24 (d, *J* = 5.6 Hz, 4H), 3.73 (s, 4H), 1.18 (t, *J* = 5.6 Hz, 2H), <sup>13</sup>C NMR (100.6 MHz, CDCl<sub>3</sub>) δ 139.9 (C), 136.9 (C), 128.9 (CH), 128.7 (CH), 126.5 (CH), 62.0 (CH<sub>2</sub>), 35.8 (CH<sub>2</sub>), MS (+ESI) calcd. *m/z* C<sub>18</sub>H<sub>20</sub>O<sub>2</sub> 291.1356 (M+Na), found *m/z* 291.1349 (M+Na).

##### Method B – Monocoupling of iodide **197a**

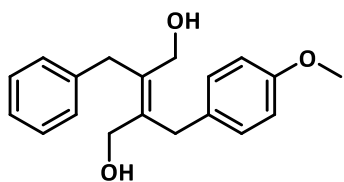
Lithium chloride (328 mg, 7.7 mmol) was dried under vacuum until free flowing, the cooled under and atmosphere of argon. Tetrahydrofuran (30 ml) was then added followed by (*Z*)-2-benzyl-3-iodobut-2-ene-1,4-diol (2.13 g, 7 mmol), forming a clear, pale yellow solution on addition. Solid SPhos (55 mg, 0.13 mmol, 1.9 mol%) was added followed by Pd(OAc)<sub>2</sub> (31 mg, 0.14 mmol, 2 mol%), forming an orange reaction mixture. Benzylzinc chloride (5.2 ml of a 1.61M solution in THF) was added promptly and the reaction became bright orange and refluxed as the addition proceeded. On

complete addition, the reaction mixture became a deep brown, almost black mixture. TLC analysis (2:1 EtOAc:Hexane) after 15 minutes of reaction time indicated complete formation of the desired product **199a** ( $R_f = 0.37$ ), with disappearance of the starting vinyl iodide ( $R_f = 0.67$ ). The reaction mixture was quenched with saturated aqueous ammonium chloride (10 ml) and extracted with ethyl acetate (3 x 20 ml). The organic layer was separated, the aqueous re-extracted with ethyl acetate (15 ml) and the organic fractions combined. The combined fractions were then dried with sodium sulfate, filtered and concentrated under reduced pressure giving a crude orange brown solid. The solid could then be triturated with Et<sub>2</sub>O and filtered to provide a colourless solid (1.64 g, 6.11 mmol, 87%).

#### **Method C – Decoupling of diiodide 200**

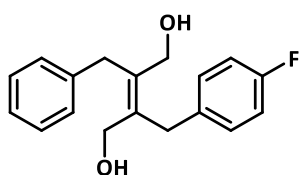
Lithium chloride (407 mg, 9.60 mmol) was dried under vacuum until free flowing, the cooled under and atmosphere of argon. Tetrahydrofuran (8.1 ml) was then added followed by (E)-2,3-diiodobut-2-ene-1,4-diol **200** (1.36 g, 4.00 mmol) and the mixture heated to 60 °C, forming a clear, pale yellow solution on addition. Solid PCy<sub>3</sub> (21.8 mg, 0.078 mmol, 1.9 mol%) was added followed by Pd(OAc)<sub>2</sub> (18.8 mg, 0.084 mmol, 2.1 mol%), forming a deep brown reaction mixture. Benzylzinc chloride (11.9 ml of a 0.81 M solution in THF) was added promptly and the reaction became bright orange and refluxed as the addition proceeded. On complete addition, the reaction mixture became a deep brown, almost black mixture. TLC analysis (2:1 EtOAc:Hexane) after 15 minutes of reaction time indicated complete formation of the desired product **199a** ( $R_f = 0.57$ ), with disappearance of the starting diiodide ( $R_f = 0.37$ ). The reaction mixture was quenched with saturated aqueous ammonium chloride (15 ml) and extracted with ethyl acetate (3 x 10 ml). The organic layer was separated, the aqueous re-extracted with ethyl acetate (15 ml) and the organic fractions combined. The combined fractions were then dried with MgSO<sub>4</sub>, filtered and concentrated under reduced pressure giving a white solid with some yellow oily residue (2.94 g). **N.B. It is key at this point that the reaction mixture is not heated on a waterbath above 30 °C, as it was found that the mixture became an intractable oil which was difficult to separate the product from.** The solid could then be triturated with Et<sub>2</sub>O and filtered to provide a colourless solid after 2 cycles (767 mg, 6.11 mmol, 72%).

Preparation of (E)-2,3-bis(4-methoxybenzyl)but-2-ene-1,4-diol **199d**



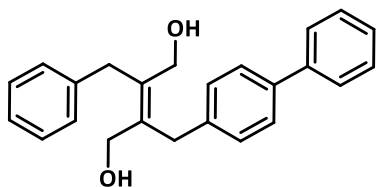
Lithium chloride (361 mg, 8.52 mmol, 1.21 eq.) was dried under vacuum until free flowing, then cooled under an atmosphere of argon. Tetrahydrofuran (14.0 ml) was then added followed by (Z)-2-benzyl-3-iodobut-2-ene-1,4-diol **197a** (2.14 g, 7.04 mmol), forming a clear, pale yellow solution on addition. Solid  $\text{PCy}_3$  (36.9 mg, 0.132 mmol, 1.9 mol%) was added followed by  $\text{Pd}(\text{OAc})_2$  (38.0 mg, 0.169 mmol, 2.4 mol%), forming a dark brown reaction mixture. 4-Methoxybenzylzinc bromide (21 ml of a 0.4M solution in THF, 8.4 mmol, 1.20 eq.) was added promptly (total volume added dropwise over 1 min) and the dark solution became bright orange and refluxed as the addition proceeded. On complete addition, the reaction mixture became a deep brown, almost black mixture. TLC analysis (2:1 EtOAc:Hexane) after 20 minutes of reaction time indicated complete formation of the desired product **199d** ( $R_f = 0.33$ ), with disappearance of the starting vinyl iodide ( $R_f = 0.55$ ). The reaction mixture was quenched with saturated aqueous ammonium chloride (20 ml) and extracted with warm EtOAc (3 x 20 ml). The organic layer was separated, the aqueous re-extracted with ethyl acetate (15 ml) and the organic fractions combined. The combined fractions were then dried warm with  $\text{MgSO}_4$ , filtered and concentrated under reduced pressure giving a crude feathery off-white solid with an orange-brown residue (6.00 g). The solid could then be triturated with  $\text{Et}_2\text{O}$  and filtered to provide a colourless solid after two cycles (1.96 g, 5.73 mmol, 82%), **m.p.** 131-132 °C, **IR** (Solid ATR)  $\nu_{\text{max}}/\text{cm}^{-1}$  3388, 3326, 3062, 3022, 2998, 2984, 2951, 2916, 2891, 2833, 1610, 1581, 1509, 1493, 1453, 1432, 1325, 1301, 1249, 1216, 1173, 1128, 1078, 1057, 1034, 1011, 992, 929, 879, 844, 832, 804, 759, 728, 701, 612, 515, 497, 454;  **$^1\text{H NMR}$**  (400.2 MHz,  $\text{D}_6\text{-DMSO}$ )  $\delta$  7.30 – 7.22 (m, 2H, H-15), 7.21 – 7.12 (m, 3H, H-14 and H-16), 7.12 – 7.07 (m, 1H, H-5), 6.85 – 6.79 (m, 1H, H-6), 4.72 (t,  $J = 5.3$  Hz, 1H, -OH), 4.69 (t,  $J = 5.3$  Hz, 1H, -OH), 3.94 (d,  $J = 5.3$  Hz, 2H, H-10), 3.92 (d,  $J = 5.3$  Hz, 2H, H-1), 3.71 (s, 3H, H-9), 3.59 (s, 2H, H-12), 3.52 (s, 2H, H-3);  **$^{13}\text{C NMR}$**  (100.6 MHz,  $\text{D}_6\text{-DMSO}$ ):  $\delta$  157.3 (C), 140.6 (C), 135.8 (C), 135.0 (C), 132.3 (C), 129.4 (CH), 128.5 (CH), 128.2 (CH), 125.7 (CH), 113.6 (CH), 59.2 ( $\text{CH}_2$ ), 59.2 ( $\text{CH}_2$ ), 54.9 ( $\text{CH}_3$ ), 34.1 ( $\text{CH}_2$ ), 33.2 ( $\text{CH}_2$ ); **HRMS** (+ESI) calcd. for  $\text{C}_{19}\text{H}_{22}\text{O}_3$   $m/z$  316.1907 ( $\text{M}+\text{NH}_4$ ), found  $m/z$  316.1902 ( $\text{M}+\text{NH}_4$ ).

Preparation of (E)-2-benzyl-3-(4-fluorobenzyl)but-2-ene-1,4-diol **199b**



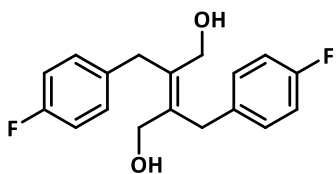
Lithium chloride (460 mg, 10.9 mmol) was dried under vacuum until free flowing, then cooled under an atmosphere of argon. Tetrahydrofuran (30 ml) was then added followed by (Z)-2-benzyl-3-iodobut-2-ene-1,4-diol **197a** (2.74 g, 9.00 mmol), forming a clear, pale yellow solution on addition. Solid  $\text{PCy}_3$  (47.8 mg, 0.170 mmol, 1.9 mol%) was added followed by  $\text{Pd}(\text{OAc})_2$  (41.1 mg, 0.183 mmol, 2 mol%), forming a deep orange/brown reaction mixture. 4-Fluorobenzylzinc chloride (11.9 ml of a 0.91M solution in THF) was added promptly and the reaction became bright orange and refluxed as the addition proceeded. On complete addition, the reaction mixture became a deep brown, almost black mixture. TLC analysis (2:1 EtOAc:Hexane) after 15 minutes of reaction time indicated complete formation of the desired product **199b** ( $R_f = 0.28$ ), with disappearance of the starting vinyl iodide ( $R_f = 0.50$ ). The reaction mixture was quenched with saturated aqueous ammonium chloride (5 ml) and extracted with warm 9:1 ethyl acetate:THF (3 x 20 ml). The organic layer was separated, the aqueous re-extracted with warm ethyl acetate (15 ml) and the organic fractions combined. The combined fractions were then dried warm with sodium sulfate, filtered and concentrated under reduced pressure giving a crude feathery off-white solid with an orange-brown residue. The solid could then be triturated with  $\text{Et}_2\text{O}$  and filtered to provide a colourless solid (2.25 g, 8.61 mmol, 96%), **m.p.** 137-138 °C, **IR** (Solid ATR)  $\nu_{\text{max}}/\text{cm}^{-1}$  3384, 3329, 3063, 3023, 2982, 2951, 2917, 2990, 1631, 1601, 1506, 1494, 1483, 1453, 1432, 1328, 1295, 1222, 1156, 1128, 1076, 1057, 1012, 993, 930, 879, 850, 834, 824;  **$^1\text{H NMR}$**  (400.2 MHz,  $\text{D}_6\text{-DMSO}$ )  $\delta$  7.25-7.18 (m, 4H, H-5), 7.11-7.04 (m, 4H, H-6), 4.69 (t,  $J = 5.1$  Hz, 2H, OH), 3.91 (d,  $J = 5.1$  Hz, 4H, H-1), 3.53 (s, 4H, H-3);  **$^{13}\text{C NMR}$**  (100.6 MHz,  $\text{D}_6\text{-DMSO}$ ):  $\delta$  160.6 (d,  $J = 240.8$  Hz, C), 136.5 (d,  $J = 2.9$  Hz, C), 135.4 (C), 130.2 (d,  $J = 8.0$  Hz, CH), 114.8 (d,  $J = 21.1$  Hz, CH), 59.2 ( $\text{CH}_2$ ), 33.4 ( $\text{CH}_2$ ); **HRMS** (+ESI) calcd. for  $\text{C}_{18}\text{H}_{18}\text{O}_2\text{F}_2$   $m/z$  322.1613 ( $\text{M}+\text{NH}_4$ ), found  $m/z$  322.1614 ( $\text{M}+\text{NH}_4$ ).

Synthesis of (*E*)-2-([1,1'-biphenyl]-4-ylmethyl)-3-benzylbut-2-ene-1,4-diol **199c**



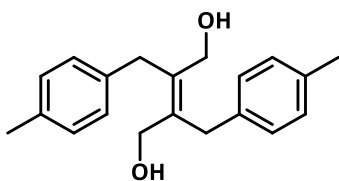
Lithium chloride (459 mg, 10.8 mmol, 1.20 eq.) was dried under vacuum until free flowing, the cooled under and atmosphere of argon. Tetrahydrofuran (22 ml) was then added followed by (*Z*)-2-benzyl-3-iodobut-2-ene-1,4-diol **197a** (2.74 g, 9.00 mmol), forming a clear, pale yellow solution on addition. Solid PCy<sub>3</sub> (47.6 mg, 0.170 mmol, 1.9 mol%) was added followed by Pd(OAc)<sub>2</sub> (40.4 mg, 0.180 mmol, 2 mol%), forming an orange reaction mixture. 4-Phenylbenzylzinc chloride (18.0 ml of a 0.61M solution in THF) was added promptly and the reaction became bright orange and refluxed as the addition proceeded. On complete addition, the reaction mixture became a deep brown, almost black mixture. After TLC indicated the reaction was complete (**199c** R<sub>f</sub> = 0.77, EtOAc), the reaction mixture was quenched with saturated aqueous ammonium chloride (10 ml) and extracted with 9:1 ethyl acetate:THF to prevent the diol crashing out of solution (3 x 20 ml). The organic layer was separated, the aqueous re-extracted with 9:1 ethyl acetate:THF (15 ml) and the organic fractions combined. The combined fractions were then dried with magnesium sulfate, filtered and concentrated under reduced pressure giving a crude orange brown solid. The solid could then be triturated with Et<sub>2</sub>O and filtered to provide a colourless solid (2.90 g, 8.43 mmol, 94%), **m.p.** 156-158 °C, **IR** (Solid ATR)  $\nu_{\max}/\text{cm}^{-1}$  3390, 3331, 3079, 3059, 3021, 2983, 2951, 2889, 1600, 1582, 1562, 1520, 1485, 1451, 1431, 1406, 1324, 1295, 1267, 1216, 1191, 1153, 1127, 1077, 1057, 1030, 1012, 994, 931, 906, 880, 843, 834, 818, 754, 738, 702, 687, 625, 593, 568, 557, 546, 497, 439, 425; **<sup>1</sup>H NMR** (400.2, D<sub>6</sub>-DMSO)  $\delta$  7.66 – 7.62 (m, 2H, H-16), 7.58 – 7.54 (m, 2H, H-13), 7.47 – 7.42 (m, 2H, H-17), 7.36 – 7.31 (m, 1H, H-18), 7.30 – 7.28 (m, 2H, H-12), 7.29 – 7.24 (m, 2H, H-6), 7.23 – 7.20 (m, 2H, H-H-5), 7.18 – 7.13 (m, 1H, H-7), 4.78 (t, *J* = 5.1 Hz, 1H, -OH), 4.77 (t, *J* = 5.1 Hz, 1H, -OH), 3.99 (d, *J* = 5.1 Hz, 2H, H-1), 3.98 (d, *J* = 5.1 Hz, 2H, H-8), 3.65 (s, 2H, H-10), 3.62 (s, 2H, H-3); **<sup>13</sup>C NMR** (100.6 MHz, D<sub>6</sub>-DMSO)  $\delta$  140.5 (C), 140.01 (C), 139.9 (C), 137.6 (C), 135.5 (C), 135.3 (C), 129.1 (CH), 128.9 (CH), 128.5 (CH), 128.2 (CH), 127.1 (CH), 126.5 (2 overlapping CH signals), 125.7 (CH), 59.4 (CH<sub>2</sub>), 59.3 (CH<sub>2</sub>), 34.2 (CH<sub>2</sub>), 33.8 (CH<sub>2</sub>); **HRMS** (+ESI) calcd. for C<sub>24</sub>H<sub>24</sub>O<sub>2</sub> *m/z* 367.1669 (M+Na), found *m/z* 367.1670 (M+Na).

Synthesis of (E)-2,3-bis(4-fluorobenzyl)but-2-ene-1,4-diol **199f**



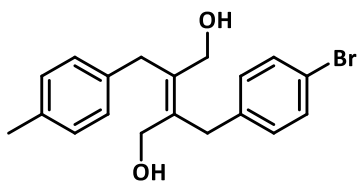
Lithium chloride (460 mg, 10.9 mmol) was dried under vacuum until free flowing, then cooled under an atmosphere of argon. Tetrahydrofuran (30 ml) was then added followed by (Z)-2-(4-fluorobenzyl)-3-iodobut-2-ene-1,4-diol **197c** (2.90 g, 9.00 mmol), forming a clear, pale yellow solution on addition. Solid  $\text{PCy}_3$  (48.0 mg, 0.171 mmol, 1.9 mol%) was added followed by  $\text{Pd}(\text{OAc})_2$  (40.7 mg, 0.181 mmol, 2 mol%), forming a dark brown mixture. 4-Fluorobenzylzinc chloride (12.0 ml of a 0.91 M solution in THF) was added promptly and the reaction became bright orange and refluxed as the addition proceeded. On complete addition, the reaction mixture became a deep brown, almost black mixture. TLC analysis (2:1 EtOAc:Hexane) after 15 minutes of reaction time indicated complete formation of the desired product **199f** ( $R_f = 0.26$ ), with disappearance of the starting vinyl iodide ( $R_f = 0.45$ ). The reaction mixture was quenched with saturated aqueous ammonium chloride (20 ml) and extracted with ethyl acetate (3 x 20 ml). The organic layer was separated, the aqueous re-extracted with ethyl acetate (15 ml) and the organic fractions combined. The combined fractions were then dried with  $\text{MgSO}_4$ , filtered and concentrated under reduced pressure giving a crude orange brown solid (8.14 g). The solid could then be triturated with  $\text{Et}_2\text{O}$  and filtered to provide a colourless solid after 3 cycles (2.25 g, 7.39 mmol, 82%), **m.p.** 129-130 °C, **IR** (Solid ATR)  $\nu_{\text{max}}/\text{cm}^{-1}$  3372, 3033, 2980, 2948, 2938, 2922, 2883, 1604, 1506, 1481, 1449, 1424, 1317, 1296, 1264, 1226, 1214, 1157, 1127, 1100, 1057, 1011, 992, 939, 932, 881, 851, 834, 820, 763, 704, 607, 573, 545, 490, 436, 416;  **$^1\text{H NMR}$**  (400.2 MHz,  $\text{D}_6\text{-DMSO}$ )  $\delta$  7.31 – 7.16 (m, 2H, H-5), 7.14 – 7.02 (m, 2H, H-6), 4.77 (t,  $J = 5.1$  Hz, 2H, -OH), 3.92 (d,  $J = 5.1$  Hz, 4H, H-1), 3.57 (s, 4H, H-3);  **$^{13}\text{C NMR}$**  (100.6 MHz,  $\text{D}_6\text{-DMSO}$ ):  $\delta$  160.6 (d,  $J = 240.8$  Hz, C), 136.5 (d,  $J = 2.9$  Hz, C), 135.4 (C), 130.2 (d,  $J = 8.0$  Hz, CH), 114.8 (d,  $J = 21.1$  Hz, CH), 59.2 ( $\text{CH}_2$ ), 33.4 ( $\text{CH}_2$ );  **$^{19}\text{F NMR}$**  (376.5 MHz,  $\text{DMSO-}d_6$ )  $\delta$  -117.80. ; **HRMS** (+ESI) calcd. for  $\text{C}_{18}\text{H}_{22}\text{O}_2\text{F}_2$   $m/z$  322.1613 (M+ $\text{NH}_4$ ), found  $m/z$  322.1614 (M+ $\text{NH}_4$ ).

### Synthesis of (*E*)-2,3-bis(4-methylbenzyl)but-2-ene-1,4-diol **199h**



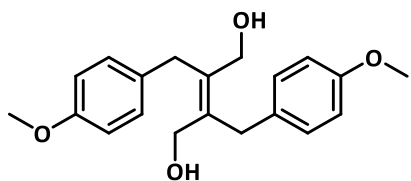
Lithium chloride (187 mg, 4.4 mmol) was dried under vacuum until free flowing, the cooled under and atmosphere of argon. Tetrahydrofuran (14 ml) was then added followed by (*Z*)-2-iodo-3-(4-methylbenzyl)but-2-ene-1,4-diol **197b** (1.27 g, 4.00 mmol), forming a clear, pale yellow solution on addition. Solid PCy<sub>3</sub> (22 mg, 0.13 mmol, 1.9 mol%) was added followed by Pd(OAc)<sub>2</sub> (19 mg, 0.14 mmol, 2 mol%), forming an orange reaction mixture. 4-Methylbenzylzinc chloride (6.9 ml of a 0.64M solution in THF) was added promptly and the reaction became bright orange and refluxed as the addition proceeded. On complete addition, the reaction mixture became a deep brown, almost black mixture. TLC analysis (2:1 EtOAc: Pentane) after 15 minutes of reaction time indicated complete formation of the desired product **199h** (*R<sub>f</sub>* = 0.39), with disappearance of the starting vinyl iodide (*R<sub>f</sub>* = 0.57). The reaction mixture was quenched with saturated aqueous ammonium chloride (5 ml) and extracted with warm 9:1 ethyl acetate:THF (3 x 20 ml). The organic layer was separated, the aqueous re-extracted with warm ethyl acetate (15 ml) and the organic fractions combined. The combined fractions were then dried warm with sodium sulfate, filtered and concentrated under reduced pressure giving a crude feathery off-white solid with an orange-brown residue. The solid could then be triturated with Et<sub>2</sub>O and filtered to provide a colourless solid (1.10 g, 6.11 mmol, 93%), **m.p.** 181-182 °C, **IR** (Solid ATR)  $\nu_{\max}/\text{cm}^{-1}$  3368, 3041, 3015, 2994, 2953, 2912, 2896, 2854, 1509, 1494, 1483, 1434, 1332, 1300, 1266, 1210, 1191, 1128, 1066, 1012, 992, 944, 925, 881, 839; **NMR** (400.2 MHz, D<sub>6</sub>-DMSO)  $\delta$  7.05 (s, 4H, H-5 and H-6), 4.69 (t, *J* = 5.2 Hz, 1H, OH), 3.91 (d, *J* = 5.2 Hz, 4H, H-1), 3.53 (s, 4H, H-3), 2.24 (s, 6H, H-8).; **<sup>13</sup>C NMR** (100.6 MHz, D<sub>6</sub>-DMSO):  $\delta$  137.4 (C, C-7), 135.3 (C, C-2), 134.5 (C, C-4), 128.7 (CH, C-6), 128.3 (CH, C-5), 59.2 (CH<sub>2</sub>, C-1), 33.6 (CH<sub>2</sub>, C-3), 20.6 (CH<sub>3</sub>, C-8); **HRMS** (+ESI) calcd. for C<sub>18</sub>H<sub>20</sub>O<sub>2</sub> *m/z* 314.2115 (M+NH<sub>4</sub>), found *m/z* 314.2112 (M+NH<sub>4</sub>).

Preparation of (E)-2-(4-bromobenzyl)-3-(4-methylbenzyl)but-2-ene-1,4-diol **199j**



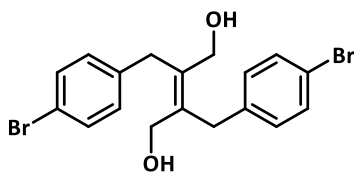
Lithium chloride (260 mg, 6.13 mmol, 1.23 eq.) was dried under vacuum until free flowing, then cooled under an atmosphere of argon. Tetrahydrofuran (18.0 ml) was then added followed by (Z)-2-iodo-3-(4-methylbenzyl)but-2-ene-1,4-diol **197b** (1.59 g, 5.00 mmol), forming a clear, pale yellow solution on addition. Solid  $\text{PCy}_3$  (48.2 mg, 0.172 mmol, 3.4 mol%) was added followed by  $\text{Pd}(\text{OAc})_2$  (40.5 mg, 0.180 mmol, 3.6 mol%), forming a dark brown reaction mixture. 4-Bromobenzylzinc chloride (7.3 ml of a 0.83M solution in THF, 8.4 mmol, 1.21 eq.) was added promptly (total volume added dropwise over 1 min) and the dark solution became bright orange and refluxed as the addition proceeded. On complete addition, the reaction mixture became a deep brown, almost black mixture. TLC analysis (2:1 EtOAc:Hexane) after 20 minutes of reaction time indicated complete formation of the desired product **199j** ( $R_f = 0.42$ ), with disappearance of the starting vinyl iodide ( $R_f = 0.57$ ). The reaction mixture was quenched with saturated aqueous ammonium chloride (20 ml) and extracted with warm EtOAc (3 x 20 ml). The organic layer was separated, the aqueous re-extracted with ethyl acetate (15 ml) and the organic fractions combined. The combined fractions were then dried warm with  $\text{MgSO}_4$ , filtered and concentrated under reduced pressure giving a crude feathery off-white solid with an orange-brown residue (8.36 g). The solid could then be triturated with  $\text{Et}_2\text{O}$  and filtered to provide a colourless solid after two cycles (1.65 g, 4.58 mmol, 92%), **m.p.** 153-154 °C, **IR** (Solid ATR)  $\nu_{\text{max}}/\text{cm}^{-1}$  3375, 3305, 3041, 3016, 2981, 2953, 2913, 2894, 2854, 1509, 1484, 1434, 1402, 1333, 1295, 1265, 1235, 1210, 1189, 1129, 1105, 1066, 1011, 994, 927, 881, 835, 808, 794, 760, 718, 611, 537, 480, 457, 438;  **$^1\text{H}$  NMR** (400.2 MHz,  $\text{D}_6\text{-DMSO}$ )  $\delta$  7.50 – 7.38 (m, 2H, H-6), 7.23 – 7.10 (m, 2H, H-5), 7.06 (s, 4H, H-12 and H-13), 4.75 (t,  $J = 5.1$  Hz, 1H, -OH), 4.72 (t,  $J = 5.1$  Hz, 1H, -OH), 3.93 (d,  $J = 5.1$  Hz, 1H, H-1), 3.90 (d,  $J = 5.1$  Hz, 1H, H-8), 3.55 (s, 2H, H-3), 3.52 (s, 2H, H-10), 2.25 (s, 3H, H-15);  **$^{13}\text{C}$  NMR** (101 MHz,  $\text{DMSO-}d_6$ )  $\delta$  140.1 (C), 137.3 (C), 135.8 (C), 134.8 (C), 134.5 (C), 131.0 (CH), 130.8 (CH), 128.8 (CH), 128.3 (CH), 118.7 (C), 59.3 ( $\text{CH}_2$ , 2 overlapping signals), 33.8 ( $\text{CH}_2$ ), 33.5 ( $\text{CH}_2$ ), 20.6 ( $\text{CH}_3$ ); **HRMS** (+ESI) calcd. for  $\text{C}_{19}\text{H}_{21}\text{BrO}_2$   $m/z$  383.0617 (M+Na), found  $\text{C}_{19}\text{H}_{21}\text{BrO}_2$   $m/z$  383.0622 (M+Na).

Preparation of (E)-2,3-bis(4-methoxybenzyl)but-2-ene-1,4-diol **199k**



Lithium chloride (326 mg, 7.69 mmol) was dried under vacuum until free flowing, then cooled under an atmosphere of argon. Tetrahydrofuran (24.6 ml) was then added followed by (Z)-2-iodo-3-(4-methoxybenzyl)but-2-ene-1,4-diol **197d** (2.36 g, 7.06 mmol), forming a clear, pale yellow solution on addition. Solid  $\text{PCy}_3$  (37.3 mg, 0.133 mmol, 1.9 mol%) was added followed by  $\text{Pd}(\text{OAc})_2$  (31.7 mg, 0.141 mmol, 2 mol%), forming a light orange reaction mixture. A small aliquot of 4-Methoxybenzylzinc bromide (roughly 100  $\mu\text{l}$  of a 0.74M solution in THF) was added promptly and the reaction became bright orange, then darkened as the catalyst activated. The remainder of the solution (10.3 ml) was added and the dark solution became bright orange and refluxed as the addition proceeded. On complete addition, the reaction mixture became a deep brown, almost black mixture. TLC analysis (2:1 EtOAc:Hexane) after 15 minutes of reaction time indicated complete formation of the desired product **199k** ( $R_f = 0.20$ ), with disappearance of the starting vinyl iodide ( $R_f = 0.40$ ). The reaction mixture was quenched with saturated aqueous ammonium chloride (5 ml) and extracted with warm EtOAc (3 x 20 ml). The organic layer was separated, the aqueous re-extracted with warm ethyl acetate (15 ml) and the organic fractions combined. The combined fractions were then dried with  $\text{MgSO}_4$ , filtered and concentrated under reduced pressure giving a crude feathery off-white solid with an orange-brown residue. The solid could then be triturated with  $\text{Et}_2\text{O}$  and filtered to provide a colourless solid (1.96 g, 5.97 mmol, 85%), **m.p.** 144-145  $^\circ\text{C}$ , **IR** (Solid ATR)  $\nu_{\text{max}}/\text{cm}^{-1}$  3384, 3332, 3065, 3029, 2990, 2950, 2929, 2915, 2891, 2831, 1608, 1580, 1506, 1461, 1439, 1323, 1300, 1245, 1215, 1129, 1109, 1062, 1032, 1010, 991, 928, 880, 843, 831, 814, 802, 756, 707, 603, 556, 512, 419;  **$^1\text{H NMR}$**  (400.2 MHz,  $\text{D}_6\text{-DMSO}$ )  $\delta$  7.13 – 7.05 (m, 4H, H-5), 6.85 – 6.79 (m, 4H, H-6), 4.68 (t,  $J = 4.9$  Hz, 2H, OH), 3.93 (d,  $J = 4.9$  Hz, 4H, H-1), 3.71 (s, 6H, H-9), 3.51 (s, 4H, H-3);  **$^{13}\text{C NMR}$**  (100.6 MHz,  $\text{D}_6\text{-DMSO}$ ):  $\delta$  157.3 (C), 135.4 (C), 132.3 (C), 129.3 (CH), 113.6 (CH), 59.1 ( $\text{CH}_2$ ), 54.9 ( $\text{CH}_3$ ), 33.2 ( $\text{CH}_2$ ); **HRMS** (+ESI) calcd. for  $\text{C}_{20}\text{H}_{24}\text{O}_4$   $m/z$  351.1567 (M+Na), found  $m/z$  351.1560 (M+Na).

### Preparation of (E)-2,3-bis(4-bromobenzyl)but-2-ene-1,4-diol **199n**



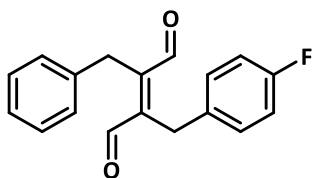
Lithium chloride (918 mg, 21.7 mmol, 2.41 eq.) was dried under vacuum until free flowing, then cooled under an atmosphere of argon. Tetrahydrofuran (19 ml) was then added followed by (E)-2,3-diiodobut-2-ene-1,4-diol **200** (3.06 g, 4.00 mmol) and the mixture heated to 65 °C, forming a clear, pale yellow solution on addition. Solid PCy<sub>3</sub> (48.2 mg, 0.172 mmol, 1.9 mol%) was added followed by Pd(OAc)<sub>2</sub> (40.8 mg, 0.181 mmol, 2.0 mol%), forming a deep brown reaction mixture. 4-Bromobenzylzinc chloride (26.0 ml of a 0.83 M solution in THF) was added promptly dropwise over 2 min and the reaction became bright orange and refluxed as the addition proceeded. On complete addition, the reaction mixture became a deep brown, almost black mixture. TLC analysis (2:1 EtOAc:Hexane) after 15 minutes of reaction time indicated complete formation of the desired product **199n** (*R<sub>f</sub>* = 0.33), with disappearance of the starting diiodide (*R<sub>f</sub>* = 0.53). The reaction mixture was quenched with saturated aqueous ammonium chloride (15 ml) and extracted with ethyl acetate (3 x 10 ml). The organic layer was separated, the aqueous re-extracted with ethyl acetate (15 ml) and the organic fractions combined. The combined fractions were then dried with MgSO<sub>4</sub>, filtered and concentrated under reduced pressure giving a white solid with some brown residue (14.1 g). The solid could then be triturated with Et<sub>2</sub>O and filtered to provide a colourless solid after 2 cycles (2.47 g, 5.81 mmol, 65%), **m.p.** 139-140 °C, **IR** (Solid ATR)  $\nu_{\text{max}}/\text{cm}^{-1}$  3373, 3305, 2991, 2957, 2911, 2894, 2850, 1899, 1619, 1484, 1433, 1400, 1339, 1294, 1267, 1232, 1187, 1129, 1104, 1069, 1010, 992, 924, 884, 834, 811, 788, 713, 636, 511, 453; **<sup>1</sup>H NMR** (400.2 MHz, D<sub>6</sub>-DMSO)  $\delta$  7.48 – 7.42 (m, 4H, H-5), 7.18 – 7.12 (m, 4H, H-6), 4.78 (t, *J* = 5.0 Hz, 2H, -OH), 3.91 (d, *J* = 5.0 Hz, 4H, H-1), 3.55 (s, 4H, H-3); **<sup>13</sup>C NMR** (100.6 MHz, D<sub>6</sub>-DMSO):  $\delta$  140.0 (C), 135.3 (C), 131.0 (CH<sub>2</sub>), 130.8 (CH<sub>2</sub>), 118.7 (C), 59.4 (CH<sub>2</sub>), 33.6 (CH<sub>2</sub>); **HRMS** (+ESI) calcd. for C<sub>18</sub>H<sub>22</sub>Br<sub>2</sub>O<sub>2</sub> *m/z* 442.0012 (M+NH<sub>4</sub>), found C<sub>18</sub>H<sub>22</sub>Br<sub>2</sub>O<sub>2</sub> *m/z* 442.0015 (M+NH<sub>4</sub>).

### General procedure for the synthesis of dialdehydes

Aerobic oxidation was carried out by modifying the procedure of Stahl. Reactions were carried out in the 100-mL apparatus shown in Figure S3a where the O<sub>2</sub> inlet pipe had an internal diameter of ca. 5 mm. The flask was charged with a suitable stirrer, diol

199a-n and DMF. Without any O<sub>2</sub> flowing the following solids and liquids were promptly added to the reaction mixture: [Cu(NCMe)<sub>4</sub>]BF<sub>4</sub> (8 mol%) [causing formation of a yellow or very pale green solution], 2,2-bipyridyl (8 mol%) [causing the solution to become very dark], TEMPO (8 mol%) [leading to a dark orange/brown solution] and finally N-methylimidazole (16 mol%). The oxygen flow was promptly started (flow rate ~5 bubbles/sec) as the reaction stirred. [NOTE: Rarely the reaction mixture turned a pale green colour within the first 5 minutes, this typically indicated premature catalyst deactivation which could be overcome by a second charge of all oxidation catalyst components.] The reaction was continued until TLC indicated formation of the dial and consumption of the diol.

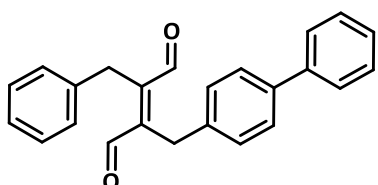
*Preparation of 2-benzyl-3-(4-fluorobenzyl)fumaraldehyde 201b*



*Following general procedure:* In the written order, [Cu(MeCN)<sub>4</sub>]BF<sub>4</sub> (78.0 mg, 0.248 mmol, 8.3 mol% in 2 ml DMF), Bipy (38.3 mg, 0.245 mmol, 8.2 mol% in 2 ml DMF), TEMPO (37.8 mg, 0.241 mmol, 8.1 mol% in 2ml DMF) and NMI (38 μl, 0.477 mmol, 15.9 mol%) to a stirred solution of (E)-2,3-bis(4-methoxybenzyl)but-2-ene-1,4-diol **199b** (859 mg, 3.00 mmol) in DMF (8 ml). On addition of all reagents, O<sub>2</sub> was bubbled into the solution until TLC analysis showed formation of the aldehyde. The reaction mixture was quenched by washing the mixture into a separatory funnel with warm 9:1 EtOAc:THF (20 ml), and quenched with aqueous 1M HCl (2 x 20 ml) then water (2 x 20ml). The aqueous was then re-extracted extracted with warm 9:1 EtOAc:THF (20 ml), the organic fractions combined and washed a final time with 1M HCl (20 ml). The combined fractions were then dried warm with MgSO<sub>4</sub>, filtered and concentrated under reduced pressure giving a yellow solid (1.10 g, 3.89 mmol, 97%), **m.p.** 113-114 °C; **IR** (Solid ATR)  $\nu_{\text{max}}/\text{cm}^{-1}$  3332, 3062, 3031, 2981, 2940, 2910, 2873, 2818, 2767, 1667, 1600, 1507, 1494, 1452, 1416, 1398, 1297, 1225, 1191, 1158, 1128, 1094, 1031, 1017, 976, 924, 901, 873, 852, 830, 809, 760, 735, 696, 608, 571, 504, 468, 418; **<sup>1</sup>H NMR** (400.2 MHz, Chloroform-*d*)  $\delta$  10.48 (s, 1H), 10.47 (s, 1H, ), 7.31 – 7.26 (m, 2H, H-14), 7.24 – 7.19 (m, 1H, H-15), 7.14 – 7.11 (m, 2H, H-13), 7.13-7.06 (m, 2H, H-5), 7.01 – 6.92 (m, 2H, H-6), 4.14 (s, 2H, H-11), 4.09 (s, 2H, H-3).; **<sup>13</sup>C NMR** (100.6 MHz, Chloroform-*d*)  $\delta$  193.4 (CH), 193.4 (CH), 161.8 (C,

d,  $J = 245.5$  Hz), 147.6 (C), 147.2 (C), 138.1 (C), 133.9 (C, d,  $J = 3.3$  Hz), 129.9 (CH, d,  $J = 8.0$  Hz), 129.1 (CH), 128.4 (CH), 127.0 (CH), 115.9 (CH, d,  $J = 21.3$  Hz), 29.4 (CH<sub>2</sub>), 28.6 (CH<sub>2</sub>); **<sup>19</sup>F NMR** (376.5 MHz, Chloroform-*d*)  $\delta$  -115.90; **HRMS** (+ESI) calcd. for C<sub>20</sub>H<sub>20</sub>O<sub>4</sub>  $m/z$  305.0948 (M+Na), found C<sub>18</sub>H<sub>15</sub>O<sub>2</sub>F<sub>1</sub>  $m/z$  305.0944 (M+Na).

*Preparation of 2-([1,1'-biphenyl]-4-ylmethyl)-3-benzylfumarylaldehyde **201c***

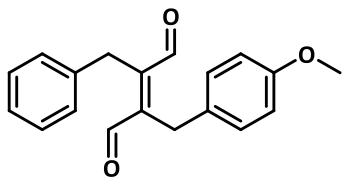


*Following general procedure:* In the written order, [Cu(MeCN)<sub>4</sub>]BF<sub>4</sub> (102 mg, 0.324 mmol, 8.2 mol% in 3 ml DMF), Bipy (50.2 mg, 0.321 mmol, 8.1 mol% in 3 ml DMF), TEMPO (52.6 mg, 0.337 mmol, 8.5 mol% in 3 ml

DMF) and NMI (51  $\mu$ l, 0.64 mmol, 16.1 mol%) to a stirred solution of (E)-2-([1,1'-biphenyl]-4-ylmethyl)-3-benzylbut-2-ene-1,4-diol **199c** (1.37 g, 3.98 mmol) in DMF (7 ml) and heated to 40 °C. On addition of all reagents, O<sub>2</sub> was bubbled into the solution, and the mixture appeared light green after 15 min, however TLC analysis (2:1 EtOAc:Hexane) showed the diol had not been consumed. The reaction mixture was redosed with [Cu(MeCN)<sub>4</sub>]BF<sub>4</sub> (80.4 mg), Bipy (39.3 mg) and TEMPO (37.8 mg) and monitored by TLC until complete formation of the dial (**R<sub>f</sub>** = 0.88). The reaction mixture was quenched by washing the mixture into a separatory funnel with EtOAc (20 ml), and quenched with aqueous 1M HCl (2 x 20 ml) then water (2 x 20ml). The aqueous was then re-extracted extracted with EtOAc (20 ml), the organic fractions combined and washed a final time with 1M HCl (20 ml). The combined fractions were then dried with MgSO<sub>4</sub>, filtered and concentrated under reduced pressure giving a yellow solid that required no further purification (1.31 g, 3.83 mmol, 96%), **m.p.** 134-135 °C, **IR** (Solid ATR)  $\nu_{\text{max}}/\text{cm}^{-1}$  3332, 3060, 3030, 2940, 2908, 2817, 2768, 1763, 1667, 1598, 1563, 1523, 1496, 1487, 1453, 1396, 1345, 1214, 1191, 1130, 1077, 1030, 1006, 977, 950, 927, 903, 875, 835, 808, 760, 737, 730, 697, 687, 641, 598, 551, 488, 474, 415; **<sup>1</sup>H NMR** (400.2 MHz, D<sub>6</sub>-DMSO)  $\delta$  10.52 (s, 1H, H-1), 10.52 (s, 1H, H-8), 7.57 – 7.53 (m, 2H, H-16), 7.53 – 7.48 (m, 2H, H-13), 7.45 – 7.40 (m, 2H, H-17), 7.37 – 7.31 (m, 1H, H-18), 7.31 – 7.26 (m, 2H, H-6), 7.24 – 7.18 (m, 3H, H-5 and H-7), 7.15 (m, 2H, H-12), 4.18 (s, 2H, H-10), 4.16 (s, 2H, H-3); **<sup>13</sup>C NMR** (100.6 MHz, D<sub>6</sub>-DMSO):  $\delta$  193.6 (CH), 193.6 (CH), 147.6 (C), 147.4 (C), 140.7 (C), 140.0 (C), 138.3 (C), 137.3 (C), 129.1 (CH), 128.9 (CH), 128.8 (CH), 128.4 (CH), 127.8 (CH), 127.5 (CH), 127.2 (CH), 127.0 (CH), 29.4 (CH<sub>2</sub>),

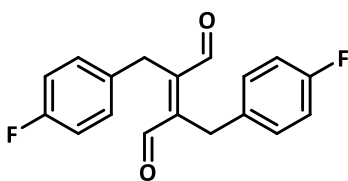
29.0 (CH<sub>2</sub>); **HRMS** (+ESI) calcd. for C<sub>24</sub>H<sub>20</sub>O<sub>2</sub> *m/z* 363.1356 (M+Na), found C<sub>24</sub>H<sub>20</sub>O<sub>2</sub> *m/z* 363.1352 (M+Na).

*Preparation of 2-benzyl-3-(4-methoxybenzyl)fumaraldehyde 201d*



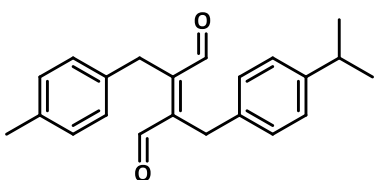
*Following general procedure:* In the written order, [Cu(MeCN)<sub>4</sub>]BF<sub>4</sub> (102 mg, 0.324 mmol, 8.1 mol% in 3ml DMF), Bipy (50.1 mg, 0.321 mmol, 8.1 mol% in 3ml DMF), TEMPO (50.2 mg, 0.321 mmol, 8.1 mol% in 3ml DMF) and NMI (52 μl, 0.652 mmol, 16.4 mol%) to a stirred solution of (E)-2-benzyl-3-(4-methoxybenzyl)but-2-ene-1,4-diol **199d** (1.19 g, 4.00 mmol) in DMF (7 ml). On addition of all reagents, O<sub>2</sub> was bubbled into the solution until TLC analysis (2:1 EtOAc:Hexanes) showed formation of the aldehyde (*R<sub>f</sub>* = 0.72). The reaction mixture was quenched by washing the mixture into a separatory funnel with warm 9:1 EtOAc:THF (20 ml), and quenched with aqueous 1M HCl (2 x 20 ml) then water (2 x 20ml). The aqueous was then re-extracted extracted with warm 9:1 EtOAc:THF (20 ml), the organic fractions combined and washed a final time with 1M HCl (20 ml). The combined fractions were then dried warm with MgSO<sub>4</sub>, filtered and concentrated under reduced pressure giving a yellow solid (1.11g, 3.76 mmol, 94%), **m.p.** 132-133 °C, **IR** (Solid ATR) *v*<sub>max</sub>/cm<sup>-1</sup> 3331, 3059, 3031, 3013, 2968, 2936, 2909, 2874, 2839, 2820, 2768, 1667, 1607, 1580, 1510, 1496, 1453, 1397, 1332, 1305, 1274, 1243, 1179, 1153, 1130, 1108, 1077, 1025, 977, 961, 925, 901, 874, 821, 807, 752, 736, 696, 609, 577, 530, 510, 493, 453; **<sup>1</sup>H NMR** (400.2 MHz, Chloroform-*d*) δ 10.49 (s, 1H, H-10), 10.47 (s, 1H, H-1), 7.31 – 7.25 (m, 2H, H-15), 7.24 – 7.18 (m, 1H, H-16), 7.13 (m, 2H, H-14), 7.08 – 7.02 (m, 2H, H-5), 6.84 – 6.78 (m, 2H, H-6), 4.12 (s, 2H, H-12), 4.07 (s, 2H, H-3), 3.77 (s, 3H, H-9).; **<sup>13</sup>C NMR** (100.6 MHz, Chloroform-*d*): δ 193.7 (CH), 193.6 (CH), 158.6 (C), 147.8 (C), 147.2 (C), 138.3 (C), 130.2 (C), 129.5 (CH), 129.0 (CH), 128.4 (CH), 126.9 (CH), 114.4 (CH), 55.4 (CH<sub>3</sub>), 29.3 (CH<sub>2</sub>), 28.5 (CH<sub>2</sub>); **HRMS** (+ESI) calcd. for C<sub>19</sub>H<sub>18</sub>O<sub>3</sub> *m/z* 317.1148 (M+Na), found C<sub>19</sub>H<sub>18</sub>O<sub>3</sub> *m/z* 317.1144 (M+Na).

### Preparation of 2,3-bis(4-fluorobenzyl)fumaraldehyde **201f**



Following general procedure: In the written order,  $[\text{Cu}(\text{MeCN})_4]\text{BF}_4$  (94.6 mg, 0.301 mmol, 8.0 mol% as a solid), Bipy (46.6 mg, 0.298 mmol, 8.0 mol% as a solid), TEMPO (46.7 mg, 0.299 mmol, 8.0 mol% as a solid) and NMI (48.0  $\mu\text{l}$ , 0.602 mmol, 16.1 mol%) to a stirred solution of (E)-2,3-bis(4-fluorobenzyl)but-2-ene-1,4-diol **199f** (1.14 g, 3.75 mmol) in DMF (16 ml). On addition of all reagents,  $\text{O}_2$  was bubbled into the solution until TLC analysis (2:1 EtOAc:Hexane) showed formation of the aldehyde ( $R_f = 0.66$ ). The reaction mixture was quenched by washing the mixture into a separatory funnel with EtOAc (20 ml), and quenched with aqueous 1M HCl (2 x 20 ml) then water (2 x 20ml). The aqueous was then re-extracted with EtOAc (20 ml), the organic fractions combined and washed a final time with 1M HCl (20 ml). The combined fractions were then dried with  $\text{MgSO}_4$ , filtered and concentrated under reduced pressure giving a yellow solid that required no further purification (859 mg, 2.68 mmol, 92%), **m.p.** 115-116  $^\circ\text{C}$ , **IR** (Solid ATR)  $\nu_{\text{max}}/\text{cm}^{-1}$  3331, 2939, 2910, 1666, 1600, 1505, 1446, 1416, 1397, 1297, 1226, 1158, 1127, 1093, 1017, 976, 877, 852, 830, 817, 763, 700, 557, 494, 428;  **$^1\text{H NMR}$**  (400.2 MHz, D-Chloroform)  $\delta$  10.46 (s, 1H), 7.09 (ddt,  $J = 8.2, 5.2, 2.5$  Hz, 2H), 7.03 – 6.91 (m, 2H), 4.09 (s, 2H).;  **$^{13}\text{C NMR}$**  (100.6 MHz, D-Chloroform)  $\delta$  193.3 (CH), 161.8 (CH, d,  $J = 245.8$  Hz), 147.3, 133.7 (C, d,  $J = 3.0$  Hz), 129.9 (CH, d,  $J = 8.0$  Hz), 115.9 (CH, d,  $J = 21.4$  Hz), 28.7 ( $\text{CH}_2$ ).;  **$^{19}\text{F NMR}$**  (376.5 MHz, D-Chloroform)  $\delta$  -115.72; **HRMS** (+ESI) calcd. for  $\text{C}_{19}\text{H}_{17}\text{Br}_1\text{O}_2$   $m/z$  379.0304 (M+Na), found  $\text{C}_{19}\text{H}_{17}\text{Br}_1\text{O}_2$   $m/z$  379.0300 (M+Na).

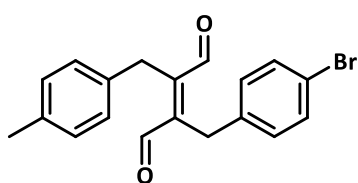
### Preparation of (E)-2,3-bis(4-methoxybenzyl)but-2-ene-1,4-diol **201i**



Following general procedure: In the written order,  $[\text{Cu}(\text{MeCN})_4]\text{BF}_4$  (102 mg, 0.243 mmol, 8.1 mol% in 2 ml DMF), Bipy (37.0 mg, 0.237 mmol, 7.9 mol% in 2 ml DMF), TEMPO (38.0 mg, 0.243 mmol, 8.1 mol% in 2 ml DMF) and NMI (38  $\mu\text{l}$ , 0.64 mmol, 16 mol%) to a stirred solution of (E)-2-(4-isopropylbenzyl)-3-(4-methylbenzyl)but-2-ene-1,4-diol **199i** (985 g, 3.00 mmol) in DMF (6 ml). On addition of all reagents,  $\text{O}_2$  was bubbled into the solution. After 2 minutes, the solution was clear green however TLC analysis indicated that the starting

material remained, so was redosed with  $[\text{Cu}(\text{MeCN})_4]\text{BF}_4$  (71.6 mg), Bipy (34.0 mg) and TEMPO (38.7 mg) and monitored until TLC analysis showed complete conversion to the aldehyde ( $R_f = 0.78$ ). The reaction mixture was quenched by washing the mixture into a separatory funnel with EtOAc (20 ml), and quenched with aqueous 1M HCl (2 x 20 ml) then water (2 x 20ml). The aqueous was then re-extracted extracted with EtOAc (20 ml), the organic fractions combined and washed a final time with 1M HCl (20 ml). The combined fractions were then dried warm with  $\text{MgSO}_4$ , filtered and concentrated under reduced pressure giving a yellow solid that required no further purification (859 mg, 2.68 mmol, 89%), **m.p.** 107-109 °C, **IR** (Solid ATR)  $\nu_{\text{max}}/\text{cm}^{-1}$  3333, 3053, 3022, 3007, 2958, 2907, 2870, 2822, 2768, 2731, 1908, 1753, 1668, 1511, 1448, 1417, 1398, 1380, 1363, 1269, 1216, 1188, 1130, 1055, 1020, 967, 880, 834, 800, 750, 693, 565, 547, 493;  **$^1\text{H NMR}$**  (400.2 MHz, Chloroform-*d*)  $\delta$  10.48 (s, 1H, H-10), 10.48 (s, 1H, H-1), 7.16 – 7.11 (m, 2H, H-6), 7.09 (m, 2H, H-15), 7.05 (m, 2H, H-5), 7.03 (m, 2H, H-14), 4.09 (s, 2H, H-3), 4.09 (s, 2H, H-12), 2.86 (hept,  $J = 6.9$  Hz, 1H, H-8), 2.31 (s, 3H, H-17), 1.22 (d,  $J = 6.9$  Hz, 6H, H-9);  **$^{13}\text{C NMR}$**  (100.6 MHz, Chloroform-*d*):  $\delta$  193.8 (CH), 193.7 (CH), 147.6 (C, 2 overlapping signals), 147.5 (C), 136.5 (C), 135.5 (C), 135.3 (C), 129.7 (CH), 128.3 (CH, 2 overlapping signals), 127.1 (CH), 33.8 (CH), 28.9 (CH<sub>2</sub>, 2 overlapping signals), 24.1 (CH<sub>3</sub>), 21.1 (CH<sub>3</sub>); **HRMS** (+ESI) calcd. for  $\text{C}_{22}\text{H}_{24}\text{O}_2$   $m/z$  343.1669 (M+Na), found  $\text{C}_{22}\text{H}_{24}\text{O}_2$   $m/z$  343.1660 (M+Na)

*Preparation of 2-(4-bromobenzyl)-3-(4-methylbenzyl)fumaraldehyde 201j*

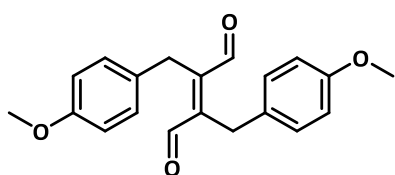


*Following general procedure:* In the written order,  $[\text{Cu}(\text{MeCN})_4]\text{BF}_4$  (76.7 mg, 0.243 mmol, 8.1 mol% in 2 ml DMF), Bipy (38.5 mg, 0.246 mmol, 8.2 mol% in 2 ml DMF), TEMPO (35.8 mg, 0.229 mmol, 7.6 mol% in 2 ml

DMF) and NMI (38  $\mu\text{l}$ , 0.64 mmol, 16 mol%) to a stirred solution of (E)-2-(4-bromobenzyl)-3-(4-methylbenzyl)but-2-ene-1,4-diol **199j** (1.08 g, 3.00 mmol) in DMF (6 ml). On addition of all reagents,  $\text{O}_2$  was bubbled into the solution until TLC analysis (2:1 EtOAc:Hexane) showed formation of the aldehyde ( $R_f = 0.76$ ). The reaction mixture was quenched by washing the mixture into a separatory funnel with EtOAc (20 ml), and quenched with aqueous 1M HCl (2 x 20 ml) then water (2 x 20ml). The aqueous was then re-extracted extracted with EtOAc (20 ml), the organic fractions

combined and washed a final time with 1M HCl (20 ml). The combined fractions were then dried with MgSO<sub>4</sub>, filtered and concentrated under reduced pressure giving a yellow solid that required no further purification (1.10 g, 3.07 mmol, >99%), **m.p.** 155-156 °C, **IR** (Solid ATR)  $\nu_{\text{max}}/\text{cm}^{-1}$  3333, 3057, 3024, 2981, 2971, 2940, 2912, 2875, 2820, 2769, 1738, 1667, 1588, 1513, 1487, 1447, 1397, 1217, 1189, 1129, 1073, 1023, 1011, 967, 944, 880, 822, 799, 790, 750, 702, 640, 582, 527, 497, 477, 460; **<sup>1</sup>H NMR** (400.2 MHz, D<sub>6</sub>-DMSO)  $\delta$  10.47 (s, 1H, H-1), 10.43 (s, 1H, H-9), 7.41 – 7.37 (m, 2H, H-6), 7.11 – 7.07 (m, 2H, H-14), 7.05 – 6.97 (m, 2H, H-13), 7.02 – 6.99 (m, 2H, H-5), 7.00 (m, 2H, H-), 4.09 (s, 2H, H-11), 4.06 (s, 2H, H-3), 2.30 (s, 3H, H-15); **<sup>13</sup>C NMR** (100.6 MHz, D<sub>6</sub>-DMSO):  $\delta$  193.4 (CH), 193.4 (CH), 148.1 (C), 146.5 (C), 137.3 (C), 136.7 (C), 134.9 (C), 132.1 (CH), 130.2 (CH), 129.8 (CH), 128.3 (CH), 120.9 (C), 29.1 (CH<sub>2</sub>), 28.8 (CH<sub>2</sub>), 21.1 (CH<sub>3</sub>); **HRMS** (+ESI) calcd. for C<sub>19</sub>H<sub>17</sub>Br<sub>1</sub>O<sub>2</sub>  $m/z$  379.0304 (M+Na), found C<sub>19</sub>H<sub>17</sub>Br<sub>1</sub>O<sub>2</sub>  $m/z$  379.0300 (M+Na)

*Preparation of (E)-2,3-bis(4-methoxybenzyl)but-2-ene-1,4-diol* **201k**

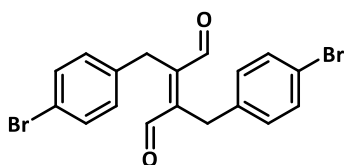


*Following general procedure:* In the written order, [Cu(MeCN)<sub>4</sub>]BF<sub>4</sub> (102 mg, 0.324 mmol, 8 mol% in 3ml DMF), Bipy (50.1 mg, 0.321 mmol, 8 mol% in 3ml DMF), TEMPO (51.0 mg, 0.326 mmol, 8.2 mol% in 3ml

DMF) and NMI (51  $\mu$ l, 0.64 mmol, 16 mol%) to a stirred solution of (E)-2,3-bis(4-methoxybenzyl)but-2-ene-1,4-diol **199k** (1.30 g, 4.00 mmol) in DMF (8 ml). On addition of all reagents, O<sub>2</sub> was bubbled into the solution until TLC analysis showed formation of the aldehyde ( $R_f$  = 0.64). The reaction mixture was quenched by washing the mixture into a separatory funnel with warm 9:1 EtOAc:THF (20 ml), and quenched with aqueous 1M HCl (2 x 20 ml) then water (2 x 20ml). The aqueous was then re-extracted extracted with warm 9:1 EtOAc:THF (20 ml), the organic fractions combined and washed a final time with 1M HCl (20 ml). The combined fractions were then dried warm with MgSO<sub>4</sub>, filtered and concentrated under reduced pressure giving a yellow solid (1.44 g). The solid could then be triturated with Et<sub>2</sub>O and filtered to provide a yellow solid (874 g, 2.69 mmol, 63%), **m.p.** 150-152 °C, **IR** (Solid ATR)  $\nu_{\text{max}}/\text{cm}^{-1}$  3332, 3063, 3036, 3013, 2969, 2937, 2908, 2876, 2840, 2821, 2769, 1668, 1606, 1581, 1509, 1455, 1443, 1397, 1327, 1305, 1284, 1241, 1178, 1131, 1109, 1025, 979, 962, 878, 833,

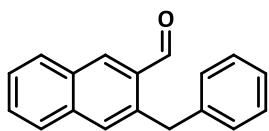
825, 811, 756, 695, 634, 565, 516, 423; **<sup>1</sup>H NMR** (400.2 MHz, D<sub>6</sub>-DMSO) δ 10.47 (s, 2H, H-1), 7.04 (d, *J* = 8.7 Hz, 2H, ), 6.81 (d, *J* = 8.7 Hz, 2H), 4.05 (s, 2H, H-3), 3.77 (s, 3H, H-9); **<sup>13</sup>C NMR** (100.6 MHz, D<sub>6</sub>-DMSO): δ 193.8 (CH), 158.5 (C), 147.5 (C), 130.2 (C), 129.5 (CH), 114.4 (CH), 55.4 (CH<sub>3</sub>), 28.5 (CH<sub>2</sub>); **HRMS** (+ESI) calcd. for C<sub>20</sub>H<sub>20</sub>O<sub>4</sub> *m/z* 342.1700 (M+NH<sub>4</sub>), found C<sub>20</sub>H<sub>20</sub>O<sub>4</sub> *m/z* 342.1695 (M+NH<sub>4</sub>).

#### Preparation of 2-(4-bromobenzyl)-3-(4-methylbenzyl)fumaraldehyde **201n**



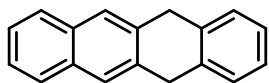
Following general procedure: In the written order, [Cu(MeCN)<sub>4</sub>]BF<sub>4</sub> (76.5 mg, 0.243 mmol, 8.1 mol% in 2 ml DMF), Bipy (38.0 mg, 0.243 mmol, 8.1 mol% in 2 ml DMF), TEMPO (38.5 mg, 0.246 mmol, 8.2 mol% in 2 ml DMF) and NMI (38 μl, 0.64 mmol, 16 mol%) to a stirred solution of (E)-2,3-bis(4-bromobenzyl)but-2-ene-1,4-diol (**5hh**) (1.28 g, 3.00 mmol) in DMF (6 ml). On addition of all reagents, O<sub>2</sub> was bubbled into the solution. After 7 minutes, the solution was clear green however TLC analysis indicated that the starting material remained, so was redosed with [Cu(MeCN)<sub>4</sub>]BF<sub>4</sub> (76.0 mg), Bipy (38.0 mg) and TEMPO (38.0 mg) and monitored until TLC analysis showed formation of the aldehyde until TLC analysis (2:1 EtOAc:Hexane) showed complete conversion to the dialdehyde (*R<sub>f</sub>* = 0.76). The reaction mixture was quenched by washing the mixture into a separatory funnel with EtOAc (20 ml), and quenched with aqueous 1M HCl (2 x 20 ml) then water (2 x 20ml). The aqueous was then re-extracted extracted with EtOAc (20 ml), the organic fractions combined and washed a final time with 1M HCl (20 ml). The combined fractions were then dried with MgSO<sub>4</sub>, filtered and concentrated under reduced pressure giving a yellow solid that required no further purification (859 mg, 2.80 mmol, 94%), **m.p.** 135-136 °C, **IR** (Solid ATR) *v*<sub>max</sub>/cm<sup>-1</sup> 3333, 2979, 2941, 2913, 2875, 2820, 2769, 1910, 1667, 1639, 1588, 1561, 1544, 1486, 1449, 1405, 1397, 1321, 1294, 1271, 1247, 1216, 1188, 1129, 1104, 1072, 1011, 981, 966, 946, 880, 822, 791, 702, 636, 499, 446; **<sup>1</sup>H NMR** (400.2 MHz, D<sub>6</sub>-DMSO) δ 10.43 (s, 2H, H-1), 7.43 – 7.37 (m, 4H, H-6), 7.03 – 6.96 (m, 4H, H-5), 4.07 (s, 4H, H-3); **<sup>13</sup>C NMR** (100.6 MHz, D<sub>6</sub>-DMSO): δ 193.0 (CH), 147.1 (C), 137.0 (C), 132.2 (CH), 130.1 (CH), 121.0 (C), 28.9 (CH<sub>2</sub>); **HRMS** (-ESI) calcd. for C<sub>18</sub>H<sub>14</sub>Br<sub>2</sub>O<sub>2</sub> *m/z* 418.9288 (M-H), found C<sub>18</sub>H<sub>14</sub>Br<sub>2</sub>O<sub>2</sub> *m/z* 418.9290 (M-H).

#### Synthesis of 3-benzyl-2-naphthaldehyde **202**



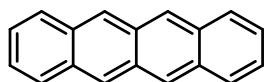
$\text{BF}_3 \cdot \text{OEt}_2$  (266  $\mu\text{l}$ , 2.15 mmol) was added to a magnetically stirred solution of **201a** (600 mg, 2.15 mmol) in DCE (8 ml) in a flame dried Schleck tube under argon at r.t. The solution was then heated to 83 °C on an oil bath until TLC indicated completion. The solution was then cooled to r.t. and quenched with saturated aqueous  $\text{NH}_4\text{Cl}$  (10 ml) and extracted with  $\text{Et}_2\text{O}$  (3 x 15 ml). The combined organic fractions were then concentrated under reduced pressure and purified by flash column chromatography (9:1 pentane:ether) and the fractions concentrated under reduced pressure giving a off white solid (439 mg, 82%). Spectroscopic data was in agreement with previously reported data.<sup>205</sup>  $R_f = 0.55$  (7:3 pentane: $\text{Et}_2\text{O}$ );  $^1\text{H NMR}$  (400.2 MHz, Chloroform- $d$ )  $\delta$  10.31 (s, 1H), 8.39 (s, 1H), 8.00 (d,  $J = 8.2$  Hz, 1H), 7.84 (d,  $J = 8.2$  Hz, 1H), 7.68 (s, 1H), 7.67 – 7.63 (m, 1H), 7.57 (ddd,  $J = 8.0, 6.9, 1.3$  Hz, 1H), 7.37 – 7.31 (m, 2H), 7.29 – 7.22 (m, 3H), 4.63 (s, 2H),  $^{13}\text{C NMR}$  (100.6 MHz, Chloroform- $d$ )  $\delta$  192.7 (CH), 140.6 (C), 137.7 (C), 136.5 (CH), 135.8 (C), 132.7 (C), 131.6 (C), 130.5 (CH), 129.4 (CH), 129.3 (CH), 129.1 (CH), 128.6 (CH), 127.6 (CH), 126.7 (CH), 126.3 (CH), 38.8 ( $\text{CH}_2$ ).

#### Synthesis of 5,12-dihydrotetracene **27**



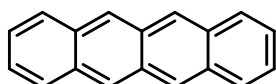
$\text{BF}_3 \cdot \text{OEt}_2$  (266  $\mu\text{l}$ , 2.15 mmol) was added to a magnetically stirred solution of **201a** (300 mg, 1.08 mmol) in DCE (4 ml) in a flame dried Schleck tube under argon at r.t. The solution was then heated to 83 °C on an oil bath until TLC indicated for 5 h. The solution was then cooled to r.t. and the crude mixture filtered through a plug of silica with  $\text{CH}_2\text{Cl}_2$ . The organic filtrate was then concentrated under reduced pressure and purified by flash column chromatography (4:1 cyclohexane: $\text{CH}_2\text{Cl}_2$ ) and the fractions concentrated under reduced pressure giving an off white solid (130 mg, 51%). Spectroscopic data was in agreement with previously reported data.<sup>63</sup>  $R_f = 0.22$  (4:1 cyclohexane: $\text{CH}_2\text{Cl}_2$ ),  $^1\text{H NMR}$  (400.1 MHz, Chloroform- $d$ )  $\delta$  7.79 (dd,  $J = 6.2, 3.3$  Hz, 2H), 7.76 (s, 2H), 7.42 (dd,  $J = 6.2, 3.3$  Hz, 2H), 7.35 (dd,  $J = 5.5, 3.3$  Hz, 2H), 7.22 (dd,  $J = 5.5, 3.3$  Hz, 2H), 4.10 (s, 4H),  $^{13}\text{C NMR}$  (100.6 MHz, Chloroform- $d$ )  $\delta$  137.2 (C), 135.9 (C), 132.5 (C), 127.4 (CH), 127.4 (CH), 126.4 (CH), 125.4 (CH), 125.3 (CH), 37.0 ( $\text{CH}_2$ ).

## Synthesis of tetracene **2**

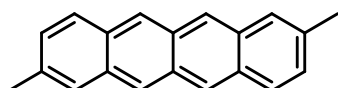


TiCl<sub>4</sub> (238  $\mu$ l, 2.16 mmol, 1.90 eq.) was added in one portion to a stirred solution of **201a** (300 mg, 1.13 mmol) in dry CH<sub>2</sub>Cl<sub>2</sub> (4 ml, c=0.25) at -30 °C. The reaction mixture was then allowed to warm to r.t. over 5 h, and stirred for 22 h, at which point NMR of the crude mixture showed complete formation of tetracene. The reaction was then quenched with 1:1 acetone:MeOH forming a bright orange precipitate and reduced under reduced pressure, washed with saturated aqueous NaHCO<sub>3</sub> (10 ml), and extracted with DCM (3 x 30 ml) (351 mg). The crude was subsequently recrystallized from hot toluene and canulla filtered giving bright orange plates (196 mg, 0.860 mmol, 76%). Tetracene can also be purified further by sublimation at 225 °C at 4.0 $\times$ 10<sup>-2</sup> mbar, **m.p.** >250 °C; **IR** (diamond-ATR):  $\nu_{\text{max/cm-1}}$  3043, (pseudo emission 2165, 2027), 1805, 1734, 1696, 1627, 1537, 1493, 1462, 1386, 1294, 1196, 1164, 1121, 995, 957, 901, 738, 469; **<sup>1</sup>H NMR** (500.2 MHz, CS<sub>2</sub>, insert referenced to D<sub>6</sub>-DMSO)  $\delta$  8.30 (s, 1H), 7.66 (dd, *J* = 6.6, 3.2 Hz, 1H), 7.08 (dd, *J* = 6.6, 3.2 Hz, 1H); **<sup>13</sup>C NMR** (125.8 MHz, CS<sub>2</sub>, insert referenced to D<sub>6</sub>-DMSO):  $\delta$  130.9 (C), 129.6 (C), 127.8 (CH), 125.9 (CH), 124.7(CH); **HRMS** (FDMS) calcd. for C<sub>18</sub>H<sub>12</sub> *m/z* 228.0298, found *m/z* 228.0934.

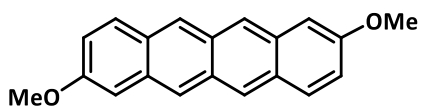
### CAM-B3LYP/6-31G(d,p) HOMO Eigenvalues and TD-DFT Calculations:



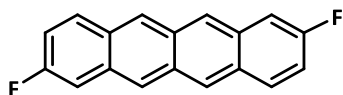
Highest alpha occupied eigenvalue:				-0.20897
Triplet-A	0.8416 eV	1473.21 nm	f=0.0000	S <sup>2</sup> =2.000
Singlet-A	2.7478 eV	451.21 nm	f=0.1478	S <sup>2</sup> =0.000



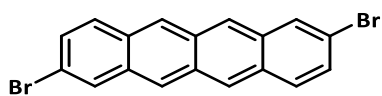
Highest alpha occupied eigenvalue:				-0.21781
Triplet-A	0.9776 eV	1268.26 nm	f=0.0000	S <sup>2</sup> =2.000
Singlet-A	2.7267 eV	454.70 nm	f=0.1386	S <sup>2</sup> =0.000



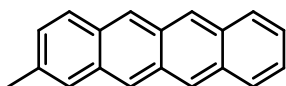
Highest alpha occupied eigenvalue:		-0.21132		
Triplet-A	0.8573 eV	1446.24 nm	f=0.0000	S <sup>2</sup> =2.000
Singlet-A	2.5641 eV	483.53 nm	f=0.1497	S <sup>2</sup> =0.000



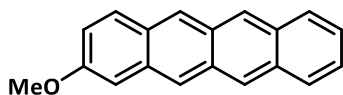
Highest alpha occupied eigenvalue:		-0.22915		
Triplet-A	0.9772 eV	1268.81 nm	f=0.0000	S <sup>2</sup> =2.000
Singlet-A	2.7292 eV	454.29 nm	f=0.1450	S <sup>2</sup> =0.000



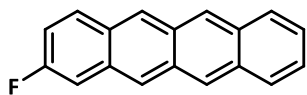
Highest alpha occupied eigenvalue:		-0.23504		
Triplet-BU	1.1602 eV	1068.63 nm	f=0.0000	S <sup>2</sup> =2.000
Singlet-BU	2.8578 eV	433.85 nm	f=0.1311	S <sup>2</sup> =0.000



Highest alpha occupied eigenvalue:		-0.21982		
Triplet-A	1.0019 eV	1237.50 nm	f=0.0000	S <sup>2</sup> =2.000
Singlet-A	2.7602 eV	449.19 nm	f=0.1430	S <sup>2</sup> =0.000



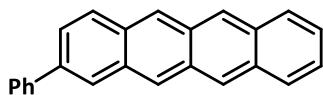
Highest alpha occupied eigenvalue:		-0.20942		
Triplet-A	1.5316 eV	809.48 nm	f=0.0000	S <sup>2</sup> =2.000
Singlet-A	3.1035 eV	399.50 nm	f=0.1350	S <sup>2</sup> =0.000



Highest alpha occupied eigenvalue: -0.21467

Triplet-A 1.6088 eV 770.68 nm f=0.0000 S<sup>2</sup>=2.000

Singlet-A 3.2116eV 386.05 nm f=0.1341 S<sup>2</sup>=0.000



Highest alpha occupied eigenvalue: -0.21018

Triplet-A 1.5731 eV 788.15 nm f=0.0000 S<sup>2</sup>=2.000

Singlet-A 3.1417 eV 394.64 nm f=0.1231 S<sup>2</sup>=0.000

## References

1. Warnes, L. A. A., *Electronic Materials*. MacMillan: 1990.
2. Rowe, D. M., *Thermoelectrics Handbook: Macro to Nano*. Taylor & Francis: 2005.
3. Hochbaum, A. I.; Chen, R.; Delgado, R. D.; Liang, W.; Garnett, E. C.; Najarian, M.; Majumdar, A.; Yang, P., Enhanced thermoelectric performance of rough silicon nanowires. *Nature (London, U. K.)* **2008**, *451* (7175), 163-167.
4. Bubnova, O.; Crispin, X., Towards polymer-based organic thermoelectric generators. *Energy Environ. Sci.* **2012**, *5* (11), 9345-9362.
5. Snyder, G. J.; Toberer, E. S., Complex thermoelectric materials. *Nat. Mater.* **2008**, *7* (2), 105-114.
6. Zhao, L.-D.; Lo, S.-H.; Zhang, Y.; Sun, H.; Tan, G.; Uher, C.; Wolverton, C.; Dravid, V. P.; Kanatzidis, M. G., Ultralow thermal conductivity and high thermoelectric figure of merit in SnSe crystals. *Nature (London, U. K.)* **2014**, *508* (7496), 373-377.
7. Beyer, H.; Nurnus, J.; Bottner, H.; Lambrecht, A.; Wagner, E.; Bauer, G., High thermoelectric figure of merit ZT in PbTe and Bi<sub>2</sub>Te<sub>3</sub>-based superlattices by a reduction of the thermal conductivity. *Physica E (Amsterdam, Neth.)* **2002**, *13* (2-4), 965-968.
8. Venkatasubramanian, R.; Slivola, E.; Colpitts, T.; O'Quinn, B., Thin-film thermoelectric devices with high room-temperature figures of merit. *Nature (London, U. K.)* **2001**, *413* (6856), 597-602.
9. Vaquero, P.; Powell, A. V., Recent developments in nanostructured materials for high-performance thermoelectrics. *J. Mater. Chem.* **2010**, *20* (43), 9577-9584.
10. Takimiya, K.; Osaka, I.; Nakano, M.,  $\pi$ -Building Blocks for Organic Electronics: Reevaluation of "Inductive" and "Resonance" Effects of  $\pi$ -Electron Deficient Units. *Chem. Mater.* **2014**, *26* (1), 587-593.
11. Katsuta, S.; Miyagi, D.; Yamada, H.; Okujima, T.; Mori, S.; Nakayama, K.-i.; Uno, H., Synthesis, Properties, and Ambipolar Organic Field-Effect Transistor Performances of Symmetrically Cyanated Pentacene and Naphthacene as Air-Stable Acene Derivatives. *Org. Lett.* **2011**, *13* (6), 1454-1457.
12. Delgado, M. C. R.; Pigg, K. R.; da Silva Filho, D. A.; Gruhn, N. E.; Sakamoto, Y.; Suzuki, T.; Osuna, R. M.; Casado, J.; Hernandez, V.; Navarrete, J. T. L.; Martinelli, N. G.; Cornil, J.; Sanchez-Carrera, R. S.; Coropceanu, V.; Bredas, J.-L., Impact of Perfluorination on the Charge-Transport Parameters of Oligoacene Crystals. *J. Am. Chem. Soc.* **2009**, *131* (4), 1502-1512.
13. Russ, B.; Glauddell, A.; Urban, J. J.; Chabinyk, M. L.; Segalman, R. A., Organic thermoelectric materials for energy harvesting and temperature control. *Nat. Rev. Mater.* **2016**, *1* (10), 16050.
14. McGrail, B. T.; Sehrioglu, A.; Pentzer, E., Polymer Composites for Thermoelectric Applications. *Angew. Chem., Int. Ed.* **2015**, *54* (6), 1710-1723.
15. Bubnova, O.; Khan, Z. U.; Malti, A.; Braun, S.; Fahlman, M.; Berggren, M.; Crispin, X., Optimization of the thermoelectric figure of merit in the conducting polymer poly(3,4-ethylenedioxythiophene). *Nat. Mater.* **2011**, *10* (6), 429-433.
16. Kim, G. H.; Shao, L.; Zhang, K.; Pipe, K. P., Engineered doping of organic semiconductors for enhanced thermoelectric efficiency. *Nat. Mater.* **2013**, *12* (8), 719-723.
17. Wang, Y.; Zhou, J.; Yang, R., Thermoelectric Properties of Molecular Nanowires. *J. Phys. Chem. C* **2011**, *115* (49), 24418-24428.
18. Shi, K.; Zhang, F.; Di, C.-A.; Yan, T.-W.; Zou, Y.; Zhou, X.; Zhu, D.; Wang, J.-Y.; Pei, J., Toward High Performance n-Type Thermoelectric Materials by Rational Modification of BDPPV Backbones. *J. Am. Chem. Soc.* **2015**, *137* (22), 6979-6982.
19. Anthony, J. E., Functionalized acenes and heteroacenes for organic electronics. *Chem. Rev. (Washington, DC, U. S.)* **2006**, *106* (12), 5028-5048.

20. Anthony, J. E., The larger acenes: versatile organic semiconductors. *Angew. Chem., Int. Ed.* **2008**, *47* (3), 452-483.
21. Fudickar, W.; Linker, T., Why Triple Bonds Protect Acenes from Oxidation and Decomposition. *J. Am. Chem. Soc.* **2012**, *134* (36), 15071-15082.
22. Von Rein, F. W.; Richey, H. G., Jr., Stereochemistry of additions of Grignard reagents to alkynols. *Tetrahedron Lett.* **1971**, (41), 3777-80.
23. Payne, M. M.; Parkin, S. R.; Anthony, J. E., Functionalized Higher Acenes: Hexacene and Heptacene. *J. Am. Chem. Soc.* **2005**, *127* (22), 8028-8029.
24. Shi, Z.-F.; Black, H. T.; Dadvand, A.; Perepichka, D. F., Pentacenebis(thiadiazole)dione, an n-Type Semiconductor for Field-Effect Transistors. *J. Org. Chem.* **2014**, *79* (12), 5858-5860.
25. Xia, D.; Marszalek, T.; Li, M.; Guo, X.; Baumgarten, M.; Pisula, W.; Mullen, K., Solution-Processable n-Type Organic Semiconductors Based on Angular-Shaped 2-(12H-Dibenzofluoren-12-ylidene)malononitrilediimide. *Org Lett* **2015**, *17* (12), 3074-7.
26. Ye, Q.; Chang, J.; Huang, K.-W.; Dai, G.; Zhang, J.; Chen, Z.-K.; Wu, J.; Chi, C., Incorporating TCNQ into Thiophene-Fused Heptacene for n-Channel Field Effect Transistor. *Org. Lett.* **2012**, *14* (11), 2786-2789.
27. Schegolev, I. E.; Yagubskii, E. B., Extended Linear Chain Compounds. Miller, J. S., Ed. 1983; Vol. 2, pp 385-431.
28. Lee, B.; Chen, Y.; Fu, D.; Yi, H. T.; Czelen, K.; Najafov, H.; Podzorov, V., Trap healing and ultralow-noise Hall effect at the surface of organic semiconductors. *Nat. Mater.* **2013**, *12* (12), 1125-1129.
29. de Boer, R. W. I.; Klapwijk, T. M.; Morpurgo, A. F., Field-effect transistors on tetracene single crystals. *Appl. Phys. Lett.* **2003**, *83* (21), 4345-4347.
30. Jiang, Y.; Peng, Q.; Geng, H.; Ma, H.; Shuai, Z., Negative isotope effect for charge transport in acenes and derivatives - a theoretical conclusion. *Phys. Chem. Chem. Phys.* **2015**, *17* (5), 3273-3280.
31. Curtis, M. D.; Cao, J.; Kampf, J. W., Solid-State Packing of Conjugated Oligomers: From  $\pi$ -Stacks to the Herringbone Structure. *J. Am. Chem. Soc.* **2004**, *126* (13), 4318-4328.
32. Coropceanu, V.; Cornil, J.; Da Silva Filho, D. A.; Olivier, Y.; Silbey, R.; Bredas, J.-L., Charge Transport in Organic Semiconductors. *Chem. Rev. (Washington, DC, U. S.)* **2007**, *107* (4), 926-952.
33. Anthony, J. E.; Facchetti, A.; Heeney, M.; Marder, S. R.; Zhan, X., n-Type Organic Semiconductors in Organic Electronics. *Adv. Mater. (Weinheim, Ger.)* **2010**, *22* (34), 3876-3892.
34. Hsu, C.-P., The Electronic Couplings in Electron Transfer and Excitation Energy Transfer. *Acc. Chem. Res.* **2009**, *42* (4), 509-518.
35. Pope, M.; Swenberg, C. E., *Electronic Processes in Organic Crystals and Polymers, Second Edition*. Oxford Univ Press: 1999; p 1376 pp.
36. Moon, H.; Zeis, R.; Borkent, E.-J.; Besnard, C.; Lovinger, A. J.; Siegrist, T.; Kloc, C.; Bao, Z., Synthesis, Crystal Structure, and Transistor Performance of Tetracene Derivatives. *J. Am. Chem. Soc.* **2004**, *126* (47), 15322-15323.
37. Albrecht, M.; Yi, H.; Pan, F.; Valkonen, A.; Rissanen, K., Connecting Electron-Deficient and Electron-Rich Aromatics to Support Intermolecular Interactions in Crystals. *Eur. J. Org. Chem.* **2015**, *2015* (15), 3235-3239.
38. Miao, Q.; Lefenfeld, M.; Nguyen, T.-Q.; Siegrist, T.; Kloc, C.; Nuckolls, C., Self-assembly and electronics of dipolar linear acenes. *Adv. Mater. (Weinheim, Ger.)* **2005**, *17* (4), 407-412.
39. Kitamura, C.; Abe, Y.; Ohara, T.; Yoneda, A.; Kawase, T.; Kobayashi, T.; Naito, H.; Komatsu, T., Synthesis and Crystallochromy of 1,4,7,10-Tetraalkyltetracenes: Tuning of Solid-

- State Optical Properties of Tetracenes by Alkyl Side-Chain Length. *Chem. - Eur. J.* **2010**, *16* (3), 890-898, S890/1-S890/38.
40. Liang, Z.; Zhao, W.; Wang, S.; Tang, Q.; Lam, S.-C.; Miao, Q., Unexpected Photooxidation of H-Bonded Tetracene. *Org. Lett.* **2008**, *10* (10), 2007-2010.
  41. Qu, H.; Chi, C., Synthetic chemistry of acenes and heteroacenes. *Curr. Org. Chem.* **2010**, *14* (18), 2070-2108.
  42. Du, C.; Guo, Y.; Chen, J.; Liu, H.; Liu, Y.; Ye, S.; Lu, K.; Zheng, J.; Wu, T.; Liu, Y.; Shuai, Z.; Yu, G., Design, Synthesis, and Properties of Asymmetrical Heteroacene and Its Application in Organic Electronics. *J. Phys. Chem. C* **2010**, *114* (23), 10565-10571.
  43. Sangaiah, R.; Gold, A., Synthesis of new cyclopenta-fused polycyclic aromatic hydrocarbon isomers of cata-annelated benzenoid systems. *J. Org. Chem.* **1987**, *52* (15), 3205-11.
  44. Patney, H. K., Synthesis of 2,3-norbornadienonaphthacene. *J. Org. Chem.* **1988**, *53* (26), 6106-9.
  45. Yagodkin, E.; Xia, Y.; Kalihari, V.; Frisbie, C. D.; Douglas, C. J., Synthesis, Solid State Properties, and Semiconductor Measurements of 5,6,11,12-Tetrachlorotetracene. *J. Phys. Chem. C* **2009**, *113* (37), 16544-16548.
  46. Gu, X.; Luhman, W. A.; Yagodkin, E.; Holmes, R. J.; Douglas, C. J., Diarylindenotetracenes via a Selective Cross-Coupling/C-H Functionalization: Electron Donors for Organic Photovoltaic Cells. *Org. Lett.* **2012**, *14* (6), 1390-1393.
  47. Odom, S. A.; Parkin, S. R.; Anthony, J. E., Tetracene Derivatives as Potential Red Emitters for Organic LEDs. *Org. Lett.* **2003**, *5* (23), 4245-4248.
  48. Woodward, R. B.; Hoffmann, R., Conservation of orbital symmetry. Verlag Chemie Academic Press: 1970
  49. Chen, Z.; Mueller, P.; Swager, T. M., Syntheses of Soluble,  $\pi$ -Stacking Tetracene Derivatives. *Org. Lett.* **2006**, *8* (2), 273-276.
  50. Rainbolt, J. E.; Miller, G. P., 4,7-Diphenylisobenzofuran: A Useful Intermediate for the Construction of Phenyl-Substituted Acenes. *J. Org. Chem.* **2007**, *72* (8), 3020-3030.
  51. Luo, J.; Hart, H., Linear acene derivatives. New routes to pentacene and naphthacene and the first synthesis of a triptycene with two anthracene moieties. *J. Org. Chem.* **1987**, *52* (22), 4833-6.
  52. Kim, B. S.; Choi, S. H.; Zhu, X. Y.; Frisbie, C. D., Molecular Tunnel Junctions Based on  $\pi$ -Conjugated Oligoacene Thiols and Dithiols between Ag, Au, and Pt Contacts: Effect of Surface Linking Group and Metal Work Function. *J. Am. Chem. Soc.* **2011**, *133* (49), 19864-19877.
  53. Somai Magar, K. B.; Xia, L.; Lee, Y. R., Organocatalyzed benzannulation for the construction of diverse anthraquinones and tetracenediones. *Chem. Commun. (Cambridge, U. K.)* **2015**, *51* (41), 8592-8595.
  54. Reichwagen, J.; Hopf, H.; Del Guerzo, A.; Belin, C.; Bouas-Laurent, H.; Desvergne, J.-P., Synthesis of 2,3-Substituted Tetracenes and Evaluation of Their Self-Assembling Properties in Organic Solvents. *Org. Lett.* **2005**, *7* (6), 971-974.
  55. Mallouli, A.; Lepage, Y., Convenient syntheses of naphthalene-, anthracene-, and naphthacene-2,3-dicarboxaldehydes. *Synthesis* **1980**, (9), 689.
  56. Lin, C.-H.; Lin, K.-H.; Pal, B.; Tsou, L.-D., Iterative synthesis of acenes via homo-elongation. *Chem. Commun. (Cambridge, U. K.)* **2009**, (7), 803-805.
  57. Bowles, D. M.; Anthony, J. E., A reiterative approach to 2,3-disubstituted naphthalenes and anthracenes. *Org. Lett.* **2000**, *2* (1), 85-87.
  58. Kitamura, C.; Takenaka, A.; Kawase, T.; Kobayashi, T.; Naito, H., Octaalkyl tetracene-1,2,3,4,7,8,9,10-octacarboxylates: synthesis by twofold [2+2+2] cocyclization and crystallochromy. *Chem. Commun. (Cambridge, U. K.)* **2011**, *47* (23), 6653-6655.

59. Pham, M. V.; Cramer, N., Aromatic Homologation by Non-Chelate-Assisted RhIII-Catalyzed C-H Functionalization of Arenes with Alkynes. *Angew. Chem., Int. Ed.* **2014**, *53* (13), 3484-3487.
60. Takahashi, T.; Kitamura, M.; Shen, B.; Nakajima, K., Straightforward method for synthesis of highly alkyl-substituted naphthacene and pentacene derivatives by homologation. *J. Am. Chem. Soc.* **2000**, *122* (51), 12876-12877.
61. Yue, W.; Gao, J.; Li, Y.; Jiang, W.; Di Motta, S.; Negri, F.; Wang, Z. H., One-Pot Synthesis of Stable NIR Tetracene Diimides via Double Cross-Coupling. *Journal of the American Chemical Society* **2011**, *133* (45), 18054-18057.
62. Geary, L. M.; Chen, T.-Y.; Montgomery, T. P.; Krische, M. J., Benzannulation via Ruthenium-Catalyzed Diol-Diene [4+2] Cycloaddition: One- and Two-Directional Syntheses of Fluoranthenes and Acenes. *J. Am. Chem. Soc.* **2014**, *136* (16), 5920-5922.
63. Dorel, R.; McGonigal, P. R.; Echavarren, A. M., Hydroacenes made easy by gold(I) catalysis. *Angew. Chem., Int. Ed.* **2016**, *55* (37), 11120-11123.
64. Link, A.; Fischer, C.; Sparr, C., Direct Transformation of Esters into Arenes with 1,5-Bifunctional Organomagnesium Reagents. *Angew. Chem., Int. Ed.* **2015**, *54* (41), 12163-12166.
65. Kimoto, T.; Tanaka, K.; Sakai, Y.; Ohno, A.; Yoza, K.; Kobayashi, K., 2,8- and 2,9-Diboryltetracenes as Useful Building Blocks for Extended  $\pi$ -Conjugated Tetracenes. *Org. Lett.* **2009**, *11* (16), 3658-3661.
66. Uttiya, S.; Miozzo, L.; Fumagalli, E. M.; Bergantin, S.; Ruffo, R.; Parravicini, M.; Papagni, A.; Moret, M.; Sassella, A., Connecting molecule oxidation to single crystal structural and charge transport properties in rubrene derivatives. *J. Mater. Chem. C* **2014**, *2* (21), 4147-4155.
67. Braga, D.; Jaafari, A.; Miozzo, L.; Moret, M.; Rizzato, S.; Papagni, A.; Yassar, A., The Rubrenic Synthesis: The Delicate Equilibrium between Tetracene and Cyclobutene. *Eur. J. Org. Chem.* **2011**, *2011* (22), 4160-4169, S4160/1-S4160/4.
68. Harrington, L. E.; Britten, J. F.; McGlinchey, M. J., Dimerisation of 9-Phenylethynylfluorene to Di-indeno-naphthacene and Dispiro-[fluorene-dihydronaphthacene-fluorene]: An X-ray Crystallographic and NMR Study. *Org. Lett.* **2004**, *6* (5), 787-790.
69. Gawel, P.; Dengiz, C.; Finke, A. D.; Trapp, N.; Boudon, C.; Gisselbrecht, J.-P.; Diederich, F., Synthesis of cyano-substituted diaryltetracenes from tetraaryl[3]cumulenes. *Angew. Chem., Int. Ed.* **2014**, *53* (17), 4341-4345.
70. Braverman, S.; Duar, Y., Thermal rearrangements of allenes. Synthesis and mechanisms of cycloaromatization of  $\pi$  and heteroatom bridged diallenes. *J. Am. Chem. Soc.* **1990**, *112* (15), 5830-7.
71. Braverman, S.; Zafrani, Y.; Gottlieb, H. E., Base catalyzed rearrangement of  $\pi$ -conjugated sulfur and selenium bridged propargylic systems. *Tetrahedron* **2001**, *57* (44), 9177-9185.
72. Chen, M.; Chen, Y.; Liu, Y., Palladium-catalyzed highly efficient synthesis of tetracenes and pentacenes. *Chem Commun (Camb)* **2012**, *48* (100), 12189-91.
73. Kitagaki, S.; Okumura, Y.; Mukai, C., Reaction of ene-bis(phosphinylallenes): [2 + 2] versus [4 + 2] cycloaddition. *Tetrahedron* **2006**, *62* (44), 10311-10320.
74. Lin, Y.-C.; Lin, C.-H., Synthesis of tetracene sulfoxide and tetracene sulfone via a cascade cyclization reaction. *Org. Lett.* **2007**, *9* (11), 2075-2078.
75. Tomita, K.; Nagano, M., Organo sulfur compounds. IV. Reaction of sodium sec- and tert- $\alpha$ -acetylenyl xanthates with alkyl halide. *Chem. Pharm. Bull. (Tokyo)* **1968**, *16* (10), 1911-17.
76. Luo, Y.-R., *Bond Dissociation Energies in Organic compounds*. CRC Press: 2003.

77. Gilbert, J. C.; Weerasooriya, U., Elaboration of aldehydes and ketones to alkynes: improved methodology. *J. Org. Chem.* **1979**, *44* (26), 4997.
78. Fleming, I., *Frontier Orbitals and Organic Chemical Reactions*. John Wiley and Sons Ltd.: 1976; p 258 pp.
79. Burroughs, L.; Ritchie, J.; Ngwenya, M.; Khan, D.; Lewis, W.; Woodward, S., Anionic sigmatropic-electrocyclic-Chugaev cascades: accessing 12-aryl-5-(methylthiocarbonylthio)tetracenes and a related anthra[2,3-b]thiophene. *Beilstein J. Org. Chem.* **2015**, *11*, 273-279.
80. Rodriguez, D.; Castedo, L.; Dominguez, D.; Saa, C., Synthesis of the Tetracyclic Core of Anthracycline Antibiotics by an Intramolecular Dehydro Diels-Alder Approach. *Org. Lett.* **2003**, *5* (17), 3119-3121.
81. DePuy, C. H.; King, R. W., Pyrolytic cis eliminations. *Chem. Rev. (Washington, DC, U. S.)* **1960**, *60*, 431-57.
82. Dhanalekshmi, S.; Venkatachalam, C. S.; Balasubramanian, K. K., Cation radical-induced Claisen rearrangement of aryl allenylmethyl ethers. *J. Chem. Soc., Chem. Commun.* **1994**, (4), 511-12.
83. He, S.; Hsung, R. P.; Presser, W. R.; Ma, Z.-X.; Haugen, B. J., An Approach to Cyclohepta[b]indoles through an Allenamide [4+3] Cycloaddition-Grignard Cyclization-Chugaev Elimination Sequence. *Org. Lett.* **2014**, *16* (8), 2180-2183.
84. Denmark, S. E.; Marlin, J. E.; Rajendra, G., Carbanion-Accelerated Claisen Rearrangements: Asymmetric Induction with Chiral Phosphorus-Stabilized Anions. *J. Org. Chem.* **2013**, *78* (1), 66-82.
85. Wilson, S. R., *Anionic-Assisted Sigmatropic Rearrangements*. Wiley: 2004; Vol. 43.
86. Koreeda, M.; Luengo, J. I., The anionic oxy-claisen rearrangement of enolates of  $\alpha$ -allyloxy ketones. A remarkable rate accelerating effect exhibited by the nature of the counterion. *J. Am. Chem. Soc.* **1985**, *107* (19), 5572-3.
87. Montgomery, J. A., Jr.; Frisch, M. J.; Ochterski, J. W.; Petersson, G. A., A complete basis set model chemistry. VI. Use of density functional geometries and frequencies. *J. Chem. Phys.* **1999**, *110* (6), 2822-2827.
88. Montgomery, J. A., Jr.; Frisch, M. J.; Ochterski, J. W.; Petersson, G. A., A complete basis set model chemistry. VII. Use of the minimum population localization method. *J. Chem. Phys.* **2000**, *112* (15), 6532-6542.
89. Zhao, Y. H.; Abraham, M. H.; Zissimos, A. M., Fast Calculation of van der Waals Volume as a Sum of Atomic and Bond Contributions and Its Application to Drug Compounds. *J. Org. Chem.* **2003**, *68* (19), 7368-7373.
90. Bordwell, F. G.; Landis, P. S., Elimination reactions. VIII. A frans Chugaev elimination. *J. Am. Chem. Soc.* **1958**, *80*, 2450-3.
91. Bredas, J.-L., Mind the gap! *Mater. Horiz.* **2014**, *1* (1), 17-19.
92. Zhang, G.; Musgrave, C. B., Comparison of DFT Methods for Molecular Orbital Eigenvalue Calculations. *J. Phys. Chem. A* **2007**, *111* (8), 1554-1561.
93. Hirata, S.; Head-Gordon, M., Time-dependent density functional theory within the Tamm-Dancoff approximation. *Chem. Phys. Lett.* **1999**, *314* (3,4), 291-299.
94. Yu, T.-Q.; Fu, Y.; Liu, L.; Guo, Q.-X., How to promote sluggish electrocyclization of 1,3,5-hexatrienes by captodative substitution. *J. Org. Chem.* **2006**, *71* (16), 6157-6164.
95. Magomedov, N. A.; Ruggiero, P. L.; Tang, Y., Remarkably facile hexatriene electrocyclizations as a route to functionalized cyclohexenones via ring expansion of cyclobutenones. *J. Am. Chem. Soc.* **2004**, *126* (6), 1624-1625.
96. Greshock, T. J.; Funk, R. L., Synthesis of Indoles via  $6\pi$ -Electrocyclic Ring Closures of Trienecarbamates. *J. Am. Chem. Soc.* **2006**, *128* (15), 4946-4947.

97. Still, W. C.; Galynker, I., Chemical consequences of conformation in macrocyclic compounds. An effective approach to remote asymmetric induction. *Tetrahedron* **1981**, *37* (23), 3981-96.
98. Murphy, S. K.; Zeng, M.; Herzon, S. B., A modular and enantioselective synthesis of the pleuromutilin antibiotics. *Science (Washington, DC, U. S.)* **2017**, *356* (6341), 956-959.
99. Brill, Z. G.; Grover, H. K.; Maimone, T. J., Enantioselective synthesis of an ophiobolin sesterterpene via a programmed radical cascade. *Science (Washington, DC, U. S.)* **2016**, *352* (6289), 1078-1082.
100. Holton, R. A.; Somoza, C.; Kim, H. B.; Liang, F.; Biediger, R. J.; Boatman, P. D.; Shindo, M.; Smith, C. C.; Kim, S.; et, a., First total synthesis of taxol. 1. Functionalization of the B ring. *J. Am. Chem. Soc.* **1994**, *116* (4), 1597-8.
101. Holton, R. A.; Kim, H. B.; Somoza, C.; Liang, F.; Biediger, R. J.; Boatman, P. D.; Shindo, M.; Smith, C. C.; Kim, S.; et, a., First total synthesis of taxol. 2. Completion of the C and D rings. *J. Am. Chem. Soc.* **1994**, *116* (4), 1599-1600.
102. Masters, J. J.; Link, J. T.; Snyder, L. B.; Young, W. B.; Danishefsky, S. J., A total synthesis of taxol. *Angew. Chem., Int. Ed. Engl.* **1995**, *34* (16), 1723-6.
103. Nicolaou, K. C.; Yang, Z.; Liu, J. J.; Ueno, H.; Nantermet, P. G.; Guy, R. K.; Claiborne, C. F.; Renaud, J.; Couladouros, E. A.; et, a., Total synthesis of taxol. *Nature (London)* **1994**, *367* (6464), 630-4.
104. Yang, Z.; He, Y.; Vourloumis, D.; Vallberg, H.; Nicolaou, K. C., Total synthesis of epothilone A: the olefin metathesis approach. *Angew. Chem., Int. Ed. Engl.* **1997**, *36* (1/2), 166-168.
105. Nelson, D. J.; Ashworth, I. W.; Hillier, I. H.; Kyne, S. H.; Pandian, S.; Parkinson, J. A.; Percy, J. M.; Rinaudo, G.; Vincent, M. A., Why is RCM Favored Over Dimerisation? Predicting and Estimating Thermodynamic Effective Molarities by Solution Experiments and Electronic Structure Calculations. *Chem. - Eur. J.* **2011**, *17* (46), 13087-13094, S13087/1-S13087/19.
106. Miller, S. J.; Kim, S.-H.; Chen, Z.-R.; Grubbs, R. H., Catalytic Ring-Closing Metathesis of Dienes: Application to the Synthesis of Eight-Membered Rings. *J. Am. Chem. Soc.* **1995**, *117* (7), 2108-9.
107. Chavan, S. P.; Thakkar, M.; Jogdand, G. F.; Kalkote, U. R., First Enantiospecific Synthesis of (-)-Parvifoline and (-)-Curcuquinone. *J. Org. Chem.* **2006**, *71* (23), 8986-8988.
108. Takao, K.-i.; Watanabe, G.; Yasui, H.; Tadano, K.-i., Total Synthesis of (±)-Mycoepoxydiene, a Novel Fungal Metabolite Having an Oxygen-Bridged Cyclooctadiene Skeleton. *Org. Lett.* **2002**, *4* (17), 2941-2943.
109. Brown, E.; Dhal, R.; Robin, J. P., A new total synthesis of (±)-steganone. *Tetrahedron Lett.* **1979**, (8), 733-6.
110. Cockerill, G. S.; Kocienski, P.; Treadgold, R., Silicon-mediated annulation. Part 2. A synthesis of β-alkoxy cyclooctanones via intramolecular directed aldol reactions. *J. Chem. Soc., Perkin Trans. 1* **1985**, (10), 2101-8.
111. Fazakerley, N. J.; Helm, M. D.; Procter, D. J., Total Synthesis of (+)-Pleuromutilin. *Chem. - Eur. J.* **2013**, *19* (21), 6718-6723.
112. Just-Baringo, X.; Clark, J.; Gutmann, M. J.; Procter, D. J., Selective Synthesis of Cyclooctanoids by Radical Cyclization of Seven-Membered Lactones: Neutron Diffraction Study of the Stereoselective Deuteration of a Chiral Organosamarium Intermediate. *Angew. Chem., Int. Ed.* **2016**, *55* (40), 12499-12502.
113. Monovich, L. G.; Le Huerou, Y.; Roenn, M.; Molander, G. A., Total Synthesis of (-)-Steganone Utilizing a Samarium(II) Iodide Promoted 8-Endo Ketyl-Olefin Cyclization. *J. Am. Chem. Soc.* **2000**, *122* (1), 52-57.
114. Kawada, H.; Iwamoto, M.; Utsugi, M.; Miyano, M.; Nakada, M., Synthetic Studies on the Taxane Skeleton: Construction of Eight-Membered Carbocyclic Rings by the

- Intramolecular B-Alkyl Suzuki-Miyaura Cross-Coupling Reaction. *Org. Lett.* **2004**, *6* (24), 4491-4494.
115. Gilbertson, S. R.; DeBoef, B., Rhodium Catalyzed [4 + 2 + 2] Cycloaddition and Alkyne Insertion: A New Route to Eight-Membered Rings. *J. Am. Chem. Soc.* **2002**, *124* (30), 8784-8785.
116. Yu, R. T.; Friedman, R. K.; Rovis, T., Enantioselective Rhodium-Catalyzed [4+2+2] Cycloaddition of Dienyl Isocyanates for the Synthesis of Bicyclic Azocine Rings. *J. Am. Chem. Soc.* **2009**, *131* (37), 13250-13251.
117. Lainhart, B. C.; Alexanian, E. J., Enantioselective Synthesis of cis-Fused Cyclooctanoids via Rhodium(I)-Catalyzed [4 + 2 + 2] Cycloadditions. *Org. Lett.* **2015**, *17* (5), 1284-1287.
118. Oonishi, Y.; Hosotani, A.; Sato, Y., Construction of monocyclic eight-membered rings: Intermolecular rhodium(I)-catalyzed [6+2] cycloaddition of 4-allenals with alkynes. *Angew. Chem., Int. Ed.* **2012**, *51* (46), 11548-11551.
119. Wender, P. A.; Snapper, M. L., Intramolecular nickel catalyzed cycloadditions of bisdienes: three approaches to the taxane skeleton. *Tetrahedron Lett.* **1987**, *28* (20), 2221-4.
120. Wender, P. A.; Ihle, N. C., Nickel-catalyzed intramolecular [4+4] cycloadditions. 2. Allylic stereoinduction and modelling studies in the preparation of bicyclo[6.4.0]dodecadienes. *Tetrahedron Lett.* **1987**, *28* (22), 2451-4.
121. Lee, P. H.; Lee, K.; Kang, Y., In situ generation of vinyl allenes and its applications to one-pot assembly of cyclohexene, cyclooctadiene, 3,7-nonadienone, and bicyclo[6.4.0]dodecene derivatives with palladium-catalyzed multicomponent reactions. *J. Am. Chem. Soc.* **2006**, *128* (4), 1139-1146.
122. Fuerstner, A.; Davies, P. W., Catalytic carbophilic activation: catalysis by platinum and gold  $\pi$  acids. *Angew. Chem., Int. Ed.* **2007**, *46* (19), 3410-3449.
123. Iwai, T.; Okochi, H.; Ito, H.; Sawamura, M., Construction of eight-membered carbocycles through gold catalysis with acetylene-tethered silyl enol ethers. *Angew. Chem., Int. Ed.* **2013**, *52* (15), 4239-4242.
124. Xu, Z.; Chen, H.; Wang, Z.; Ying, A.; Zhang, L., One-Pot Synthesis of Benzene-Fused Medium-Ring Ketones: Gold Catalysis-Enabled Enolate Umpolung Reactivity. *J. Am. Chem. Soc.* **2016**, *138* (17), 5515-5518.
125. Winkler, J. D.; Hey, J. P.; Williard, P. G., Inside-outside stereoisomerism: the synthesis of trans-bicyclo[5.3.1]undecane-11-one. *J. Am. Chem. Soc.* **1986**, *108* (20), 6425-7.
126. Winkler, J. D.; Lee, C. S.; Rubo, L.; Muller, C. L.; Squattrito, P. J., Stereoselective synthesis of the tricyclic skeleton of the taxane diterpenes. The first C-silylation of a ketone enolate. *J. Org. Chem.* **1989**, *54* (19), 4491-3.
127. Benchikh-le-Hocine, M.; Do Khac, D.; Cervantes, H.; Fetizon, M., Model studies in taxane diterpene synthesis. Part II. *Nouv. J. Chim.* **1986**, *10* (12), 715-21.
128. Grayson, D. H.; Wilson, J. R. H., Synthesis of the fusicoccin H aglycone. Construction of the carbon framework. *J. Chem. Soc., Chem. Commun.* **1984**, (24), 1695-6.
129. Mehta, G.; Krishnamurthy, N., A route, via tetraquinane, to the 5-8-5 carbocyclic nucleus of fusicoccins and ophiobolins. *J. Chem. Soc., Chem. Commun.* **1986**, (17), 1319-21.
130. Mehta, G.; Murty, A. N., Synthetic studies toward the novel tetracyclic diterpene longipenol. Construction of the ABD tricyclic framework. *J. Org. Chem.* **1990**, *55* (11), 3568-72.
131. Trost, B. M.; Vincent, J. E., A three-carbon condensative expansion. Application to muscone. *J. Am. Chem. Soc.* **1980**, *102* (17), 5680-3.
132. Martin, S. F.; White, J. B.; Wagner, R., Alkoxide-accelerated sigmatropic rearrangements. A novel entry to the bicyclo[5.3.1]undec-7-ene system of the taxane diterpenes. *J. Org. Chem.* **1982**, *47* (16), 3190-2.

133. Paquette, L. A.; Liang, S.; Galatsis, P., Expedient construction of the dicyclopenta[a,d]cyclooctene core of ceroplastin di- and sesterterpenes. *Synlett* **1990**, (11), 663-5.
134. Ma, S.; Gu, Z., Sequential Rearrangement of 1,2,4,7-Tetraenes Involving [1,5]-Hydrogen Migration and Electrocyclization: An Efficient Synthesis of Eight-Membered Cyclic Compounds. *J. Am. Chem. Soc.* **2006**, *128* (15), 4942-4943.
135. Petasis, N. A.; Patane, M. A., The synthesis of carbocyclic eight-membered rings. *Tetrahedron* **1992**, *48* (28), 5757-821.
136. Taylor, R. J. K., *Organocopper reagents: a practical approach*. Oxford University Press: 1994.
137. Eccleshare, L.; Lozada-Rodriguez, L.; Cooper, P.; Burroughs, L.; Ritchie, J.; Lewis, W.; Woodward, S., Diversification of ortho-Fused Cycloocta-2,5-dien-1-one Cores and Eight to Six-Ring Conversion by  $\sigma$  Bond C-C Cleavage. *Chem. - Eur. J.* **2016**, *22* (35), 12542-12547.
138. Burroughs, L.; Eccleshare, L.; Ritchie, J.; Kulkarni, O.; Lygo, B.; Woodward, S.; Lewis, W., One-Pot Cannizzaro Cascade Synthesis of ortho-Fused Cycloocta-2,5-dien-1-ones from 2-Bromo(hetero)aryl Aldehydes. *Angew. Chem., Int. Ed.* **2015**, *54* (36), 10648-10651.
139. Texier-Boullet, F.; Foucaud, A., Knoevenagel condensation catalyzed by aluminum oxide. *Tetrahedron Lett.* **1982**, *23* (47), 4927-8.
140. Rao, P. S.; Venkataratnam, R. V., Zinc chloride as a new catalyst for Knoevenagel condensation. *Tetrahedron Lett.* **1991**, *32* (41), 5821-2.
141. Rand, L.; Haidukewych, D.; Dolinski, R. H., Reactions catalyzed by potassium fluoride. V. The kinetics of the Knoevenagel reaction. *J. Org. Chem.* **1966**, *31* (4), 1272-4.
142. Sepiol, J. J.; Wilamowski, J., New aromatic rearrangement accompanying ring closure of 2-arylpropylidenemalonodinitriles to 1-aminonaphthalene-2-carbonitriles. *Tetrahedron Lett.* **2001**, *42* (31), 5287-5289.
143. Dufraisse, C.; Etienne, A.; de Pradene, H. V., peri-Diaminonaphthacene. *Compt. rend.* **1954**, *239*, 1744-7.
144. Hammett, L. P., Effect of structure upon the reactions of organic compounds. Benzene derivatives. *J. Am. Chem. Soc.* **1937**, *59*, 96-103.
145. Doyle, M. P.; Siegfried, B.; Dellaria, J. F., Jr., Alkyl nitrite-metal halide deamination reactions. 2. Substitutive deamination of arylamines by alkyl nitrites and copper(II) halides. A direct and remarkably efficient conversion of arylamines to aryl halides. *J. Org. Chem.* **1977**, *42* (14), 2426-31.
146. Li, X.-L.; Wu, W.; Fan, X.-H.; Yang, L.-M., A facile, regioselective and controllable bromination of aromatic amines using a CuBr<sub>2</sub>/Oxone system. *RSC Adv.* **2013**, *3* (30), 12091-12095.
147. Brown, H. C.; Kim, S. C.; Krishnamurthy, S., Selective reductions. 26. Lithium triethylborohydride as an exceptionally powerful and selective reducing agent in organic synthesis. Exploration of the reactions with selected organic compounds containing representative functional groups. *J. Org. Chem.* **1980**, *45* (1), 1-12.
148. Su, X.; Chen, C.; Wang, Y.; Chen, J.; Lou, Z.; Li, M., One-pot synthesis of quinazoline derivatives via [2+2+2] cascade annulation of diaryliodonium salts and two nitriles. *Chem. Commun. (Cambridge, U. K.)* **2013**, *49* (60), 6752-6754.
149. Sheng, J.; Wang, Y.; Su, X.; He, R.; Chen, C., Copper-Catalyzed [2+2+2] Modular Synthesis of Multisubstituted Pyridines: Alkenylation of Nitriles with VinylIodonium Salts. *Angew. Chem., Int. Ed.* **2017**, *56* (17), 4824-4828.
150. Wang, Y.; Chen, C.; Peng, J.; Li, M., Copper(II)-catalyzed three-component cascade annulation of diaryliodoniums, nitriles, and alkynes: A regioselective synthesis of multiply substituted quinolines. *Angew. Chem., Int. Ed.* **2013**, *52* (20), 5323-5327.
151. Flynn, A. B.; Ogilvie, W. W., Stereocontrolled Synthesis of Tetrasubstituted Olefins. *Chem. Rev. (Washington, DC, U. S.)* **2007**, *107* (11), 4698-4745.

152. Itami, K.; Kamei, T.; Yoshida, J., Diversity-oriented synthesis of tamoxifen-type tetrasubstituted olefins. *J. Am. Chem. Soc.* **2003**, *125* (48), 14670-14671.
153. Gourdet, B.; Lam, H. W., Stereoselective Synthesis of Multisubstituted Enamides via Rhodium-Catalyzed Carbozincation of Ynamides. *J. Am. Chem. Soc.* **2009**, *131* (11), 3802-3803.
154. Nishimae, S.; Inoue, R.; Shinokubo, H.; Oshima, K., Manganese(II) chloride-catalyzed alkylmagnesiumation of 2-alkynylphenols. *Chem. Lett.* **1998**, (8), 785-786.
155. Zhang, D.; Ready, J. M., Iron-Catalyzed Carbometalation of Propargylic and Homopropargylic Alcohols. *J. Am. Chem. Soc.* **2006**, *128* (47), 15050-15051.
156. Murakami, K.; Yorimitsu, H., Recent advances in transition-metal-catalyzed intermolecular carbomagnesiumation and carbozincation. *Beilstein J Org Chem* **2013**, *9*, 278-302.
157. Labaudiniere, L.; Hanaizi, J.; Normant, J. F., Reactivity of allylic dimetallic zinc reagents. 1. *J. Org. Chem.* **1992**, *57* (25), 6903-8.
158. Anastasia, L.; Dumond, Y. R.; Negishi, E.-I., Stereoselective synthesis of exocyclic alkenes by Cu-catalyzed allylmagnesiumation, Pd-catalyzed alkylation, and Ru-catalyzed ring-closing metathesis: highly stereoselective synthesis of (Z)- and (E)- $\gamma$ -bisabolenes. *Eur. J. Org. Chem.* **2001**, (16), 3039-3043.
159. Negishi, E.; Zhang, Y.; Cederbaum, F. E.; Webb, M. B., A selective method for the synthesis of stereodefined exocyclic alkenes via allylmetalation of propargyl alcohols. *J. Org. Chem.* **1986**, *51* (21), 4080-2.
160. Forgiione, P.; Wilson, P. D.; Fallis, A. G., Magnesium mediated carbometallation of propargyl alcohols: direct routes to furans and furanones. *Tetrahedron Lett.* **2000**, *41* (1), 17-20.
161. Creton, I.; Marek, I.; Normant, J.-F., Stereoselective synthesis of polysubstituted olefins via the formation of 1,1-bimetalloalkenes. *Tetrahedron Lett.* **1995**, *36* (41), 7451-4.
162. Huewe, F.; Steeger, A.; Kostova, K.; Burroughs, L.; Bauer, I.; Strohmriegl, P.; Dimitrov, V.; Woodward, S.; Pflaum, J., Low-cost and sustainable organic thermoelectrics based on low-dimensional molecular metals. *Adv. Mater. (Weinheim, Ger.)* **2017**, *29* (13), n/a.
163. Barluenga, J.; Moriel, P.; Valdes, C.; Aznar, F., N-Tosylhydrazones as reagents for cross-coupling reactions: a route to polysubstituted olefins. *Angew. Chem., Int. Ed.* **2007**, *46* (29), 5587-5590, S5587/1-S5587/23.
164. Barluenga, J.; Tomas-Gamasa, M.; Aznar, F.; Valdes, C., Metal-free carbon-carbon bond-forming reductive coupling between boronic acids and tosylhydrazones. *Nat. Chem.* **2009**, *1* (6), 494-499, S494/1-S494/46.
165. Fang, G.-H.; Yan, Z.-J.; Yang, J.; Deng, M.-Z., The first preparation of 4-substituted 1,2-oxaborol-2(5H)-ols and their palladium-catalyzed cross-coupling with aryl halides to prepare stereodefined 2,3-disubstituted allyl alcohols. *Synthesis* **2006**, (7), 1148-1154.
166. Cui, C.-X.; Li, H.; Yang, X.-J.; Yang, J.; Li, X.-Q., One-Pot Synthesis of Functionalized 2,5-Dihydrofurans via an Amine-Promoted Petasis Borono-Mannich Reaction. *Org. Lett.* **2013**, *15* (23), 5944-5947.
167. Korner, C.; Starkov, P.; Sheppard, T. D., An Alternative Approach to Aldol Reactions: Gold-Catalyzed Formation of Boron Enolates from Alkynes. *J. Am. Chem. Soc.* **2010**, *132* (17), 5968-5969.
168. Roscales, S.; Csaky, A. G., Transition-Metal-Free Direct anti-Carboboration of Alkynes with Boronic Acids To Produce Alkenylheteroarenes. *Org. Lett.* **2015**, *17* (6), 1605-1608.
169. Dixon, D. D.; Lockner, J. W.; Zhou, Q.; Baran, P. S., Scalable, Divergent Synthesis of Meroterpenoids via "Borono-sclareolide". *J. Am. Chem. Soc.* **2012**, *134* (20), 8432-8435.
170. Dean, J. A., *Lange's Handbook of Chemistry, Fourteenth Edition*. McGraw-Hill: 1992; p Unpaged.

171. Bauer, I.; Knoelker, H.-J., Iron Catalysis in Organic Synthesis. *Chem. Rev. (Washington, DC, U. S.)* **2015**, *115* (9), 3170-3387.
172. Hamze, A.; Brion, J.-D.; Alami, M., Synthesis of 1,1-diarylethylenes via efficient iron/copper co-catalyzed coupling of 1-arylvinyl halides with Grignard reagents. *Org Lett* **2012**, *14* (11), 2782-5.
173. Manolikakes, G.; Schade, M. A.; Munoz Hernandez, C.; Mayr, H.; Knochel, P., Negishi Cross-Couplings of Unsaturated Halides Bearing Relatively Acidic Hydrogen Atoms with Organozinc Reagents. *Org. Lett.* **2008**, *10* (13), 2765-2768.
174. Manolikakes, G.; Munoz Hernandez, C.; Schade, M. A.; Metzger, A.; Knochel, P., Palladium- and nickel-catalyzed cross-couplings of unsaturated halides bearing relatively acidic protons with organozinc reagents. *J. Org. Chem.* **2008**, *73* (21), 8422-8436.
175. Amatore, C.; Carre, E.; Jutand, A.; M'Barki, M. A., Rates and Mechanism of the Formation of Zerovalent Palladium Complexes from Mixtures of Pd(OAc)<sub>2</sub> and Tertiary Phosphines and Their Reactivity in Oxidative Additions. *Organometallics* **1995**, *14* (4), 1818-26.
176. Muniz, K., High-Oxidation-State Palladium Catalysis: New Reactivity for Organic Synthesis. *Angew. Chem., Int. Ed.* **2009**, *48* (50), 9412-9423.
177. Luo, L.; Resch, D.; Wilhelm, C.; Young, C. N.; Halada, G. P.; Gambino, R. J.; Grey, C. P.; Goroff, N. S., Room-Temperature Carbonization of Poly(diiododiacetylene) by Reaction with Lewis Bases. *J. Am. Chem. Soc.* **2011**, *133* (48), 19274-19277.
178. Hoover, J. M.; Stahl, S. S., Highly Practical Copper(I)/TEMPO Catalyst System for Chemoselective Aerobic Oxidation of Primary Alcohols. *J. Am. Chem. Soc.* **2011**, *133* (42), 16901-16910.
179. Semmelhack, M. F.; Schmid, C. R.; Cortes, D. A.; Chou, C. S., Oxidation of alcohols to aldehydes with oxygen and cupric ion, mediated by nitrosonium ion. *J. Am. Chem. Soc.* **1984**, *106* (11), 3374-6.
180. Mata-Perez, F.; Perez-Benito, J. F., The kinetic rate law for autocatalytic reactions. *J. Chem. Educ.* **1987**, *64* (11), 925-7.
181. Farcasiu, D.; Ghenciu, A., Evaluation of acidity of strong acid catalysts. II. The strength of boron trifluoride-water systems. *J. Catal.* **1992**, *134* (1), 126-33.
182. Huang, R.; Zhang, X.; Pan, J.; Li, J.; Shen, H.; Ling, X.; Xiong, Y., Benzylolation of arenes with benzyl halides synergistically promoted by in situ generated superacid boron trifluoride monohydrate and tetrahaloboric acid. *Tetrahedron* **2015**, *71* (10), 1540-1546.
183. Zhang, S.; Zhang, X.; Ling, X.; He, C.; Huang, R.; Pan, J.; Li, J.; Xiong, Y., Superacid BF<sub>3</sub>-H<sub>2</sub>O promoted benzylolation of arenes with benzyl alcohols and acetates initiated by trace water. *RSC Adv.* **2014**, *4* (58), 30768-30774.
184. Prakash, G. K. S.; Panja, C.; Shakhmin, A.; Shah, E.; Mathew, T.; Olah, G. A., BF<sub>3</sub>-H<sub>2</sub>O Catalyzed Hydroxyalkylation of Aromatics with Aromatic Aldehydes and Dicarboxaldehydes: Efficient Synthesis of Triarylmethanes, Diarylmethylbenzaldehydes, and Anthracene Derivatives. *J. Org. Chem.* **2009**, *74* (22), 8659-8668.
185. Athans, A. J.; Briggs, J. B.; Jia, W.; Miller, G. P., Hydrogen-protected acenes. *J. Mater. Chem.* **2007**, *17* (25), 2636-2641.
186. Kimura, K.; Yamazaki, T.; Katsumata, S., Dimerisation of the perylene and tetracene radical cations and electronic absorption spectra of their dimers. *J. Phys. Chem.* **1971**, *75* (12), 1768-74.
187. Malachuk, P. A.; Marcoux, L. S.; Adams, R. N., Improved methods for preparing hydrocarbon cation radicals. *J. Phys. Chem.* **1966**, *70* (6), 2064-5.
188. Tius, M. A.; Gomez-Galeno, J., Aromatic annelation. Synthesis of naphthalenes. *Tetrahedron Lett.* **1986**, *27* (23), 2571-4.
189. Hansch, C.; Leo, A.; Taft, R. W., A survey of Hammett substituent constants and resonance and field parameters. *Chem. Rev.* **1991**, *91* (2), 165-95.

190. Sokolov, A. N.; Atahan-Evrenk, S.; Mondal, R.; Akkerman, H. B.; Sanchez-Carrera, R. S.; Granados-Focil, S.; Schrier, J.; Mannsfeld, S. C. B.; Zoombelt, A. P.; Bao, Z.; Aspuru-Guzik, A., From computational discovery to experimental characterization of a high hole mobility organic crystal. *Nat. Commun.* **2011**, *2* (Aug.), 1451/1-1451/8.
191. Armarego, W. L. F.; Chai, C., *Purification of Laboratory Chemicals, 5th Edition*. Butterworth-Heinemann: 2003; p 608 pp.
192. Eaton, P. E.; Carlson, G. R.; Lee, J. T., Phosphorus pentoxide-methanesulfonic acid. Convenient alternative to polyphosphoric acid. *J. Org. Chem.* **1973**, *38* (23), 4071-3.
193. Gottlieb, H. E.; Kotlyar, V.; Nudelman, A., NMR chemical shifts of common laboratory solvents as trace impurities. *J. Org. Chem.* **1997**, *62* (21), 7512-7515.
194. Sun, H.; DiMugno, S. G., Anhydrous Tetrabutylammonium Fluoride. *J. Am. Chem. Soc.* **2005**, *127* (7), 2050-2051.
195. Bredas, J. L.; Silbey, R.; Boudreaux, D. S.; Chance, R. R., Chain-length dependence of electronic and electrochemical properties of conjugated systems: polyacetylene, polyphenylene, polythiophene, and polypyrrole. *J. Am. Chem. Soc.* **1983**, *105* (22), 6555-9.
196. Tauc, J., Optical properties and electronic structure of amorphous germanium and silicon. *Mater. Res. Bull.* **1968**, *3* (1), 37-46.
197. Gaussian 09, R. A., M. J. Frisch, G. W. Trucks, H. B. Schlegel, G. E. Scuseria, M. A. Robb, J. R. Cheeseman, G. Scalmani, V. Barone, G. A. Petersson, H. Nakatsuji, X. Li, M. Caricato, A. Marenich, J. Bloino, B. G. Janesko, R. Gomperts, B. Mennucci, H. P. Hratchian, J. V. Ortiz, A. F. Izmaylov, J. L. Sonnenberg, D. Williams-Young, F. Ding, F. Lipparini, F. Egidi, J. Goings, B. Peng, A. Petrone, T. Henderson, D. Ranasinghe, V. G. Zakrzewski, J. Gao, N. Rega, G. Zheng, W. Liang, M. Hada, M. Ehara, K. Toyota, R. Fukuda, J. Hasegawa, M. Ishida, T. Nakajima, Y. Honda, O. Kitao, H. Nakai, T. Vreven, K. Throssell, J. A. Montgomery, Jr., J. E. Peralta, F. Ogliaro, M. Bearpark, J. J. Heyd, E. Brothers, K. N. Kudin, V. N. Staroverov, T. Keith, R. Kobayashi, J. Normand, K. Raghavachari, A. Rendell, J. C. Burant, S. S. Iyengar, J. Tomasi, M. Cossi, J. M. Millam, M. Klene, C. Adamo, R. Cammi, J. W. Ochterski, R. L. Martin, K. Morokuma, O. Farkas, J. B. Foresman, and D. J. Fox,, *Gaussian 09, Revision D.01* , Gaussian, Inc., Wallingford CT, **2009**
198. Lee, C.; Yang, W.; Parr, R. G., Development of the Colle-Salvetti correlation-energy formula into a functional of the electron density. *Phys. Rev. B: Condens. Matter* **1988**, *37* (2), 785-9.
199. Becke, A. D., Density-functional exchange-energy approximation with correct asymptotic behavior. *Phys. Rev. A: Gen. Phys.* **1988**, *38* (6), 3098-100.
200. Becke, A. D., A new mixing of Hartree-Fock and local-density-functional theories. *J. Chem. Phys.* **1993**, *98* (2), 1372-7.
201. Raghavachari, K., Perspective on "Density functional thermochemistry. III. The role of exact exchange". *Theor. Chem. Acc.* **2000**, *103* (3-4), 361-363.
202. Yanai, T.; Tew, D. P.; Handy, N. C., A new hybrid exchange-correlation functional using the Coulomb-attenuating method (CAM-B3LYP). *Chem. Phys. Lett.* **2004**, *393* (1-3), 51-57.
203. Blake, A. J.; Shannon, J.; Stephens, J. C.; Woodward, S., Demonstration of promoted zinc Schlenk equilibria, their equilibrium values and derived reactivity. *Chem. - Eur. J.* **2007**, *13* (9), 2462-2472.
204. Baker, K. V.; Brown, J. M.; Hughes, N.; Skarnulis, A. J.; Sexton, A., Mechanical activation of magnesium turnings for the preparation of reactive Grignard reagents. *J. Org. Chem.* **1991**, *56* (2), 698-703.
205. Tso, H.-H.; Hwang, T.-K.; Chen, Y.-J., Convenient synthesis of 2-(methoxymethyl)-3-alkyl-, 2,3-dialkylated naphthalenes and 3-alkyl-2-naphthaldehydes. *Bull. Inst. Chem., Acad. Sin.* **1994**, *41*, 25-32.

---

.